The application of the Multi-Component Reaction (MCR) strategy in the design and synthesis of new antiplasmodial and antimycobacterial agents

Matshawandile Tukulula

University of Cape Town
Department of Chemistry
February 2012

The application of the Multi-Component Reaction (MCR) strategy in the design and synthesis of new antiplasmodial and antimycobacterial agents

A thesis submitted to the University of Cape Town for the fulfillment of the requirement for the degree of Doctor of Philosophy

By

Matshawandile Tukulula

Supervisor: Professor Kelly Chibale

February 2012

Department of Chemistry
University of Cape Town
Rondebosch, 7701,
Cape Town

DECLARATION

The application of the Multi-Component Reaction (MCR) strategy in the design and synthesis of new antiplasmodial and antimycobacterial agents.

I, Matshawandile Tukulula, hereby declare that:

- The work contained in the above-titled thesis is my own unaided work and that no part of it has been submitted previously for a degree or examination at this or any other university.

- Relevant sources used and people that contributed are referenced and acknowledged.

- I grant the University of Cape Town free license to reproduce this work, in whole or in part, for the purpose of research.

M. Tukulula:_____ Date:_____

Witness:_____ Date:_____

DEDICATION

This work is dedicated to my late great-grandmother, **Mrs Buyelwa Maria Tukulula-Madlavu**, whom herself was illiterate but educated her children and three generation of grandchildren thereafter. May Your Soul Rest In Peace MaNcobeni, Khuzekasi.

ACKNOWLEDGEMENTS

First and foremost, I would like to acknowledge the Heavenly Father Almighty for the blessings that he has bestowed upon me. Without his grace, guidance and limitless love I would not have been able to partake in and bring this project to completion. I will forever be grateful.

I would also like to extend my heartfelt gratitude to my supervisor, Prof. Kelly Chibale, for his guidance, enthusiasm and motivation throughout the duration of this project. I am also thankful for the opportunity to further my training in his world-class research group. Also acknowledged is Mrs Elaine Rutherfoord-Jones, the mother to all of us in the Chibale Research Group, and Dr Aloysius Nchinda for the assistance they have given to me over the past three years.

To my family, ndiyabulela for the unconditional love, support, prayers, encouragement and patience during my long absence from home due to my studies. Ndithi nangamso, ningadinwa.

Thanks are also due to the staff and students in the Department of Chemistry for their direct or indirect contribution to this project. Worth of a mention is Mr Noel Hendricks and Mr Pete Roberts for running the NMR analyses, Mr Pierro Benincasa for performing microanalysis and low resolution mass spectrometry, Dr Stefan Louw, Mrs Nina Lawrence and Ms Nersia Barnes, in no particular order, for conducting HPLC purification and mass spectrometry on my compounds. I am also thankful to Mr Mathew Njoroge for conducting solubility experiments and other ongoing *in vitro* ADME studies.

I would also like to acknowledge the contribution made by our collaborators in this project: Prof. Philip Rosenthal and Jiri Gut of the Department of Medicine, San Francisco General Hospital, University of California, USA, and the staff at the London School of Hygiene and Tropical Medicine, UK, and at the Swiss Tropical and Public Health Institute, Switzerland, for performing *in vitro* antiplasmodial evaluation against the W2, 3D7 and K1 (and *T.b. brucei Rhodesian* parasite) strains of *P. falciparum*, respectively. Prof Scott Franzblau and Dr Bao Wan from the Institute of Tuberculosis Research at the University of Illinois at Chicago, USA, and Dr Digby Warner and Ms Kupra Naran from the Institute of Infectious Disease and Molecular Medicince (IIDMM), University of Cape, SA, for performing *in vitro* antimycobacterial evaluation.

To the Chibale Research Group members, past and present, it has been an honor and a privilege to have worked alongside all of you. Thank you to Mr Dennis Ongarora for allowing me to stay at his place over the December holidays, much of this thesis write-up would have been extremely difficult if it were not for his generosity.

I am grateful to the NRF for the SARChI grant-holder bursary and to the University of Cape Town (Equity Development Program Scholarship in Chemistry and Equity Scholarship) for the generous financial support.

I would also like thank all my friends, especially Malibongwe Phillip, Luthando Funani, Thabo Poti, Sthule Xanga, Nkosana Yeye, Samkele Nsumiwa, Dr Andrew Andayi and Manare Sejeng, and my girlfriend, Nokubonga “Sma” Ngcamu, for all the prayers and moral support.

Abstract

Malaria and tuberculosis are ancient diseases that continue to have a profound impact on mankind, 5 millennia after their first documentation. Malaria is endemic in more than 100 countries and about 50% of the world's population is at risk of infection. Sub-Saharan Africa accounts for nearly 91% of malaria-related deaths annually. Tuberculosis on the other hand infects about one third of the world's population and is the second major cause of death in adults worldwide, with about 1.8 million deaths reported annually. The major challenge to the control of these diseases has been the rapid emergence of multi-drug resistant strains to the currently administered drugs, as such, these exert an enormous pressure on health care systems, especially in resource-limited areas. Alleviation of this pressure requires the development of highly efficacious new chemical entities (NCEs) to curb or manage these pathogens. The main aim of this study was to design NCEs based on the quinoline-, PA-824-, and tetrazole-scaffolds, which exhibit *in vitro* antiplasmodial and antimycobacterial activity. A series of quinoline-based compounds bearing the deoxyamodiaquine-, chloroquine-, primaquine-, and 4-arylamino quinoline-tetrazole scaffolds were rationally designed, profiled *in silico* and synthesized *via* the modified $TMSN_3$-Ugi multi-component reaction (MCR) strategy. These were then evaluated for antiplasmodial activity against the chloroquine-resistant (K1 and W2) and chloroquine-sensitive (3D7) strains of *P. falciparum*, as well as for antimycobacterial activity against the drug sensitive H_{37}Rv strain of *M. tuberculosis*.

In the deoxyamodiaquine series, the designed target compounds were profiled *in silico* to have predicted aqueous solubilities that were comparable to amodiaquine at both pH 5.0 and 7.5. Furthermore, all the proposed compounds were predicted to have acceptable Caco-2 permeation and intermediate hepatic metabolic stabilities. The *in silico* aqueous solubility predictions were compared to and/or verified with experimentally determined solubility studies on key compounds.

In this series, compounds **3.9a-f**, **3.9k** and **3.10c** (IC_{50} values ranging from 0.040 to 0.194 µM) were more potent than amodiaquine in both K1 and W2 strains. Also, compounds **3.9b-c** and **3.9k** exhibited greater *in vitro* potency than chloroquine in the K1 strain, while only compound **3.9k** was also more active than chloroquine in the W2 strain. These compounds also possessed potent antimycobacterial activity, with compounds **3.9a**, **3.9c-f** inhibiting over 90% of the replicating bacteria. Against the non-replicating persistent form of the bacteria, compounds **3.9a** (MIC_{90} =118.7 µM), **3.9c** (MIC_{90} = 74 µM) and **3.9k** (MIC_{90} = 15.1 µM) were the most active.

In the chloroquine-like series, of the 14 compounds tested against K1 strain, 6 showed greater activity than chloroquine, the most active compound, **3.15a5** (IC_{50} = 0.001 µM), was 36-fold more active than the reference drug. Against the W2 strain, almost all the compounds tested were more active than chloroquine except compound **3.15a1**, which was 1.2 times less active. Moreover, compounds **3.15a3-a5** completely inhibited the growth of the replicating bacteria, with MIC_{90} values in the range of 5.6 to 14.3 µM. Additionally, compounds **3.15a3** and **3.15a4** were also active against the non-replicating bacteria, while also exhibiting better activity than two standard TB drugs, isoniazid and moxofloxacin.

Primaquine-based compounds showed modest activity against the K1 strain. The most active compound in this series was **3.19d** (IC_{50} = 1.311 µM), which was 2 times less active than primaquine. However, none of these compounds showed any (MIC_{90} >160 µM) activity against the *M. tuberculosis* H_{37}Rv strain.

The 4-arylamino quinoline derivatives did not show significant activity against K1 strain except compounds **4.12a** (IC_{50} = 1.310 µM) and **4.12f** (IC_{50} = 1.228 µM). Also, none of these compounds inhibited the growth of the W2 strain at the highest concentration (IC_{50} > 10 µM) tested. Against the 3D7 sensitive strain, the most active compound was **4.12d** (IC_{50} = 0.647

μM). Furthermore, compounds **4.12b** (MIC_{90} = 123.2 μM) and **4.12d** (MIC_{90} = 92.5 μM) were the only ones in this series that exhibited inhibitory activity against the non-replicating and replicating *M. tuberculosis* bacteria, respectively.

The majority of the designed PA-824 derivatives were predicted to have improved aqueous solubilities than PA-824 at both pH 5.0 and 7.5. However, some of these derivatives were also predicted to have an affinity for binding to proteins and were susceptible to hepatic metabolic degradation. In addition, these compounds, including PA-824, were predicted to have acceptable Caco-2 permeation. As before, *in silico* aqueous solubility predictions were compared to and/or verified with experimentally determined kinetic solubility studies of key compounds. Among the PA-824 derivatives, the PA-824-aminoquinoline hybrids were the most active against the K1 strain, with hybrids **4.19d** (IC_{50} = 0.100 μM) and **4.19f** (IC_{50} = 0.164 μM) being more active than chloroquine. In addition, all the tested hybrids were more efficacious than mefloquine. Finally, these PA-824 derivatives exhibited potent antimycobacterial activity with MIC_{90} values between 0.25-125 μM. All these compounds were more active than kanamycin and streptomycin, standard TB drugs, in the 7 and 14 day assays.

Lastly, a limited number of *β*-lactams were synthesized *via* the Staudinger reaction, demonstrated activity against K1 strain. The most active compound, **4.22c** (IC_{50} = 0.209 μM), had comparable to the activity to chloroquine. Additionally, these *β*-lactams were inactive against the replicating bacteria at the highest concentration (MIC_{90} >160 μM) tested.

ABBREVIATIONS

ACT	Artemisinin Combination Therapy
ADME(T)	Absorption, Distribution, Metabolism, Excretion (Toxicity)
BBB	Blood-Brain Barrier
n-BuLi	*n*-Butyl lithium
CaH	Calcium hydride
$CDCl_3$	Deuterochloroform
$CHCl_3$	Chloroform
^{13}C NMR	Carbon Nuclear Magnetic Resonance
CYPs	Cytochrome P450 isozymes
DCM	Dichloromethane
DFV	Digestive food vacuole
DMF	Dimethylformamide
DMPK	Drug Metabolism and Pharmacokinetics
DMSO	Dimthylsulfoxide
DNA	Deoxyribonucleic acid
DOTS	Directly Observed Therapy, Short-course
ESI	Electron Spray Ionization
Et_3N	Triethylamine
EtOAc	Ethylacetate
EtOH	Ethanol
FGI	Functional group interconversion
HIV	Human Immunodeficiency Virus
^1H NMR	Proton Nuclear Magnetic Resonance
HPLC	High Pressure Liquid Chromatography
IC_{50}	50% Inhibitory Concentration
IR	Infrared
KBr	Potassium bromide
LORA	Low Oxygen Recovery Assay
MABA	Microplate Alamar Blue Assay
MCR	Multi-Component Reaction
MDR	Multi-drug resistant
MIC_{90}	90% Minimum Inhibitory Concentration
µM	MicroMolar

MeOH	Methanol
m.p.	Melting point
MS	Mass Spectroscopy
m/z	mass to charge ratio
NaH	Sodium Hydride
PB	Protein Binding
PBr_3	Phosphorus tribromide
PBS	Phosphate buffered saline
Pgp	P-glycoprotein
PfCRT	*Plasmodium falciparum* Chloroquine Resistance Transporter
Pfcrt	*Plasmodium falciparum* chloroquine resistance transporter gene
PfMDR1	*Plasmodium falciparum* Multi-Drug Resistance-1 Transporter
Pfmdr1	*Plasmodium falciparum* multi-drug resistance-1 transporter gene
PK	Pharmacokinetics
PM	Plasmepsin
$POBr_3$	Phosphorus oxy-tribromide
ppm	Parts per million
$Py.SO_3$	Pyridine sulphur trioxide
R_f	Retention factor
R_t	Retention time
RI	Resistance Index
SAR	Structure-Activity Relationships
TB	Tuberculosis
TDR	Totally-Drug Resistant
$TMSN_3$	Trimethylsilane azide
WHO	World Health Organization
XDR	Extensive-Drug Resistant

TABLE OF CONTENTS

Chapter One

Introduction

1.1 Malaria

1.1.1 Historical overview

Malaria is an ancient disease that has had a profound impact on the history of mankind for over 5000 years.[1] The first documented evidence of the disease characterized by intermittent fevers and enlargement of the spleen dates as far back as 2700 BC in the Chinese medical writings, *Nei Ching* (the canon of medicine), and in the Egyptian, Greek and Hindu texts in about 400 BC.[2,3] For some time malaria fevers were believed to be caused by poisonous vapors that arose from swamps and stagnant water. As a result of this ancient belief the word malaria derived from a Roman term "*mal aria*", which directly translates to "bad air" was adopted as the name for this disease.

The search for the cause of malaria intensified in the 19th century resulting in major advances and discoveries. In 1847, a German pathologist, Heinrich Meckel observed the presence of black-brown granules (Haemozoin) in the blood and spleen of patients who died of fever but did not link these observations to malaria.[4] In 1880 the true cause of malaria was identified to be a protozoan parasite by Charles Louis Alphonse Laveran.[2] Subsequent to this great discovery, Ronald Ross and Giovanni Battista Grassi identified the mosquito as the vector for both human and bird malaria.[2] Both Ross and Laveran were awarded the Nobel prize in 1902 and 1907 respectively.

1.1.2 Global distribution

Malaria remains one of the most important health and economic burdens facing the developing world. The World Health Organization (WHO) estimates malaria to be endemic in more than 100 countries and about 50% of the world's population is at risk of infection worldwide.[5] Although malaria is a global problem, more than 70% of the total morbidity is in Africa, followed by some parts of Asia and Latin America (Fig. 1.1 and Table 1.1).[6,7a,7b] The global distribution pattern suggests this disease is centered in the tropical and sub-tropical regions where the conditions are conducive for the survival and multiplication of the vector mosquitoes. To date, over 255 million new infections and 781 000 deaths are reported annually, 91% of which occur in sub-Saharan Africa, mostly to children under the age of 5 years and pregnant women.[8,9a,9b] These staggering mortality figures are exacerbated by co-infection with other opportunistic diseases such as human immunodeficiency virus (HIV) and tuberculosis (TB) in people with compromised immune systems.[10a,10b]

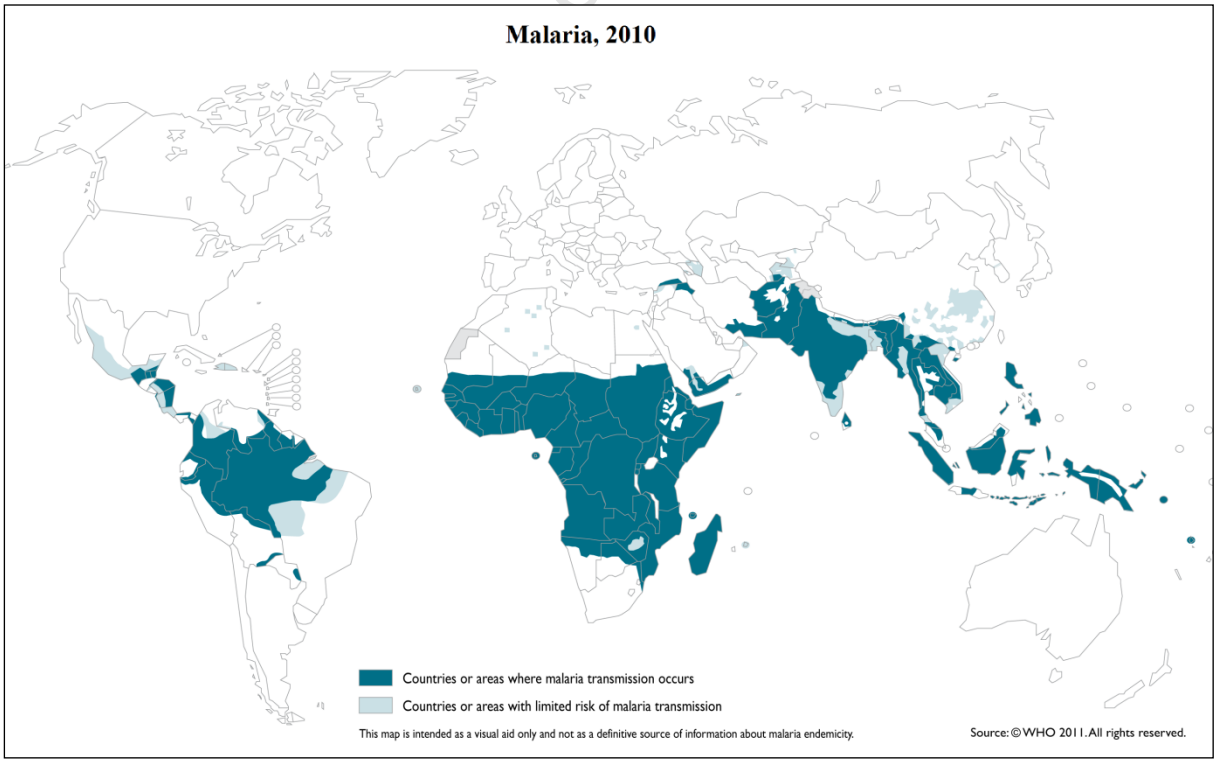

Figure 1.1: Global distribution of Malaria, 2010.[7a]

Table 1.1: Estimated malaria incidence and deaths by region, 2009 (adapted from the US GLOBAL HEALTH AND FACT SHEET, March 2011) [7b]

WHO Region (No. of Endemic Countries)	Estimated No. (%) of Malaria Cases, 2009	Estimated No. (%) of Deaths, 2009
Global Total (106)	**225 million (100%)**	**781,000 (100%)**
Africa (43)	176 million (78%)	709,000 (91%)
South-East Asia (10)	34 million (15%)	49,000 (6%)
Eastern Mediterranean (12)	12 million (5%)	16,000 (2%)
Western Pacific (10)	2 million (1%)	5,300 (1%)
Americas (23)	1 million (<1%)	1,300 (<1%)
Europe (8)	1 million (<1%)	0

1.2 Malaria vector and *Plasmodium falciparum*

Malaria is a parasitic blood infection caused by the intracellular-protozoan parasite belonging to the genus *Plasmodium*. It is transmitted from one human to another by the blood-feeding female *Anopheles* mosquitoes.[3,11] There are currently 41 known *Anopheles* mosquito species and sub-species complex worldwide that are implicated as vectors of *Plasmodium falciparum* malaria, *Anopheles gambiae* being the most important and efficient.[12] This species feeds predominantly on humans and has a longer life span compared to other mosquitoes. The genome sequence of the *Anopheles gambiae* was recently completed by Holt *et al.*,[13] in 2002.

The *Plasmodium* genus is comprised of unicellular protozoan parasites and currently there are 156 different known species, and among these, *P. falciparum*, *P. vivax*, *P. ovale*, *P. malariae* and *P. knowlesi* are the only known species able to cause human malaria.[14] *P. falciparum* is the most lethal and causes malignant malaria globally, while *P. vivax* is the most prevalent species outside Africa.[15]

1.2.1 Life cycle of the *Plasmodium falciparum*

The understanding of malaria parasite biochemistry and molecular biology over the last two decades increased extensively. The highlight of which was the full disclosure of *P. falciparum* genome sequence in 2002 and the elucidation of the highly conserved molecular

mechanisms that the parasite uses during host-cell invasion.[16,17] The life cycle of the *Plasmodium* parasite alternates between a human host (asexual reproduction) and the mosquito vector (sexual reproduction) (Fig. 1.2).[18]

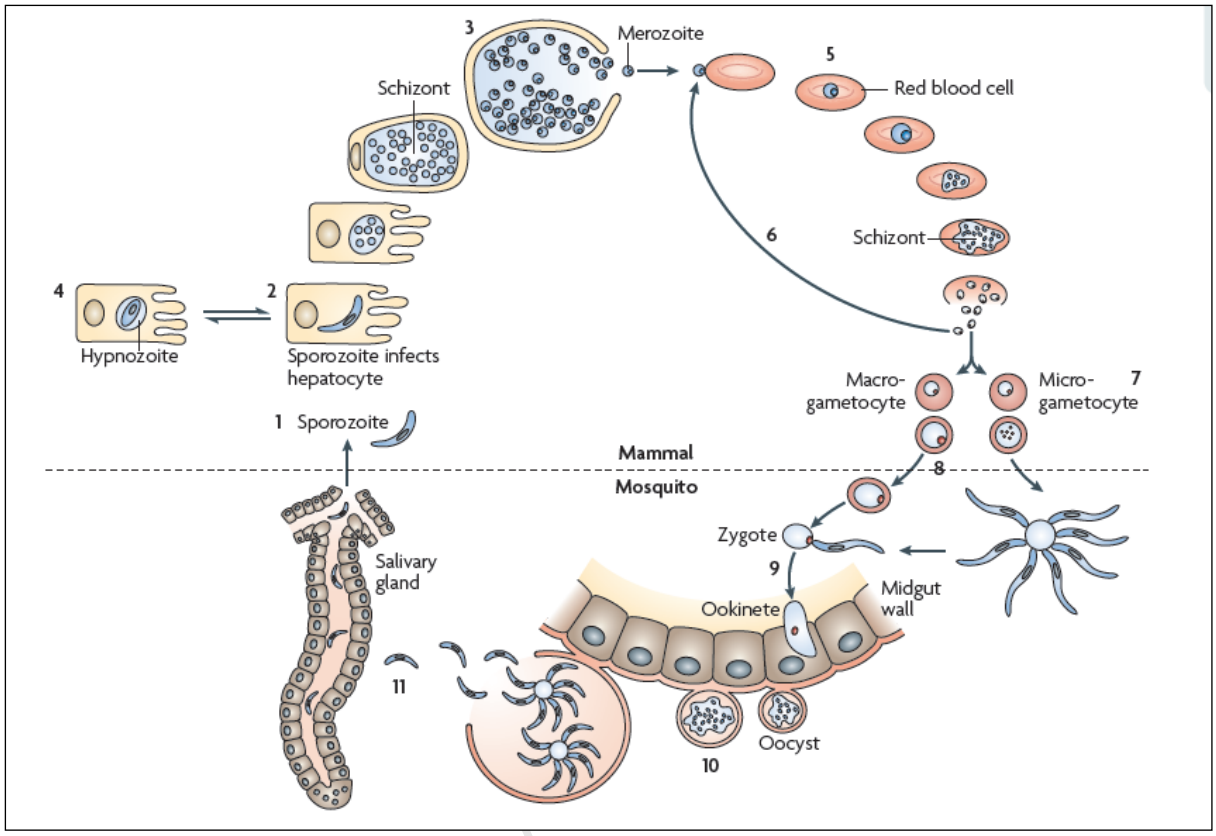

Figure 1.2: The malaria parasite's life cycle. [18]

Asexual reproduction: When an infected *Anopheles* female mosquito feeds on humans it injects saliva containing infective worm-like, unicellular organelles called sporozoites into the bloodstream (**1**, Fig. 1.2). These sporozoites rapidly migrate to the liver where they invade hepatocytes. Here they undergo replication that results in the production of uninucleate merozoites (**2-3** and **4**, Fig. 1.2). At this stage, the pre-erythrocytic stage, the human host is asymptomatic. After a period of about 9-16 days (depending on the infecting species), the hepatocytes burst releasing merozoites into the bloodstream where they invade red-blood cells and initiate the second phase of asexual multiplication (erythrocytic schizogony) (**5**, Fig. 1.2).[14] The merozoites undergo differentiation into early trophozoites (small ring forms), that develop over 48 hours into larger metabolically active trophozoites.

The erythrocyte cytoplasm is ingested and haemoglobin digested to form multinucleated schizonts. Haeme, the by-product of this haemoglobin digestion, is toxic to the parasite and as a result the parasite has developed a detoxification mechanism of converting the toxic material to an insoluble non-toxic haemozoin. The rupture of the schizont-containing erythrocyte releases merozoites into the bloodstream, which invade other red blood cells or differentiate into gametocytes, the male and female sexual forms (**6-7**, Fig. 1.2). The human host at this stage will show malaria symptoms such as high fever, chills and anaemia.[2]

Sexual reproduction: The gametocytes circulating in the bloodstream are taken up by another female mosquito feeding on an infected human (**8**, Fig. 1.2). Upon entering the stomach of the mosquito, the parasite receives environmental signals such as temperature drop and pH increase, which indicate a switch from a warm-blooded host to an insect vector.[19] The gametocytes mature into male and female gametes. Fertilization occurs forming zygotes and then ookinetes which penetrate the gut wall to become oocysts (**9-10**, Fig. 1.2).[20] The mature oocysts in the body cavity of the mosquito rupture to release infectious sporozoites, which migrate to and infect the mosquito salivary gland. Release of sporozoites in the next blood meal restarts the cycle (**11**, Fig. 1.2).

1.3 Targets for Antimalarial Chemotherapy

Certain phases of the parasite life cycle reveal various critical biological processes that are essential for the survival and development of the parasite. Mapping of the *P. falciparum* genome has contributed considerably in the identification and elucidation of these processes as potential drug targets. Many of these have been validated and shown to be localized inside unique parasitic organelles, such as the acidocalcisome,[21] vestigial mitochondria,[22] the acidic digestive food vacuole and the apicoplast among others (Fig. 1.3).[23, 24,25]

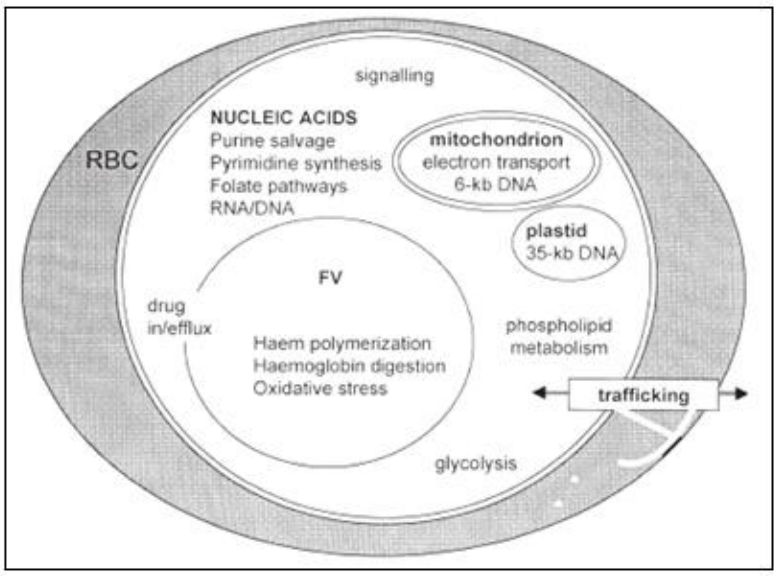

Figure 1.3: Schematic representation of drug targets for antimalarial chemotherapy.[24]

1.3.1 Biochemistry of the parasite digestive food vacuole (DFV)

The digestive, lysosomal food vacuole is an acidic (pH 5.2-5.8) single-membrane organelle that is unique to the genus *Plasmodium*.[26,27] Electron microscopy (EM) studies suggest that the formation of the DFV occurs immediately after the erythrocyte invasion through the coalescing of several cytostomic-derived vesicles, sometimes known as small vacuoles.[27,28,29] The formation of these cytostomic-derived vacuoles is mediated by the double-membrane endocytic invagination called the cytostome.[29] This cytostome is in turn made from the merozoite surface protein 1 (MSP1) of the parasitophorous vacuolar membrane.[30,31] Merozoite surface proteins protect the infective merozoites from attack by the host's immune system while they are circulating in the bloodstream. In addition, these merozoite surface proteins also play a significant role in the initial recognition and attachment to the red-blood cells.[14]

The digestive food vacuole of the malaria parasite is a site for a number of biochemical processes that are essential for growth and survival of the parasite. Two of the most important

are haemoglobin degradation and haeme polymerization, only the former will be discussed in this report.

1.3.2 Haemoglobin degradation

The malaria parasite has a limited ability to synthesize its own amino acids for proliferation.[32] During the intraerythrocytic stage of its life cycle the parasite degrades about 80% of the host haemoglobin to create space for growth, as a source of amino acids required for protein synthesis and in maintaining osmotic stability.[28,30,33] Haemoglobin degradation is believed to be a semi-ordered sequence of proteolytic events involving various DFV-residing protease enzymes such as: (i) the aspartic plasmepsin (PM) proteases [PM-I, PM-II and PM-IV and five others, and closely related histo-aspartic protease],[34a,34b,34c] (ii) cysteine falcipain (FP) proteases [FP-2, FP-2' and FP-3],[35,36a,36b] (iii) metalloprotease [falcilysin],[35] and (iv) dipeptidyl aminopeptidase 1 [DAPD1][35,37a] (Fig. 1.4).[37b]

The *P. falciparum* genome project has identified a family of ten aspartic plasmepsin protease enzymes that play an important role in the degradation of the erythrocyte haemoglobin.[16] PM-I and II initiate the degradation of the native hemoglobin by hydrolyzing the peptide-bond between Phe-33 and Leu-34 to generate acid denatured-globin fragments and haeme (Fig 1.4).[38] The globin fragments are further broken down by a second set of enzymes, PM-IV to PM-10, histo-aspartic protease and cysteine falcipain proteases (FP-2, FP-2' and FP-3) into peptides containing no more than 20 amino acids.[35,37a] The resulting peptides are hydrolyzed further into smaller peptides or oligopeptides of 6-8 amino acids by the metalloprotease (falcilysin) and dipeptidyl aminopeptidase which are thought to act downstream in the degradation pathway. These oligopeptides are then pumped out of the DFV into the cytoplasm where they are converted into amino acids by the aminopeptidase enzyme.[27,37a]

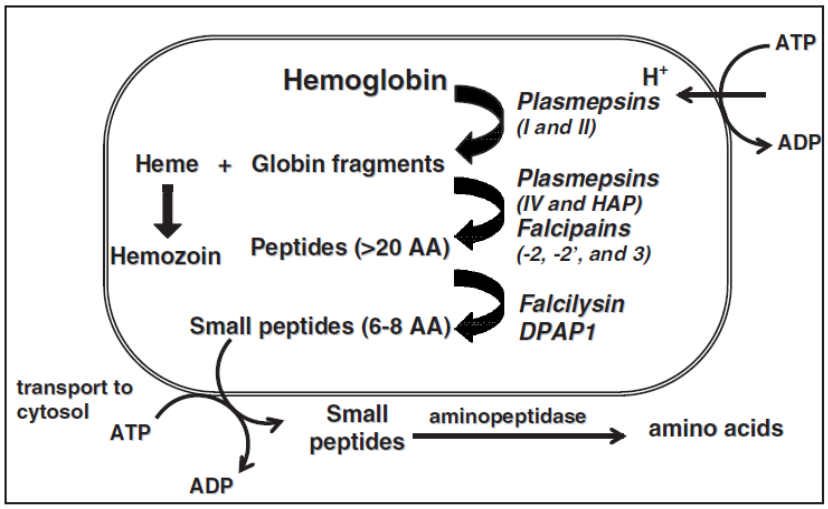

Figure 1.4: Haemoglobin degradation pathway inside the *Plasmodium* DFV.[37a]

Unlike plasmepsin I-IV, plasmepsin V (PM-V) is not localized to the DFV, but is restricted to the endoplasmic reticulum (ER) membrane.[39] Plasmepsin V is responsible for cleaving the Plasmodium Export Element (PEXEL) sequence motif, which is essential for the export of 200-300 PEXEL-containing parasite proteins into the erythrocyte cytosol.[40,41] This export of parasite proteins allow the parasite to remodel the host cell functions, such as nutrient permeation pathway, adhesion to endothelial cells and mechanical stability, and as such PM-V is essential for parasite viability.[41,42]

Interruption and/or inhibition of these proteolytic events could have detrimental effects on the parasite development and proliferation, thus these present important targets for antimalarial chemotherapy.

1.4 The battle for malaria control

Malaria is complex and difficult to control largely due to the political and socioeconomic circumstances of the malaria endemic countries, as well as the highly adaptable nature of the *Anopheles* mosquito and the malaria parasite.[43] For over half a century the battle for malaria control has been waged on two main fronts, namely, vector control and chemotherapy. Vector

control has been highly successful and is being achieved through reduction and/or eradication of the mosquito breeding sites using insecticides.[44,45] However, given the increase in mosquito resistance to most of the currently administered insecticides, there is an urgent need to develop more potent and environmentally friendly insecticides in order to curb the spread of the disease.[43]

In the recent past there have been positive developments in the malaria vaccine research. The most encouraging and significant of these developments came from the largest malaria vaccine study ever undertaken. RTS,S/AS01, the most advanced vaccine candidate, currently undergoing phase III clinical trials showed up to 50% protection against both clinical and severe malaria in children between the ages of 5 and 17 months during the 12 months after vaccination.[46a,46b] In addition, this vaccine exhibited acceptable side-effect profiles and could be administered safely with other childhood vaccines.[46b] Although the study is far from being concluded, this vaccine has the potential to play a very important role on the burden of malaria in young children residing in malaria endemic regions. However, chemoprophylaxis and chemotherapy are still the major players in combating malaria infections and will continue to be for the foreseeable future. This role is, however, compromised by the limited number of the available antimalarial drugs currently in use and the relentless emergence and spread of parasite strains that are resistant to these drugs.

1.4.1 Antimalarial chemotherapy

The majority of the antimalarial drugs currently available today have been in use for over three decades and they act on the intra-erythrocytic stage of development.[47] Many of these drugs were not rationally developed, but rather were serendipitously discovered from natural products with inherent antimalarial activity.[48] Thus, there is an urgent need to develop drugs

possessing certain characteristics such as activity against multi-drug resistant parasite strains, minimal toxicity and affordability.

1.4.2 Classification of antimalarial drugs

The majority of the antimalarial drugs in use today can be classified according to the three main categories; (i) life-cycle stage upon which they act, (ii) their mode of action and (iii) their structural features.

1.4.2.1 Classification according to the life cycle stage

Antimalarial drugs can be classified as blood schizonticides, tissue schizonticides, hypnozointicides and sporontocides or gametocytocides depending on which stage of the life cycle they target.[49,50,51] Blood schizonticides act on the asexual blood form of the parasite by inhibiting asexual growth within erythrocytes, whereas tissue schizonticides act on the primary tissue of the *P. falciparum* by killing hepatic schizonts and preventing erythrocyte invasion. The "radical cure of malaria", eradication of both the exo-erythrocytic and intra-erythrocytic stages of malaria infection, uses both the blood and tissue schizonticidal drugs in clearing the parasitaemia caused by *P. vivax* and *P. ovale*.[52] Hypnozointicides kill the persistent intrahepatic parasitic forms thus preventing a malaria relapse from the dormant parasite. Gametocytocides and sporontocides function by destroying the intra-erythrocytic sexual forms of the parasites in the infected human blood and by inhibiting the development of oocysts in the mosquito gut, ultimately preventing inter-host transmissions.[50,51]

1.4.2.2 Classification according to their mode of action

Antimalarial drugs can also be classified according to their mode of action as compounds acting on haeme-detoxification, inhibitors of nucleic acids and DNA synthesis, inhibitors of protein synthesis and as drugs generating oxidative stress.[53]

1.4.2.3 Classification according to their structural features

Structurally, antimalarial drugs can be broadly classified into two groups, namely, "nitrogen- and "non-nitrogen containing heterocyclic compounds".[54] In the following discussion antimalarial drugs are grouped according to this classification.

1.4.2.3.1 Nitrogen containing heterocyclic compounds

This subclass of compounds contains many of the common antimalarial drugs and can further be subdivided into two groups, (**A**) the aminoquinoline and arylamino alcohols, and (**B**) antifolates.

A: Aminoquinoline and arylamino alcohols

The majority of the aminoquinoline and arylamino alcohols exert their activity during the blood stages of the *P. falciparum* by interfering with the detoxification of haeme, while a few of these are also believed to target the hepatic stage.[55,56] Quinine, chloroquine, amodiaquine, piperaquine, primaquine, halofantrine, mefloquine, pyronaridine, lumefantrine and tafenoquine are some of the known aminoquinoline and arylamino alcohol drugs (Fig. 1.5).

Chloroquine and amodiaquine are the most common and widely used of all the 4-aminoquinoline drugs. These blood schizonticidal drugs are effective for the treatment and prophylaxis of malaria.[50] Chloroquine is effective against the erythrocytic forms of all the plasmodial species and together with amodiaquine they are believed to act by inhibiting haeme dimerization (through the formation of double protonated species in the DVF) and haeme-dependent parasitic protein synthesis, although their exact mechanism of action is still debated.[54] The attractive features of chloroquine are its mild side-effects and affordability, while its use is hampered by the spread of drug-resistant strains of the parasite. Amodiaquine, piperaquine and pyronaridine on the other hand are effective against chloroquine-resistant

strains of the parasite.[57] However, their use is restricted because of side effects such as hepatotoxicity and agranulocytosis due to amodiaquine, while pyronaridine metabolite causes toxicity to neutrophils.[54,58] Other safety concerns with the 4-aminoquinolines include cardiovascular and central nervous system (CNS) effects.[8,57]

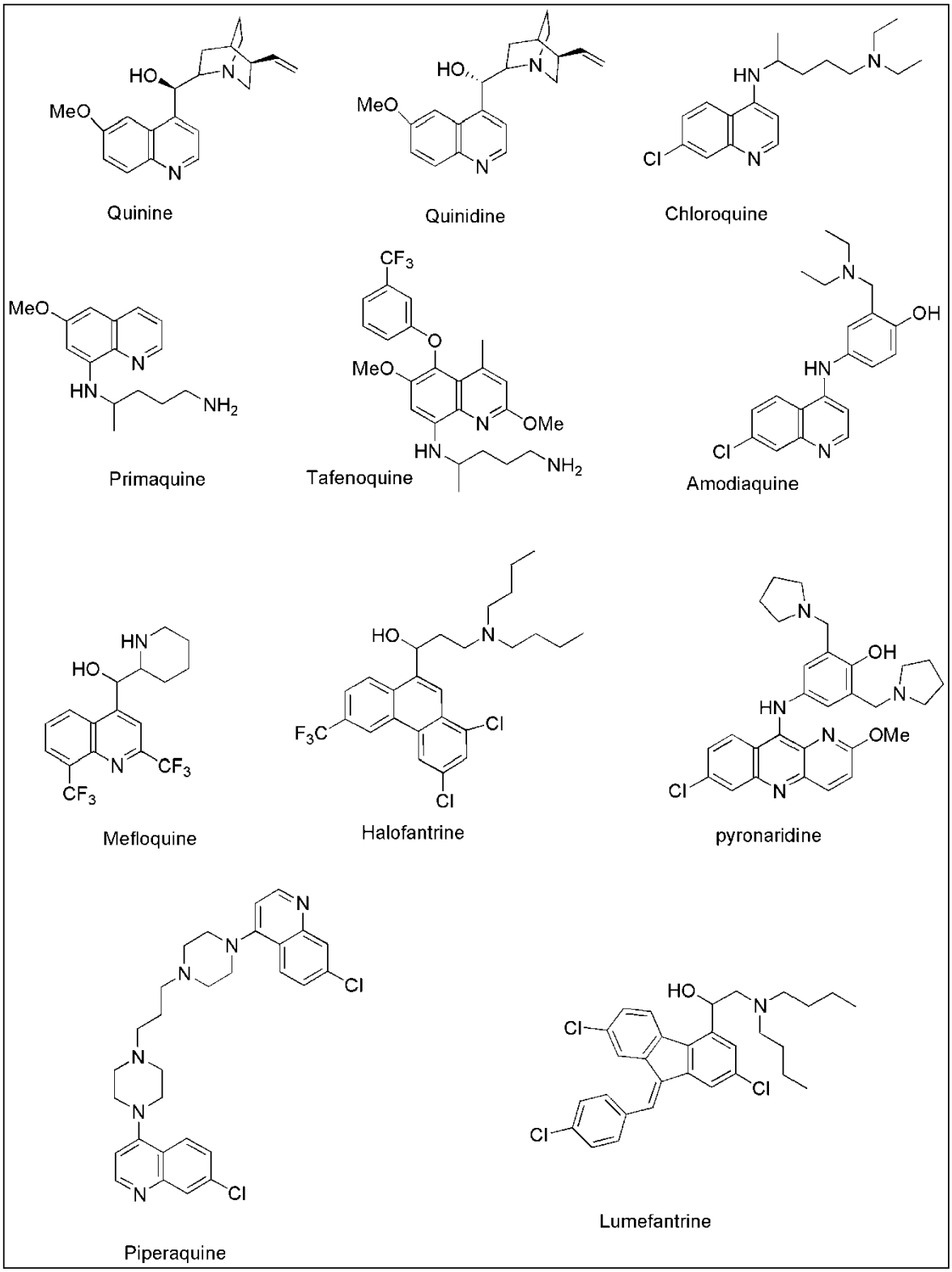

Figure 1.5: Chemical structures of aminoquinoline and arylamino alcohol compounds.
The 8-aminoquinoline family of compounds consists of primaquine and tafenoquine, the former being the most widely used. Primaquine is the only tissue schizonticidal drug currently available for the treatment of *P. vivax* and it acts by inhibiting the maturation of the fertile gametocytes.[8,59] Primaquine is also used as a chemoprophylactic but its use is compromised by its association with hemolytic anaemia in people with glucose-6-phosphate dehydrogenase (G6PD) deficiency.[54,57] Consequently, a less toxic and more active primaquine analogue, tafenoquine, was synthesized. Tafenoquine is currently undergoing phase (III) clinical trials and has demonstrated activity against all parasitic forms of malaria.[54,60] It is hoped that tafenoquine will someday replace primaquine as the antimalarial drug of choice against relapsing malaria.

Another major class of antimalarial drugs is the arylamino alcohol family which can be sub-divided into quinoline containing, *i.e.* quinoline-methanols (quinine and mefloquine) and non-quinoline-containing (halofantrine and lumefantrine) arylamino alcohols. Quinine and its diastereomer, quinidine, originally extracted from the bark of the Peruvian Cinchona tree, were the first antimalarial drugs to be used for treating malaria about 400 years ago.[60,61] The schizonticidal quinine drug is still widely used today for the treatment of uncomplicated and severe malaria because of the availability of its intravenous preparation.[50,54] Quinine is associated with multiple side-effects such as hypoglycemia and α-adrenergic blocking effect, while quinidine which is 2-3-fold more active than quinine has been implicated to induce cardiac arrhythmia.[50,57,62]

The emergence of the multi-drug resistant strains of the malaria parasite to quinine necessitated the development of mefloquine, its synthetic analogue, by the Walter Reed Army Institute of Research in 1971.[8] Mefloquine and halofantrine are both active against chloroquine-resistant strains of *P. falciparum* and the former is widely used as a

chemoprophylactic.[50] However, the use of mefloquine is linked to adverse events such as sleep and seizure disorders, insomnia and gastro-intestinal disorders.[8,50,57] Currently, mefloquine is used as part of combination therapy with artesunate due to the rapid spread of mefloquine-resistance.

B: Antifolate-based drugs

This class of drugs act by inhibiting the enzymes involved in the folate metabolic pathway of the parasite.[26,56] In addition, the antifolate drugs are thought to inhibit the early phases of the parasite liver stage as well as the development of the infective stages in the mosquito.[60] The antifolate drugs include pyrimethamine, proguanil, chlorproguanil, sulphadoxine and dapsone (Fig. 1.6). These drugs are usually administered as part of a combination therapy due to the rapid emergence and spread of parasite resistance to these drugs.[50,60] Development of resistance to antifolates is believed to be the consequence of mutation in the target enzymes.[49]

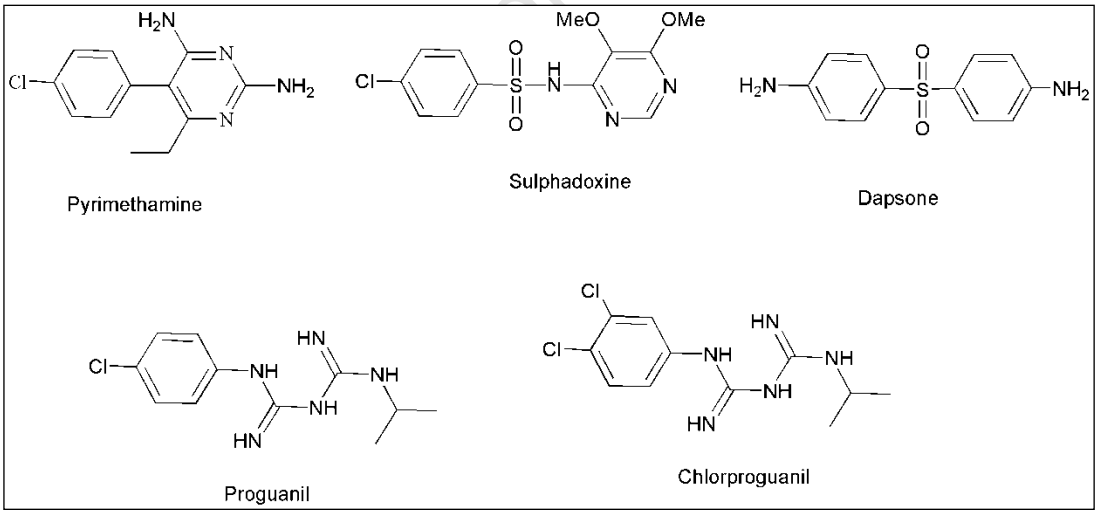

Figure 1.6: Chemical structures of antifolate drugs.

Pyrimethamine and sulfadoxine (SP) combination therapy has played a pivotal role in the fight against malaria mainly because of its affordability and effectiveness against the drug-susceptible strains of *P. falciparum*. However, the use of this combination therapy has been limited by the development of the parasite resistance.[8,63] Antifolates possess minimal side-

effects except on excessive use of pyrimethamine which causes megaloblastic anemia and hepatitis.[57]

1.4.2.3.2. Non-nitrogen containing heterocyclic compounds

This subclass of antimalarial drugs can also be subdivided into two groups, (**A**) sesquiterpene endoperoxide lactones (artemisinins) and (**B**) naphthoquinones and antibiotics.

A: Sesquiterpene endoperoxide lactones

This class of compounds is unique and structurally different from all the other known antimalarial drugs, an attractive feature for circumventing resistance and cross-resistance. Artemisinin, also known as *Qinghaosu*, is a sesquiterpene endoperoxide lactone that originates from the Chinese herb *Artemisia Annua*, whose use in China as an antipyretic remedy dates as far back as 2000 years ago.[8,54,64] Artemisinin was first isolated in 1971, used as an antimalarial a year later in China, and its active principle was identified to be the 1,2,4-trioxane moiety or the endoperoxide bridge.[50] The low bioavailability of artemisinin has necessitated the development of a number of its synthetic analogues such as the water soluble artesunate and lipid soluble dihydroatermisinin, artemether and arteether (Fig. 1.7). All these are active against all stages of the *P. falciparum* life cycle and multi-drug resistant strains.[47,51] The one disadvantage of these derivatives is their short half-lives which are associated with the high levels of recrudescence following artemisinin-based monotherapy. As such these drugs are used as part of the artemisinin-based combination therapy (ACT) with other drugs that have longer half-lives and possibly different modes of action to artemisinins in an attempt to reduce recrudescence and resistance development.[55] Although resistance to this class of compounds is yet to be observed, there are indications that reveal reduced sensitivity of the parasite to artemether and the increasing evidence of resistance to artemisinin-based

combination therapy in the Thai-Cambodian-border and some parts of southern Cambodia.[65,66]

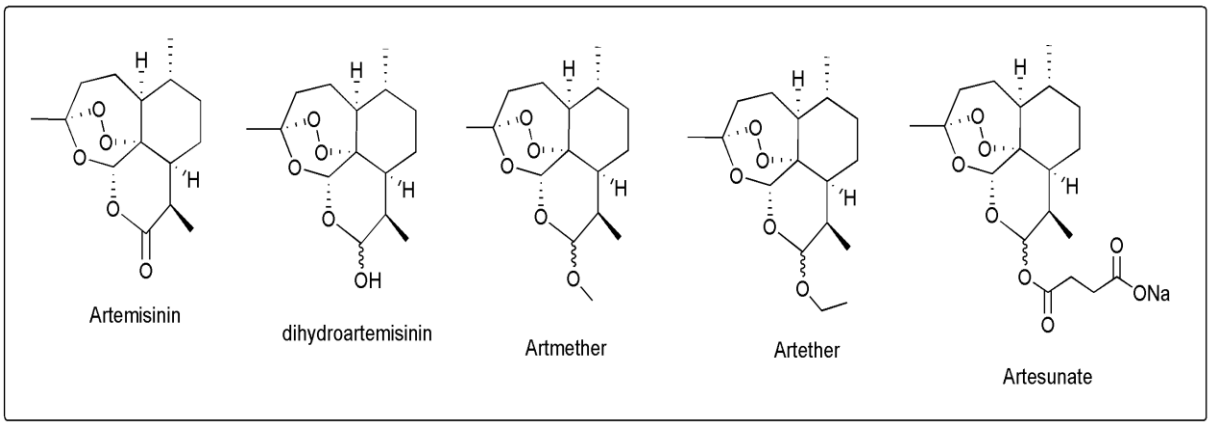

Figure 1.7: Artemisinin-based drugs.

Despite their importance in the fight against malaria, the exact mode of action of artemisinin-based compounds is still not well understood. However, a number of putative modes of action have been reported and in some cases contradicted. The majority of these, however, concur that the formation of the *C*-centred radicals from hemolytic cleavage of the intact endoperoxide bridge in the presence of Fe^{2+} plays an important role.[8,67a,67b,68] These radicals are believed to be involved in the formation of haeme-artemisinin adducts that inhibit haemozoin formation.[69] In addition, these radicals are also postulated to be involved in protein alkylation, parasite membrane damage, interference with the mitochondria, inhibition of food vacuole cysteinyl proteases and *Pf*ATP6, a homologue of the mammalian sarco/endoplasmic reticulum Ca^{2+}-dependent ATPase (SERCA), resulting in the death of the parasite.[8,50,64,68] Neurotoxicity seem to be the major side-effect of these drugs although this is disputed by some studies.[50]

B: Naphthoquinones and antibiotics

Naphthoquinones (atovaquone and hydrolapachol) is another promising class of antimalarial drugs (Fig. 1.8). In 1946 Wendel observed the antimalarial activity possessed by these

compounds when they inhibited the growth of *P. vivae*.[9b] Atovaquone, initially marketed for *Pneumocsytis* pneumonia,[63] is active against the multi-drug resistant strains of the malaria parasite. It is known to inhibit the parasite mitochondrial respiratory system through the mitochondrial electron transport chain.[8] As a result this interferes with the mitochondrial membrane potential.[8,50] Due to the rapid emergence of resistance to this class of compounds, atovaquone is used in combination with other drugs such as proguanil to target the liver stage of the parasite.[8,9b] Rash, fever, vomiting and abdominal pains are some of the side-effects associated with the use of atovaquone.[57]

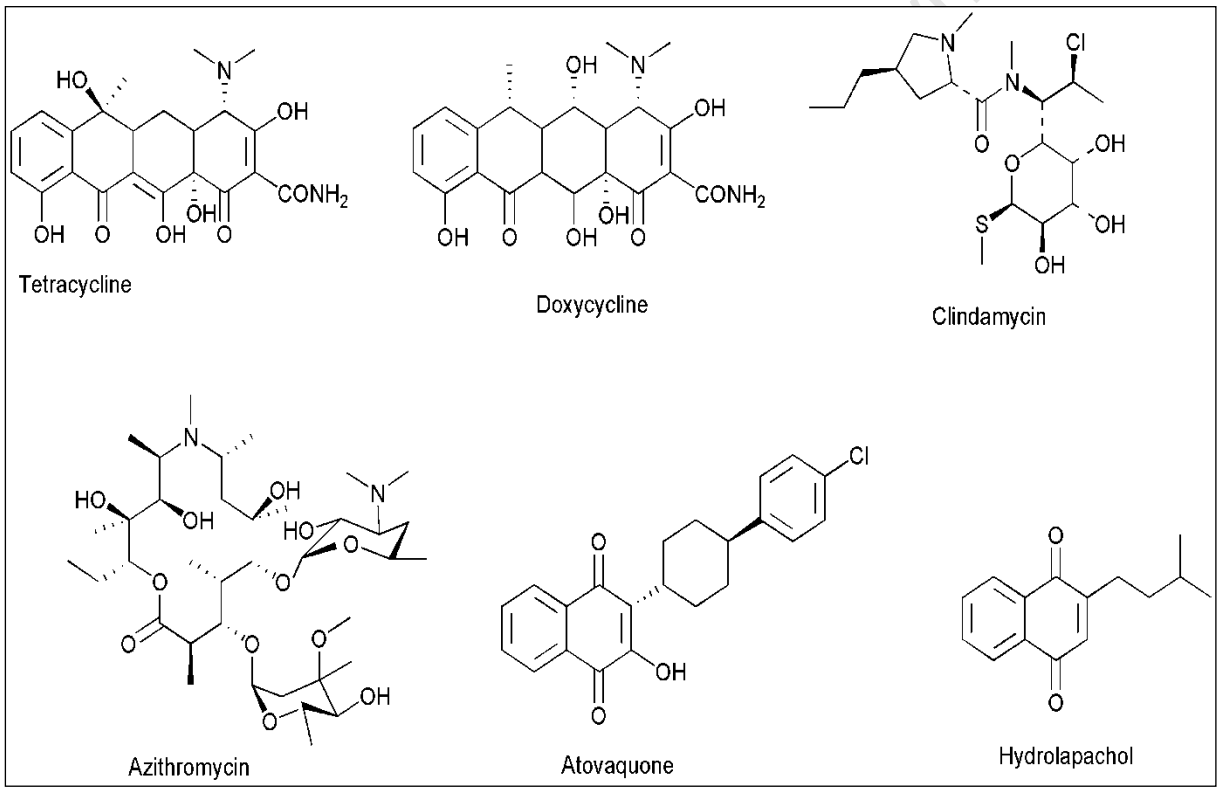

Figure 1.8: Naphthoquinones and antibiotics.

Several antibacterial agents are known to possess considerable activity against the eukaryotic *P. falciparum* parasite and as such they represent another interesting class of antimalarial drugs. Antibiotics with antimalarial activity such as tetracycline, doxycycline, clindamycin and azithromycin have been used to treat multi-drug resistant strains of the malaria parasite for over thirty years (Fig. 1.8).[70] These antibiotics are characterized by the lack of an

immediate killing effect during the first intracellular asexual replication cycle of the parasite, but exert their activity on the second cycle, a phenomenon known as the "delayed-death phenotype".[50,71]

Tetracycline, a secondary metabolite from *Stremptomyces actinobacteria*, is believed to act against the mitochondrion by inhibiting protein synthesis while its derivative, doxycycline, acts by blocking the expression of apicoplast genes.[8,50] Because of their slow acting effect, these antibiotics can be used prophylactically as a single agent or in combination with the fast acting antimalarial drugs.[50,72] Azithromycin and clindamycin are known to have excellent safety profiles in pregnant women and they target the 50S ribosomal subunits of the apicoplast and further inhibit the polypeptide development, and subsequently protein synthesis.[8,72] However, the use of tetracycline and doxycycline is impaired by side-effects such as gastrointestinal disturbances, esophageal ulceration and the possibility of oral contraception failure.[50,57]

1.5 Antimalarial drug resistance

Drug resistance, including multi-drug resistance, has been highlighted as one of the major contributing factors to malaria resurgence and malaria-induced morbidity and mortality.[49] Antimalarial drug resistance is defined as the "ability of the parasite strain to survive and/or multiply despite the administration or adsorption of a drug given in doses equal to or higher than the usually recommended; but within tolerance of the subject".[54] The drug in question must "gain access to the parasite or the infected red blood-cell for the duration of the time that is necessary for its action".[73] Malaria parasite resistance arises as a result of overuse of antimalarial drugs for prophylaxis, inadequate or incomplete therapeutic treatments of active infections, high level of parasite adaptability at the genetic or metabolic levels, and the extensive proliferation rate that permits the selected population to emerge relatively quickly

among other factors.[74] Resistance to all currently available antimalarial drugs emerged during the last three decades, the exception being the artemisinin derivatives although there have been reports of reduced *in vitro* susceptibility to artemether.[65] The exact molecular mechanism of resistance has been a matter of debate, thus the following discussion will be limited to the universally accepted mechanisms of resistance to the aminoquinoline and arylamino alcohols only

1.5.1 Mechanism of resistance of aminoquinolines and arylamino alcohols

Development of resistance of the malaria parasite to quinoline-based antimalarial drugs was first observed in 1910 to quinine then in 1957 to chloroquine in Thailand, by 1988 it had spread to the major parts of the sub-Saharan Africa.[74] As early as the 1960s, it was observed that chloroquine resistant parasites exhibit lower levels of drug inside the digestive food vacuole (DFV) when compared to their sensitive counterparts.[55] This is an indication that the parasite is capable of either accumulating less drug or increasing its efflux. This ability of the parasite to accumulate low drug concentrations inside the DFV is facilitated by three major genes; *P. falciparum* chloroquine resistant transporter (*pfcrt*), *P. falciparum* multi-drug resistant-1 (*pfmdr1*) and *P. falciparum* Na^+/H^+ exchanger (*pfnhe*) genes which are located in the membrane of the DFV. [68,75,76]

Parasites with the point mutation at position 76 of the *pfcrt* gene have been shown to expel chloroquine at a much higher rate than those without.[68] The PfCRT protein is a ten transmembrane-domain transporter that belongs to the superfamily of transporters called drug and metabolite transporters (DMT), located in the membrane of the DFV of the parasite.[77] Recent studies pointed out that mutations in the *pfcrt* gene alone are insufficient for chloroquine resistance and as such mutations in the *pfdmr1* and *pfnhe* genes were also implicated, suggesting a multi-genic process.[55,78] The *pfdmr1* gene encodes for another

membrane transporter protein known as the *P. falciparum* multi-drug resistance-1 transporter (PfMDR1) which is linked to the overexpression and/or presence of the P-glycoprotein homologue 1 that resemble the mammalian *Pgp*.[51,75] Mammalian *Pgp* are suspected of "pumping out" a number of drugs in chemo-resistant mammalian cell-lines resulting in drug resistance.[55] Amplification of the *pfdmr1* gene is implicated as one of the major modulators of resistance for the arylamino alcohols and for the reduced sensitivity of artemisinins.[50,75] Lastly, the gene *pfnhe*, also known to play a crucial role in the resistance of quinoline compounds, encodes for another family of proteins, Na^+/H^+ exchanger (NHE), the second largest eukaryotic identified so far.[76,79]

1.5.2 Strategies used to avert and manage drug resistance

The 17th meeting of the Roll back Malaria (RBM) consortium devised the following strategies in counteracting the emergence and spread of antimalarial drug resistance; (i) use of combination therapy, (ii) use of parasite-resistance reversers, (iii) drug-repositioning, and (iv) rationally designing analogues of the currently administered drugs in such a way that cross-resistance is circumvented.[63,80] The rationale behind the use of combination therapy is well documented in the treatment of other diseases such as HIV and Tuberculosis.[54] This concept is based on the synergistic or additive potentials of two or more drugs with different modes of action, different mechanisms of resistance and acting on different targets of a particular disease.[54,68] In 2001 the WHO issued guidelines for the treatment of malaria, and among these was the recommendation of using artemisinin-based combination therapy (ACT) to treat uncomplicated *P. falciparum* malaria.[48,81] ACT increases the rate of clinical and parasitological cure, and also reduces the probability of drug resistance development.[68] However, the emergence of resistance to some ACT combinations is posing a big threat to this by far the most effective way of dealing with the malaria burden.[81]

Another interesting approach that has recently garnered support is the use of previously effective antimalarial drugs in combination with compounds that are known to reverse parasite resistance to those drugs.[75] This strategy uses compounds with weak antimalarial activity such as calcium channel blockers, antidepressants drugs (e.g. desipramine), antihypertensive drugs (e.g. verapamil) and antihistaminic drugs (e.g. cyproheptadine) among others.[68,77]

1.6 Tuberculosis

Tuberculosis (TB) is a curable and preventable ancient disease that has plagued humankind throughout history. The earliest recorded evidence of this disease comes from the 9000 year-old skeletal fossils found in the Neolithic settlements of the Eastern Mediterranean.[82] TB is associated with skeletal abnormalities (Pott's disease) and has long been found in Egyptian mummies dating back as far as 5000 years.[83] In addition, early texts found in India and China depicting a disease with TB characteristics suggests the disease occurred around these parts of the world between 2300 and 3300 years ago.[83]

1.6.1 A Global Epidemic

One third of the world population harbour the latent form of TB and this poses a risk of disease reactivation in immunocompromised individuals such as those co-infected with the human immunodeficiency virus (HIV).[84] TB is the second major cause of death due to an infectious disease in adults worldwide, most severely felt in poverty stricken areas such as Asia and Africa.[85] This airborne disease is spread through sneezing and coughing, and it predominantly affects the lungs (pulmonary TB) but it can also affect other parts of the body (extrapulmonary TB). The 2011 WHO report estimates 9.2 million new cases of TB and 1.8 million deaths among HIV-negative people and an additional 0.35 million from HIV-assisted TB deaths annually (Fig. 1.9).[86] The epicenter of the HIV-TB co-infection lies in Sub-

Saharan Africa, accounting for 79% of the worldwide disease burden and more noticeably 25% of these are found in South Africa alone.[87] In 1993, the WHO declared TB a global emergence and in an attempt to stem the tide on drug-susceptible TB, the directly observed therapy, short-course (DOTS) was launched in 1994. In this therapy patients are observed taking the drugs until completion of the course.[88] However, despite the adoption of DOTS strategy, treatment success in some areas remains low due to poor management of TB control programs and patient non-compliance.[88]

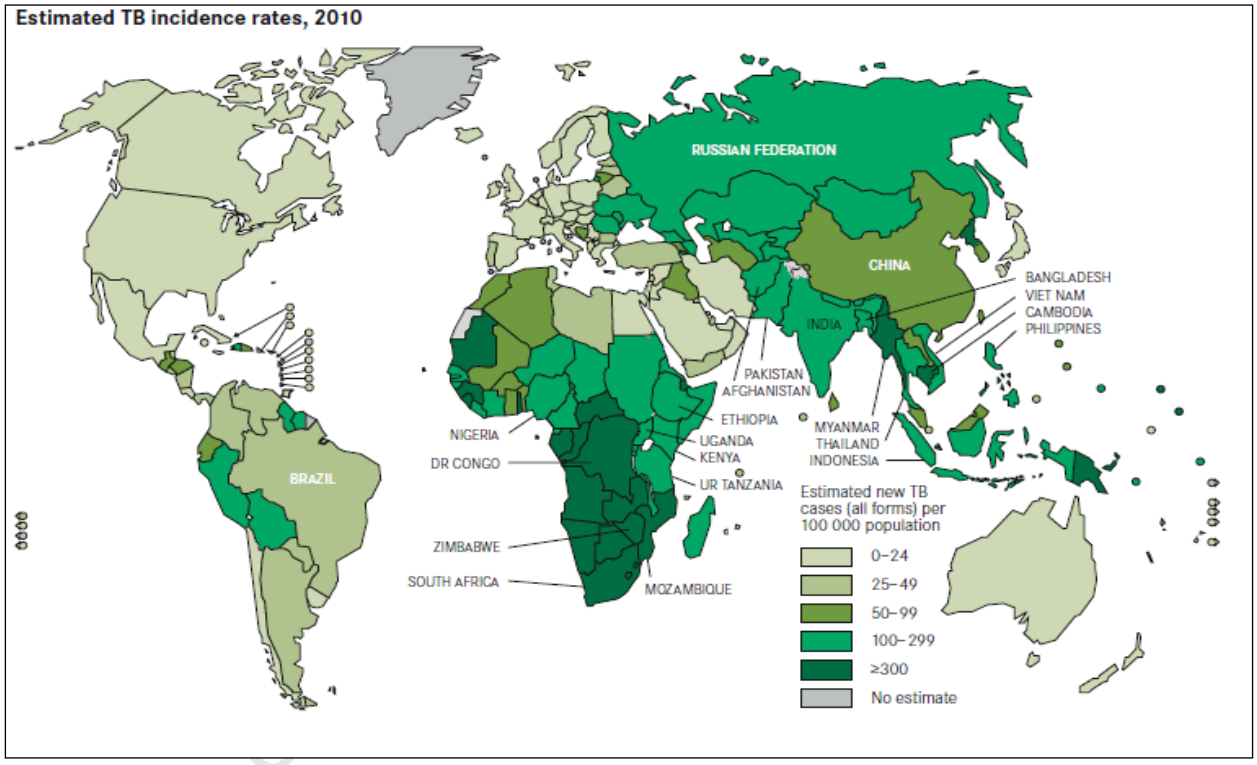

Figure 1.9: Global distribution and estimated new TB cases, 2010.[86]

The burden of TB is not only compounded by its synergy with HIV/AIDS but also by the widespread emergence of multi-drug resistant (MDR), extensive-drug resistant (XDR) and totally drug-resistant (TDR) strains of the disease.[85] MDR-TB is defined as the TB infection caused by the strain of the disease that is resistant to at least two (*i.e.* isoniazid and rifampicin) powerful first-line anti-TB drugs while XDR-TB denotes MDR-TB with additional resistance to fluoroquinolones and to one or more of the second-line injectable

drugs (kanamycin, amikacin, etc).[89] In 2010 there were 650 000 estimated cases of MDR-TB and its current treatment (DOTS-plus strategy) can take anything from 1.5 to 2.5 years while XDR-TB is extremely difficult to treat and TDR-TB is virtually untreatable.[85,90]

1.6.1.1 *Mycobacterium tuberculosis*

Tuberculosis (TB) is caused by a group of closely related bacterial species belonging to the genus *Mycobacterium* and to the family of *Mycobacteriaceae*.[91] There are currently 85 species known to belong to this genus; *Mycobacterium tuberculosis* is responsible for the majority of all TB cases but other species such as *Mycobacterium bovis*, *Mycobacterium africanum*, *Mycobacterium microtti* and *Mycobacterium canetti* are also known to cause TB but this is not common.[92,93,94] Discovered in 1882 by Robert Koch, *Mycobacterium tuberculosis* is a slow-growing rod-shaped intracellular organism enclosed by a mycobacterial cell envelope.[95] This envelope is composed of a cell wall, a capsule-like layer and the cytoplasmic membrane which accommodates enzymes required for metabolic processes including energy generation.[91] The cytoplasmic membrane is surrounded by a cell wall that protects cell contents, provides mechanical support and is responsible for the characteristic shape of the bacterium.[96] The cell wall consists of a capsule, a core and an inner membrane (Figure 1.10).[97] The capsule is made up of free lipids and mycolates (phosphatidylinosistol, PIMs, and lipoarabinomannan, LAM), while the core is composed of *N*-glycolylated peptidoglycan linked to a heteropolyschariде, the D-arabino-D-galactan, which in turn is esterified by long chain (C60 to C90) α-branched, β-hydroxylated fatty acids called mycolic acid.[98]

In addition, the core also contains porin proteins which are responsible for passive diffusion of aqueous solute through the mycolic acid layer .[91,96] The majority of TB drugs target the functional development of the mycobacterial cell wall envelope.

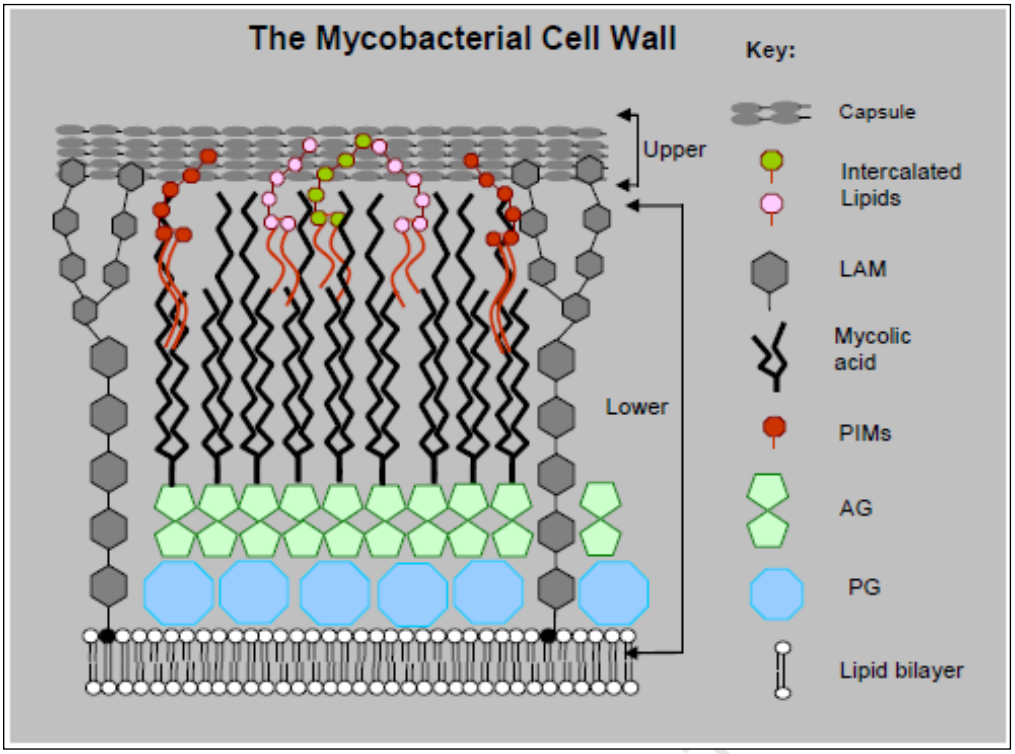

Figure 1.10: *Mycobacterial tuberculosis* cell wall.[97]

1.6.2 Current status of chemotherapy and biological targets

TB is one of the most challenging infectious diseases to treat mainly due to the long treatment term prone to patients' non-compliance and subsequently, the emergence of MDR-TB and XDR-TB.[92] The DOTS strategy used to treat drug-susceptible *Mycobacterium tuberculosis* is initiated by taking a multidrug therapy consisting of the four first line drug combinations (isoniazid, pyrazinamide, ethambutol and rifampicin or streptomycin) over a period of 2 months (Fig. 1.11). These drugs target and act on the replicating and the semi-dormant infective bacilli and in the process reduce the bacterial population by about 95%, thereby decreasing the potential for TB transmision.[99] This phase is followed by a further 4 months of treatment with rifampicin and isoniazid alone and this is aimed at killing the non-replicating bacilli.[94]

Isoniazid, the most powerful mycobactericidal drug, exerts its activity by inhibiting mycolic acid synthesis while rifampicin inhibits transcription by interacting with the β-subunit of the

bacterial RNA polymerase enzyme.[85,100] Pyrazinamide functions by lowering the pH of the intracellular environment thus inactivating the fatty acid synthase enzyme, while ethambutol inhibits arabinosyl transferase involved in the cell wall synthesis.[100] Streptomycin on the other hand inhibits protein synthesis, thus leading to the death of the bacterium.[101]

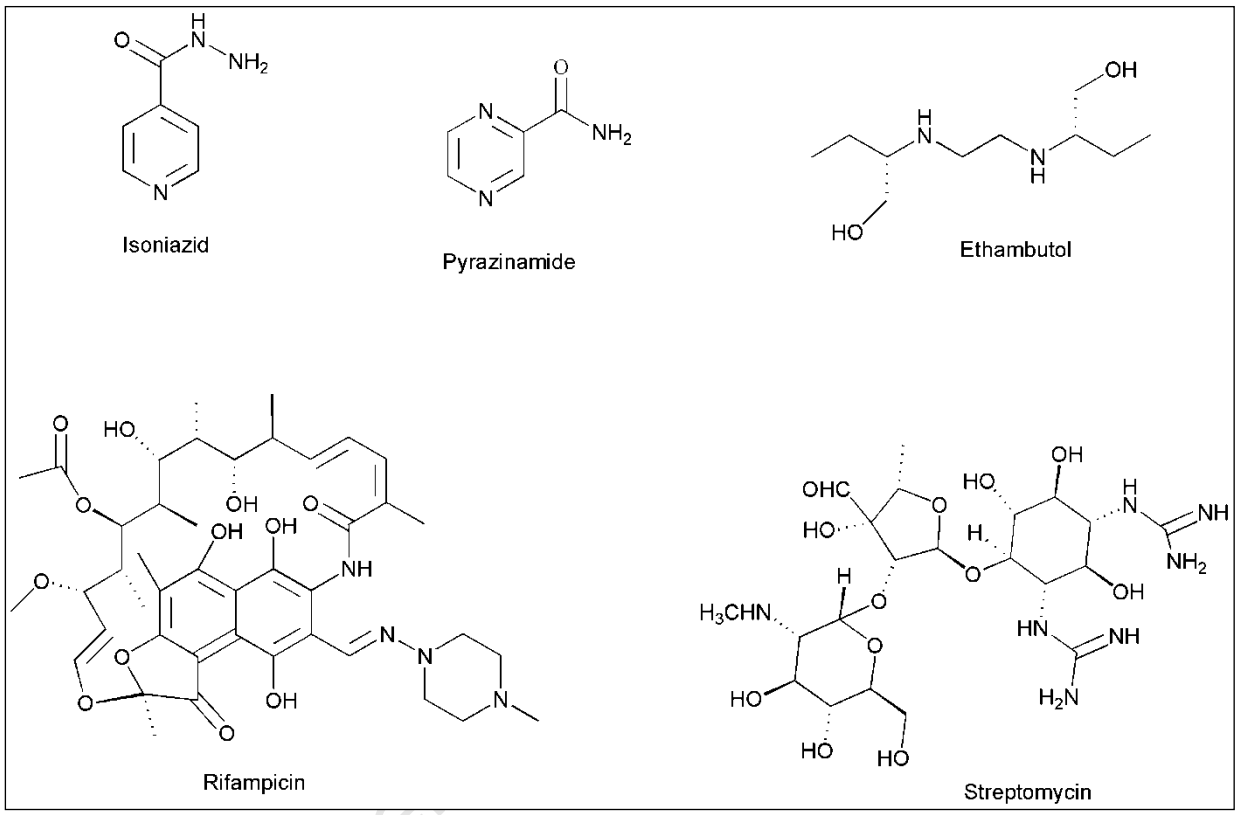

Figure 1.11. Chemical structures of the first-line anti-TB drugs.

The first-line anti-TB drug therapy is inadequate against MDR-TB and as such effective second-line drugs were introduced (Figure 1.12).[94] Although these second-line drugs are used to treat MDR-TB for a period of up to 2 years, they are less effective, toxic and more expensive compared to the first–line drugs.[92] Cycloserine inhibits cell wall biosynthesis, ethionamide inhibits lipid biosynthesis and cell wall assembly, and fluoroquinolones (moxifloxacin, gatifloxacin and levofloxacin) act by inhibiting DNA topoisomerase and DNA gyrase enzymes which are responsible for DNA replication.[92,94] *p*-Aminosalicylic acid is believed to act by targeting folate biosynthesis although this is still disputed.[11]

Campreomycin inhibits protein synthesis while aminoglycosides (kanamycin and amikacin) inhibit protein synthesis by binding to the 16S rRNA of the bacterial 30S ribosomal subunit, resulting in mycobacterial cell death.[85,102] Although difficult to treat, XDR-TB can be successfully managed using the third-line anti-TB drugs, the cure rate currently ranges from 30 to 75%.[85] Third-line drugs are currently poorly understood since few *in vivo* human studies were done on them, they are toxic and are currently not recognized or accepted by the WHO.[102]

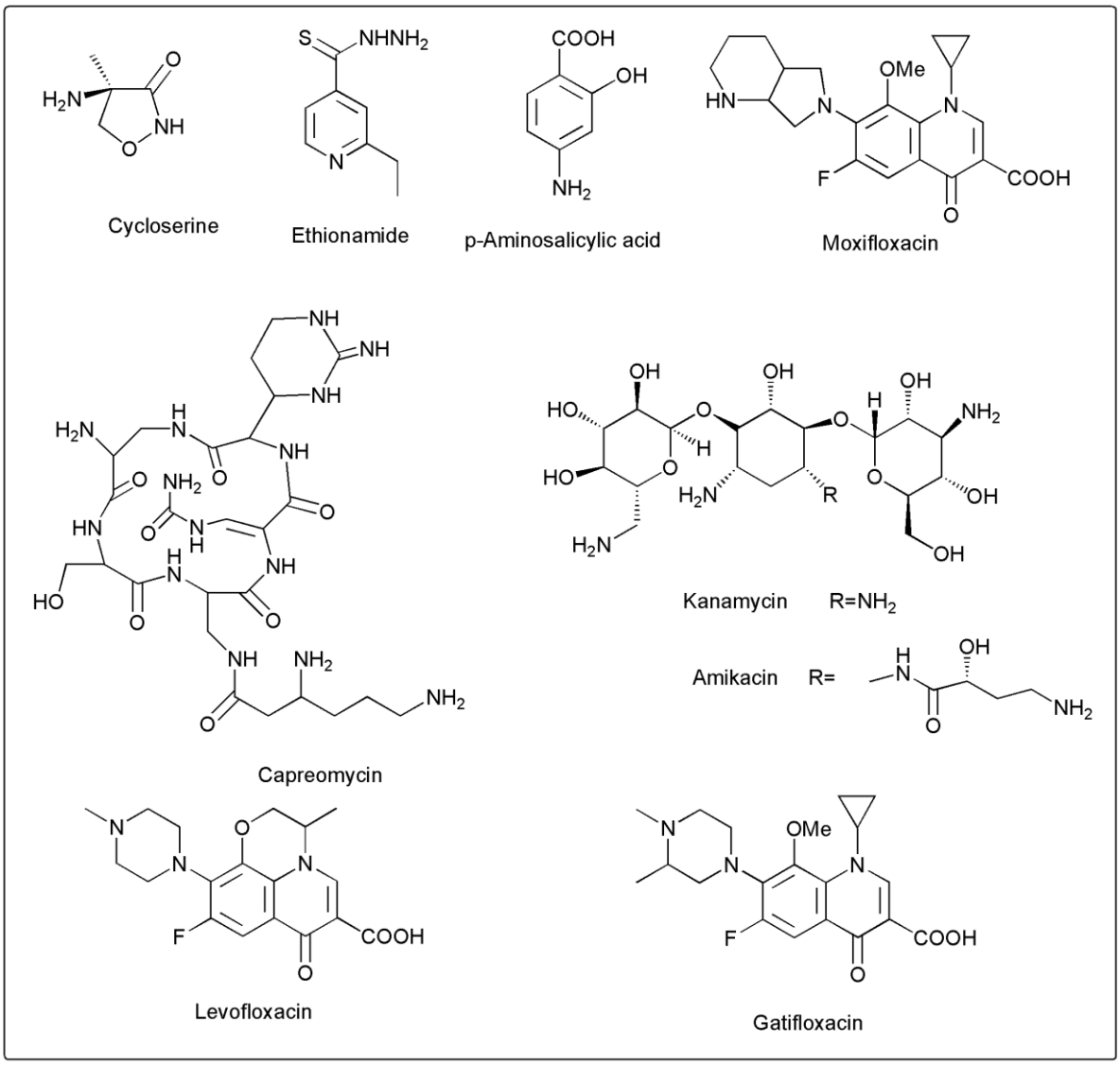

Figure 1.12. Chemical structures of the second-line anti-TB drugs.

TB chemotherapy has its shortcomings and the four widely accepted primary objectives for improving TB therapy are; (i) shortening and simplifying the treatment of drug-sensitive TB,

(ii) improving treatment efficacy, safety and duration for drug-resistant TB, (iii) avoiding drug-drug interactions and improving the safety of co-therapy for TB patients co-infected with HIV and (iv) establishing an effective therapy for latent, persistent TB.[82]

There are currently a number of different classes of compounds undergoing clinical development with the aim of addressing the four primary objectives mentioned above. These include nitroimidazooxazines (lead compound; PA-824),[103] diaryquinolines (lead compound; TMC207),[104] oxazolidinones (lead compounds; eperezolid and linezolid),[105] and ethylenediamines (lead compound; SQ109) (Fig. 1.13).[97] Nitroimidazooxazines inhibit cell wall lipids and protein synthesis and diarylquinolines are active against drug-resistant strains and they inhibit membrane bound ATP synthase.[85,93] Oxazolidinones inhibit protein synthesis by binding to bacterial 20S rRNA of the 50S ribosomal subunits, and ethylenediamines target cell wall synthesis.[99]

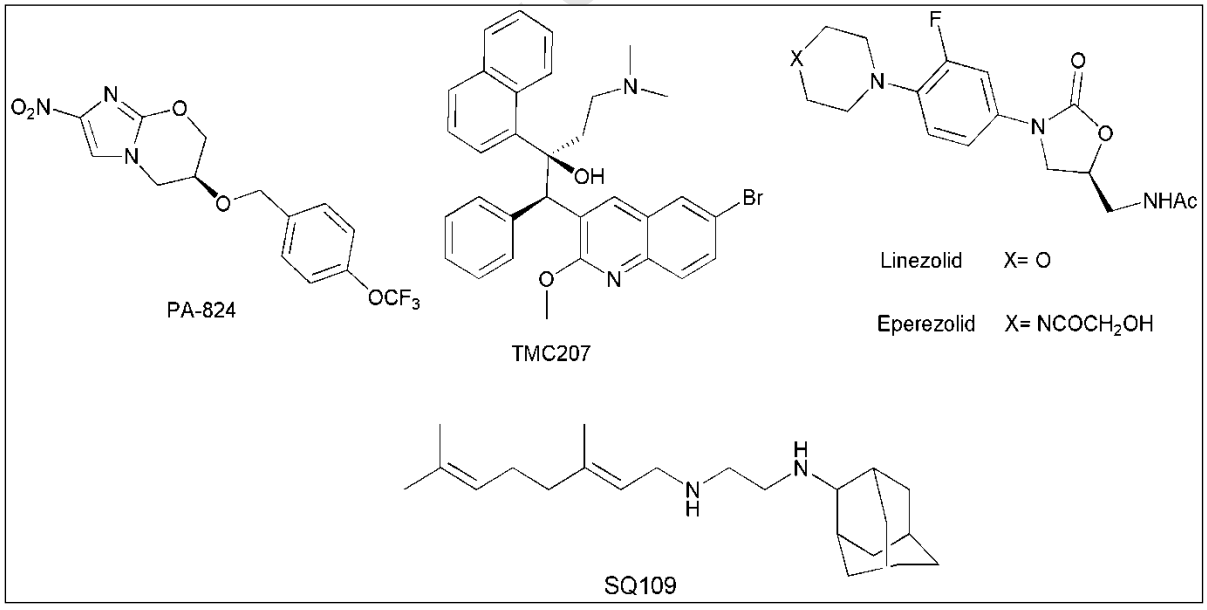

Figure 1.13. Chemical structures of lead compounds of drugs in clinical development for TB.

1.6.3 Mechanism of drug resistance

The emergence of anti-TB drug resistance is a serious problem for TB control programs and is attributed to two factors; (i) erroneous prescribing practices by clinicians, and (ii) inappropriate and irregular intake of medication by patients.[105] In 2008, a global project for anti-TB drug resistance surveillance reported prevalence of drug resistance of more than 10% in 30 countries and also identified 14 countries with prevalence for MDR-TB strains.[106,107] The majority of resistance towards isoniazid and rifampicin is thought to occur primarily through point mutations in the *katG* or *inhA* genes and in the 81bp region of the RNA polymerase β-subunit (*rpoB*) gene.[85,102] Toxic side-effects associated with the use of isoniazid and rifampicin include mild influenza, hepatotoxicity and hepatic enzyme abnormalities which lead to hepatitis.[108] Resistance to streptomycin is a result of mutation in the 16S rRNA genes, *rrs* and *rpsL*, that encode ribosomal protein S12 and the associated side-effects are otovestibular toxicity and nephrotoxicity in children.[85,109]

Resistance to flouroquinolones is due to specific mutation in the *gyrA* and *gyrB* genes that encode for DNA gyrase A and subunits, while resistance in ethionamide is acquired through mutation in the *emB* gene that encodes for the arabinosyl transferase that ethionamide inhibits.[85,109]

The injectable aminoglycosides' (kanamycin and amikacin) resistance is similar to that of streptomycin and is due to mutation in the *rrs* gene encoding for 16S rRNA.[88] Common side-effects due to these drugs include nephrotoxicity and ototoxicity.[85]

1.7 Rationale for research undertaken

Development of multi-drug resistant (MDR) and extensive-drug resistant (XDR) strains of *Plasmodium falciparum* and *Mycobacterium tuberculosis* has reduced the efficacy of the currently administered drugs. Thus, there is an urgent need for new chemical entities (NCE) with novel modes of action that will provide maximal anti-infective activity against these infectious diseases. Our interest in discovering new anti-infective agents is focused primarily on the quinoline-based compounds that can exert their activity against *P. falciparum* and *Mycobacterium tuberculosis*. This approach is supported by the fact that the quinoline nucleus is known to exhibit a wide spectrum of biological activity such as antiviral,[110] anticancer,[111] antibacterial,[112] antifungal[113] and anti-inflammatory.[114]

The fact that quinoline-based antimalarial drugs such as quinine, chloroquine, mefloquine, primaquine and amodiaquine, have been shown to possess moderate activity against *Mycobacterium tuberculosis* further supports the choice of using the quinoline nucleus.[115,116,117] Another important reason for searching for new chemical entities (NCE) based on the quinoline nucleus is the diarylquinoline TMC207 which is in phase IIB clinical trials for TB.[118] This compound is active against drug-sensitive and drug-resistant *Mycobacterium tuberculosis*, and has bactericidal effect against the dormant bacilli.[119] Furthermore, this compound possesses a new mechanism of action by inhibiting ATP synthase subunit C, an energy source for the bacterium.[120] The enzyme, ATP synthase, is an attractive target since there is limited similarity between the mycobacterial and human AtpE protein sequence.[121,122] As such TMC207 is a viable alternative for the treatment of multi-drug resistant *Mycobacterium tuberculosis* strain.

1.8 References

1. Frey, C.; Troare, C.; De Allegri, M.; Kouyate, B.; Mueller, O., *Malarial. J.*, **2006**, *5*, 70.

2. Cox, F. E. G., *Parasite & Vectors.*, **2010**, *3*, 5.

3. Carter, R.; Mendis, K. N., *Clin. Microbiol. Rev.*, **2002**, *15*, 564.

4. Opiz, J. M.; Schultka, R.; Göbbel, L., *Am. J. Med. Genetics.*, **2006**, *140A*, 115.

5. World Health Organization, *World Malaria Report*, Geneva, **2010**.

6. Snow, R. W.; Marsh, K., *Lancet.*, **2010**, *376*, 137.

7. (a). World Health Organization's (WHO) Malaria's Global distribution estimates, **2010**; gamapserver.who.int/mapLibrary/Files/Maps/Global_Malaria_2010.png (accessed on the 12.10.2011).

(b) www.kff.org/globalhealth/upload/7882-03.pdf (accessed on the 12.10.2011)

8. Burrows, J. N., Chibale, K.; Wells, T. N. C., *Curr. Topics Med. Chem.*, **2011**, *11*, 1226.

9. (a). Joshi, A. A.; Viswanathan, C. L., *Anti-infect. Agents. Med. Chem.*, **2006**, *5*, 105.

(b) Fotie, J., *Anti-infect. Agents. Med. Chem.*, **2006**, *5*, 357.

10. (a) Uneke, C. J.; Ogbonna, O., *Trans. R. Soc. Trop. Med. Hyg.*, **2009**, *103*, 761.

(b) Skinner-Adams, T. S.; McCarthy, J. S.; Gardiner, D. L.; Andrews, K. T., *Trends Parasitol.*, **2008**, *24*, 264.

11. Bousema, T.; Drakeley, C., *Clin. Microbiol. Rev.*, **2011**, *24*, 377.

12. Sinka, M. E.; Rubio-Palis, Y.; Manguin, S.; Patil, A. P.; Temperley, W. H.; Gething, P. W.; Boeckel, T. M.; Kabaira, C. W.; Harbach, R. E.; Hay, S. I., *Parasite & Vectors.*, **2010**, *3*, 72.

13. Holt, R. A.; Subramanian, G. M.; Halpern, A.; Sutton, G. G.; Charlab, R. S.; Nusskern, D. R.; Wincker, P.; Clark, A. G.; Ribeiro, J. M. C.; Wides, R.; Salzberg, S. L.; loftus, B.; Yandell, M.; Majoros, W. H.; Rusch, D. B.; Lai, Z.; Kraft, C. L.; Abril, J. F.; Anthouard, V.; Arensburger, P.; Atkinson, P. W.; Baden, H.; De Berardinis, V.; Baldwin, D.; Benes, V.; Biedler, J.; Blass, C.; Bolanos, R.; Boscus, D.; Barnstead, M.; Cai, S.; Center, A.; Chaturvedi, K.; Christophides, G. K.; Chrystal, M. A.; Clamp, M.; Cravchik, A.; Curwel, V.; Dana, A.; Delcher, A.; Dew, I.; Evans, C. A.; Flanigan, M.; Grundschober-Freimoser, A.; Friedli, L.; Gu, Z.; Guan, P.; Guigo, R.; Hillenmeyer, M. E.; Hladun, S. L.; Hogan, J. R.; Hong, Y. S.; Hoover, J.; Jaillon, O.; Ke, Z.; Kodira, C.; Kokoza, E.; Koutsos, A.; Letunic, I.; Levitsky, A.; Liang, Y.; Lin, J-J.; Lobo, N. F.; Lopez, J. R.; Malek, J. A.; McIntosh, T. C.; Meister, S.; Miller, J.; Mobarry, C.; Mongin, E.; Murphy, S. D.; O'Brochta, D. A.; Pfannkoch, C.; Qi, R.; Regier, M. A.; Remington, K.; Shao, H.; Sharakhova, M. V.; Sitter, C. D.; Shetty, J.; Smith, T. J.; Strong, R.; Sun, J.; Thomasova,

D.; Ton, L. Q.; Topalis, P.; Tu, Z.; Unger, M. F.; Walenz, B.; Wang, A.; Wang, J.; Wang, M.; Wang, X.; Woodford, K. J.; Wortman, J. R.; Wu, M.; Yao, A.; Zdobnov, E. M.; Zhang, H.; Zhao, Q.; Zhao, S.; Zhu, S. C.; Zhimulev, I.; Coluzzi, M.; Della Torre, A.; Roth, C. W.; Louis, M.; Kalush, F.; Mural, R. J.; Myers, E. W.; Adams, M. D.; Smith, H. O.; Broder, S.; Gardner, M. J.; Fraser, C. M.; Birney, E.; Bork, P.; Brey, P. T.; Venter, J. C.; Weissenbach, J.; Kafatos, F. C.; Collins, F. H.; Loffman, S. L., *Science.*, **2002**, *298*, 129.

14. Wipasa, J.; Elliot, S.; Xu, H.; Good, M. F., *Immunol. Cell Biol.*, **2002**, *80*, 401.
15. Andrade, B. B.; Reis-Filho, A.; Souza-Neto, S. M.; Clarencio, J.; Camargo, L. M.; Barral, A.; Barral-Neto, M., *Malaria. J.*, **2010**, *9*, 13.
16. Gardner, M. J.; Hall, N.; Fung, E.; White, O.; Berriman, M.; Hayman, R. W.; Carlton, J. M.; Pain, A.; Nelson, K. E.; Bowman, S.; Paulsen, I. T.; James, K.; Eisen, J. A.; Rutherford, K.; Salzberg, S. L.; Craig, A.; Kyes, S.; Chan, M. S.; Nene, V.; Shallom, S. J.; Suh, B.; Peterson, J.; Angiuolli, S.; Pertea, M.; Allen, J.; Selengut, J.; Haft, D.; Mather, M. W.; Vaidya, A. B.; Martin, D. M.; Fairlamb, A. H.; Fraunholtz, M. J.; Ross, D. S.; Ralph, S. A.; McFadden, G. I.; Cummings, L. M.; Subramanian, G. M.; Mungall, C.; Venter, J. C.; Carucci, D. J.; Hofmann, S. L.; Newbold, C.; Davis, R. W.; Fraser, C. M.; Barrell, B., *Nature.*, **2002**, *419*, 498.
17. Baum, J.; Gilberger, T-M.; Frischknecht, F.; Meissner, M., *Trends Parasitol.*, **2008**, *24*, 557.
18. Wells, T. N. C.; Alonso, P. L.; Gutteridge, W. E., *Nature Rev. Drug Discov.*, **2009**, *8*, 879.
19. de Macedo, C. S.; Schwartz, R. T.; Todeschini, A. R.; Previato, J. O.; Mendonça-Previato, L., *Mem. Inst. Oswaldo Cruz, Rio de janeiro*, **2010**, *105*, 949.
20. Kuehn, A.; Pradel, G., *J. Biomed. Biotechnol.*, **2010**, *97*,6827.
21. Decampo, R.; Moreno, S. N., *Curr. Pharm. Descov.*, **2008**, *14*, 882.
22. Mather, M. W.; Henry, K. W.; Vaidya, A. B., *Curr. Drug Target*, **2007**, *8*, 49.
23. Roepe, P. D., *F1000 Biol. Rep.*, **2009**, 1:18.
24. Olliaro, P. L.; Yuthavong, Y., *Pharmacol. Ther.*, **1999**, *81*, 91.
25. Jana, S.; Paliwal, J., *Internat. J. Antimicrob. Agents*, **2007**, *30*, 4.
26. Choi, S-R.; Mukherjee, P.; Avery, M. A., *Curr. Med. Chem.*, **2008**, *15*, 161.
27. Klemba, M.; Beatty, W.; Gluzman, I.; Goldberg, D. E., *J. Cell Biol.*, **2004**, *164*, 47.
28. Abu Bakar, N., Klonis, N.; Hanssen, E.; Chen, C.; Tilley, L., *J. Cell Biol.*, **2009**, *123*, 441.
29. Banister, L. H.; Hopkins, J. M.; Fowler, R. E.; Krishna, S.; Mitchell, G. H., *Parasitol. Today*, **2000**, *16*, 427.

30. Lamarque, M.; Tastet, C.; Poncet, J.; Demettre, E.; Jouin, P.; Vial, H.; Dubremetz, J-F., *Proteomics. Clin. Appl*., **2008**, *2*, 1361.

31. Kuhn, Y.; Sanchez, C. P.; Ayoub, D.; Saridaki, T.; van Dorsselaer, A.; Lanzer, M., *Traffic*, **2010**, *11*, 236.

32. Francis, S. E.; Sullivan Jr, D. J.; Goldberg, D. E., *Annu. Rev. Microbiol*., **1997**, *51*, 97.

33. Lew, V. L.; Tiffert, T.; Ginsburg, H., *Blood*, **2003**, *101*, 4189.

34. (a) Glutzman, Y. I.; Francis, S. E.; Oksman, A.; Smith, E. C.; Duffins, K. L.; Goldberg, D. E., *J. Clin. Invest.*, **1994**, *93*, 1602.

(b) Francis, S. E.; Glutzman, Y. I.; Oksman, A.; Knickerbocker, A.; Mueller, K.; Bryant, M. L.; Sherman, D. R.; Russel, D. G.; Goldberg, D. E., *EMBO J.*, **1994**, *13*, 306

(c) .Banerjee, R.; Liu, J.; Beatty, W.; Pelosof, L., Klemba, M.; Goldberg, D. E., *PNAS*, **2002**, *99*, 990.

35. Errati, R.; Bova, F.; Zappalá, M.; Grasso, S.; Micale, N., *Med. Chem. Rev.*, **2010**, *30*, 136.

36. (a) Drew, M. E.; Banerjee, R.; Uffman, E. W.; Gilbertson, S., Rosenthal, P. J.; Goldberg, D. E., *J. Bio. Chem.*, **2008**, *283*, 12870

(b) Coombs, G. H.; Goldberg, D. E.; Klemba, M.; Berry, C.; Kay, J.; Mottram, J. C., T., *Trends Parasitol.*, **2001**, *17*, 532.

37. (a) Moon, S-U.; Kang, J-M.; Kim, T-S.; Kong, Y.; Sohn, W-K.; Na, B-K., *Exp. Parasitol.*, **2011**, *128*, 127.

(b) Chemlay, S. M.; Chen, C-T.; Van Zyl, R. L., *J. Inorg. Biochem.*, **2007**, *101*, 764.

38. Tekwani, B. L.; Walker, L. A., *Comb. Chem. High Throughput Screen*, **2005**, *8*, 63.

39. Pick, C.; Ebersberger, I.; Spielmann, T.; Bruchhaus, I.; Burmester, T., *BMC Evol. Biol.*, **2011**, *11*, 167.

40. de Koning-Ward, T.; Gilson, P. R.; Boddey, J. A.; Rug, M.; Smith, B. J.; Papenfuss, A. T.; Sanders, P. R.; Lundie, R. J.; Maier, A. G.; Cowman, A. F.; Crabb, B. S., *Nature*, **2009**, *459*, 945.

41. Russo, I.; Babbitt, S.; Muralidharan, V.; Butler, T.; Oksman, A.; Goldberg, D. E., *Nature*, **2011**, 463, 632.

42. Gil, A. L.; Valiente, P. A.; Pascutti, P. G.; Pons, T., J. *J. Trop. Med*., **2011**, doi:10.1155/2011/657483.

43. Greenwood, B. M.; Fidock, D. A.; Kyle, D. E.; Kappe, S. H. I.; Alonso, P. L.' Collins, F. H.; Duffy, P. E., *J. Clin. Invest.*, **2008**, *118*, 1266.

44. Takken, W.; Knols, B. G. J., *Trends Parasitol.*, **2008**, *25*, 101.

45. Shiff, C., *Clin. Microbiol. Rev.*, **2002**, *15*, 278.

46. (a) Lusingu, J.; Olotu, A.; Leach, A.; Lievens, M.; Vekermans, J.; lie Olivier, A.; Benns, S.; Olomi, R.; Msham, S.; Lang. T.; Gould, J.; Hallez, K.; Guerra, Y.; Njuguna, P.; Awuondo, K. O.; Malabeja, A.; Abdul, O.; Gesase, S.; Dekker, D.; Malle, L.; Ismael, S.; Mturi, N.; Drakely, C. J.; Savarese, B.; Villafana, T.; Ballou, W. T.; Cohen, J.; Riley, E. M.; Lemnge, M. M.; Marsh, K.; Bejon, P.; von Seidlein, L., *PLoS ONE*, **2011**, *5*, e14090.
(b) Agnandji, S. T.; Lell, B.; Soulanoudjingar, S. S.; Fernandes, J. F.; Abossolo, B. P.; Conzelmann, C.; Methogo, B. G. N. O.; Doucka, Y-N.; Flamen, A.; Mordmúller, B.; Issifou, M.; Kremsner, P. G.; Sacarlal, J.; Aide, P.; Lanaspa. M.; Aponte. J. J.; Nhamuave, A.; Quelhas, D.; Bassat, Q.; Mandjate, S.; Macete, E.; Alonso, P.; Abdulla, S.; Salim, N.; Juma, O.; Shomari, M.; Shubis, K.; Machera, F.; Hamad, A. S.; Minja, R.; Mpina, M.; Mtoro, A.; Sykes, A.; Ahmed, S.; Urassa, A. M.; Ali, A. M.; Mwangoka, G.; Tanner, M.; Tinto, H.; D'Alessendro, U.; Sorgho, H.; Valea, I.; Tahita, M. E.; Kaboré, W.; Ouédraogo, S.; Sadrine, Y.; Guiguémdé, T.; Ouédraogo, J. B.; Hamel, M. J.; Kariuki, S.; Odero, C.; Oneko, M.; Otieno, K.; Awino, N.; omoto, J.; Williamson, J.; Muturi-Kioi, V.; Laserson, K. F.; Slutsker, L.; Otieno, W.; Otieno, L.; Nekoye, O.; Gondi, S.; Otieno, A.; Ogutu, B.; Wasuna, R.; Owira, V.; Jones, D.; Onyango, A. A.; Njuguna, P.; Chilengi, R.; Akoo, P.; Kerubo, C.; Gitaka, J.; Maingi, C.; Lang, T.; Olotu, A.; Tsofa, B.; Bejon, P.; Peshu, N.; Marsh, K.; Owusu-Agyei, S.; Asante, K. P.; Osei-Kwakye, K.; Boahen, D.; Ayamba, S.; Keyan, K.; Owusu-Ofori, R.; Dosoo, D.; Asante, I.; Adjei, G.; Kwana, E.; Chandramohan, D.; Greenwood, B.; Lusingu, J.; Gesase, S.; Malabeja, A.; Lemnge, M.; Theander, T.; Drakeley, C.; Anasong, D.; Agbenyega, T.; Adjei, S.; Boateng, H. D.; Rettig, T.; Bawa, J.; Sylverken, J.; Sambian, D.; Agyekum, A.; Owusu, L.; Martinson, F.; Hoffman, I.; Mvalo, T.; Kamthunzi, P.; Nkomo, R.; Msika, A.; Jumbe, A.; Chome, N.; Nyakuipa, D.; Chitedza, J.; Ballou, W. R.; Bruls, M.; Cohen, J.; Guerra, Y.; Jongert, E.; Lipirre, D.; Leach, A.; Lievens, M.; Ofori-Anyinam, O.; Vekemans, J.; Carter, T.; Leboullex, D.; Loucq, C.; Redford, A.; Savarese, B.; Schellenberg, D.; Sillman, M.; Vansadia, P., *N. Engl. J. Med.*, **2011**; 10.1056/NEJMOA1102287.

47. Olliaro, P., *Pharmacol. Ther.*, **2001**, *89*, 207.

48. Fidock, D. A.; Rosenthal, P. J.; Croft, S. L.; Brun, R.; Nwaka, S., *Nature Rev. Drug Discov.*, **2004**, *3*, 509.

49. Vangapandu, S.; Jain, M.; Kaur, K.; Patil, P.; Patel, S. R.; Jain, R., *Med. Chem. Rev.*, **2007**, *27*, 65.

50. Schlitzer, M., *ChemMedChem.*, **2007**, *2*, 944.

51. Ibezim, E. C.; Odo, U., *Afr. J. Biotechnol.*, **2008**, *7*, 349.

52. Kumar, A.; Katiyar, S. B.; Agarwal, A.; Chauhan, P. M. S., *Curr. Med. Chem.*, **2003**, *10*, 1137.

53. Debyshire, E. R.; Mota, M. M.; Clardy, J., *PLoS Pathog.*, **2011**, *7*, e1002178.

54. Dhanawat, M.; Das, N.; Nagarwal, R. C.; Schrivastava, S. K., *Mini-Rev. Med. Chem.*, **2009**, *9*, 1447.

55. Cravo, P.; Culleton, R.; Afonso, A.; Ferreira, I. D.; do Rosário, V. E., *Anti-Infect. Agents Med. Chem.* **2006**, *5*, 63-73.

56. Nzila, A.' Ward, S. A.; Marsh, K. A.; Sims, P. F. G.; Hyde, J. E., *Trends Parasitol*., **2005**, *21*, 334.

57. Alkadi. H. O., *Chemother*., **2007**, *53*, 385.

58. Biagini, G. A.; O'Neil, P. M.; Nzila, A.; Ward, S. A.; Bray, P. G., *Trends Parasitol.*, **2003**, *19*, 479.

59. Kouznetsov, V. V.; Gómes-Barrio, A., *Eur. J. Med. Chem*., **2009**, *44*, 3091.

60. Mital, A.; *Curr. Med. Chem*., **2009**, *14*, 759.

61. Kumar, V.; Mahajan, A.; Chibale, K., *Bioorg. Med. Chem.*, **2009**, *17*, 2236.

62. Achan, J.; Talisuna, A. O.; Erhart, A.; Yeka, A.; Tibenderana, J. K.; Buliraine, F. N.; Rosenthal, P. J.; D'Alessandro, U., *Malaria J*., **2011**, *10*, 144.

63. Rosenthal, P. J., *J. Exp. Biol*., **2003**, *206*, 3735.

64. O'Neill, P. M.; Barton, V. E.; Ward, S. A., *Molecules*, **2010**, *15*, 1705.

65. Noedl, H.; Se, Y.; Schaecher, K.; Smith, B. L.; Socheat, D,; Fukuda, M. M., *N. Engl. J. Med.*, **2008**, *24*, 359.

66. Hartwig, C. L.; Rosenthal, A. S.; D'Angelo, J.; Griffin, C. E.; Posner, G. H.; Cooper, R. A., *Biochem. Pharmacol.* **2009**, *77*, 322.

67. (a) Krishna, S.; Uhlemann, A-C.; Haynes, R. K., *Drug Resistance Updates* **2004**, *7*, 233.
(b) Krishna, S.; Bustamante, L.; Haynes, R. K.; Staines, H. M., *Trends Parasitol.*, **2008**, *29*, 520.

68. Parija, S. C.; Praharaj, I., *Indian J. Med. Microbiol*., **2011**, *29*, 243.

69. Meshnick, S.R., *Int. J. Parasitol.* **2004**, *32*, 1655.

70. Starzengruber, P.; Thriemer, K.; Haque, A.; Khan, W. A.; Fuehrer, H. P.; Siedl, A.; Hofecker, V.; Ley, B.; Wernsdorfer, W. H., *Antimicrob. Agents Chemother.*, **2009**, *53*, 404.

71. Friesen, J.; Silve, O.; Patrianti, E. D.; Hafalla, J. L. R.; Mutuschweski, K.; Borrman, S., *Sci. Transl. Med.*, **2010**, *2*, 40ra49.

72. Chico, R. M.; Pittrof, R.; Greenwood, B.; Chandramohan, D., *Malaria J*., **2008**, *7*, 225.

73. Bruce-Chwatt, L. J.; Black, R. H.; Canfield, C. J.; Clyde, D. F.; Peters, W.; Wernsdorfer, W. H., *Chemotherapy of malaria.* Second Edition (**1986**), WHO, Geneva, 102.

74. Hyde, J. E., *FEBS J*., **2007**, *274*, 4688.

75. Guantai, E.; Chibale K., *Curr. Drugs Delivery*, **2010**, *7*, 312.

76. Roepe, P. D.; *Future Microbiol*., **2009**, 4, 441.

77. Henry, M.; Alibert, S.; Orlandi-Pradines, E.; Bogreau, H.; Fusai, T.; Rogier, C.; Barbe, J.; Pradines, B., *Curr. Drug Targets*, **2006**, *7*, 935.

78. Lehane, A. M.; Kirk, K., *Mol. Microbiol.*, **2010**, *77*, 1039.

79. (a) Wünsh, S.; Sanchez, C. P.; Gekle, M.; Groβe-Wortmann, C.; Weisner, J.; Lanzer, M., *J. Cell Biol*., **1998**, *140*, 335.

(b) Sanchez, C. P.; Horrocks, P.; Lanzer, M., *Cell*, **1998**, *92*, 601.

80. RBM 17th Meeting on Global Malaria Programme: *Strategy paper on Management of antimalarial drug resistance* by Ringwald, P.; Mendis, K., Barrette, A.; Meek; S.; WHO, Geneva, **2009**.

81. Egan, T. J., *Future Microbiol.*, **2009**, *4*, 637.

82. Hershkovitz, I.; Donoghue, H. D.; Minnikin, D. E.; Bersa, G. S.; Lee, O. Y-C.; Gernaey, A. M.; Galili, E.; Eshed, V.; Greenblatt, C. L.; Lemma, E.; Bar-Gal, G. K.; Spigelman, M., *PLoS ONE*, **2008**, *3*, e3426.

83. Daniel, T. M., *Respirat. Med*., **2006**, *100*, 1862.

84. Koul, A.; Arnoult, E.; Lounis, N.; Guillemont, J.; Andries, K., *Nature Res. Rev.,* **2011**, *469*, 483.

85. Marriner, G. A.; Nayyar, A.; Uh, E.; Wong, S. Y.; Mukherjee, T.; Via, L. E.; Carroll, M.; Edwards, R. L.; Grubber, T. D.; Choi, I.; Lee, J.; Arora, K.; England, K. D.; Boshoff, H. I., M.; Barry III, C. E., *Top. Med. Chem.*, **2011**, *7*, 47.

86. *Global Tuberculosis Control*, WHO Report **2011**, WHO/HTM/TB/2011.16

87. Hanekom, W. A.; Lawn, S. D.; Dheda, K.; Whitelaw, A., *Trop. Med. Int. Health*, **2010**, *15*, 981.

88. Johnson, R.; Streicher, E. M.; Louw, G. E.; Warren, R. M.; van Helden, P. D.; Victor, T. C., *Curr. Issue Mol. Biol.*, **2006**, *8*, 97.

89. Matteeli, A.; Carvalho, A.; C. C.; Dooley, K. E.; Kritski, A., *Future Microbiol.*, **2010**, *5*, 849.

90. Aziz, M. A.; Wright, A.; Lazlo, A.; De Muynck, A.; Portaels, F.; Van Deun, A.; Wells, C.; Nunn, P.; Blanc, L.; Raviglione, M., *Lancet*, **2006**, *368*, 2142.

91. Chhabria, M.; Patel, S.; Jani, M., *Anti-Infect. Agents Med. Chem.*, **2010**, *9*, 59.

92. Liu, J.; Ren, H. P., *Anti-infect. Agents. Med. Chem.* **2006**, *5*, 331.

93. Rivers, E. C.; Mancera, R. L., *Curr. Med. Chem.* **2008**, *15*, 1956.

94. Gutierrez-Lugo, M-T.; Bewley, C. A., *J. Med. Chem.* **2008**, *51*, 2606.

95. Manganelli, R.; Dubnau, E.; Tyagi, S.; Kramer, F. R.; Smith, I., *Mol. Microbiol.*, **1999**, *31*, 715.

96. Beran, V.; Havelkova, M.; Kaustova, J.; Dvorska, L.; Pavlik, I., *Vet. Med-CZECH*, **2006**, *51*, 365.

97. Brennan, P. J., *Tuberculosis*, **2003**, *83*, 91.

98. Rezwan, M.; Lanéelle, M-A.; Sander, P.; Daffé, M., *J. Microbiol. Methods*, **2007**, *68*, 32.

99. Dover, L. G.; Bhatt, A.; Bhowruth, V.; Willcox, B. E.; Bersa, G. S., *Expert Rev. Vaccines*, **2008**, *7*, 481.

100. Jayaprakash, S.; Iso, Y.; Wan, B.; Franzblau, S. G.; Kozikowski, A. P., *ChemMedChem* **2006**, *1*, 593.

101. Rodrĭguez, J. C.; Escribano, I.; Gỏmez, R. A.; Pachỏn, E. G.; Navarro, A.; Royo, G., *Anti-Infect. Agents. Med. Chem.* **2006**, *7*, 1.

102. Caminero, J. A.; Sotgiu, G.; Zumla, A.; Migliori, B., *Lancet Infect Dis.*, **2010**, *10*, 621.

103. Denny, W. A.; Palmer, B. D., *Future Med. Chem.*, **2010**, *2*, 1295.

104. Protopopova, M.; Hanrahan, C.; Nikonenko, B.; Samala, R.; Chen, P.; Gearhart, J.; Einck, L.; Nancy, C. A., *J. Antimicrob. Chemother.*, **2005**, *56*, 968.

105. Chan, E. D.; Iseman, M. D., Curr. *Opinions Infect. Dis.*, **2008**, *21*, 587.

106. Assam-Assam, J-P.; Penlap, V. B.; Cho-Ngwa, F.; Teldom, J-C.; Ane-Anyangwe, I.; Titanji, V. P., *BMC Infect. Dis.*, **2011**, 11:94.

107. Chiang, C-Y.; Centis, R.; Migliori, G. B., *Respirology*, **2010**, *15*, 413.

108. Frydenberg, A. R.; Graham, S. M., *Trop. Med. Int. Health*, **2009**, *14*, 1329.

109. Rattan, A.; Kalia, A.; Ahmad, N., *Emerg. Infect. Dis.*, **1998**, *4*, 195.

110. Font, M.; Monge, A.; Ruiz, I.; Heras, B., *Drug Des. Discovery*, **1997**, *14*, 259.

111. Nakamara, T.; Oka, M.; Aizawa, K.; Soda, H.; Fukuda, M.; Terashi, K.; Ikeda, K.; Mizuta, Y.; Noguchi, Y.; Kimura, Y.; Tsururo, T.; Kohno, S., *Biochem. Biophys. Res. Commun.*, **1999**, *255*, 618.

112. Kaminsky, D.; Meltzer, R. I., *J. Med. Chem.*, **1968**, *11*, 60.

113. Musiol, R.; Jampilek, J.; Buchta, V.; Silva, L.; Niedbala, H.; Podeszwa, B.; Palka, A.; Majerz-Maniecka, K.; Oleksyn, B.; Polanski, J., *Bioorg. Med. Chem.*, **2006**, *14*, 3592.

114. Sloboda, A. E.; Powell, D.; Poletto, J. F.; Pickett, W. C.; Gibbons Jr, J. J.; Bell, D. H.; Oronsky, A. L.; Kerwar, S. S., *J. Rheumatol.*, **1991**, *18*, 855.

115. de Souza, M. V. N.; Pais, K. C.; Kaiser, C. R.; Peralta, M. A.; Ferreira, M. L.; Lourenço, M. C. S., *Bioorg. Med. Chem.*, **2009**, *17*, 1474.

116. Lilienkampf, A.; Mao, J.; Wan, B.; Wang, Y.; Franzblau, S. G.; Kozikowski, A. P., *J. Med. Chem.*, **2009**, *52*, 2109.

117. Loughheed, K. E. A.; Taylor, D. L.; Osborne, S. A.; Bryans, J. S.; Buxton, R. S., *Tuberculosis(Edinb)*, **2009**, *89*, 364.

118. Diacon, A. H.; Pym, A.; Grobush, M.; Patienta, R.; Rustomjee, R.; Page-Shipp, L.; Pistorius, C.; Krause, R.; Bogoshi, M.; Churchyard, G.; Venter, A.; Allen, J.; Palominoa, J. C.; De Merez, T.; van Heeswijk, R. P. G.; Lounis, N.; Meyvisch, P.; Verbeeck, J.; Parys, W.; de Beule, K.; Andries, K.; McNeeley, D. F., *N. Engl. J. Med*., **2009**, *360*, 2397.

119. Veziris, N.; Ibrahim, M.; Lounis, N.; Andries, K.; Jarlier, V., *PLoS ONE*, **2011**, *6*, e17556.

120. Guillenmont, J.; Meyer, C.; Poncelet, A.; Xavier, B.; Andries, K., *Future Med. Chem*., **2011**, *3*, 1345.

121. Burman, W. J., *Clin. Infect. Dis.*, **2010**, *50*, S165.

122. Keller, T. H.; Shi, P-Y.; Wang, Q-Y., *Curr. Opinion Chem. Biol*., **2011**, *15*, 529.

Chapter Two

Multi-component reactions and DMPK/ADMET

2.0 General introduction

Diversity-orientated synthesis (DOS) continues to grow as an area of importance in drug discovery. The introduction of structural diversity in a focused library of potential therapeutic compounds is believed to have a greater chance of delivering positive hits.[1,2] The majority of potential therapeutics are natural products or drug-like molecules that often contain a heterocyclic ring.[3] The chemistry of heterocyclic compounds has attracted a great deal of interest in recent times due to the increasing importance of the heterocyclic scaffold in pharmaceuticals. However, the range of easily accessible and suitable functionalized heterocyclic building blocks for the synthesis of structurally diverse libraries of therapeutics is somehow limited.[4] Therefore, the development of simple, elegant and facile methodologies towards focused libraries of such compounds is one of the most important aspects of drug discovery.[5] The multi-component reaction (MCR) strategy is arguably the most efficient method for rapid synthesis of heterocyclic compounds.[4] Large libraries of MCR heterocyclic products are particularly attractive for drug discovery efforts because they provide rapid access to complex molecules for biological evaluation.

2.1 Multi-component reactions (MCRs)

The synthesis of an α-aminonitrile (**2.4**) from the reaction of ammonia (**2.1**) and hydrogen cyanide (**2.2**) in the presence of a carbonyl compound (**2.3**) was reported by Strecker in 1850, and is considered to be the first MCR (Scheme 2.1).[6] Multi-component reactions are chemical reactions that combine three or more different starting materials in a one-pot synthesis to yield a final product that incorporates structural features of all inputs. In these reactions

starting materials do not all react simultaneously in one step but rather proceed in a series of ordered steps.[7] Multi-component reactions can be grouped into three basic types,[7] Table 2.1.

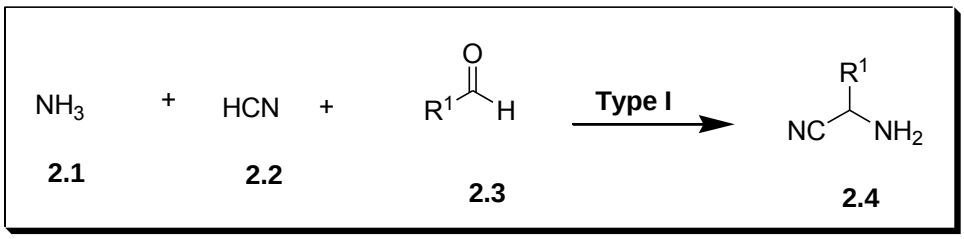

Scheme 2.1: Strecker three-component reaction.

Table 2.1: The basic types of MCR.[6]

MCR Type	General reaction scheme
I	A + B ⇌ C ⇌ D ⇌ ... O ⇌ P
II	A + B ⇌ C ⇌ D ⇌ ... O → P
III	A + B → C → D → ... O → P

Multi-component reactions in which starting materials, intermediates and product are in dynamic equilibrium is classified as type I. In this case yields range between 0 and 100% depending on the state of balance that prevails. In most cases type I reactions do not go to completion, have a greater chance of side product formation and desired products are usually difficult to isolate because they occur as mixtures with intermediates and/or starting materials. This is not an ideal type of MCR and an example is the Strecker reaction (Scheme 2.1).

Multi-component reactions whose elementary reactions are in reversible equilibria and the only irreversible step being the product forming step belong to type II. These reactions are advantageous in that they are high yielding due to the total equilibrium shift towards the direction of the products by the irreversible last step. This is an ideal type of MCR especially

in drug discovery programs where rapid generation of a library of compounds is of utmost importance. An example of type II reaction is the Biginelli reaction (Scheme 2.2).[8a,8b]

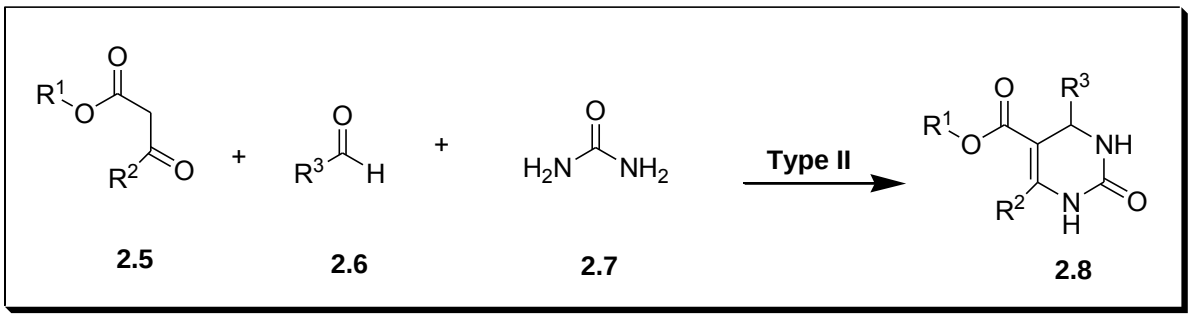

Scheme 2.2: Biginelli three-component reaction.

Multi-component reactions of type III consist of a sequence of irreversible elementary reactions that rarely occur in preparative chemistry, but found mostly in biochemical reactions of living organisms.

A number of other multi-component reactions such as the Hantzsch (1912),[7,9] Biginelli (1891),[10] Mannich (1912), Robinson-Schlöpf (1917),[11] Passerini (1921)[12,13] and Ugi (1959)[7] reactions came to light after Strecker's discovery. Many different variations of these reactions are known and some utilize as many as seven different starting materials. An example of this is the Dömling-Ugi seven-component reaction.[15] To date more than 400 different Multi-component reactions are known, 20-25% of them utilize isocyanides as one of the starting materials.[16] Isocyanide-based multi-component reactions are by far the most important and widely used of all the MCRs. In addition, the isocyanide based MCRs have been extensively exploited in drug discovery programs and in the synthesis of biologically active heterocyclic compounds.

2.1.1 Isocyanide-based multi-component reaction

In 1921, Passerini synthesized a carbamoylmethyl ester (**2.12**) from a three-component reaction of a carboxylic acid (**2.9**), an isocyanide (**2.11**) and a carbonyl compound (**2.10**), and this was to be regarded as the first isocyanide-based MCR (Scheme 2.3).[12,17]

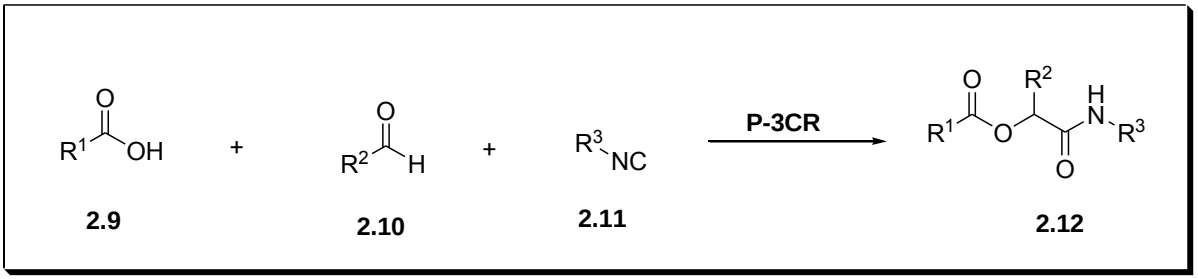

Scheme 2.3: Passerini three-component reaction.

After forty years of non-activity on isocyanide-based MCRs, Ugi discovered an aza version of the Passerini reaction in 1959 and this reaction became known as the Ugi reaction.[6] This reaction is discussed further in section 2.1.1.2. The advantages of using these reactions include; (i) high efficiency and versatility, (ii) functional group tolerance, and (iii) high levels of chemoselectivity, regioselectivity and stereoselectivity often observed.[12] In addition, both these reactions serve as a powerful tool for the production of a diverse array of biologically active compounds with high atom economy from readily accessible or easily prepared starting materials.[8a,17] Furthermore, isocyanide-based MCRs are being employed in the discovery of novel agents against infectious diseases caused by viruses, bacteria and parasites.[18]

2.1.1.1 Isocyanides

Isocyanides, formerly known as isonitriles, are a class of compounds containing an unusually extraordinary functional group whose structure and reactivity have been discussed for over one and a half century.[7] The majority of isocyanides or compounds containing an isocyano functional group are largely found in marine species. The first naturally occurring isocyanide

was isolated from *Penicillium notatum Westling* by Rothe in 1950 and was later used as an antibiotic, Xanthocillin (**2.13**) (Fig. 2.1).[8a,19] A larger number of simple and volatile isocyanides are characterized by an extremely unpleasant "odor" and the majority are only slightly toxic except for a select few.[20] However, prolonged exposure and inhalation of isocyanides has been reported to increase the intensity of dreams at night.[7]

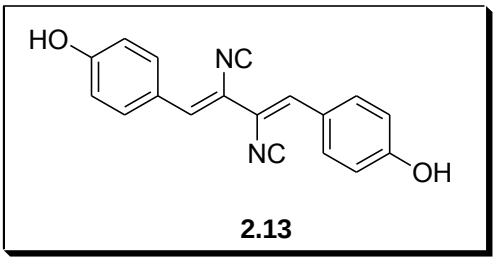

Figure 2.1: Xanthocillin, a naturally occurring isocyanide.

Isocyanides are the only class of stable organic compounds with a formally divalent carbon (C^{II}) capable of undergoing oxidation to a tetravalent carbon (C^{IV}) under mild reaction conditions.[7] In addition, the divalent carbon has a unique ability to react with both nucleophiles and electrophiles to give rise to α-adducts.[8a] The structural representation of isocyanides is depicted in Figure 2.2 and conformer **I** has been shown to contributes significantly more than **II** to the overall isocyanide structure.[21]

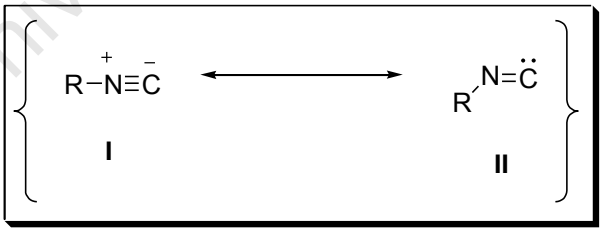

Figure 2.2: Resonance structures of isocyanides.

Carbenes and carbon monoxide are the only organic compounds with a divalent carbon and by virtue of this are structurally related to isocyanides. Reactivity of isocyanides is characterized by three properties: (i) the α-acidity, (ii) the α-addition, and (iii) the easy formation of radicals.[7]

The first synthetic isocyanide, allyl isocyanide (**2.16**), was accidentally made by Lieke in 1859 from the reaction of allyl iodide (**2.14**) and silver cyanide (**2.15**) (Scheme 2.4).[19] In the original synthesis Lieke believed he had formed nitriles only to be surprised in obtaining formamides instead of carboxylic acids when he tried to hydrolyze his product.[7] Unfortunately Lieke had to abandon his experiments as a result of the awful smell of isocyanides.[7] Eight years later Gauntier and Hoffman independently described the isomeric relationship of isocyanides and nitriles, and in the process developed the classical synthesis of isocyanides.[8a]

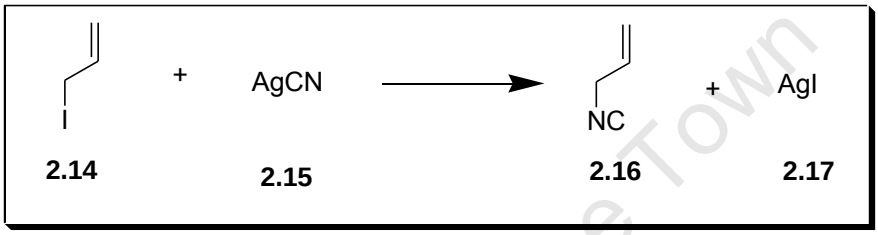

Scheme 2.4: Lieke synthesis of allyl isocyanide.

Currently there are dozens of methods reported in literature for the synthesis of isocyanides but the method of choice involves dehydrating *N*-formamides (**2.18**) (Scheme 2.5).[8a] Various dehydrating agents such as phosgene,[22] phosphorus oxychloride,[23] thionyl chloride,[7] *p*-toluenesulfonyl chloride[24] and triphenylphosphine[25] among others have been used to great effect in dehydrating formamides. Generally, dehydration of *N*-formamides is associated with high yields, ease of synthesis and low costs.[7]

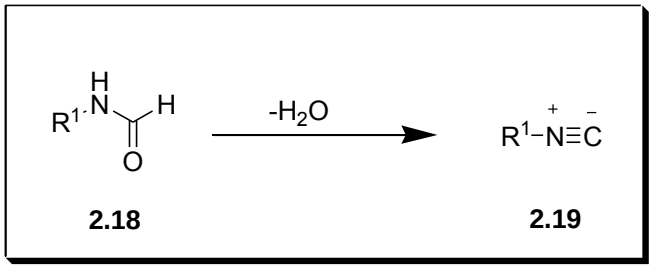

Scheme 2.5: General dehydration of *N*-formamides.

2.1.1.2 The Ugi multi-component reaction

In 1959, Ugi described the synthesis of an α-acylamino amide (**2.21**) from the reaction of a carboxylic acid (**2.9**) with an aldehyde (**2.10**) and an isocyanide (**2.11**) in the presence of an amine (**2.20**), and this reaction became known as the Ugi four-component reaction (Scheme 2.6).[26] Many variations of this reaction that are known today were discovered in a matter of weeks after this disclosure in 1959.[7] From the early 1990s until today, this reaction in conjunction with the enabling technologies such as high-throughput screening became one of the most utilized and investigated transformations.[27]

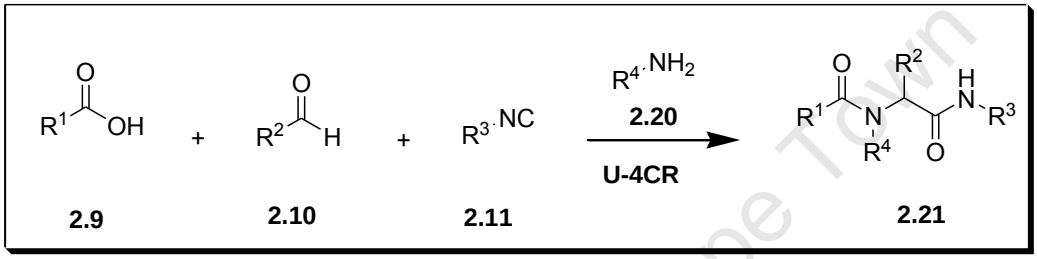

Scheme 2.6: Ugi four-component reaction (U4CR).

The reaction mechanism of the Ugi four-component reaction begins with the formation of a imine (**2.22A**) from the condensation of an amine (**2.20**) with the aldehyde (**2.10**) as depicted in Scheme 2.7. Protonation of the Schiff base nitrogen by the carboxylic acid (**2.9**) increases the electrophilicity of the C=N bond, thereby generating an activated iminium ion (**2.22B**). Addition of the isocyanide (**2.11**) to the activated imminium ion and subsequent nucleophilic addition of the carboxylate ion generates an α-adduct (**2.22D**), which is analogues to an acid anhydride *via* an intermediate nitrilium ion (**2.22C**). Irreversible intramolecular acylation, also known as the Mumm rearrangement, generates a hydroxyimine-amide (**2.22E**) which subsequently undergoes rearrangement and proton transfer to form a stable Ugi adduct (**2.21**). All the intermediate steps of this reaction sequence are equilibria. However, the acyl transfer and the rearrangement step lie exclusively on the product side, characteristic of type II MCRs. The major driving force for this reaction is the oxidation of the isocyanide divalent

carbon (C^{II}) to the amide tetravalent carbon (C^{IV}). In the course of this reaction, one C-C and several heteroatom-C bonds are created.[7]

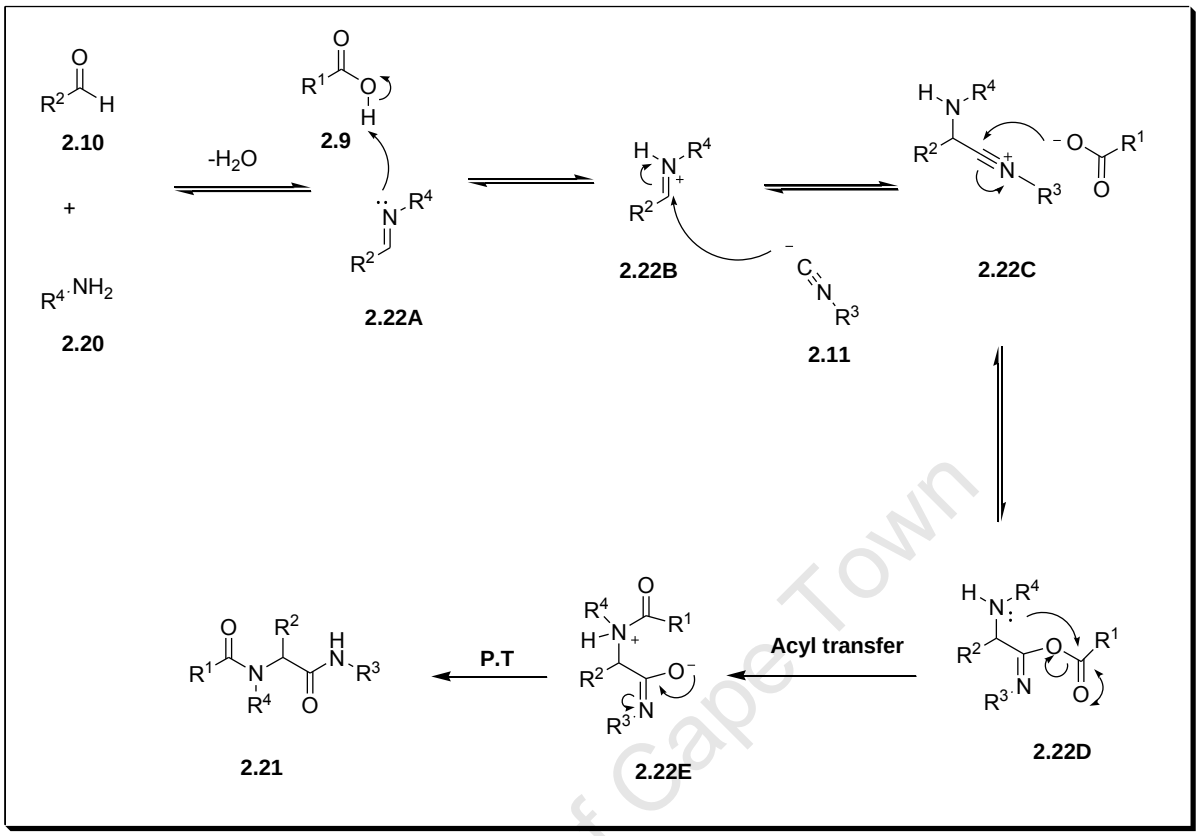

Scheme 2.7: Ugi four-component reaction (U4CR) mechanisms.

Reactivity series studies as a function of solvent and concentration established that this reaction is mainly influenced by inductive and mesomeric effects, and to a lesser extent by steric effects.[7] Conducting this reaction in polar aprotic solvents or in low-molecular weight alcohols has been found to be advantageous. However, the concentration of the reactants is postulated to be the most important factor.[12] The main drawbacks of this reaction are poor diastereoselectivity often observed when chiral reagents are used and the limited number of isocyanides currently available.[28]

2.2 Application of the Ugi MCR in drug discovery

2.2.1 Drugs already in the market

The increasing demand for rapid synthesis of biologically active compounds in the pharmaceutical industry has encouraged the use of MCRs in drug discovery and generic drug synthesis.[29] In addition, the possibility of performing post-condensation modifications on Ugi products gives access to new biologically relevant molecules. Furthermore, the fact that this reaction enables automated parallel synthesis further highlights its importance in the drug discovery process.[30] Application of the Ugi reaction in the synthesis of marketed drugs is exemplified by the following: The first application of the Ugi reaction was in the synthesis of Xylocain® (**2.26**), a local anesthetic (Scheme 2.8).[26]

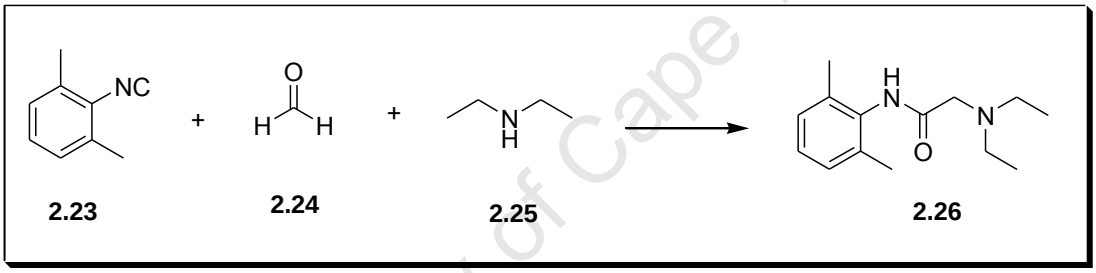

Scheme 2.8: Ugi synthesis of a local anesthetic, Xylocain®.

Secondly, the Ugi reaction was also used in the modified synthesis of known marketed drugs such as Plavix® (**2.31**), a antiplatelet agent (Scheme 2.9).[29,31]

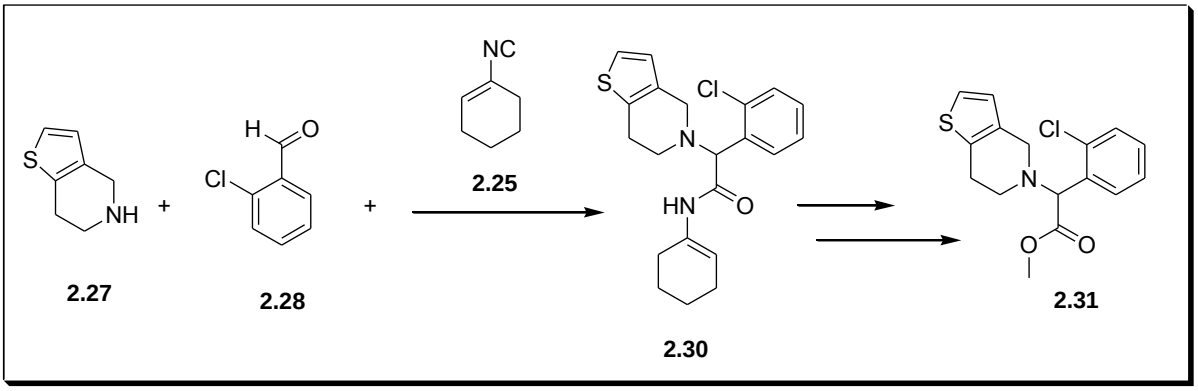

Scheme 2.9: Ugi synthesis of an antiplatelet agent, Plavix®.

Lastly, scientists at Merck & Co utilized the Ugi four-component reaction in synthesizing the core fragment (**2.35**) of an HIV-1 protease inhibitor, Crixivan® (**2.38**) (Scheme 2.10).[32]

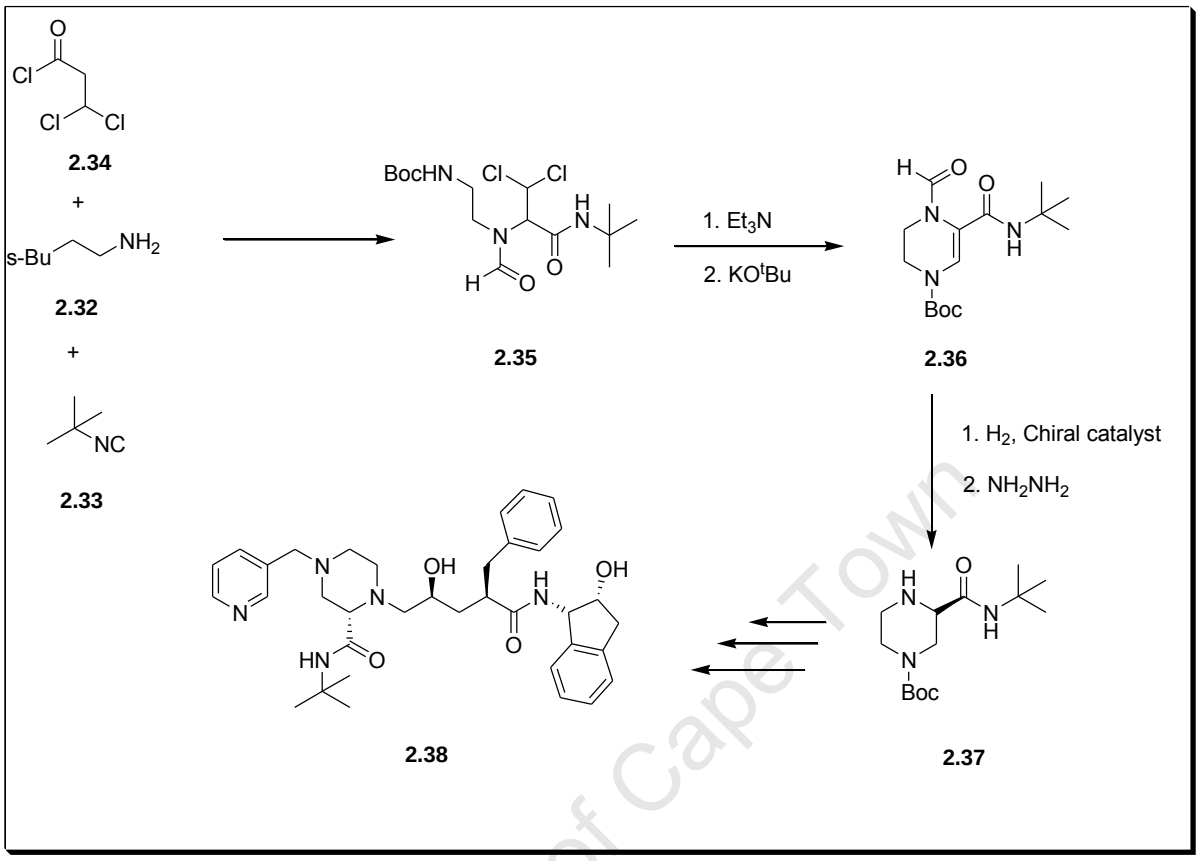

Scheme 2.10: Application of the Ugi MCR in the synthesis of HIV protease inhibitor, Crixivan®.

2.2.2 Application in early drug discovery programs

A number of compounds obtained *via* the Ugi multi-component reaction have found successful use in lead discovery and lead optimization stages of drug discovery programs. As such, various research institutes and academic research labs are also utilizing Ugi multi-component reactions in search of biologically active molecules for screening purposes in "hit to lead" campaigns. The following three examples illustrate the application of Ugi multi-component reactions in the discovery of potential hits and/or possibly lead compounds.

Musonda *et al.*,[33] functionalized a quinoline pharmacophore found in a number of antimalarial drugs by synthesizing a series of novel 4-aminoquinoline γ- and δ-lactams (**2.42**)

using the "Ugi 3-component 4-centre multi-component reaction" (Scheme 2.11). In addition, these γ- and δ-lactams showed activity against a chloroquine-resistant strain of the *P. falciparum* parasite as well as against the causative agent of human African Trypanosomiasis, *Trypanosoma brucei*.

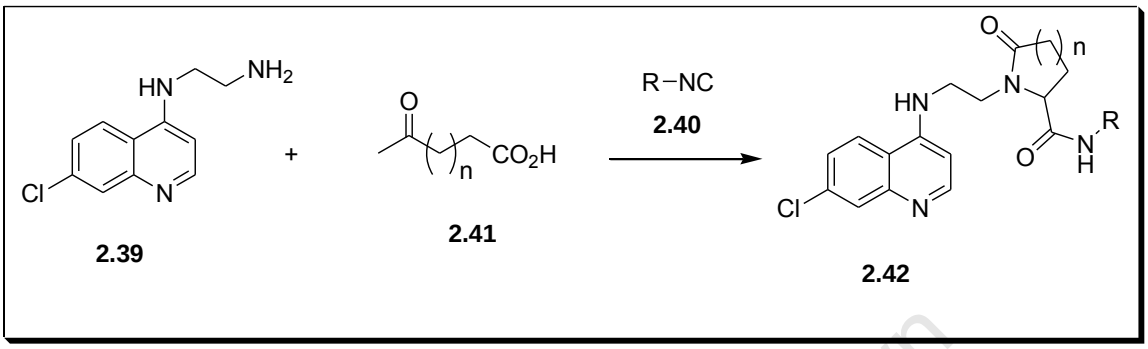

Scheme 2.11: Application of the Ugi MCR in the synthesis of 4-aminoquinoline γ- and δ-lactams.

In 2007 Dömling and co-workes at Morphochem disclosed the Ugi four-component synthesis of novel anti-TB agents (**2.45**) based on the isoniazid and pyrazineamide pharmacophores (Scheme 2.12).[34] These anti-TB agents possessed activity against the $H_{37}Rv$ drug-sensitive strain of *Mycobacterium tuberculosis*.

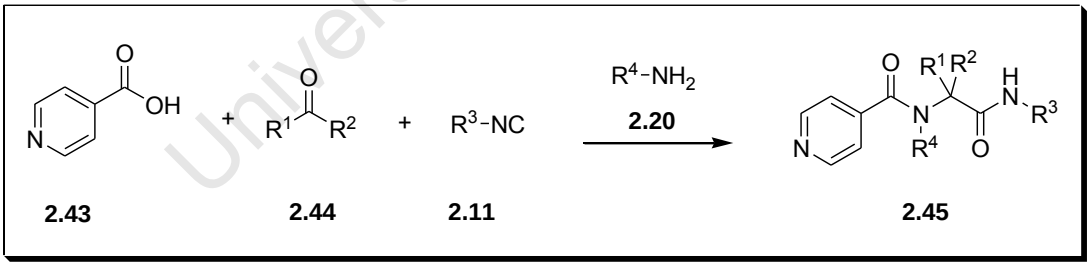

Scheme 2.12: Application of the Ugi MCR in the synthesis of novel anti-TB agents.

Scientists from the Korean's Institute of Science and Technology synthesized potent morpholin-2-one based T-type Ca^{2+}-ion channel blockers *via* the Ugi five-centre three-component reaction (Scheme 2.13).[35]

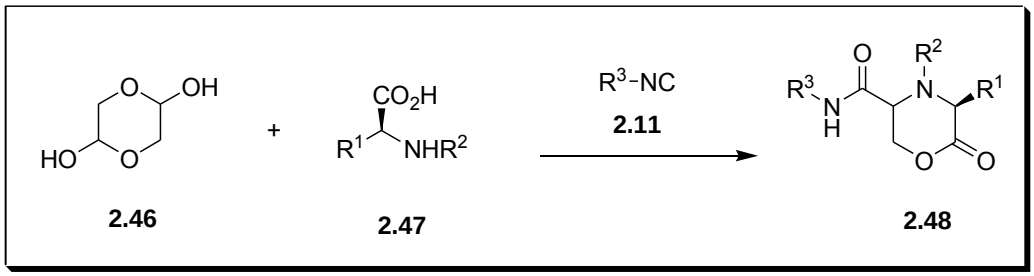

Scheme 2.13: Application of the Ugi MCR in the synthesis of novel Ca^{2+}-channel blockers.

In addition, some of the products synthesized using the Ugi multi-component reactions contain biologically relevant and privileged heterocyclic structures such as tetrazoles,[36] imidazoles,[37] thiazoles,[38] and oxazoles[39].

2.3 Tetrazoles as biologically relevant heterocycles

The tetrazole moiety is a doubly unsaturated heterocyclic five-membered ring system consisting of one carbon atom and four nitrogen atoms. Tetrazoles have not been found in nature and they exist as 1H- (**A**) and 2H-tetrazole (**B**) tautomers, the latter being more stable in the gas phase (Fig. 2.3).[40] They usually possess a significantly high acidic and weak basic characteristics, and as such, many of their physical, chemical, physico-chemical, and biological properties are linked to this amphoteric character.[41] Tetrazole-based compounds have found a wide range of applications in explosives, in photography, in agriculture, in medicine, and information recording and imaging systems.[42] In addition, tetrazoles are normally used in synthetic chemical transformations as building blocks or derivatizing agents and as ligands in coordination chemistry.[43,44] This latter property has been successfully exploited by analytical chemists in removing heavy metal ions from liquids and chemical systems formulated for metal protection against corrosion.[45,46]

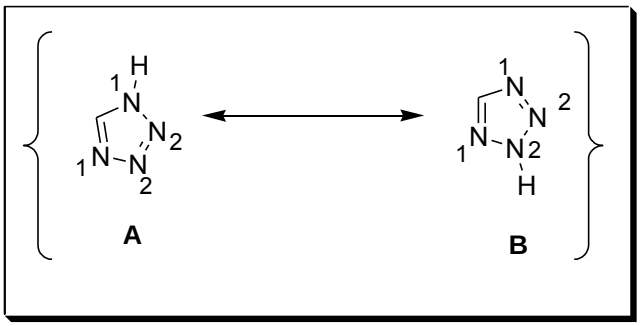

Figure 2.3: General representation of tetrazoles.

Tetrazoles belong to the family of biologically active compounds known as the "azole pharmacophoric compounds" which include imidazoles, thiazoles and triazoles among others.[46] The majority of medical applications of tetrazole-based compounds are a result of the acidic property of the tetrazole ring. Medicinal chemists are interested in the tetrazole moiety due to the fact that this scaffold possesses excellent physico-chemical properties and thus is used as a bioisostere for carboxylic acids in biologically active molecules.[48,49] The tetrazolic acid fragment has similar acidity to carboxylic acids but is more metabolically stable at physiological pH and has been shown to be at least ten times more lipophilic than the corresponding carboxylate.[50] Lipophilicity is an important drug property as this is a measure of how effectively a particular drug will pass through the cell membrane. Isosteric replacement of functional groups is of particular interest in drug discovery efforts because it allows one to alter unfavourable ADME (**A**bsoprtion, **D**istribution, **M**etabolism and **E**xcretion) properties which have been shown to have a major impact on the attrition rate of new chemical entities.[51]

Tetrazoles are found in a number of marketed pharmaceutical agents particularly the angiotensin II antagonists such as Losartan (**2.49**) and its analogues; Irbesartan (**2.50**) and Valsartan (**2.51**) (Fig. 2.4).[52] On the other hand, several tetrazole derivatives have been screened for various biological activities such as antibacterial,[53] anti-inflammatory,[54] antifungal (TAK-456, **2.52**),[55] antitubercular,[56]antiprotozoan,[57] antiviral,[58] and anticancer[59].

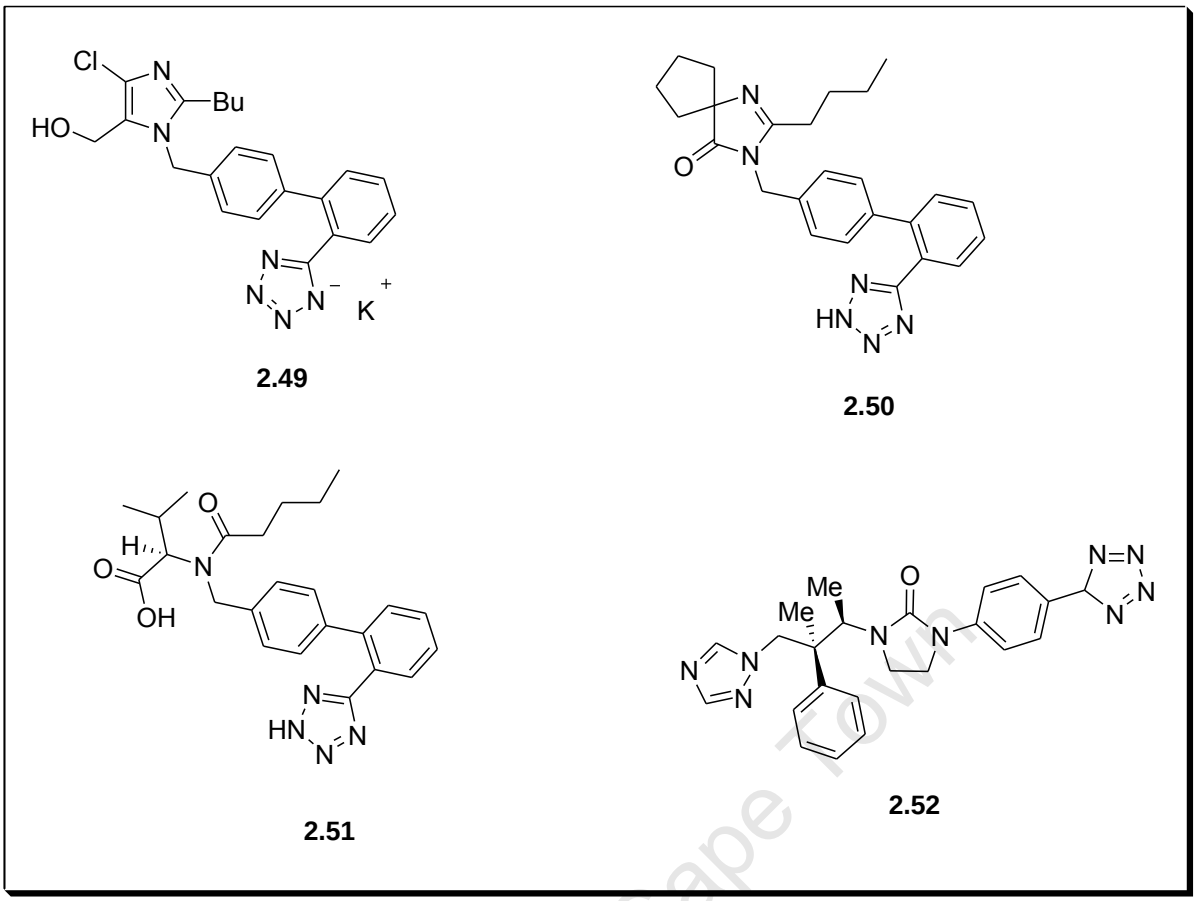

Figure 2.4: Drugs on the market with the tetrazole scaffold.

2.3.1 Synthesis of tetrazoles

Various methods for preparing tetrazoles, especially 1,5-disubstituted tetrazoles, are widely reported in literature and these include; (i) amides reacting with PCl_5 or triflic anhydride or HN_3 or NaN_3,[60] (ii) thioamides with trimethylsilyl azide,[61] (iii) imidoyl chlorides with NaN_3,[62] (iv) ketones with NaN_3 or trimethylsilyl azides,[63] (v) oximes with HN_3,[64] (vi) nitriles with alkyl chlorides and trimethylsilyl azide or alkyl azide,[65] (vii) nitrillium triflate with NaN_3,[66] and (viii) amidrazones with N_2O_4 or HNO_2[67] (Scheme 2.14).[68] The majority of these methods suffer from drawbacks such as long reactions times, use of toxic and/or explosive reagents, tedious work-up and low yields, use of dangerously high temperatures, and use of uncommon starting materials among others.[68,69] Isocyanide based multi-component reactions, particularly the modified $TMSN_3$-Passerini and Ugi reactions, provide an efficient and

convenient alternative method for synthesizing 1,5-disubstituted tetrazoles from readily available non-toxic starting materials and in far better yields.

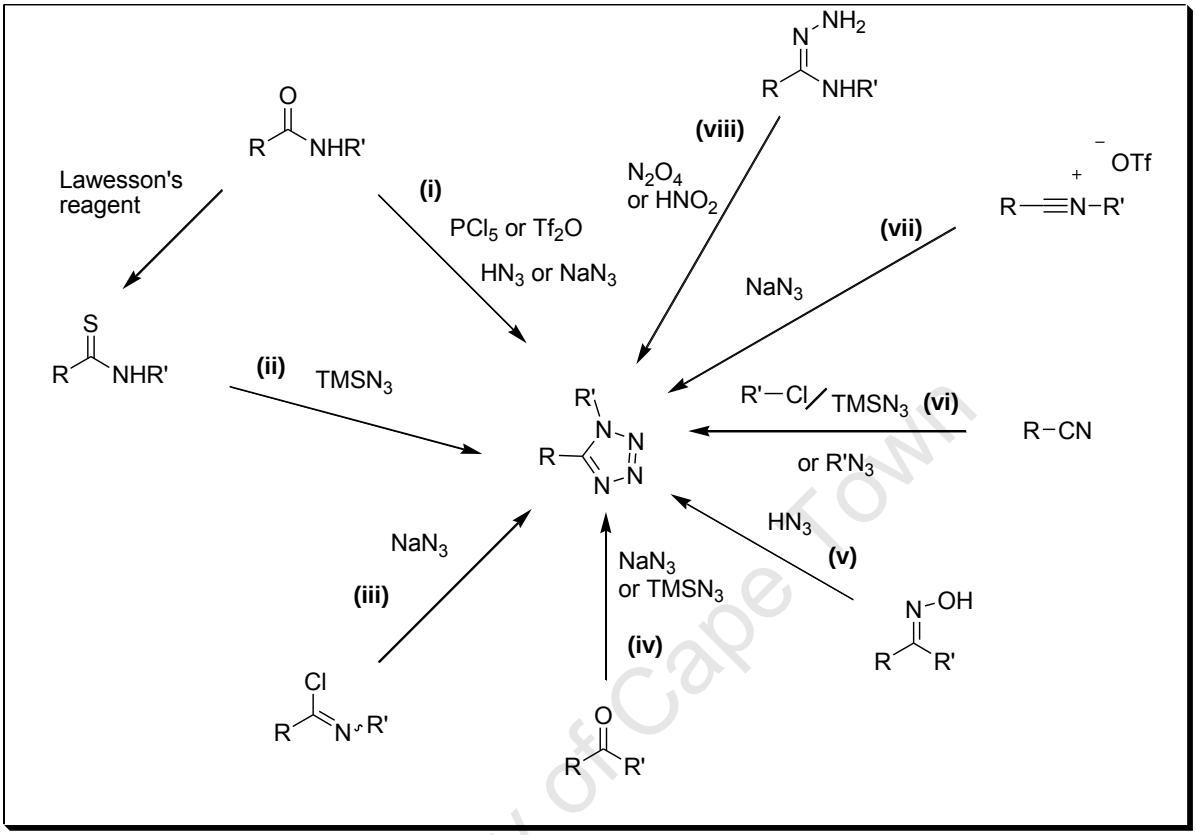

Scheme 2.14: Various methods for synthesizing 1,5-disubstituted tetrazole (Adapted from ref. 68)

2.3.1.1 Synthesis of tetrazoles from isocyanide-based MCRs

For the first time Nixely *et al.*,[58c] utilized the modified $TMSN_3$-Passerini reaction to synthesize norstatine tetrazoles as a new class of HIV-1 protease inhibitors in 2002. They achieved this by replacing the standard carboxylic acid input in the classical Passerini reaction with $TMSN_3$. The *N*-Boc-α-aminoaldehydes (**2.53**) were reacted with an isocyanide (**2.11**) in the presence of $TMSN_3$ (**2.54**) to furnish protected tetrazoles (**2.55**) (Scheme 2.15). Subsequent deprotection and *N*-capping with **2.56** gave the desired *cis*-constrained norstatine-tetrazole mimetics (**2.57**).

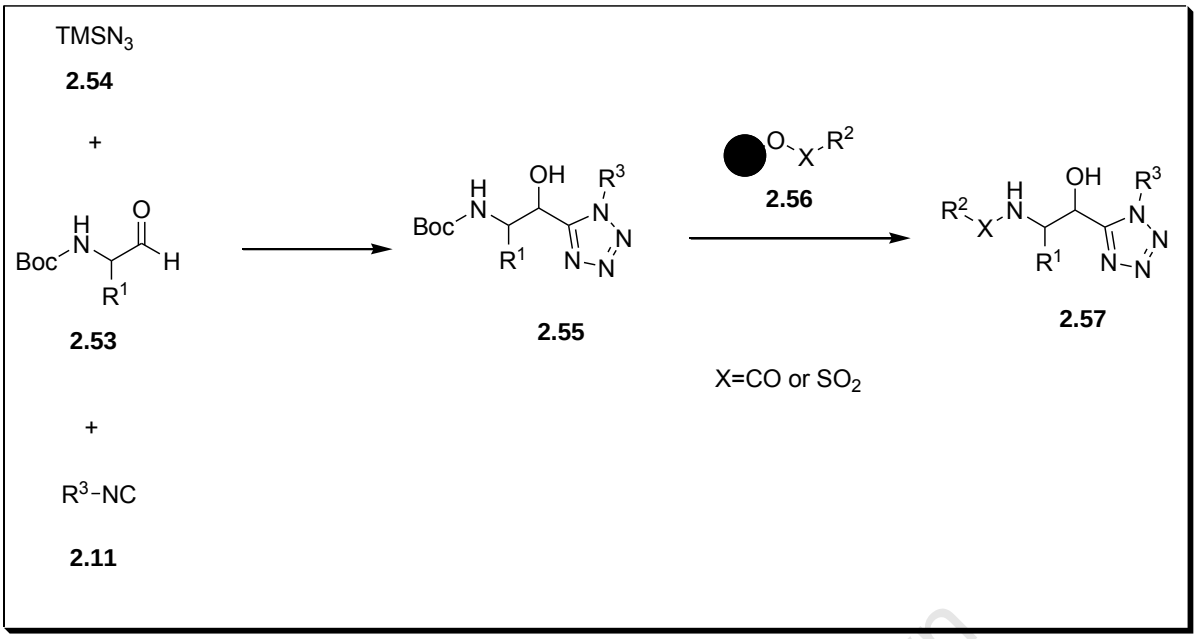

Scheme 2.15: Synthesis of tetrazoles using the modified $TMSN_3$-Passerini reaction.

In 1960 Ugi accomplished the synthesis of tetrazoles (**2.58**) by replacing the carboxylic acid with hydrazoic acid. The modified reaction involved reacting aldehydes with amines in the presence of isocyanides and hydrazoic acid (Scheme 2.16).[70] The main problem with this reaction was the use of a highly poisonous and potentially explosive hydrazoic acid, and low yields.[71]

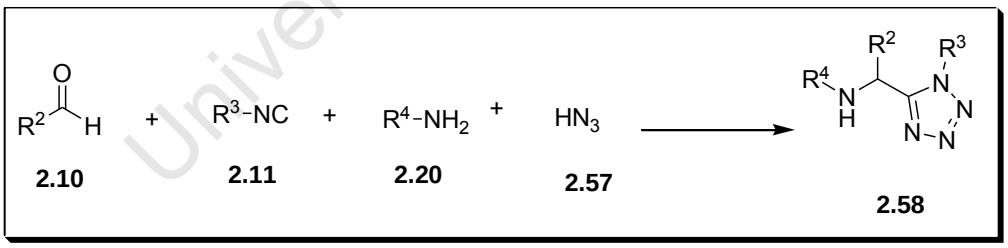

Scheme 2.16: Synthesis of tetrazoles using the HN_3 based Ugi reaction.

The drawbacks of using HN_3 prompted the research into alternative reagents such as $TMSN_3$. Mayer *et al.*,[72] and Dömling *et al.*,[48] have synthesized a number of tetrazoles (**2.61**) using the modified $TMSN_3$-Ugi reaction in conjunction with cleavable isocyanides (Scheme 2.17). $TMSN_3$ is slightly toxic as well but it is not explosive and it gives better yields than HN_3.[71]

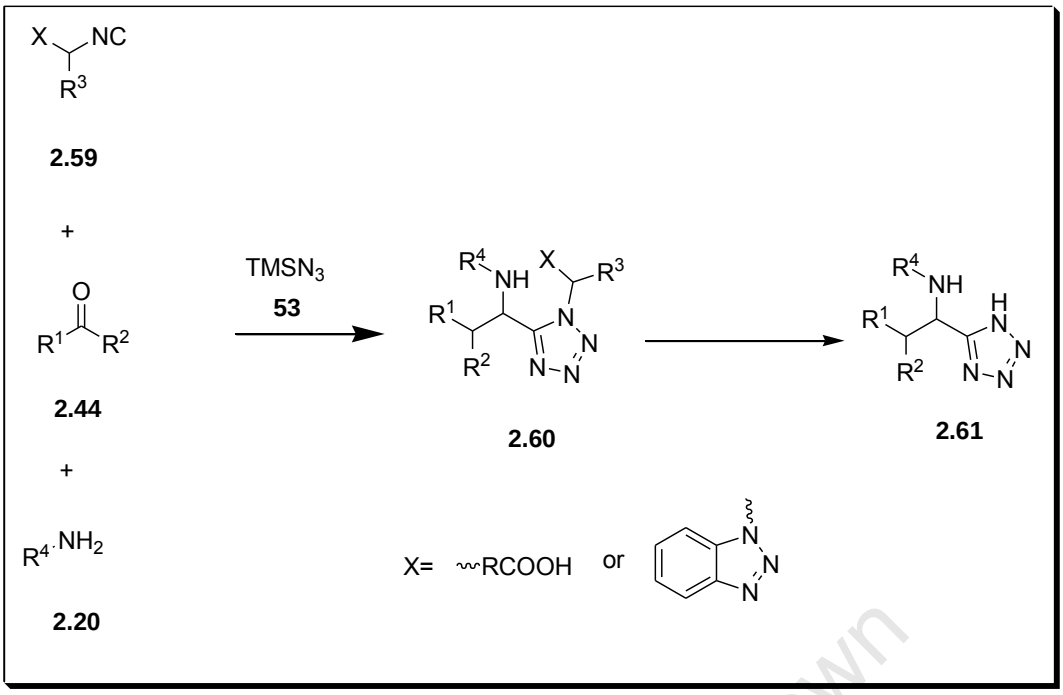

Scheme 2.17: Synthesis of tetrazoles using the $TMSN_3$ modified Ugi reaction.

2.4 DMPK/ADMET

A large numbers of new chemical entities (NCEs) are developed in drug discovery programs, thus the understanding of drug-metabolism and pharmacokinetic (DMPK) properties involved in the absorption, distribution, metabolism, excretion and toxicity (ADMET) of such NCEs is of utmost importance. Prior to the year 2000 the major reason for the high failure rate of drugs in clinical development was largely due to the DMPK related issues, with rates around 40%.[73,74] The incorporation of DMPK in early drug discovery dropped this rate to below 10% from the year 2000 onwards (Fig. 2.5).

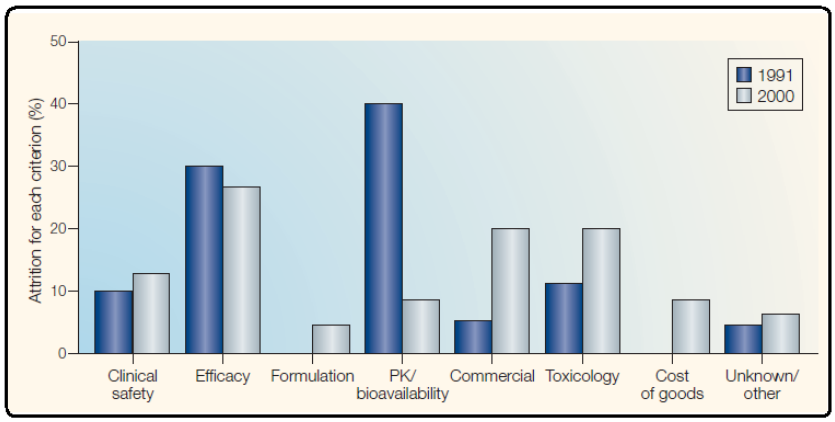

Figure 2.5: Reasons for attrition rate of drugs in clinical development.[74]

Drug metabolism (DM) comprises of biological processes that are involved in the conversion of potential drugs into toxic or non-toxic metabolites before and after they reach their site of action in the body.[75] Most of these processes are enzyme-catalyzed; uridine-diphosphate-glucuronosyl-transferases, cytochrome P-450 and carboxylesterases are some of the drug-metabolizing enzymes.[75,76] DM is dived into two phases, oxidative (phase I) and conjugative (phase II) metabolism, and predominantly takes place in the liver, gastrointestinal tract, kidneys, lungs and the plasma through a series of reactions.[77] The establishment of the *in vitro* and *in vivo* ADMET technologies has resulted in a better understanding of the DM properties of potential drug candidates. Pharmacokinetics (PK) is the study of the rate at which a potential drug is transported to its site of action in sufficient concentrations and in long enough time to course a significant pharmacological response.[78,79] PK encapsulate the efficiency of drug absorption, the rate of drug metabolism, rate of distribution, and the rate of excretion by measuring the amount of drug concentration in the blood or plasma.[77,80,81,82] The role of DMPK in early drug discovery is to identify and eliminate compounds exhibiting poor metabolic and/or pharmacokinetic properties that would reduce their chances of successful development as drug candidates.[83]

2.4.1 Physico-chemical properties affecting ADME

Much of the work on drug metabolism and pharmacokinetics (DMPK) within drug discovery programs is mainly concerned with the oral delivery of drugs.[84] An orally administered drug will first dissolve in the gastrointestinal tract and followed by one of the two processes; the drug will either (i) be excreted without modification or (ii) some of it will be absorbed through the gut wall, modified by first pass metabolism (phase I) and distributed to the liver (Fig. 2.6).[85] Once it reaches the liver, the drug will be metabolized further (phase II), distributed in systematic circulation to tissues, organs, and finally, to its molecular target. The fraction of a dose of a drug reaching systemic circulation is referred to as its bioavailability.

Dosage form, dissolution, permeation through the gastrointestinal tract, and metabolic stability are some of the factors that influence drug bioavailability.[84,86] In addition, these factors are largely dependent on physico-chemical properties of drugs such as lipophilicity, solubility and permeability among others.

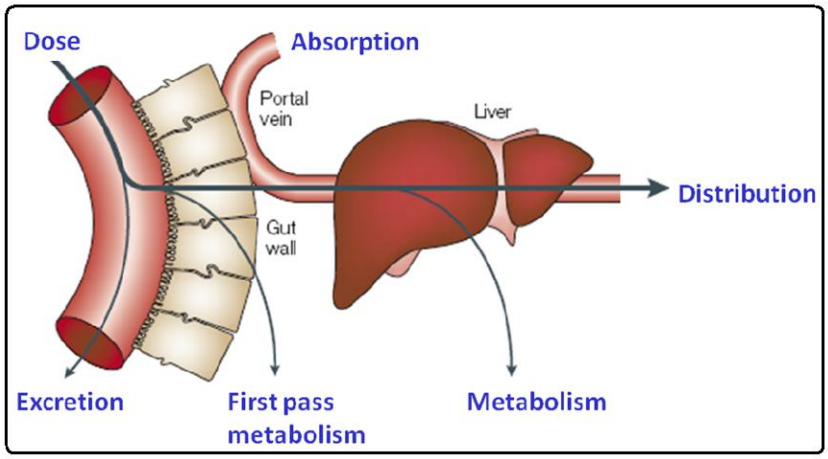

Figure 2.6: Fate of an orally administered drug.[74]

2.4.2.1 Lipophilicity

Lipophilicity represents an affinity of a molecule or moiety to partition in the oily phase or biological membrane (lipophilic environment).[87] This is expressed as the logarithm of partition coefficient or distribution coefficient (log P or log D) of a drug in an octanol/water system. This physico-chemical property greatly affects solubility, dissolution and absorption of drugs. Poor aqueous solubility and slow dissolution of drugs can lead to poor oral absorption and thus low oral bioavailability.[85]

2.4.2.2 Solubility

Solubility measures the ability of a drug or drug candidate to dissolve and remain in aqueous or other physiological media. Low solubility is detrimental to good or complete oral absorption and/or bioavailability. As such early measurements of this parameter are of great importance in drug discovery programs.

2.4.2.3 Permeability

Permeability is an ability of a drug or drug candidate to pass through biological membranes after dissolution in the gastrointestinal tract. Permeability can occur *via* transcellular diffusion, paracellular diffusion, and transporter mediated-mechanism.[88] Permeability of compounds through Caco-2 cells is used to model human intestine absorption and this approach is commonly referred to as the membrane-interaction quantitative structure-activity relationship (MI-QSAR).[89] This physico-chemical property is influenced largely by the molecular weight of compounds because as molecules increase in size their ability to permeate through membranes decreases.[88]

The majority of these physico-chemical properties can be predicted by *in silico* tools such as Moka, Volsurf+, and MetaSite among others.[91] *In silico* predictions are advantageous in that they utilize a virtual library of compounds and generate ADME data to assess which compounds to prioritise in synthesis. This approach reduces the cost and time involved in discovering new compounds which have high potential to be positive hits. However, such predictions should be corroborated by *in vitro* and/or *in vivo* ADME experiments whenever possible.

2.5 Objective, Hypothesis and Aims

Objective

The overall objective of this research program is to identify and develop bi-therapeutic chemically hybridized new anti-infective agents in a quest to overcome or delay drug resistance in malaria and tuberculosis.

Hypothesis

The questions to be addressed at the conclusion of this project are two-fold:

- Using MCR, is it possible to identify single agents that provide inhibition of multiple disease-causing organisms or cells?

- Is it possible to improve the physico-chemical and DMPK properties of antiplasmodial and anti-mycobacterium tuberculosis pharmacophores or bioactiphores?

Specific aims

Specific aims include:

- The synthesis new tetrazole-based compounds as potential anti-malaria and anti-tuberculosis agents *via* Multi-Component Reaction (MCR) strategies.

- Pharmacological evaluation of synthesized compounds, *In silico* ADME profiling of the most promising compounds.

2.6 Reference

1. Bon, R. S.; Hong, C.; Bouma, M. J.; Schmitz, R. F.; de Kanter, F. J. J.; Lutz, M.; Spek, A. L.; Orru, R. V. A., *Org. Lett*., **2003**, *5*, 3759.

2. Keserü, G. M.; Makata, G. M., *Drug Discov. Today*, **2006**, *11*, 741.

3. Sunderhaus, J. D.; Martin, S. F., *Chemistry*, **2009**, *15*, 1300.

4. Akritopoulou-Zanze, I.; Djuric, S. W., *Top. Heterocycl. Chem*., **2010**, *25*, 231.

5. Sadjadi, S.; Heravi, M. M., *Tetrahedron*, **2011**, *67*, 2707.

6. Ivachtchenko, A. V.; Ivanenkov, Y. A.; Kysil, V. M.; Krasavin, M. Y.; Ilyin, A. P., *Russian Chem. Rev.*, **2010**, *79*, 787.

7. Dömling, A.; Ugi, I., *Angew. Chem. Int. Ed.*, **2000**, *39*, 3168.

8. (a) Ugi, I.; Werner, B.; Dömling, A.; Ugi, I., *Molecules*, **2003**, *8*, 53.
(b) Weber, L.; Illgen, K.; Almstetter, M., *Synlett.*, **1999**, *3*, 366.

9. Ranu, C.; Harja, A.; Jana, U., *Synlett*, **2000**, 75.

10. Kappe, C. O., *Acc. Chem. Res.*, **2000**, *33*, 879.

11. List, B.; *J. Am. Chem. Soc.*, **2000**, *122*, 9336.

12. Dömling, A.; Ugi, I., *Chem. Rev.*, **2006**, *106*, 17.

13. Ramon, D. J., *Angew. Chem. Int. Ed.*, **2005**, *44*, 1602.

14. Ganem, B.; Ugi, I., *Chem. Res.*, **2009**, *106*, 17.

15. Kolb, J.; Beck, B.; Almstetter, M.; Heck, B.; Hertweck, E.; Dömling, A., *Mol. Divers.*, **2003**, *6*, 297.

16. Weber, L., *Curr. Med. Chem.*, **2002**, *9*, 2085.

17. Huang, Y.; Dömling, A., *Mol. Divers.*, **2011**, *15*, 13.

18. Akritopoulou-Zanze, I.; *Curr. Opinion Chem. Biol.*, **2008**, *12*, 324.

19. Ugi, I., *Pure Appl. Chem.*, **2001**, *73*, 187.

20. Lygin, A. V.; de Meijere, A., *Angew. Chem. Int. Ed.*, **2010**, *49*, 9094.

21. Ugi, I., *Isonitrile Chemistry*, Academic Press, London, **1971**.

22. Skorna, G.; Ugi, I., Angew. *Chem. Int. Ed. Engl*., **1977**, *16*, 259.

23. Obrecht, R.; Herrmann, R.; Ugi, I., *Synthesis*, **1985**, 400.

24. Hertler, W. R.; Corey, E. J., *J. Am. Chem. Soc*., **1958**, 1221.

25. Appel, R.; Kleinstak, R.; Zeihn, K-D.; *Angew. Chem. Int. Ed*., **1971**, *2*, 132.

26. Hulme, C.; Gore, V., *Curr. Med. Chem*., **2003**, *10*, 51.

27. Bonne, D.; Dekhane, M.; Zhu, J., *Org. Lett*., **2004**, *6*, 4771.

28. Banfi, L.; Basso, A.; Cerulli, V.; Roca, V.; Riva, R., *Beilstein J. Org. Chem*., **2011**, *7*, 976.

29. Kalinski, C.; Umkehker, M.; Weber, L.; Kolb, J.; Burdack., C.; Ross, G., *Mol. Devers*., **2010**, *14*, 513.

30. Armstrong, R. W.; Combs, A. P.; Tempest, P. A.; Brown, S. D.; Keating, T. A., *Acc. Chem. Res*., **1996**, *29*, 123.

31. Kalinski, C.; Lemoine, H.; Schmidt, J.; Burdack, C.; Kolb, J.; Umkehker, M.; Ross, G., *Synthesis*., **2008**, *24*, 4007.

32, Rossen, K.; Pye, P. J.; diMechele, L. M.; Voante, R. P.; Reider, P. J., *Tetrahedron Lett*., **1998**, *39*, 6823.

33. Musonda, C. C.; Gut, J.; Rosenthal, P. J.; Yardley, V.; Carvalho de Souza, R. C.; Chibale, K., *Bioorg. Med. Chem.*, **2006**, *14*, 5605.

34. Dömling, A.; Achatz, S.; Beck, B., Bioorg. *Med. Chem. Lett.*, **2007**, *17*, 5483.

35. (a) Kim, Y. B.; Chooi, E. H.; Keum, G.; Kang, S. B.; Lee, D. H.; Koh, H. Y.; Kim, Y., *Org. Lett*., **2001**, *3*, 4149.

(b) Ku, W.; Cho, S.; Doddaredy, M. R.; Jang, M. S.; Keum, G.; Lee, J-H.; Chung, B. Y.; Kim, Y.; Rhim, H.; Kang, S. B., *Bioorg. Med. Chem. Lett*., **2006**, *16*, 5244.

36. Kalinski, C.; Umkehrer, M,; Gonnard, S.; Nadine, J.; Ross, G.; Hiller, W., *Tetrahedron Lett*., **2006**, *47*, 2041.

37. Gulecich, A. V.; Balenkova, E. S.; Wenajdenko, V. G., *J. Org. Chem*., **2007**, *72*, 7878.

38. Kazmaier, U.; Ackermann, S., *Org. Biomol. Chem*., **2005**, *3*, 3184.

39. Thompson, M. J.; Chen, B., *J. Org. Chem*., **2009**, *74*, 7084.

40. Mazurek, A. P.; Sadlej-Sosnowska, N., *Chem. Phys. Lett*., 2000, 33, 212.

41. Ostrovskii, V. A.; Koren, A. O., *Heterocycles*, **2000**, *53*, 1421.

42. Upadhayaya, R. S.; Jain, S.; Sinha, N.; Kishore, N.; Chandra, R.; Arora, S. K., *Eur. J. Med. Chem.*, **2004**, *39*, 579.

43. Frija, L. M. T.; Fausto, R.; Loureiro, R. M. S.; Cristiano, M. L. S., *J. Mol. Cat. A Chem*., **2009**, *305*, 142.

44. Popova, E. A.; Trifonov, R. E.; Ostrovskii, V. A., *ARKIVOC*, **2011**(i), 552.

45. Moore, D. S.; Robinson, S. D., *Adv. Inorg. Chem.*, **1998**, 32, 171.

46. Frija, L. M. T.; Ismael, A.; Cristiano, M. L. S., *Molecules*., **2010**, *15*, 3757.

47. Rostom, S. A. F.; Ashour, H. M. A.; Abd El Razik., H. A.; Abd El Fattah, A. E. F. H.; El-Din, N. N., *Bioorg. Med. Chem*., **2009**, *17*, 2410.

48.Dömling, A.; Beck, B.; Magnin-Lachaux, M., *Tetrahedron Lett*., **2006**, *47*, 4289.

49. Herr, R. J., *Bioorg. Med. Chem*., **2002**, *10*, 3379,

50. Yella, R.; Khatun, N.; Rout, S. K.; Patel, B. K., *Org. Biomol. Chem*., **2011**, *9*, 3235.

51. Kassel, D. B., *Curr. Opinion Chem. Biol.*, **2004**, *8*, 3389.

52. Myznikov, L. V.; Hrabalek, A.; Koldobskii, G. I., *Chem. Heterocycl. Compounds*, **2007**, *43*, 1.

53. (a) Bekhit, A. A.; El-Sayed, O. A.; Aboulmagd, E.; Park, J., *Eur. J. Med. Chem*., **2004**, *39*, 249.

(b) Mohamed, M. S.; El-Domany, R. A.; abd El-Hameed, R. H., *Acta. Pharm*., **2009**, *59*, 145.

54. Mohite, P. B.,; Bhaskar, V. H., *Int. J. Pharm. Tech. Res*., **2011**, 3, 1557.

55. Mohite, P. B.,; Bhaskar, V. H., *Electron. J. Chem*., **2010**, *2*, 311.

56. Wachter, G. A.; Davis, M. C.; Martin, A. R.; Franzblau, S. G., *J. Med. Chem*, **1998**, *44*, 2436.

57. Biot, C.; Bauer, H.; Schirmer, R.; Davioud-Charvet, E., *J. Med. Chem*., **2004**, *47*, 5972.

58. (a) Zhan, P.; Liu, H.; Liu, X.; Wang, Y.; Pannecouque, L.; Witvrow, M, De Clerq, E., *Med. Chem. Res.*, **2010**, *19***,** 652

(b) Habich, D., *Synthesis*, **1992**, 358.

(c) Nixely, T.; Hulme, C., *Tetrahedron Lett.*, **2002**, *43*, 6839.

59. Kumar, C. N. S.; Parida, D. K.; Santhoshi, A.; Kota, A. K.; Sridhar, B.; Rao, V. J., *Med. Chem. Commun.*, **2011**, *2*, 486.

60. Hegarty, A. F.; Tynan, N. M.; Fergus, S. J., *J. Chem. Soc. Perkin Trans. 2*, **2002**, *7*, 1328.

61. Lehnholf, S.; Ugi, I., *Heterocycles*, **1995**, *43*, 801.

62. Artamonova, T. V.; Zhivich, A. B.; Dubisnkii, M. Y.; Koldobskii, G. I., *Synthesis*, **1996**, 1428.

63. Suzuki, H.; Hwang, Y. S.; Nakaya, L.; Matano, Y., *Synthesis*, **1993**, 1218.

64. Burtler, R. N.; O'Donoghue, D. A., *J. Chem. Res. (S)*, **1983**, 18.

65. Ueyama, N.; Yanagisawa, T.; Kawai, T.; Sonegawa, M.; Baba, H.; Mochizuki, S.; Kosakai, K.; Tomiyama, T., *Chem. Pharm. Bull*., **1994**, *42*, 1841.

66. Amer, M. I. K.; Booth, B. L., *J. Chem. Res. (S)*, **1993**, 4.

67. Deady, L. W.; Devine, S. M. J., *Heterocyclc. Chem*., **2004**, *41*, 549.

68. Katritzky, A. R.; Rogovoy, B. V.; Kovalenko, K. V., *J. Org. Chem*., **2003**, *68*, 4941.

69. Koldobskii, G. I., *Russian J. Org. Chem*., **2006**, *42*, 469.

70. Ugi, I., *Angew. Chem*., **1960**, *72*, 639.

71. Gowd, M. R. M. B.; Pasha, M. A., *J. Chem. Sci*., **2011**, *123*, 75.

72. Mayer, J.; Umkehrer, M.; Kalinski, C.; Ross, G.; Kolb, J.; Burdack, C.; Hiller, W., *Tetrahedron Lett*., **2005**, *46*, 7393.

73. Kola, I.; Landis, J., *Nature Rev*., **2004**, *3*, 711.

74. Carlson, J. J.; Fisher, M. B., *Comb. Chem. High Throughput Screening*, **2008**, *11*, 258.

75. Thomas, A., *Medicinal Chemistry*-An introduction, John-Wiley & Sons Ltd, **2000**.

76. Lin, J. H.; Lu, A. Y. H., *Pharmacol. Rev.*, **1997**, *49*, 403-440.

77. Smith, D. A.; van de Waterbeemd, H.; Walker, D. K.; Manhold, R.; Kubiyisi, H.; Tremmerman, H., *Pharmacokinetics and Metabolism in drug design*, Wiley-VCH, **2001**.

78. Riley, R. J.; Martin, I. J.; Cooper, A. E., *Curr. Drug. Metab*., **2002**, *3*, 527-550.

79. Harrigan, G. G.; Brackett, D. J.; Boros, L. G., *Mini-Rev. Med. Chem*., **2005**, *5*, 13-20.

80. Eddershaw, P. J.; Beresford, A.P.; Bayliss, M.K., *Ther. Focus-Rev.*, **2000**, *5*, 409.

81. Baumann, A., *Curr. Drug Metab*., **2006**, *7*, 15-21.

82. Yang, M.; Ge, J-F.; Arai, C.; Itoh, I.; Fu, Q.; Ihara, M., *Bioorg. Med. Chem*., **2009**, *17*, 1481.

83. Baillie, T. A., *Chem. Res. Toxicol.*, **2008**, *21*, 129-137.

84. Smith, D.; Schmid, E.; Jones, B., *Clin. Pharmacokinet.*, **2002**, *41*, 1005.

85. van de Waterbeemd, H.; Gifford, E., *Nature Rev*., **2003**, *2*, 192.

86. Fasinu, P.; Pillay, V.; Ndesendo, V. M. K.; du Toit, L. C.; Choonara, Y. E., *Biopharm. Drug Dispos*., **2011**, *32*, 185.

87. Wang, J.; Skonik, S., *Chem. Biodiversity*, **2009**, *6*, 1887.

88. Gleeson, M. P., J. *Med. Chem*., **2008**, *51*, 817.

89. Kulkarni, A.; Yi, H.; Hopfinger, A. J., *J. Chem. Inf. Comput. Sci*., **2002**, *42*, 331.

90. Avdeef, A., *Curr. Topics Med. Chem*., **2001**, *1*, 277.

91. These can be downloaded from the Molecular Discovery website for a certain amount of licence fee (http://www.moldiscovery.com/software.pnp)

Chapter Three

Design, synthesis and biological evaluation of novel tetrazole-based aminoquinoline derivatives

3.1 Preface

This chapter describes the design, synthesis and biological evaluation of a series of novel tetrazole-based aminoquinoline derivatives. Specifically, these derivatives are based on the deoxyamodiaquine, 4-amino-7-chloroquinoline and primaquine scaffolds. Prior to synthesis, *in silico* prediction tools were utilized in selecting a small number of compounds predicted to possess favourable ADME properties (solubility and metabolic stability). The multi-component reaction (MCR) strategy was then used to synthesize these target compounds, which were all fully characterized by spectroscopic methods. The synthesized compounds were all evaluated *in vitro* for antiplasmodial and antimycobacterial activity.

3.2 General overview

Aminoquinoline-based antimalarial drugs have been the most important class of compounds used for treating malaria over the years. This was largely due to their excellent clinical efficacy, limited host toxicity, ease of use and most importantly, their simple and cost-effective synthesis.[1] The precise mode of action of aminoquinolines is believed to involve Π-stacking of the quinoline ring to the porphyrin units of the haeme-moiety, resulting in the accumulation of the "free-haeme" inside the parasite digestive food vacuole, and subsequently death of the parasite.[2,3] Although aminoquinoline-based drugs are useful in treating and managing malaria, their use has been limited by the emergence of drug-resistant strains of the parasite.[4] Thus, the search for new and improved aminoquinoline derivatives that will be equally effective against both the sensitive and resistant *P. falciparum* strains is of utmost importance in the fight against malaria.

One good starting point in antimalarial drug discovery is an existing antimalarial drug in which the validated chemical scaffold critical for inhibition of the parasite growth, at least *in vitro*, has been identified and newer derivatives designed around it.[5]

3.3 General rationale

The general rationale used in designing target compounds is illustrated by the generic rationale representation in Figure 3.1. Based on the design, the tetrazole scaffold is fused with one or two known biologically active bioactiphores that will form part of the inputs envisaged for the MCR. The choice of the tetrazole R' substituent was deliberately limited to two convertible isocyanides, namely, 4-ethylmorpholine- and the *tert*-butyl isocyanide, whose resulting product would lend themselves to post MCR modification if desired. The tetrazole moiety was chosen as an integral part of this design mainly for three reasons. First, this scaffold possesses excellent physico-chemical/ADME properties.[6] Second, it is found in a number of synthetic biologically active compounds.[7] Third, molecules containing this scaffold are known to exhibit excellent activity against infectious disease-causing organisms (Chapter 2, section 2.3).[8,9,10] There are various methods reported in literature for synthesizing substituted tetrazoles but the MCR strategy appears to be the most convenient because of its high efficiency and versatility, functional group tolerance, and use of non-toxic and readily available starting materials.

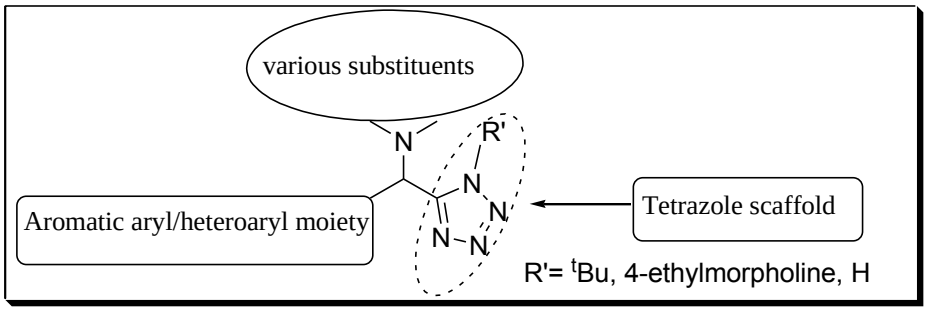

Figure 3.1: Generic rationale design for target compounds.

3.4 Deoxyamodiaquine-based tetrazole compounds

Amodiaquine (AQ) (**3.1**) is a Mannich base derivative that was first synthesized by Burckhalter in 1948 as an alternative to quinine (Fig. 3.2).[11,12] Amodiaquine possesses excellent activity against a variety of chloroquine-resistant strains of *P. falciparum*. In the 1980s the use of amodiaquine was discouraged as a result of its association with adverse effects such as hepatotoxicity and agranulocytosis in people taking the drug prophylactically.[13] However, following wide-spread development of resistance to chloroquine, the use of amodiaquine was reconsidered in the 1990s. Currently, the WHO recommends the use of amodiaquine in combination with artesunate or with sulfadoxine/pyrimethamine as a first-line treatment for uncomplicated malaria.

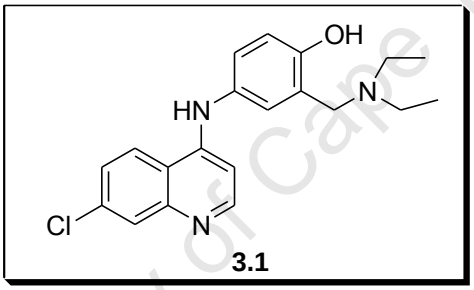

3.1

Figure 3.2: Amodiaquine, an antimalarial drug.

Amodiaquine is rapidly metabolized by the hepatic CYP2C8 enzyme into *N*-desethylamodiaquine (DEAQ) metabolite, which has a longer half-life and is three-times less active than the parent drug.[14] Toxic episodes of amodiaquine are manifested by *in vivo* biotransformation of its *p*-aminophenol moiety into an electrophilic metabolite, amodiaquine quinoneimine (ADQI) (**3.2A**) (Scheme 3.1).[15,16] This CYP450-mediated biotransformation is accompanied by the expression of drug-related antigens on the cell surface caused by the amodiaquine-protein complex (**3.3A**), an indication of a type II hypersensitivity reaction.[17]

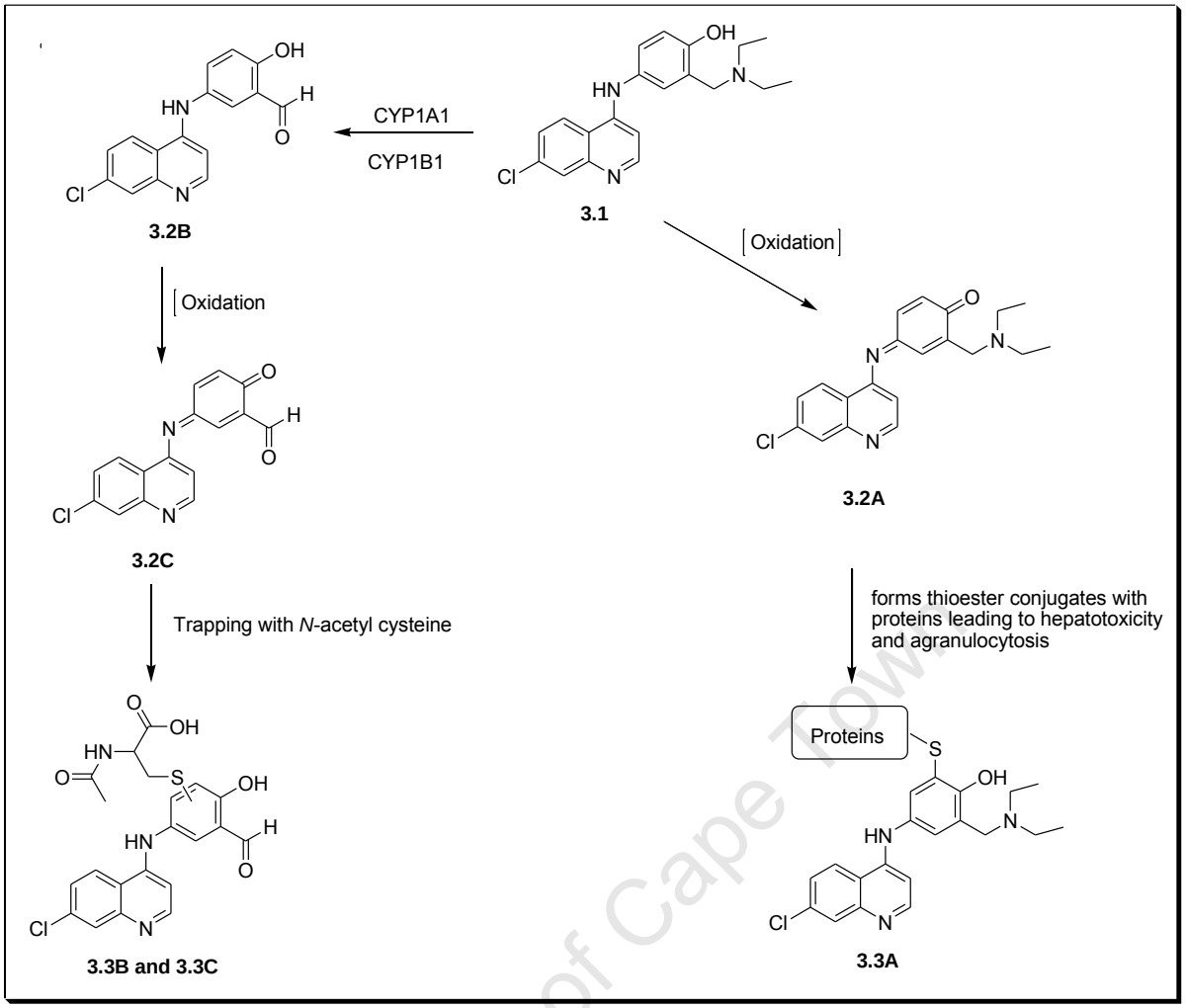

Scheme 3.1: CYP450 mediated biotransformation of amodiaquine and subsequent protein binding.

Recently, another metabolite (aldehyde, **3.2B**) of amodiaquine was identified from *in vitro* incubation studies of amodiaquine with recombinant human CYP1A1 and CYP1B1 enzymes.[18] Subsequent trapping of metabolite **3.2B** with *N*-acetyl cysteine revealed that this metabolite undergoes further oxidation into an aldehyde quinoneimine intermediate (**3.2C**) (Scheme 3.1), as evidenced by the formation of **3.3B** and **3.3C**. The formation of intermediate **3.2C** implies that aldehyde **3.2B** also has the potential to cause type II hypersensitivity reaction. However, no *in vivo* studies have so far been performed in order to establish whether or not this metabolite contributes to the toxicity of amodiaquine.

Various strategies for improving the toxicity profile of amodiaquine while retaining and/or bettering its activity involved modification of the Mannich base side-chain,[17,19] blockade of the biotransformation pathways,[20,21] and total replacement of the phenyl moiety.[22] Modification of the Mannich base side-chain with cyclic amines or with a *tert*-butylamino group resulted in compounds that were more active *in vivo* against *P. beghei* than amodiaquine. Moreover, interchanging the Mannich base side-chain and the hydroxyl group of the phenyl moiety of amodiaquine resulted in more metabolically stable compounds that had comparable activity to amodiaquine. Unfortunately, replacement of the phenyl ring has thus far not yielded any lead compound that is more active than amodiaquine.

Judging from various studies undertaken on amodiaquine, it appears that the blockade of the biotransformation pathway is a method of choice in developing new amodiaquine analogues, one of which is isoquine (also known as GSK369796) (**3.4**) (Fig. 3.3).[23] However, in 2008 the development of isoquine by Medicine for Malaria Venture (MMV), in partnership with GlaxoSmithKline (GSK) and the University of Liverpool was discontinued due to unexpected toxicity.[24]

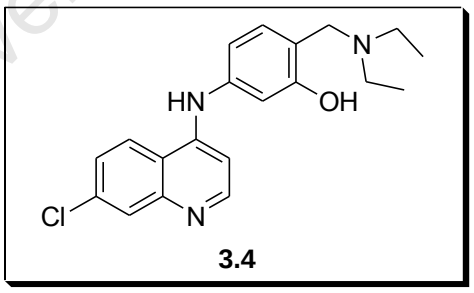

3.4

Figure 3.3: Isoquine, also known as GSK 369796.

Other modifications that have been performed on amodiaquine include replacement of the metabolically susceptible *p*-hydroxyl group with a fluorine (fluoroamodiaquines) or hydrogen atom (deoxyamodiaquines) in order to circumvent the formation of the quinoneimine metabolite.[25] However, these deoxyamodiaquines exhibited reduced activity when compared

to amodiaquine but their observed IC_{50} remain stable across all chloroquine-reistant strains. Recently, Chibale *et al*.,[26] utilized the deoxyamodiaquine scaffold fused with chalcones in developing potent inhibitors of Plasmodial and tumor growth. This suggests that fusion of deoxyamodiaquine scaffold "to appropriate moieties" could potentially deliver potent deoxyamodiaquine analogues. As such, the rationale adopted in this project involved the incorporation of a tetrazole moiety and protonatable nitrogen into the deoxyamodiaquine scaffold (Fig. 3.4). The substituent on the phenyl ring, which consists of the tetrazole and the tertiary amine, was varied between the *ortho*-, *meta*- and *para*-positions. Furthermore, the choice of the tertiary amine R-groups was based on favourable *in silico* ADME (Absorption, Distribution, Metabolism and Excretion) predictions and/or on commercial availability of the secondary amines.

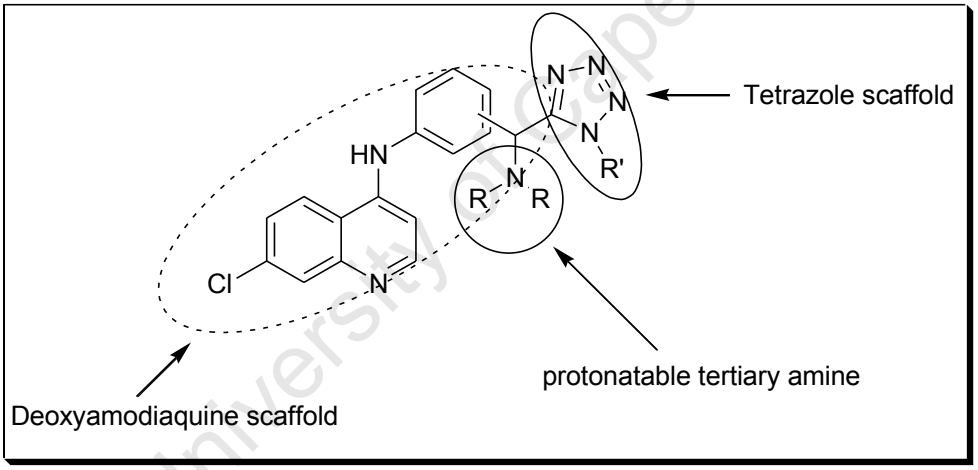

Figure 3.4: Rationale for the tetrazole-based deoxyamodiaquine target compounds.

3.4.1 *In Silico* profiling

Drug discovery programs have traditionally relied on identifying potential drug candidates through *in vitro* and/or *in vivo* screening, followed by optimization for potency and specificity for molecular targets while optimization of ADME parameters was reserved for clinical development.[27,28] However, this approach led to high attrition rates of drug candidates in late stages of development due to poor pharmacokinetic and ADME properties, which could have been addressed early on in the drug discovery process. In an attempt to

circumvent and/or reduce such attrition rates, *in silico* prediction tools are being utilized in selecting and eliminating compounds with ADME liabilities before any substantial resources are invested.[29,30] Thus, *in silico* ADME prediction models and tools complement *in vitro* and *in vivo* ADME experiments by facilitating the characterization of compounds prior to their synthesis, hence significantly reducing the costs involved.[31,32]

Models for predicting ADME parameters are usually based on empirical approaches such as quantitative structure-activity relationship (QSAR)[33] and/or quantitative structure-permeability relationship (QSPR)[27]. Chemometric methods such as multi-linear regression (MLR),[33] principal compact analysis (PCA),[35] and partial least square (PLS)[36] analysis are used in constructing QSAR/QSPR models. These models are often employed in programs such as Volsurf+[37,38] in predicting physico-chemical properties from molecular structures. Volsurf+ is an automated procedure for the conversion of 3D molecular interaction fields (MIFs) into simple physico-chemically relevant molecular descriptors.[39,40] A number of these descriptors are based on models of solubility, permeability, blood-brain barrier (BBB) and metabolic stability among others.

Bioavailability of an orally administered drug largely depends on solubility, permeability and metabolic stability.[41] In this study *in silico* prediction tools were applied in the ADME profiling of a focused library of proposed tetrazole-based deoxyamodiaquine compounds (Fig. 3.5). It is important to note that these predictions were merely used as a guide in these studies. The predicted Volsurf+ parameters were aqueous solubility at two pHs (5.0 and 7.5), Caco-2 permeability and metabolic stability of the proposed compounds. The style and format of the presentation of *in silico* results reported by Guantai *et al*.,[41] was followed and adopted in profiling the proposed compounds. In addition, amodiaquine was selected as a reference compound to be profiled and compared to the study compounds.

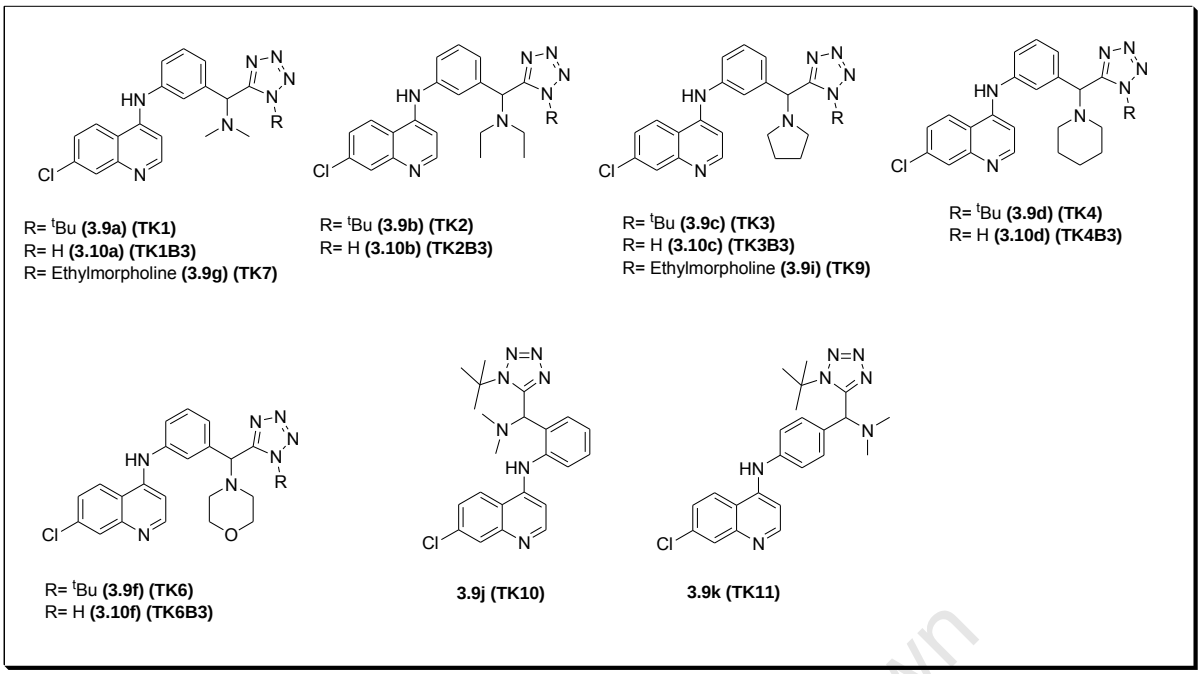

Figure 3.5: Structures of the proposed tetrazole-based deoxyamodiaquine compounds.

The majority of the proposed compounds had predicted aqueous solubilities that were comparable to that of the reference drug, amodiaquine, at both pH 5.0 and 7.5. However, two compounds, **3.9g** and **3.9i**, exhibited significantly superior predicted solubility compared to amodiaquine and other test compounds at pH 5.0 (Fig. 3.6A). This observation might be due to the fact that both these compounds contain an additional protonatable morpholine nitrogen attached to the tetrazole side-chain when compared to the other test compounds, and this is postulated to be aiding the ionization of these compounds at low pHs. Also not surprisingly, the free tetrazole-based compounds (grey) had a slightly superior predicted aqueous solubility compared to the protected analogues (yellow) at both pHs, except for compounds **3.9g** and **3.9i** at pH5.0. This is anticipated because the free tetrazole moiety usually possess a significantly high acidic and weak basic characteristics, an amphoteric character, and as such these would be ionized at both pHs, thus facilitating the solubility of the free tetrazole-based analogues.[42] The conclusion that can be drawn from this exercise is that the predicted aqueous solubility of the proposed compounds is significantly influenced by the two pH regions as anticipated.

The prediction of the Caco-2 permeability and metabolic stability were qualitative. The study sets of compounds were projected onto the inbuilt two-dimensional PLS scores plot to generate the Caco-2 permeation model. All the test compounds, including amodiaquine, showed acceptable predicted Caco-2 permeation, falling within the permeation (Blue) zone of the plot, indicating an efficacious permeation of intestinal epithelium cells (Fig. 3.6B).

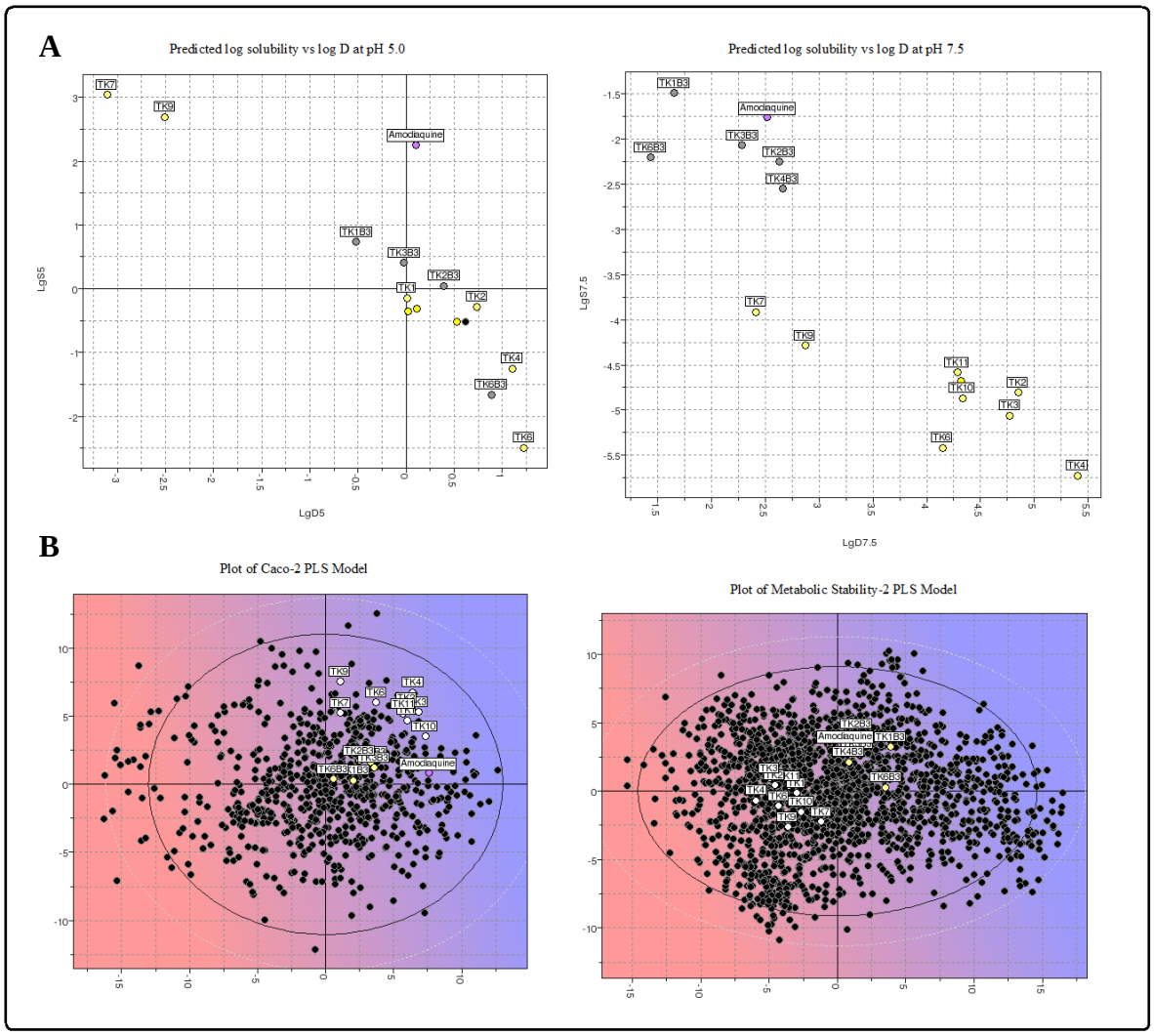

Figure 3.6: **A**: Plots of predicted solubility (log S) against predicted n-Octanol-water partition coefficient (log D) at pH 5.0 and 7.5; **B**: Plots showing the proposed compounds projected onto PLS models used to predict Caco-2 permeability and metabolic stability- the black dots represent compounds comprising the models' training data sets while the yellow and white dots represent the test compounds. The blue regions indicate acceptable predicted zones while the red region indicates poor predicted properties.

In addition, the free tetrazole-based compounds (yellow) were predicted to have an intermediate but acceptable metabolic stability that is comparable to amodiaquine, while the protected tetrazole (white) were shown to be less metabolically stable (red region) (Fig. 3.6B). To get a better picture of the metabolic pathway of the proposed compounds, MetaSite[43,44] was used to predict the site of metabolism (SOM). The site of metabolism refers to the part of the molecule where the metabolic reaction is predicted to occurs. MetaSite is a computational tool that is able to predict human cytochrome P450 (CYP450) mediated metabolism using only the 3D structure of the proposed compounds to generate the probable site of metabolism.[44] Furthermore, these 3D structures are automatically generated by the software in the cytochrome enzyme cavity from the 2D input structures.

Figure 3.7 shows the probable hepatic metabolic positions on each proposed compound as suggested by MetaSite; the blue circles indicate highest probable site of metabolism. For compounds **3.9a**, **3.10a**, **3.9g**, **3.9b** and **3.10b** the main routes of metabolism is predicted to be *N*-dealkylation of the tertiary amine of the alkyl side-chain, similar to amodiaquine. This predicted route of metabolism for amodiaquine is in agreement with the reported experimental observations, where the *N*-desethylamodiaquine is identified as the major metabolite.[14,45] In addition, *N*-oxidation of the quinoline moiety is also predicted to be another major route of metabolism for amodiaquine. However, this route is not favoured.[41] The protected tetrazole analogues contain an extra group (*i.e*. the *t*-butyl or the 4-ethylmorpholine group) that is predicted to be susceptible to metabolism, and this may partly explain why these are predicted to be less stable than the free tetrazole analogues.

In conclusion, at pH 7.5 the free tetrazole compounds were profiled to have predicted aqueous solubility that is similar to amodiaquine but superior to the other analogues. However, their predicted solubility at pH 5.0 was comparable to the other analogues except

for compounds **3.9g**, **3.9i** and amodiaquine, which had better solubilities. Furthermore, all the proposed compounds were predicted to have acceptable permeation on Caco-2 cells. The metabolic stability of the free tetrazole-based compounds was predicted to be superior on both Volsurf+ and MetaSite packages than the protected analogues. Overall, the free tetrazole analogues were predicted to have better physico-chemical properties than the protected ones.

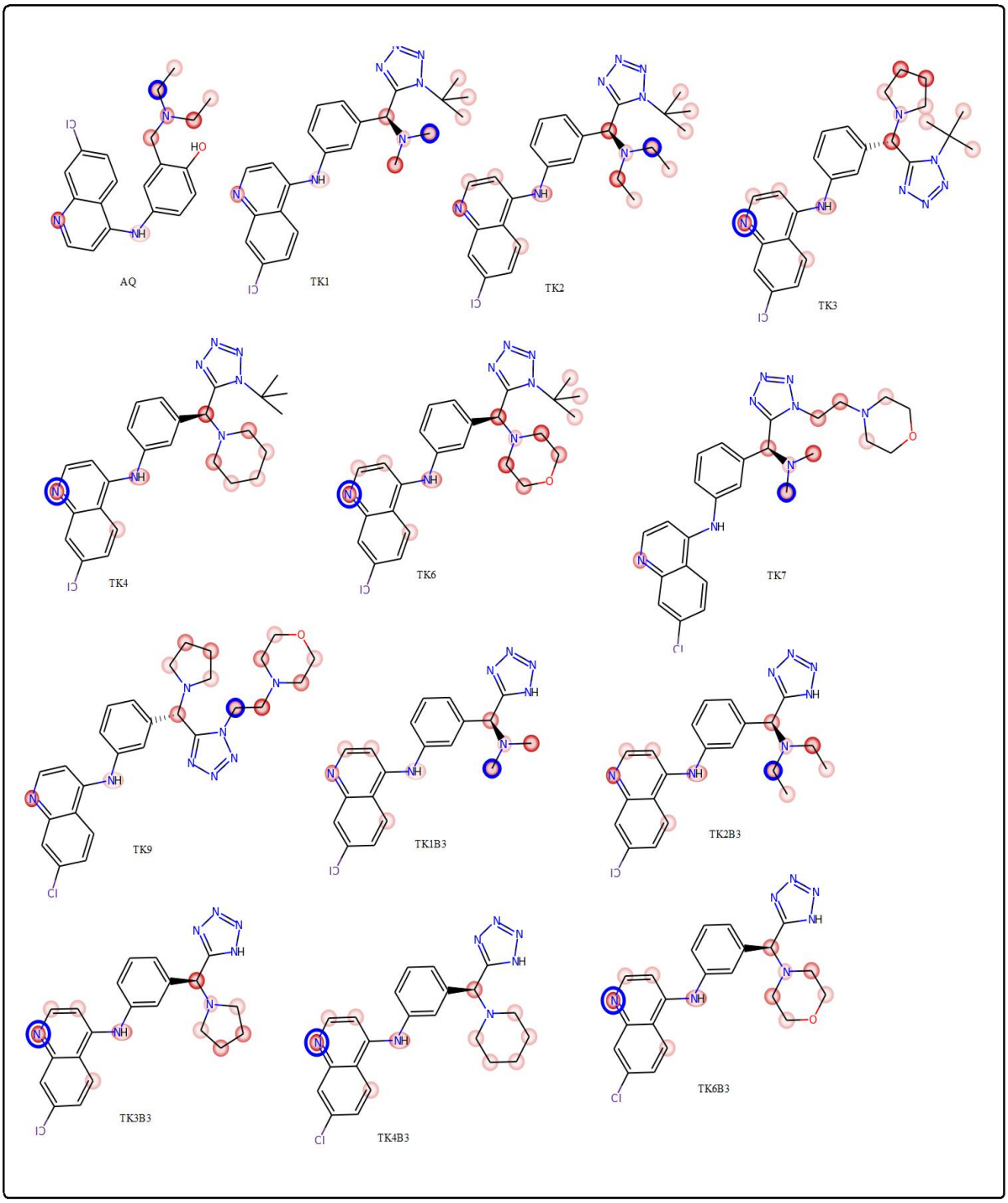

Figure 3.7: Predicted sites of metabolism of the proposed compounds obtained from MetaSite.

3.4.2 Synthesis of tetrazole-based deoxyamodiaquine derivatives

3.4.2.1 Retrosynthetic analysis

The synthesis of the target compounds (**3.10**) was envisaged as achievable from the de-*tert*-butylation of compounds (**3.9**) which in turn can be prepared from the modified $TMSN_3$-Ugi reaction. Intermediates **3.8** can be obtained from oxidation of benzyl alcohols (**3.7**) that would be synthesized from a nucleophilic aromatic substitution reaction of commercially available 4,7-dichloroquinoline (**3.6**) and various aminobenzyl alcohols (**3.5**) (Scheme 3.2).

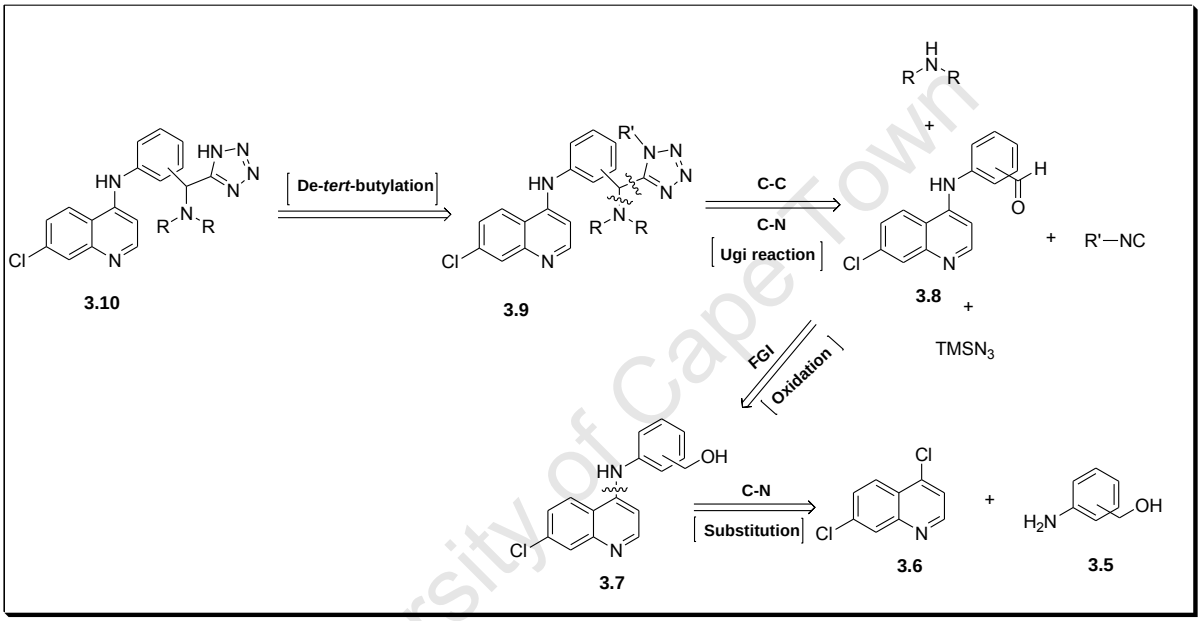

Scheme 3.2: Retrosynthesis of tetrazole-based deoxyamodiaquine compounds.

3.4.2.2 Synthesis

3.4.2.2.1 Synthesis of 4-aminoquinoline benzaldehydes

The procedure followed for the synthesis of the intermediate compounds (**3.8a-c**) was previously reported in our research group[26,46] and commenced with the preparation of 4-aminoquinoline benzyl alcohols (**3.7a-c**) in reasonable yields from the nucleophilic aromatic substitution reaction of aminobenzyl alcohols (**3.5a-c**) with 4,7-dichloroquinoline (**3.6**) in refluxing EtOH (Scheme 3.3). The *ortho*- and *meta*-quinoline-4-aminobenzyl alcohols (**3.7a-b**) were obtained as precipitates after 3 hrs of refluxing while the *para* analogue (**3.7c**) was obtained in low yields with an unidentified side product after 18 hrs. The possible reason for

the low yields observed for the *para*-analogue (**3.7c**) might be due to the rapid polymerization of the commercially available 4-aminobenzyl alcohol[47] at room temperature. Evidence of the correct products was confirmed by ^{1}H NMR spectra which had the characteristic singlet, or a doublet in some instances (due to coupling with the hydroxyl group), around 4.5 ppm that belongs to the benzylic methylene protons.

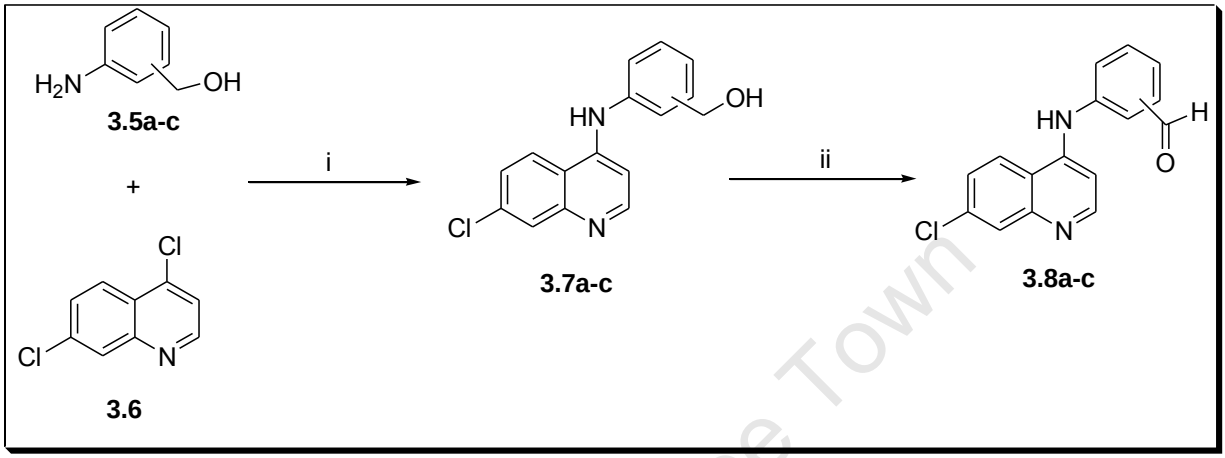

Scheme 3.3: *Reagents and conditions*: (i) EtOH, reflux at 85-90 °C, 3 hrs to 18hrs; (ii) SO_3.Py (2.0 eq), Et_3N (4.0 eq), DMSO, 26 °C, 3 days.

The quinoline-4-aminobenzaldehydes (**3.8a-c**) were then obtained in modest yields from the Parikh-Doering[48] oxidation of the primary quinoline-4-aminobenzyl alcohols (**3.7a-c**) (Scheme 3.3, Table 3.1). This reaction is analogous to the Swern oxidation[49] except that the oxayl chloride used to oxidise alcohols in the Swern reaction is replaced with a milder reagent, Py.SO_3. Complete oxidation was furnished after three days of stirring at 26 °C in anhydrous DMSO-Et_3N mixture. The main drawback of this reaction is the long reaction times required for the reaction to go to completion and the awful smell that results from the production of dimethylsulfide. The presence of the desired aldehydes (**3.8a-c**) was confirmed by NMR spectroscopy (^{1}H and ^{13}C) and mass spectrometry. Using compounds **3.8b** and precursor alcohol **3.7b** as an example, the disappearance of the key benzylic methylene protons resonating at approximately 4.5 ppm, and the appearance of a characteristic aldehyde

signal at approximately 10.0 ppm in the ^{1}H NMR spectra serve as confirmation of the oxidation of the alcohols (Fig. 3.8).

Table 3.1: Percentage yields of the intermediate products.

Entry	3.7	Yield/[%]	3.8	Yield/[%]
a	2-CH_2OH	25	2-CHO	87
b	3-CH_2OH	88	3-CHO	84
c	4-CH_2OH	30	4-CHO	19

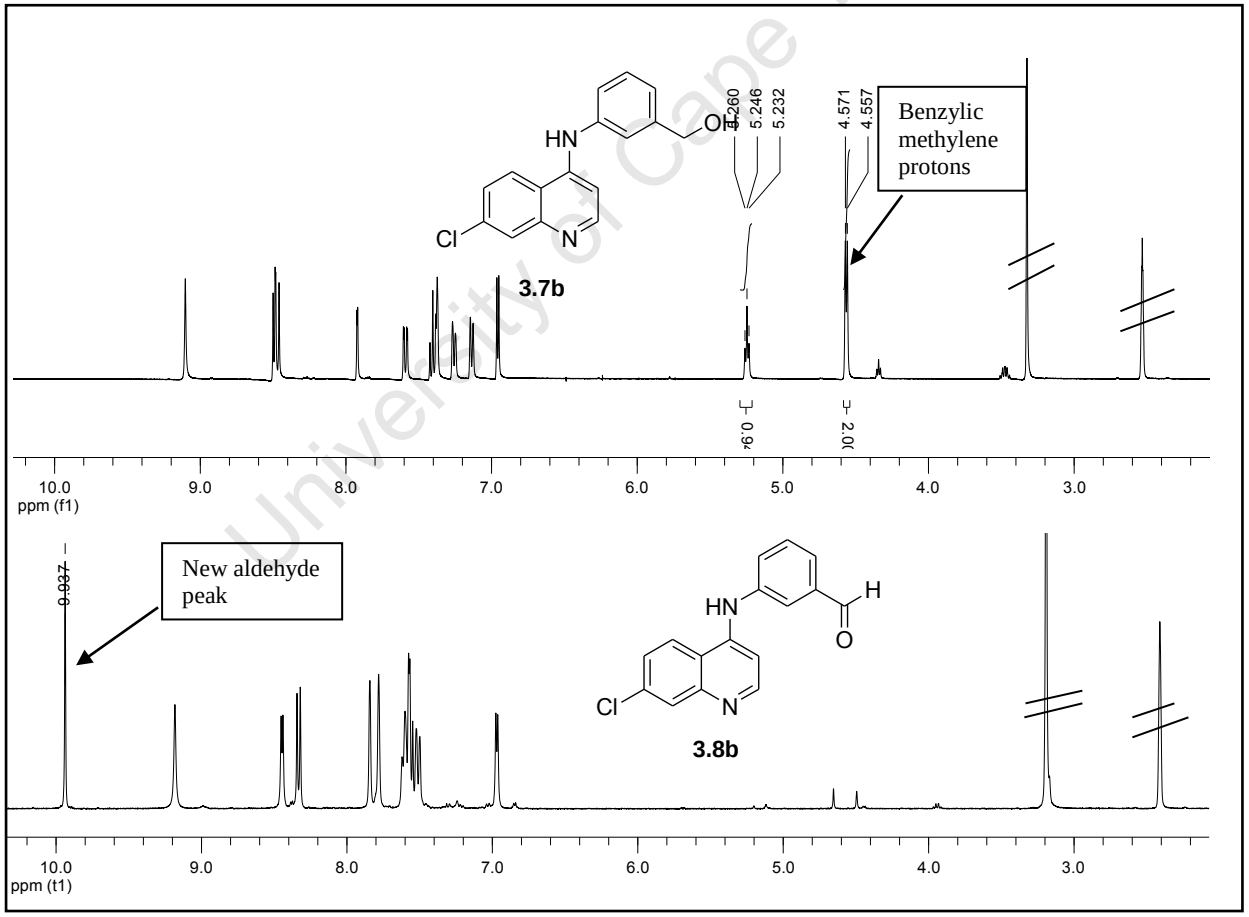

Figure 3.8: Superimposed 400 MHz ^{1}H NMR spectra of intermediates **3.7b** and **3.8b** in DMSO-d*6*.

3.4.2.2.2 Synthesis of tetrazole-based deoxyamodiaquine

The synthesis of the novel tetrazole-based deoxyamodiaquine derivatives was achieved using the multi-component reaction strategy. Following the modified $TMSN_3$-Ugi procedure described by Dömling *et al*.,[50] and Mayer *et al*.,[51] quinoline-4-aminobenzaldehydes (**3.8a-c**) were allowed to react at ambient temperature with various commercially available secondary amines and *tert*-butyl isocyanide or the 4-(2-isocyanoethyl)morpholine, in the presence of $TMSN_3$ in anhydrous MeOH for a period of 24 hrs. The reaction progress was monitored by thin layer chromatography (TLC). On completion of the reaction, the novel tetrazole-based deoxyamodiaquine compounds (**3.9a-k**) were obtained in moderate to good yields after purification by column chromatography (Scheme 3.4, Table 3.2). In addition, these compounds were further purified by high pressure liquid chromatography (HPLC) to give compounds with purity exceeding 98%.

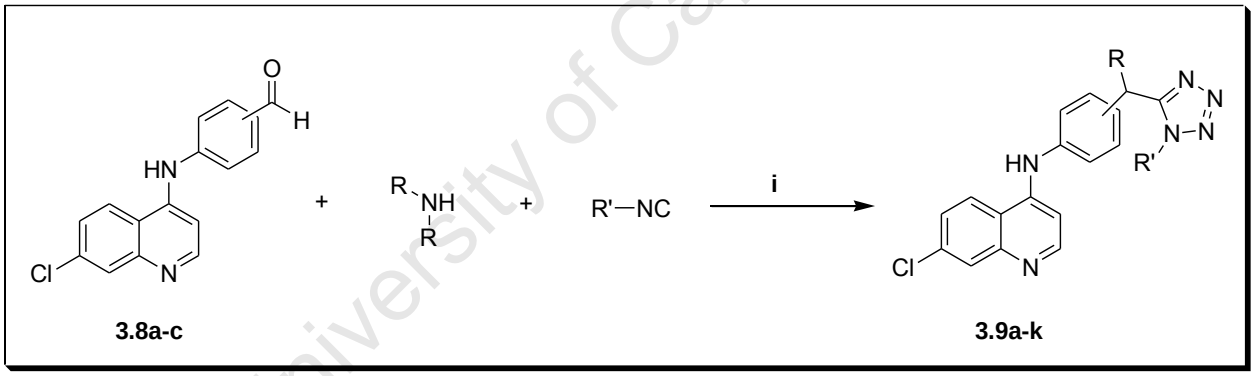

Scheme 3.4:. *Reagents and conditions*: (i) $TMSN_3$ (2.0 eq to the aldehyde and 1.0 eq to the other reagents used), MeOH, 25 °C, 24 hrs.

The generalized mechanism for the formation of target compounds (**3.9a-k**) is shown in Scheme 3.5. The reaction is initiated by the condensation of the aldehyde with the secondary amine to give rise to an intermediate (**A**), iminium ion, *in situ*. This iminium ion then reacts with an isocyanide *via* a nucleophilic addition reaction to form a key intermediate (**B**), the nitrilium ion. Azide trapping of this nitrilium ion produces intermediate (**C**), which undergoes sigmatropic rearrangement to give rise to the desired substituted tetrazole (**D**).[51,52]

Table 3.2: Yields and HPLC purity of synthesized target compounds, **3.9a-k**.

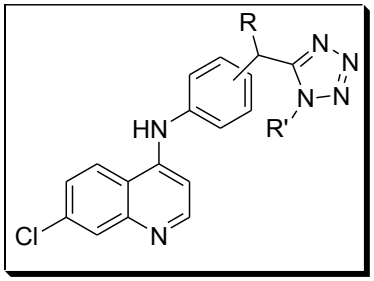

R'	Position	Code	Product	R	Yield/ [%]	HPLC‡ Purity/[%]
	*meta*	**TK1**	**3.9a**		86	99.5
	"	**TK2**	**3.9b**	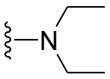	25	98.7
	"	**TK3**	**3.9c**	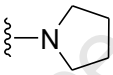	87	99.0
	"	**TK4**	**3.9d**	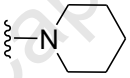	55	99.5
	"	**TK5**	**3.9e**	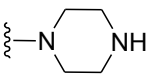	19	99.5
	"	**TK6**	**3.9f**	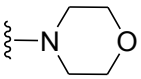	53	98.6
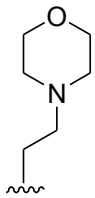	"	**TK7**	**3.9g**		35	97.5
	"	**TK8**	**3.9h**	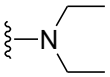	32	98.9
	"	**TK9**	**3.9i**	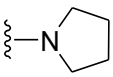	40	98.2
	*ortho*	**TK10**	**3.9j**		12	98.2
	para	**TK11**	**3.9k**		16	99.5

‡HPLC purity: purity judged from High Performance Liquid Chromatography.

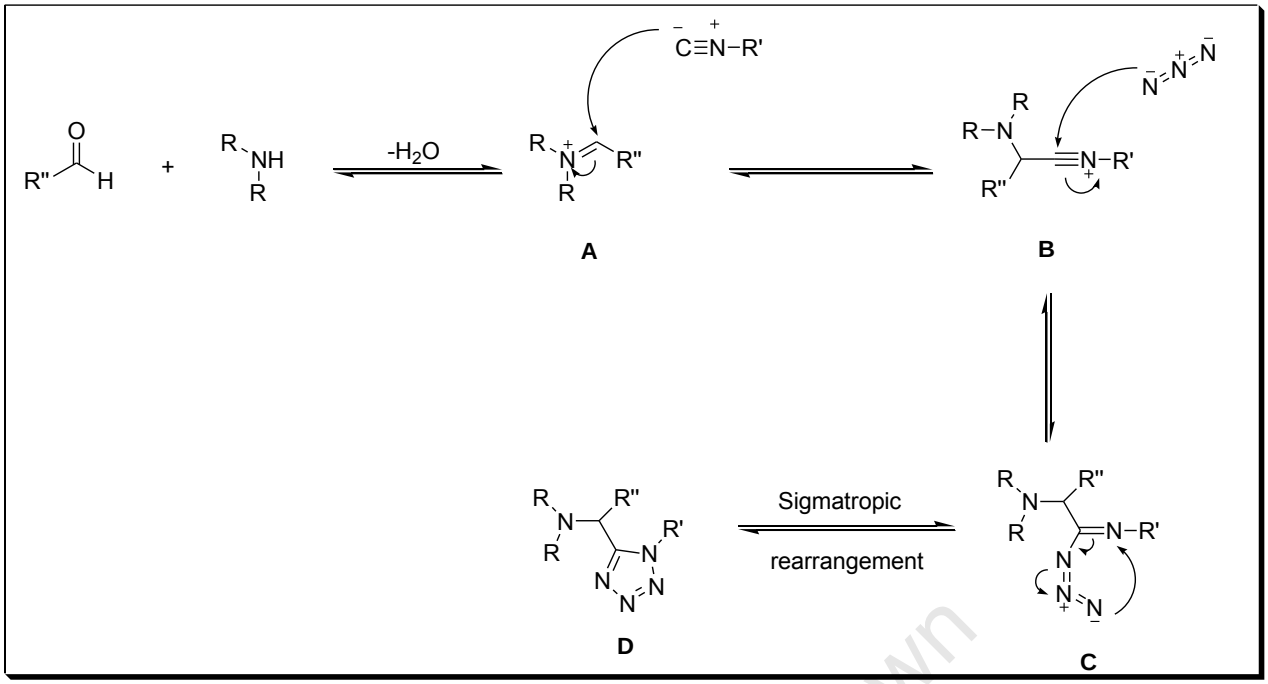

Scheme 3.5: Mechanism for the synthesis of tetrazole using $TMSN_3$-modified Ugi reaction.

The desired compounds (**3.9a**-**k**) were characterized by NMR spectroscopy (^{1}H and ^{13}C) and mass spectrometry. Figures 3.9 and 3.10 represent the ^{1}H and ^{13}C NMR spectra of representative compound **3.9a**. The absence of the characteristic aldehyde peak at approximately 10.0 ppm in the ^{1}H NMR spectrum served to confirm that the reaction did occur, and the singlets at 1.68, 2.27 and 5.50 ppm correspond to the H-14 *t*-butyl methyl, H-15 methyl, and H-13 methine protons, respectively (Fig. 3.9). These signals represent the new structural motifs that had been incorporated into the starting 4-aminoquinoline benzaldehydes. The C-13 is the newly created stereogenic centre in the final products. The signals resonating at 1.18, 2.00 and 4.04 ppm are due to the solvent peaks, *i.e.* ethyl acetate residual peaks. In Figure 3.10, the carbon peaks at 29.9, 40.2, 61.3 and 62.8 ppm correspond to these new structural features that are incorporated into the final product, while the rest of the signals are due to the starting 4-aminoquinoline benzaldehyde moiety.

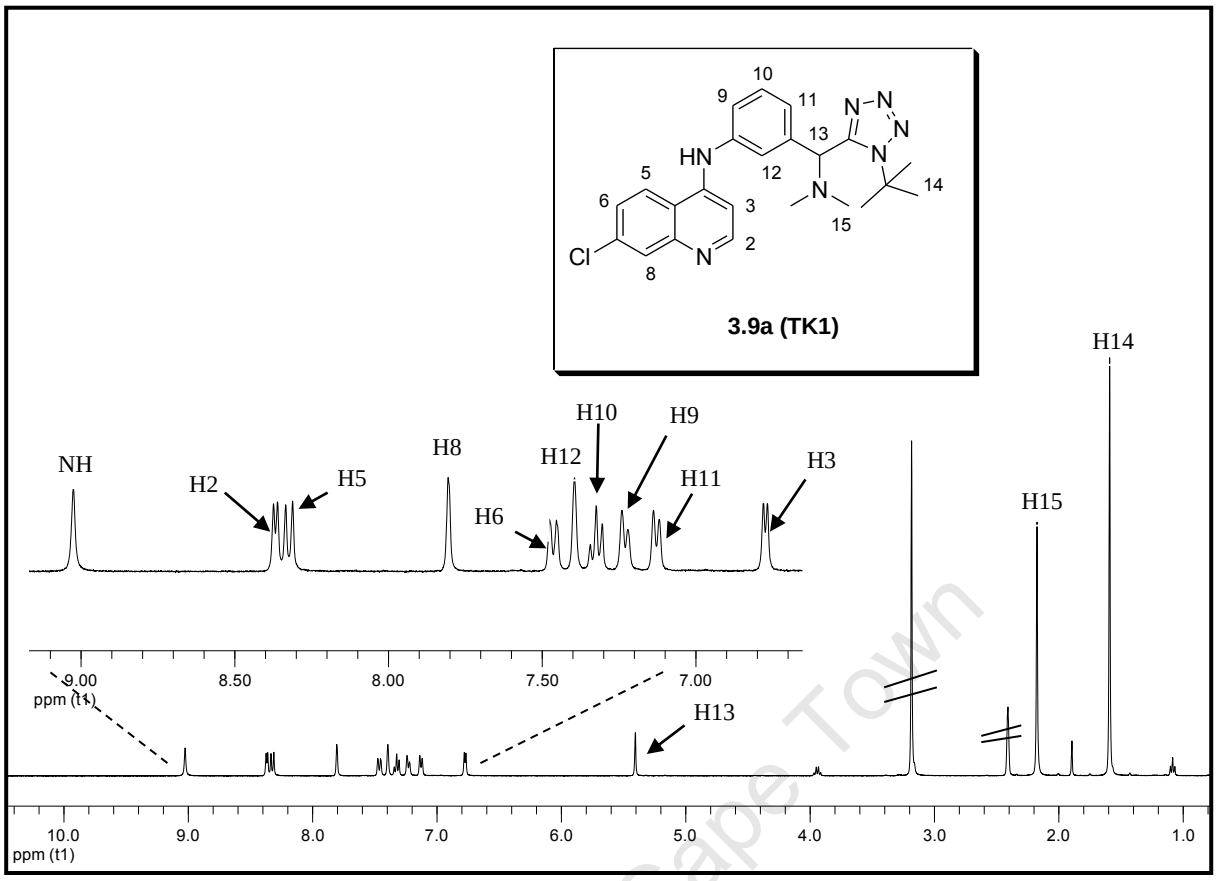

Figure 3.9: 400 MHz ^{1}H NMR spectrum of product **3.9a** in DMSO-*d6*.

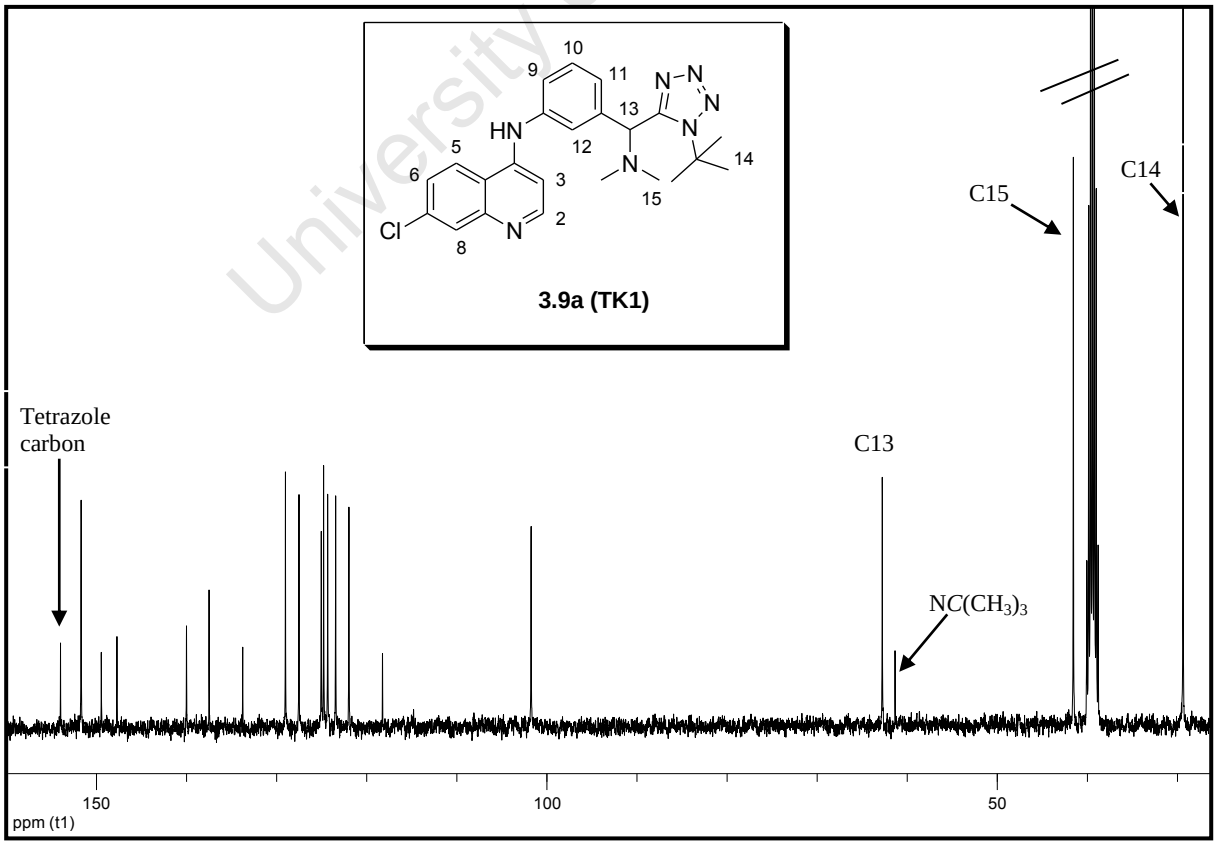

Figure 3.10: 100 MHz ^{13}C NMR spectrum of product **3.9a** in DMSO-*d6*.

3.4.2.2.3 Post MCR modification of previously synthesized target compounds

The next phase in the synthesis involved the deprotection of the tetrazole moiety in compounds synthesized in section 3.4.2.2.2. It is important to note that only the *tert*-butylated tetrazoles were deprotected in this study mainly due to the feasibility of the de-*tert*-butylation reactions. Furthermore, only the *meta*-substituted compounds (**3.9a-f**) were intentionally deprotected to provide representative compounds.

There are various methods reported in literature for the de-*tert*-butylation of the tetrazole ring. The majority of these methods use harsh reaction conditions such as refluxing strong mineral acids like hydrobromic acid (HBr)[53], sulphuric acid (H_2SO_4)[54], methanolic-hydrochloric acid (mixture of methanol and HCl gas)[55] *etc*, at high temperatures and long reaction times. However, in our study it was observed that the use of hydrobromic acid (40%) and sulphuric acid (98%) resulted in the destruction of the starting material as suggested by the complex TLC and ^{1}H NMR of the crude reaction mixture. It was also noted that when a "milder" methanolic-hydrochloric acid was used, no reaction occurred. This was evidenced by the recovery of starting material in the reaction flask. Thus, there was a need to find reaction conditions that fitted between these two extremes. The method that worked efficiently in our case involved heating the starting materials (**3.9a-f**) at 120 °C for 4 to 8 hours in neat hydrochloric acid (32%) (Scheme 3.6). Upon cooling and neutralization of the reaction mixture, the intended product (**3.10a-f**) precipitated in reasonable yields after standing overnight in the fume hood (Table 3.3). These compounds were then purified by HPLC (greater than 95 % purity) (Table 3.3) to give the desired products.

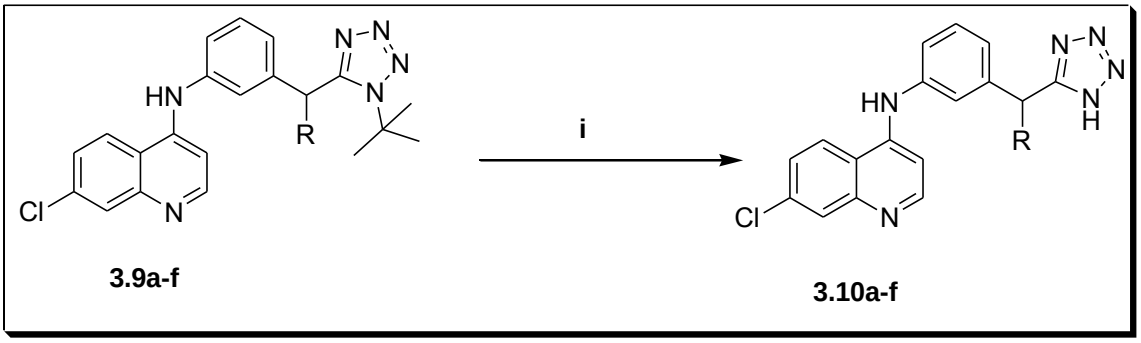

3.9a-f **3.10a-f**

Scheme 3.6: *Reagents and conditions*: (i) neat 32% HCl (excess), 120 °C, 4 to 8 hrs.

Table 3.3: Yields, melting points and and HPLC purity of the target compounds, **3.10a-f.**

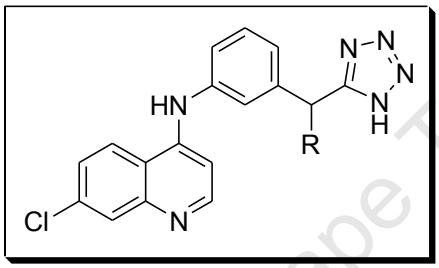

Code	Product	R	Yield/ [%]	HPLC Purity/[%]	Melting point/ [°C]
3.10a	**TK1B3**		59	98	174-176
3.10b	**TK2B3**	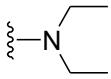	40	95.7	185-187
3.10c	**TK3B3**	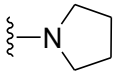	55	99.4	189-192
3.10d	**TK4B3**	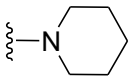	39	96.4	193-195
3.10f	**TK6B3**	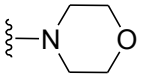	45	99.4	190-192

Scheme 3.7 shows a simplified mechanism for thermally induced de-*tert*-butylation of the tetrazole ring.[56] The initial phase of the mechanism is protonation of one of the tetrazole nitrogens (**I**). This then leads to the formation of a partially protonated tetrazole ring (**II**). The positive charge of the partially protonated tetrazole ring is subsequently delocalized around the ring due to the resonance effect from the neighbouring nitrogens, thus leading to a fully protonated and positively charged ring (**III**). This delocalization of the positive charge on the tetrazole ring facilitates the cleavage (or de-*tert*-butylation) of a relatively stable *tert*-butyl carbocation to form a free tetrazole ring system (**IV**). This "carbenium" further reacts spontaneously with the chloride ions *in situ* to form a colourless, volatile and flammable liquid, *tert*-butyl chloride (**V**), *via* the S_N1 reaction mechanism.[57,58]

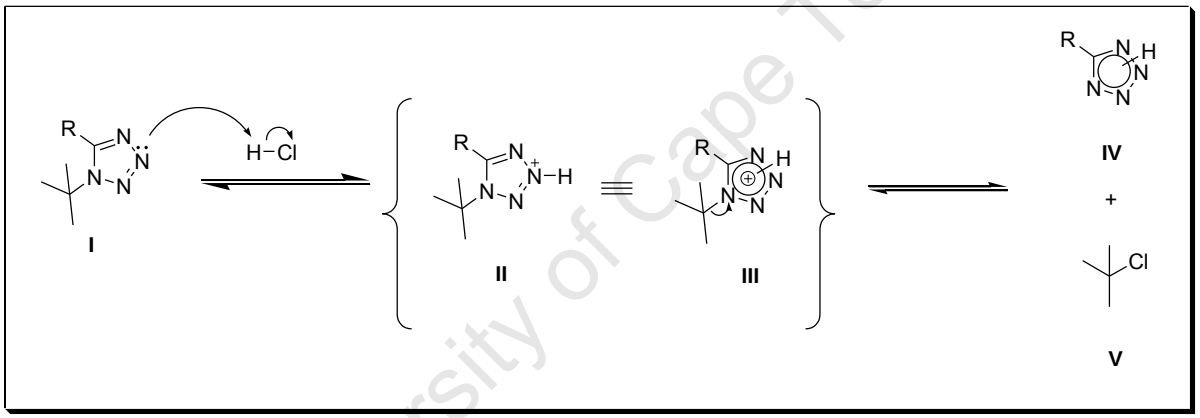

Scheme 3.7: Proposed mechanism for de-*tert*-butylation of tetrazoles.

The presence of the de-*tert*-butylated compounds was confirmed by NMR spectroscopy (^{1}H and ^{13}C) and mass spectrometry. Figure 3.11 shows superimposed ^{1}H NMR spectra of product **3.10a**, the desired de-*tert*-butylated product, and **3.9a**, the parent compound. The absence of the singlet at 1.68 ppm corresponding to the *tert*-butyl group (H-14) in the spectrum of compound **3.10a** when compared to that of compound **3.9a** is evident, thus confirming de-*tert*-butylation of the tetrazole ring.

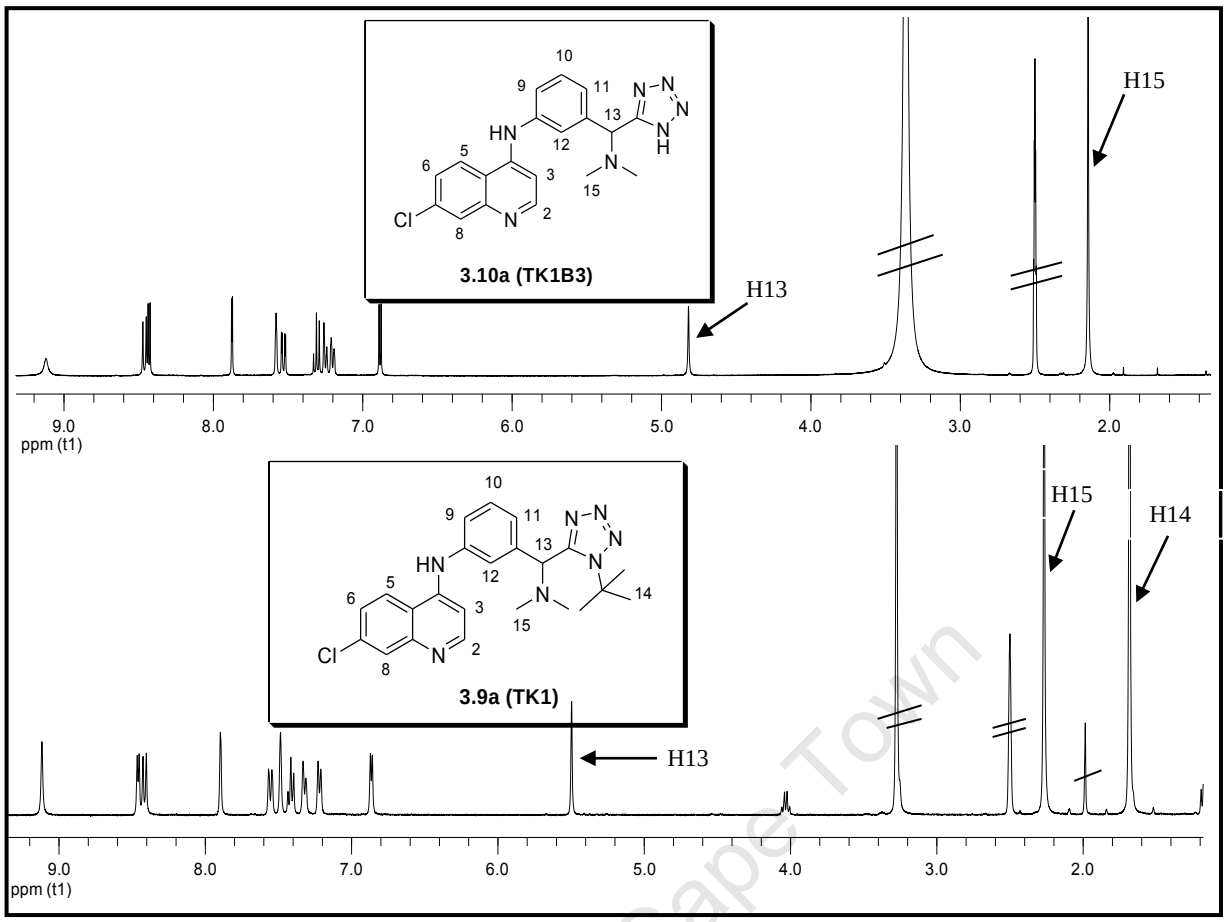

Figure 3.11: Superimposed 400 MHz ^{1}H NMR spectra of products **3.9a** and **3.10a** in DMSO-*d6*.

3.4.3 Experimental determination of solubility

Aqueous solubility was determined using a high-throughput plate-based kinetic solubility assay. This method measures the onset of precipitation of any given compound by absorbance change. Precipitation occurs when the maximum aqueous solubility level is reached, and solubility is measured using LC-UV spectrophotometry at 620 nm and the mass of the compound is confirmed by MS spectrometry.

Concentrations of 10mM stock solutions of test compounds were prepared in 100% DMSO, followed by dilution with phosphate buffered saline (PBS), pH 7.0 (and in some case pH 7.4), to 200 µM solutions. These dilutions were effected such that the final DMSO concentration does not exceed 2%. The 200 µM solutions were then shaken for 2 hours at 25 °C on an

orbital shaker and filtered, and the filtrate used to determine kinetic solubility. Aqueous solubility of each compound was ranked according to the following criteria: <5 μM = insoluble; 5- 50 μM = partially soluble; 50- 100 μM = soluble; and > 100 μM = highly soluble.

Experimentally determined kinetic solubility results at pH 7.0 of selected key compounds are shown in Table 3.4. These results corroborated the trend observed in the *in silico* solubility predictions described in section 3.4.1. The de-*tert*-butylated compounds were found to be highly soluble while the protected analogues varied from being insoluble to partially soluble.

Table 3.4: Results for experimentally determined kinetic solubility at pH 7.0

Code	Product	Solubility at pH 7.0 (μM)	Conclusion
TK1	**3.9a**	83.8 ± 2.97	soluble
TK2	**3.9b**	27.8 ± 0.86	Partially soluble
TK3	**3.9c**	1.70 ± 0.14	Insoluble
TK4	**3.9d**	2.31 ± 0.15	Insoluble
TK1B3	**3.10a**	65.5 ± 6.08	soluble
TK2B3	**3.10b**	207 ± 6.08	Highly soluble
TK3B3	**3.10c**	191 ± 1.66	Highly soluble
TK4B3	**3.10d**	207 ± 3.48	Highly soluble
Amodiaquine HCl		Did not dissolve in DMSO[a]	

[a] Tested at pH 7.4.

3.5 Chloroquine-based tetrazole compounds

Chloroquine (**3.11**) (Fig. 3.12), a 4-aminoquinoline drug, has a long history of being a first choice antimalarial drug. However, widespread resistance to chloroquine and other quinoline-based antimalarials has exacerbated the problem of endemic malaria. Various researchers have postulated and shown that lengthening or shortening the chloroquine alkyl side chain leads to compounds which are effective against drug-resistant strains.[59] However, recently Roepe *et al.*,[60] concluded that these observations only hold for quinolone derivatives with the

diethyl substituetnt on the terminal nitrogen. Although, there is still some debate among researchers regarding the influnce that result from the modification of the alkyl side-chain length, they all however agree that these modifications do not improve the metabolic stability of these chloroquine derivatives, especially *N*-dealkylation at the terminal tertiary amine that is normally observed in chloroquine and/or amodiaquine. This *N*-dealkylation at the terminal tertiary amine has been shown to be the cause of a reduced lipid solubility of these drugs, and as such it increases the potential for cross-resistance with chloroquine.[61] As a result of this observation, Stocks *et al*.,[62] and Madrid *et al.*,[63] suggested and showed that substitutions on the terminal tertiary amine by a bulkier group increased the *in vivo* efficacy and decreased the potential for emergency of cross-resistance, presumably by circumventing metabolic *N*-dealkylation. The mode of action of chloroquine is believed to involve the inhibition of polymerization of the toxic heme inside the digestive food vacuole of the parasite.[64]

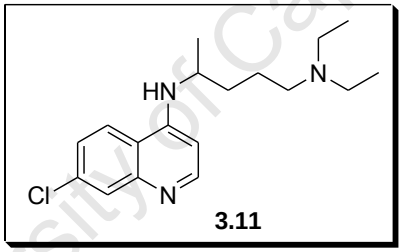

3.11

Figure 3.12: Chloroquine, an antimalarial drug.

Considering the facts highlighted above, the rationale for the design of the target compounds included an attempt to circumvent metabolic *N*-dealkylation of the tertiary amine by incorporating bulkier substituents such as the aromatic and tetrazole rings, while varying the length of the 4-amino alkyl side-chain in the proposed target compounds (Fig. 3.13). With the incorporation of the tetrazole ring, it was hypothesized that this would also significantly enhance the physico-chemical and ADME properties of these target compounds.

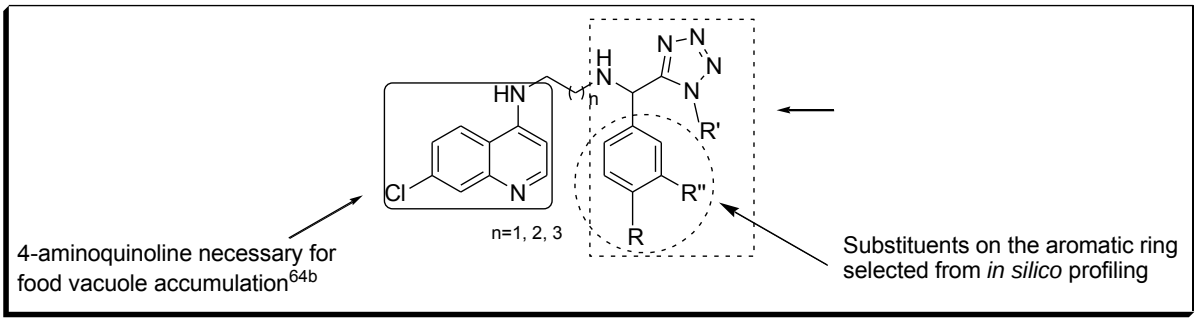

Figure 3.13: Rationale design for chloroquine-based target compounds.

3.5.1 *In Silico* profiling

In light of the rationale given above, the aim of performing *in silico* profiling in this sections was to get a sense of the metabolic degradation of the designed compounds. During the design, emphasis was placed specifically on circumventing *N*-dealkylation of the terminal amine found in 4-aminoquinoline alkyl side-chain by introducing bulkier substituents. Thus, the discussion in this section will only focus on this aspect of *in silico* profiling. Figure 3.14 shows a series of 14 chloroquine-based tetrazole compounds that were profiled *in silico* for metabolic stability. In addition, the route of metabolism was also investigated *via* the *in silico* predictions in order to confirm the circumvention of *N*-dealkylation in these new analogues.

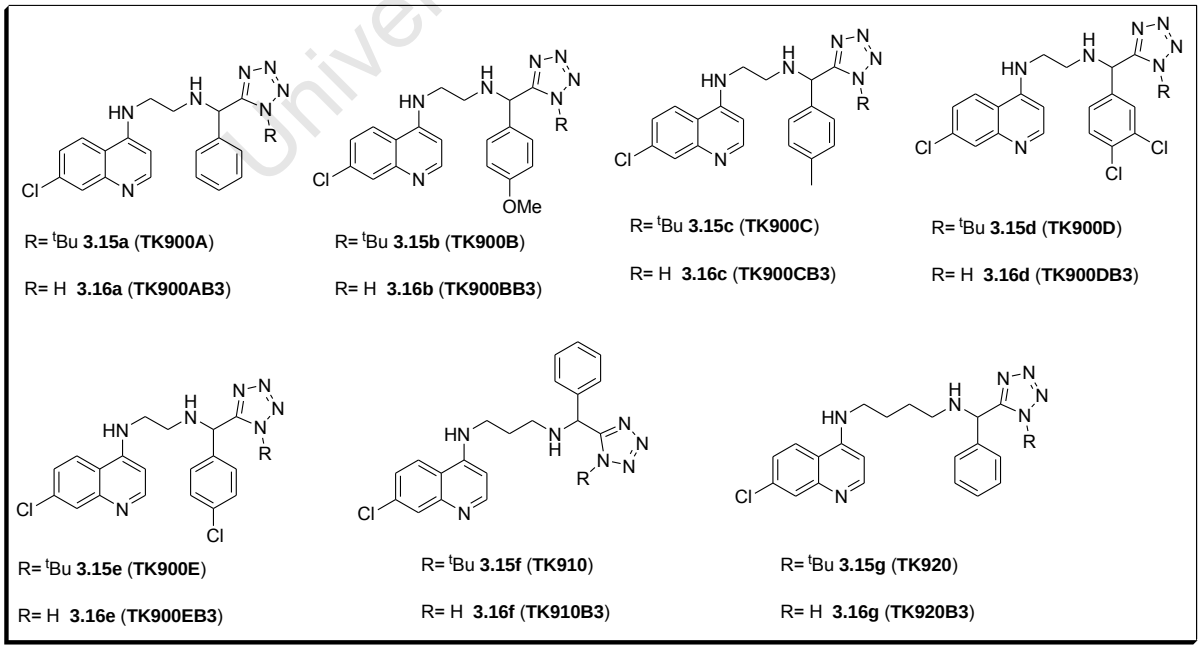

Figure 3.14: Structures of tetrazole-based chloroquine compounds.

Chloroquine (**3.11**) was selected as a reference compound and compared to the designed chloroquine-based tetrazole compounds. The metabolic stability trend observed on the deoxyamodiaquine analogues (section 3.4.1) was also evident in this class of compounds, and this is to be expected since all these are 4-aminoquinoline-based compounds. The free tetrazole compounds (white) were predicted to have acceptable metabolic stabilities which were comparable to and in some instances better than chloroquine, while the protected tetrazoles (yellow) were shown to be metabolically unstable (red region) (Fig. 3.15).

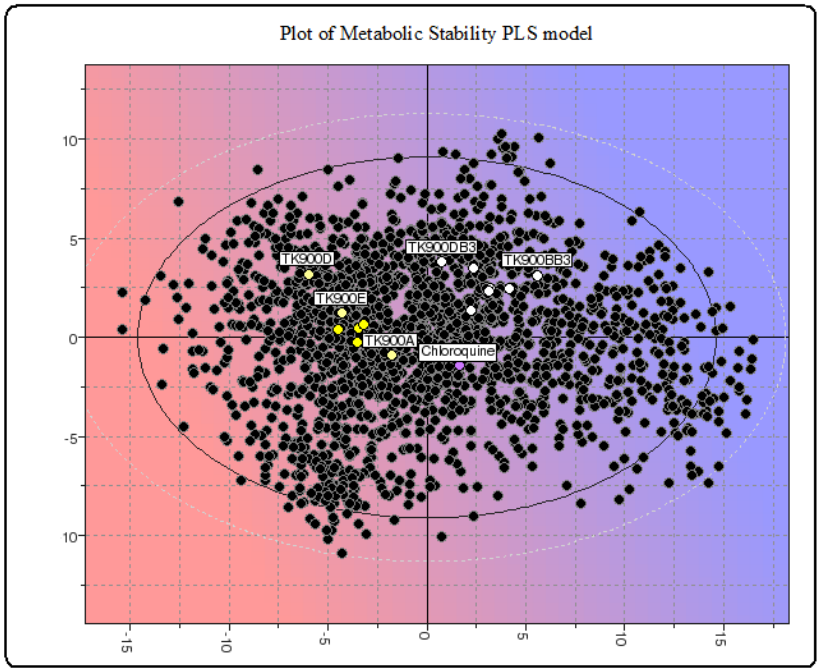

Figure 3.15: Plot of the proposed compounds projected onto metabolic stability PLS models.

As mentioned earlier the route of metabolism of these compounds was investigated by MetaSite. Again, the software predicted correctly the experimentally observed metabolite of chloroquine, *N*-desethylchloroquine (Fig. 3.16).[62,65,66] *N*-oxidation of the quinoline moiety was predicted to be the major route of metabolism for most of these compounds, except for **3.15b** and **3.16b**, which were predicted to undergo *O*-demethylation of the *para*-methoxy group of the phenyl ring. In addition to the above mentioned likely sites of metabolism, *p*-hydroxylation of the phenyl ring was predicted to be another possible route of metabolism for compounds **3.15a**, **3.16a**, **3.15f**, **3.16f**, **3.15g**, and **3.16g**. Furthermore, aromatic methyl

oxidation was predicted to be another likely route of metabolism for compounds **3.15c** and **3.16c**. Similar to the deoxyamodiaquine series, the protected tetrazole compounds were predicted to be less stable than the unprotected compounds. In summary, these predictions appear to suggest that *N*-dealkylation of the terminal amine alkyl side-chain is not a major route of metabolism in these proposed compounds.

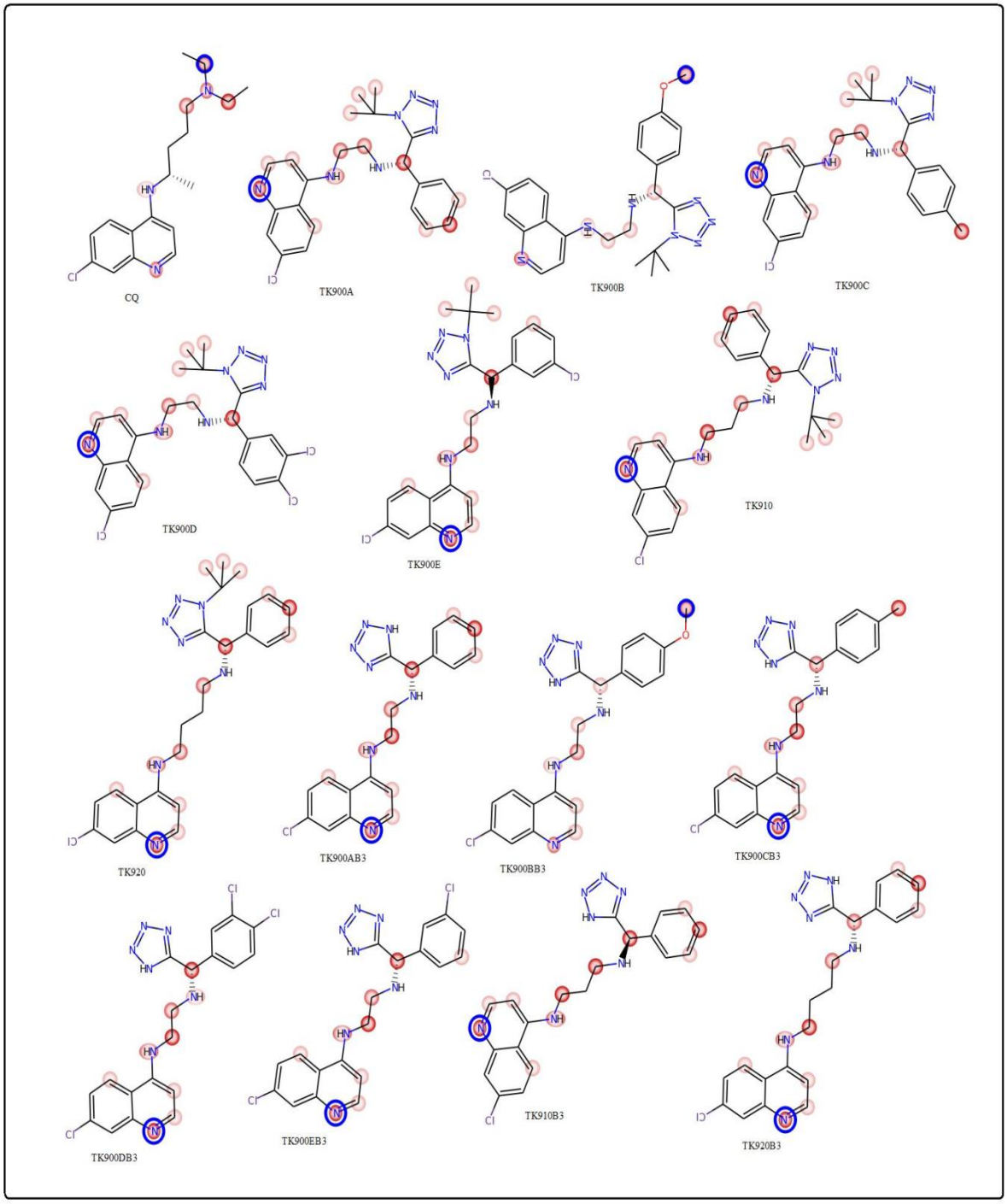

Figure 3.16: Predicted sites of metabolism of chloroquine-based tetrazole compounds.

3.5.2 Synthesis of chloroquine-based tetrazole derivatives

3.5.2.1 Synthesis of precursor quinoline diamines

The synthesis of the precursor quinoline diamines (**3.13a-c**) was achieved following known standard procedures reported in literature.[67,68,69] A nucleophilic substitution reaction involving excess diamines (**3.12a-c**) (5.0 equivalents) and 4,7-dichloroquine (**3.6**) in neat reflux gave the desired quinoline diamines (**3.13a-c)** in good yields (Scheme 3.8, Table 3.5). The required quinoline amines were confirmed by NMR spectroscopy (^{1}H and ^{13}C) and by comparison of their melting points with those reported in literature[68].

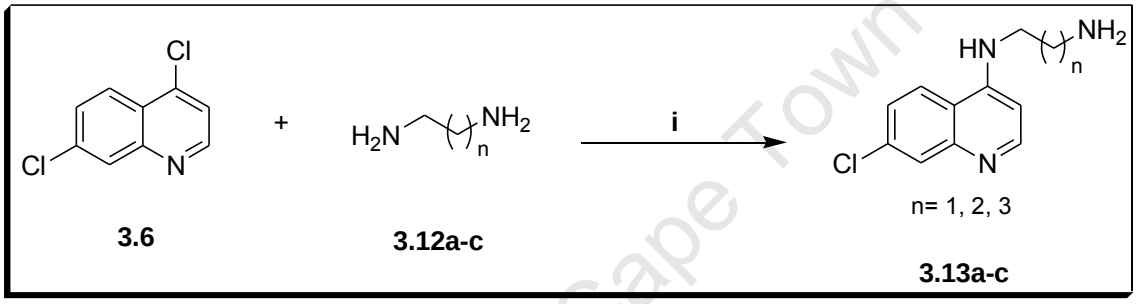

Scheme 3.8: *Reagents and conditions*: (i) Neat reflux 80 °C, 1 hrs, then 135 °C, 4 hrs.

Table 3.5: Yields and melting points quinoline amines, **3.13a-c.**

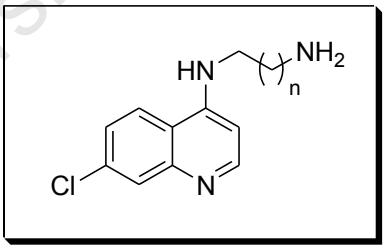

Compound	n	Yield/[%]	Melting point/[°C]	
			Measured	Literature[66]
3.13a	1	65	138-140	137-139
3.13b	2	66	120-122	124-127
3.13c	3	77	40-41	43-47

3.5.2.1.1 Mechanistic comments

Before one can fully appreciate the mechanism of this nucleophilic substitution reaction, reactivity of the quinoline ring towards nucleophiles needs to be explained first; Quinoline (**I**) is a fused benzo[*b*]pyridine heterocyclic system, and as such its reactivity can be likened to that of benzene towards nucleophiles, and to that of pyridine towards electrophiles. The quinoline nitrogen atom causes the ring to be π-electron deficient through mesomeric and inductive effects, which are largely felt at the C-2 and C-4 positions due to their close proximity to the nitrogen atom (Fig. 3.17).[70] Thus, these two positions are susceptible to nucleophilic attack and their reactivity is further enhanced by the presence of electron-withdrawing substituents such as halogens in the ring. In the mechanism, nucleophilic attack at position C-4 by the amine (nucleophile) is facilitated by the nitrogen atom's ability to act as an electron 'sink', and by resonance effect, which drives the observed regioselectivity (Scheme 3.18).

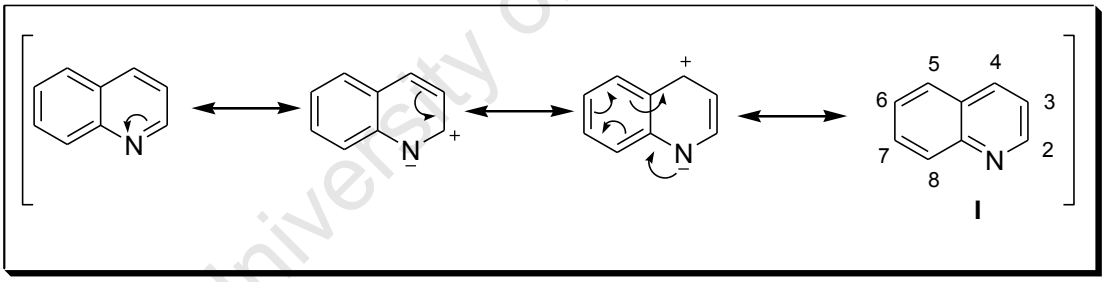

Figure 3.17: Canonical structures for the inductive and mesomeric effects of the quinoline nitrogen.

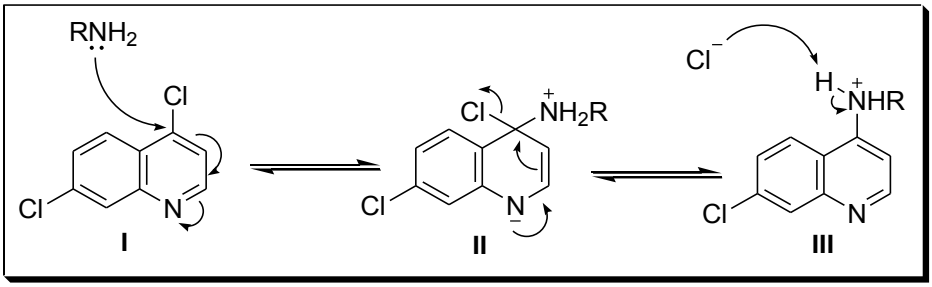

Figure 3.18: Mechanism of formation of 7-chloroquinoline-4-amine derivatives.

3.5.2.2 Synthesis of the target compounds

The quinoline diamines (**3.13a-c**) were then reacted with various aromatic aldehydes (**3.14**) following a similar procedure used in the synthesis of deoxyamodiaquine-based target compounds, except these reactions were conducted at 40 °C instead of 26 °C. Target compounds (**3.15a1-a5**, **3.15b** and **3.15c**) were obtained in poor to moderate yields after purification by column chromatography (Scheme 3.9, Table 3.6). Thereafter, these compounds were deprotected by refluxing at 120 °C in neat hydrochloric acid over a period of 8 hours to give the free tetrazole-based target compounds (**3.16a1-a5**, **3.16b** and **3.16c**), also in low to moderate yields (Scheme 3.9, Table 3.6). All the synthesized compounds were purified to acceptable levels of purity by HPLC. In addition, characterization was achieved by NMR spectroscopy (^{1}H and ^{13}C) and mass spectrometry.

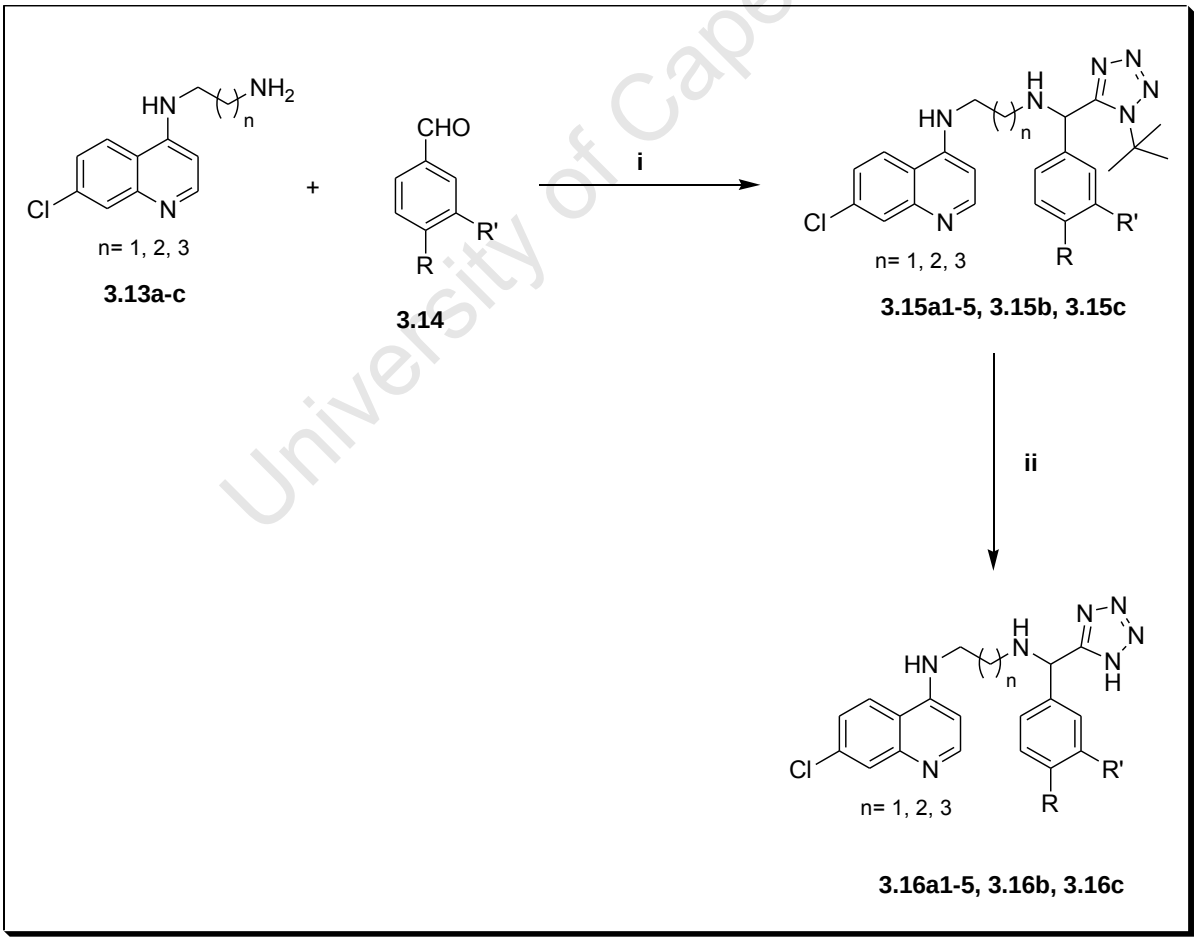

Scheme 3.9: *Reagents and conditions*: (i) $TMSN_3$ (1.0 eq), *t*-Butyl isocyanide (1.0 eq), MeOH, 40 °C, 24 hrs; (ii) neat 32% HCl (excess), 120 °C, 4 to 8 hrs.

Table 3.6: Yields and HPLC purity of the chloroquine-based target compounds.

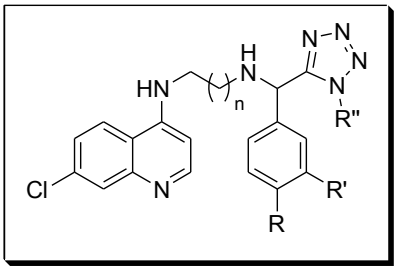

Compound	Code	n	R''	R'	R	Yield/[%]	HPLC Purity/[%]
3.15a1	**TK900A**	1	^{t}Bu	H	H	65	98.5
3.15a2	**TK900B**	1	^{t}Bu	H	OCH_3	57	99.0
3.15a3	**TK900C**	1	^{t}Bu	H	CH_3	61	99.5
3.15a4	**TK900D**	1	^{t}Bu	Cl	Cl	11	99.2
3.15a5	**TK900E**	1	^{t}Bu	H	Cl	28	99.5
3.15b	**TK910**	2	^{t}Bu	H	H	51	96.5
3.15c	**TK920**	3	^{t}Bu	H	H	57	95.9
3.16a1	**TK900AB3**	1	H	H	H	8	99.0
3.16a2	**TK900BB3**	1	H	H	OCH_3	38	97.4
3.16a3	**TK900CB3**	1	H	H	CH_3	31	98
3.16a4	**TK900DB3**	1	H	Cl	Cl	58	99
3.16a5	**TK900EB3**	1	H	H	Cl	27	99.2
3.16b	**TK910B3**	2	H	H	H	52	98.3
3.16c	**TK920B3**	3	H	H	H	72	97.6

The superimposed ^{1}H NMR spectra confirming the presence of the desired products **3.15a1**, **3.15b** and **3.15c** is shown in Figure 3.19. The main differences between the spectra of these compounds are the extra signals due to the methylene and twice the methylene protons for compounds **3.15b** and **3.15c**, respectively, when compared to the spectrum of compound **3.15a1**. Since all the other inputs were constant in the synthesis of these compounds, the aromatic region is similar in all cases. Furthermore, the observed singlets resonating at approximately 5.3- 5.6 ppm are due to the protons of the newly created stereogenic centre, thus confirm the presence of the desired products.

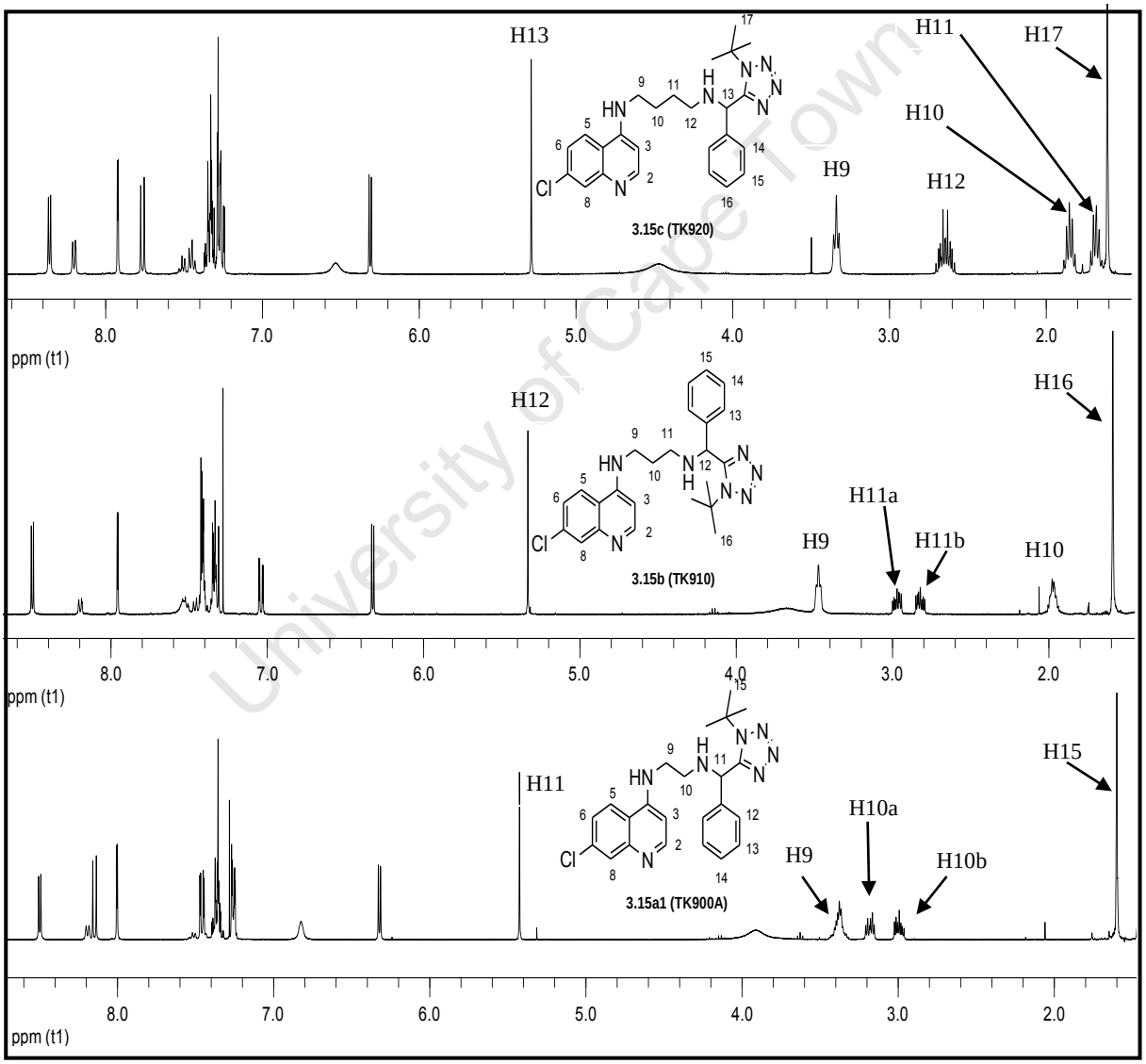

Figure 3.19: Superimposed 400 MHz ^{1}H NMR spectra of products **3.15a1**, **3.15b** and **3.15c** in $CDCl_3$.

Confirmation of the deprotected compounds is exemplified by the superimposed ^{1}H NMR spectra of compounds **3.15a2** and **3.16a2** (Fig. 3.20). It is important to note that the two compounds were analyzed in two different solvents ($CDCl_3$ and DMSO-*d6*). However, the spectra suffice in terms of comparison purposes. From the ^{1}H NMR spectrum of compound **3.16a2**, the absence of a singlet resonating at 1.62 ppm which corresponds to the three methyl protons of the *tert*-butyl group when compared to that of compound **3.15a2** confirms the de-*tert*-butylation of the tetrazole ring. Furthermore, all the other signals are accounted for and appear to be similar in both spectra as expected since the only difference between the two compounds is the absence of the *tert*-butyl group in compound **3.16a2**.

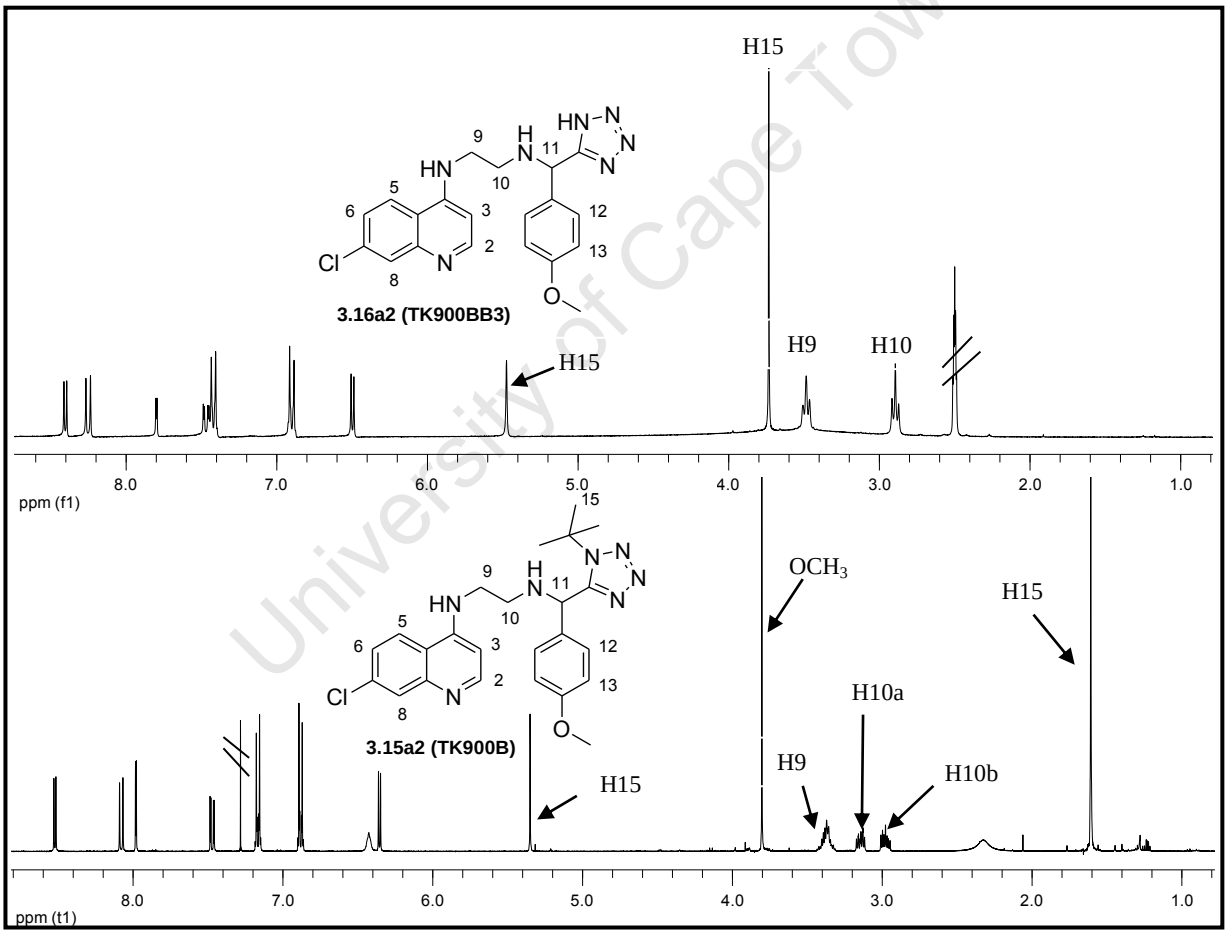

Figure 3.20: Superimposed 400 MHz ^{1}H NMR spectra of **3.15a2** in $CDCl_3$ and **3.16a2** in DMSO-d_6.

3.5.3 Experimental determination of solubility

Similar to the deoxyamodiaquine-based compounds, the de-*tert*-butylated chloroquine-like compounds exhibited superior aqueous solubility than the protected analogues (Table 3.7). However, the majority of compounds in this series had acceptable solubilities, with **3.16a5** (207 ± 4.08 µM) being the most soluble at pH 7.0 while **3.15a4** (30.3 ± 0.47 µM) was the least soluble. Also, compounds **3.15b** and **3.15c** were found to be insoluble (< 5 µM). Commercially available chloroquine diphosphate was not determined because it was insoluble in 100% DMSO.

Table 3.7: Results for experimentally determined solubility at pH 7.0

Code	Product	Solubility at pH 7.0 (µM)	Conclusion
TK900A	**3.15a1**	181 ± 4.76	Highly soluble
TK900C	**3.15a3**	110 ± 2.25	Highly soluble
TK900D	**3.15a4**	30.3 ± 0.47	partially soluble
TK900E	**3.15a5**	119 ± 1.16	Highly soluble
TK910	**3.15b**	<5[a]	Insoluble
TK920	**3.15c**	<5[a]	Insoluble
TK900DB3	**3.16a4**	143 ± 2.77	Highly soluble
TK900EB3	**3.16a5**	207 ± 4.08	Highly soluble
TK910B3	**3.16b**	157.23[a]	Highly soluble
TK920B3	**3.16ac**	196.12[a]	Highly soluble
Chloroquine diphosphate		Did not dissolve in DMSO[a]	

[a] Kinetic solubility performed at pH 7.4

3.6 Primaquine-based target compounds

Primaquine (**3.17**), an 8-aminoquinoline derivative, is currently the only available antimalarial drug that is active against both *Plasmodium vivax* and *Plasmodium ovale* latent liver forms of relapsing malaria.[71] Primaquine is also the only available transmission-blocking (from human host to mosquitoes) antimalarial drug which is active against the gametocytes from all species of parasite causing human malaria, including chloroquine-

resistant *P. falciparum*.[72] Recently, for the first time Lougheed *et al*.,[73] observed anti-tuberculosis activity of primaquine and suggested that this scaffold could represent a new class of anti-TB drugs with a novel mode of action against the *M. tuberculosis* pathogen. On this basis it may be hypothesized that primaquine and its analogues could potentially find use in killing the dormant forms of *M. tuberculosis* bacteria given their activity against the dormant liver forms of the malaria parasite. However, this speculation remains to be proven experimentally. As effective as primaquine is, its clinical use is impaired by toxic side effects such as its implication in hemolytic anaemia in humans who are glucose-6-phosphate dehydrogenase (G6PD) deficient, a genetic condition commonly associated with African males, and intravascular hemolysis in pregnant women.[74] Primaquine is rapidly metabolized *via* deamination into its inactive but toxic metabolite, carboxyprimaquine (**3.18**), which causes blood toxicity as a result of an induced oxidation of oxyhemoglobin to methemoglobin.[63] Thus, there is a dire need for the design and synthesis of novel primaquine derivatives which are devoid of the formation of **3.18**, but exert the same or improved efficacy against all forms of the human malaria parasite and *M. tuberculosis* without the associated toxic side-effects.

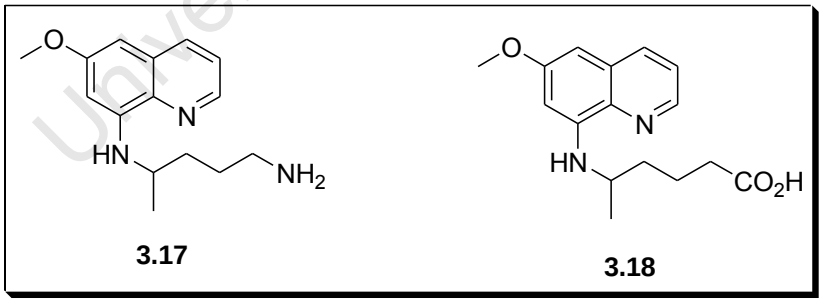

Figure 3.21: Primaquine, an antimalarial drug and its metabolite, carboxyprimaquine.

The rationale used in the design of primaquine-based target compounds is shown in Figure 3.22. Similar to chloroquine-based compounds in section 3.4, a bulky moiety (consisting of a tetrazole and various aromatic rings) is introduced at the terminal amine. The aim of this design was to introduce steric bulk in order to potentially circumvent the problem of rapid

metabolism at that site while keeping the primaquine backbone intact. In addition, this was done in order to exploit the efficacy of primaquine while simultaneously limiting the potential for rapid metabolism, and the inherent toxicity.

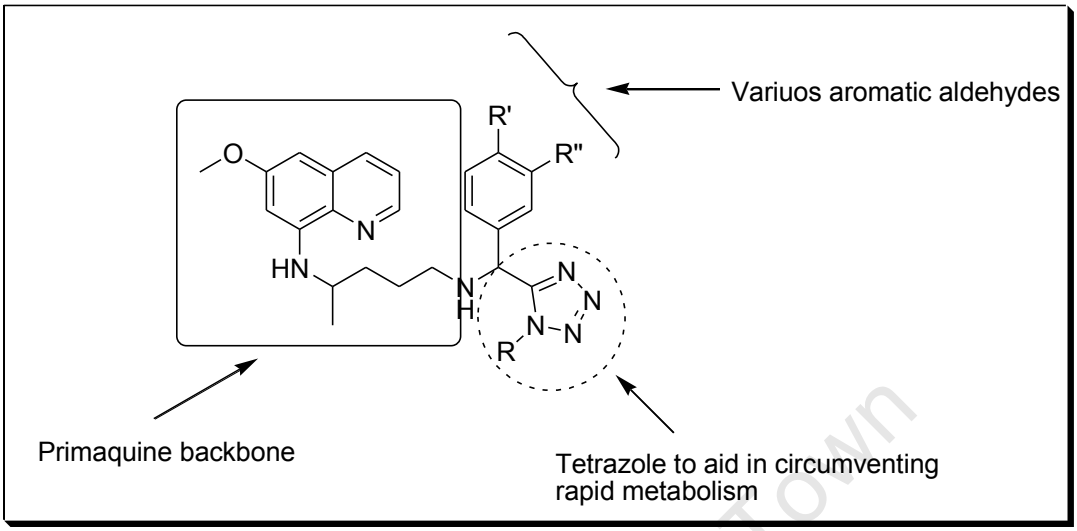

Figure 3.22: Rationale behind the design of primaquine-based compounds.

3.6.1 Synthesis of the target compounds

The first step in the synthesis of primaquine-based target compounds (**3.19a-e**) was neutralization of a commercially available primaquine diphosphate salt (**3.17**) using triethylamine as a base, followed by the MCR strategy similar to that used in the synthesis of chloroquine-based target compounds (Scheme 3.10). The desired compounds **3.19a-e** were obtained as racemic diastereomeric mixtures (1:1) in poor to moderate yields after purification (Table 3.8). Varying the mobile phase gradient and pH were undertaken in attempting to separate and/or resolve the diastereomers without success, and Figure 3.23 shows an HPLC chromatogram of a diastereomeric mixture of compound **3.19a**. From Figure 3.23 it is evident that the diastereomers coalesce into a single sharp peak and this complicates matters when trying to separate these. Perhaps the best option of separating these diastereomeric mixtures would be to use a chiral column or chiral resolving agent. Due to time constraints, the use of superior separating methods on these distereomeric mixtures were not attempted in this study.

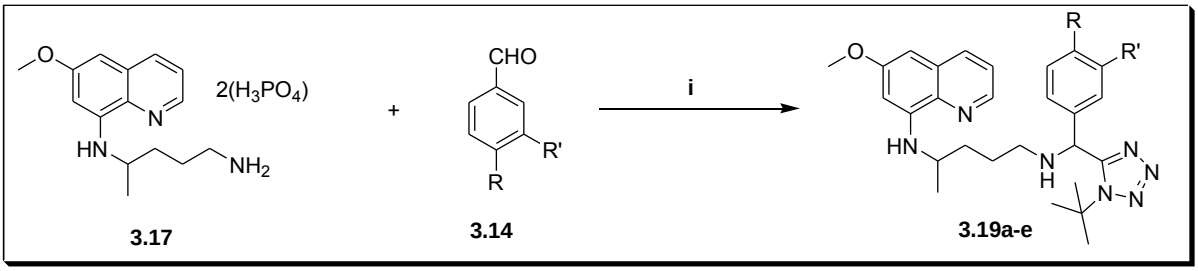

Scheme 3.20: *Reagents and conditions*: (**i**) $TMSN_3$ (1.0 eq to the aldehyde and primaquine salt), *t*-Butyl isocyanide (1.0 eq), Et_3N (4.0 eq), MeOH, 40 °C, 24 hrs.

Table 3.8: Yields of Primaquine-based target compounds.

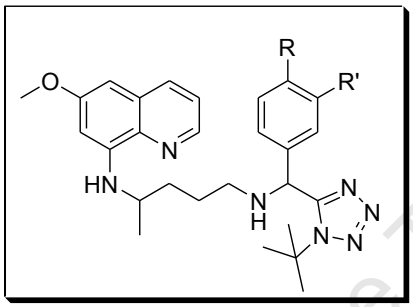

Compound	Code	R'	R	Yield/[%]	HPLC Purity/[%]
3.19a	**TK1000A**	H	H	21	99.3
3.19b	**TK1000B**	H	OCH_3	40	99.5
3.19c	**TK1000C**	H	CH_3	50	99.4
3.19d	**TK1000D**	Cl	Cl	17	99.5
3.19e	**TK1000E**	H	Cl	41	99.7

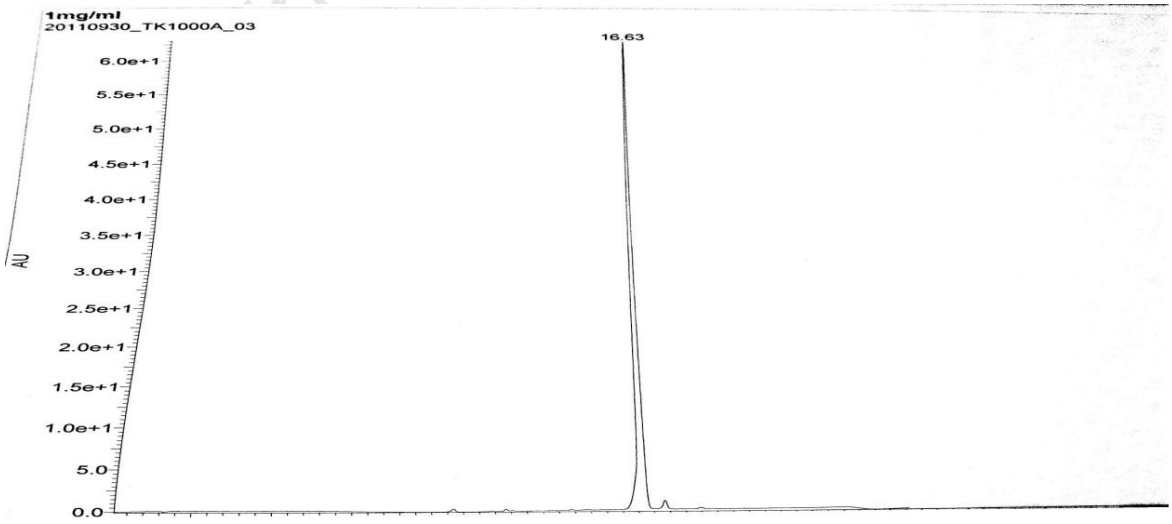

Figure 3.23: HPLC chromatogram of compound **3.19a** (**TK1000A**).

All the synthesized compounds were characterized fully (^{1}H, ^{13}C and mass spectrometry). Figure 3.24 shows a typical ^{1}H NMR of one of the desired target compounds (**3.19c**). The important signals to note in this spectrum are the two sets of overlapping singlets between 1.54 and 1.56 ppm, and between 5.20 and 5.23 ppm, which correspond to the *tert*-butyl protons and the H14 methine proton of each diastereomer in the racemic mixture. The appearance of these signals as overlapping singlets is a clear confirmation of the diastereomeric mixture of the target compound, and this is to be expected because of the presence of two stereogenic centres. The appearance of signals at 20.5, 30.0 and 47.9 ppm corresponding to carbons C10, C18 and C19, respectively, as multiplets in the ^{13}C NMR spectrum (Fig. 3.25) also confirm the presence of a diastereomeric mixture.

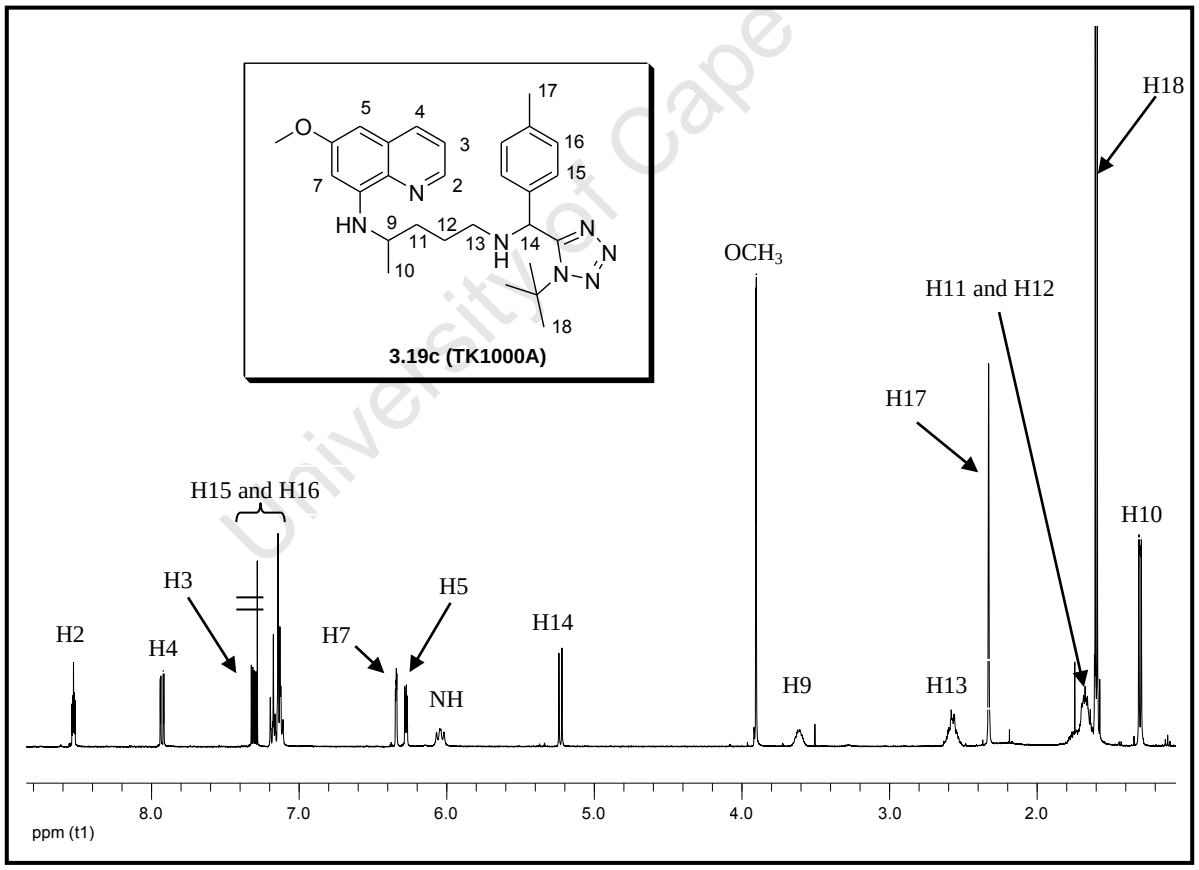

Figure 3.24: 400 MHz ^{1}H NMR spectrum of product **3.19c** in $CDCl_3$.

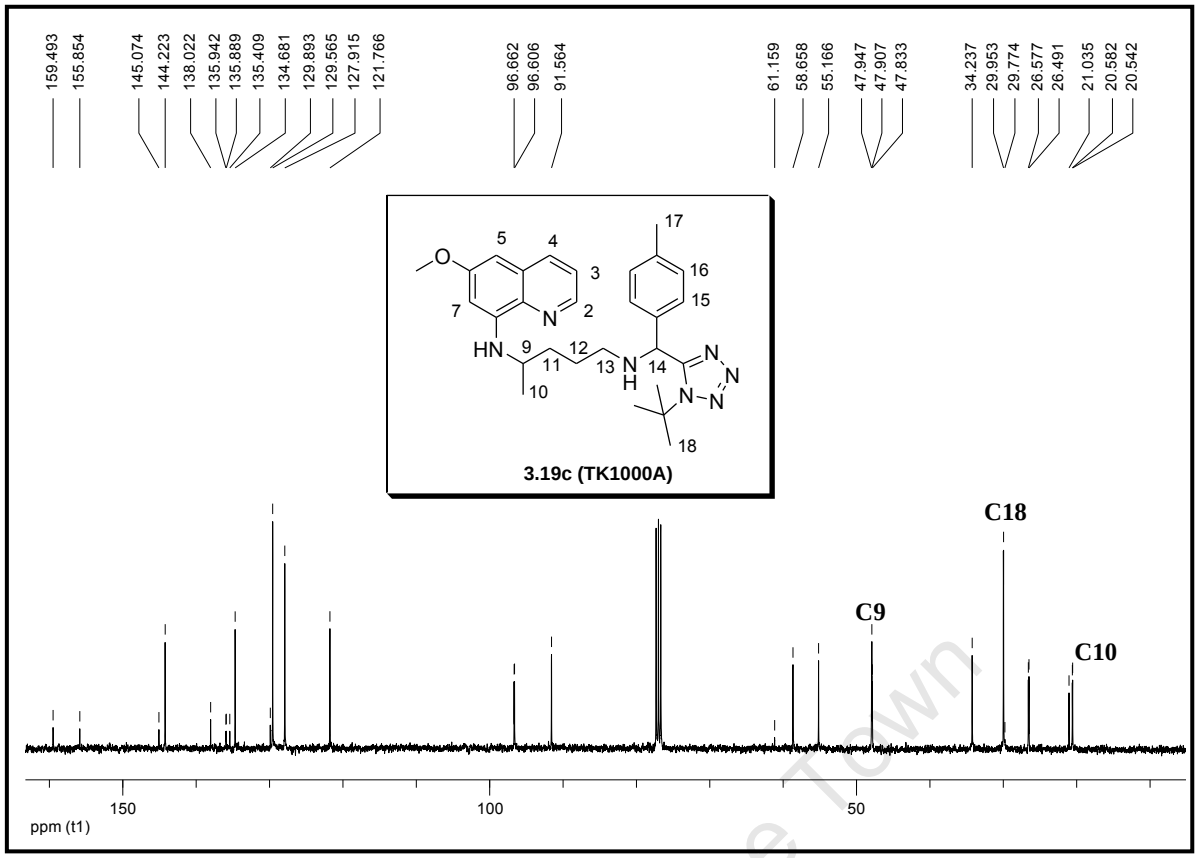

Figure 3.25: 100 MHz ^{13}C NMR spectrum of product **3.19c** in $CDCl_3$.

3.7 Biological results and discussion

In vitro antiplasmodial and antimycobacterial evaluation of all synthesized compounds were conducted in collaboration with: (i) London School of Hygiene and Tropical Medicine, University of London (LSHTM) (3D7 and K1); (ii) Department of Medicine, San Francisco General Hospital, University of San Francisco (W2); (iii) Swiss Tropical and Public Health Institute, Switzerland (STPH) (K1); (iv) Institute of Tuberculosis Research, College of Pharmacy, University of Illinois at Chicago (MABA and LORA assays); and (v) Institute of Infectious Disease and Molecular Medicine (IIDMM), University of Cape Town (7 and 14 days MABA experiments).

In all antiplasmodial assays, chloroquine, amodiaquine and primaquine were used as reference drugs for growth inhibition of *P.falciparum* chloroquine-sensitive (3D7) and chloroquine-resistant (K1 and W2) strains. The antiplasmodial activities are expressed as

50% inhibitory concentration (IC_{50}), and this describes the concentration of a drug necessary to cause 50% inhibition of growth or activity in the test sample. In antimycobacterial evaluation, the MABA (Microplate Alamar Blue Assay) and LORA (Low Oxygen Recovery Assay) were conducted and antimycobacterial activities are expressed as minimum inhibitory concentration (MIC_{90}). Furthermore, streptomycin (SM), kanamycin (KAN), rifampin (RMP), isoniazid (INH), and PA-824 were used as controls. Cytotoxicity testing of selected compounds were conducted in Vero cell-lines (Institute of Tuberculosis Research, University of Chicago), in Chinese Hamster ovarian (CHO) cell-lines, using emetine as a reference drug in the standard MTT assay, which was used to measure cellular growth and chemosensitivity (Department of Pharmacology, University of Cape Town), and in L6 mammalian cell-lines, using podophylotoxin as a reference drug (STPH). Experimental details pertaining the assays can be found in the experimental section (Chapter 6).

3.7.1 *In vitro* antiplasmodial evaluation of the target compounds

3.7.1.1. Antiplasmodial activity of deoxyamodiaquine-based compounds

The antiplasmodial activities of compounds **3.9a-3.10f** against 3D7, K1 and W2 strains were determined and the results are shown in Table 3.9. This data revealed that most of these compounds had *in vitro* antiplasmodial activity against all three strains of the parasite, and the protected tetrazole-based compounds were generally more active than the deprotected analogues. Compounds **3.9b-c** and **3.9k** showed greater activity in the K1-resistant strain (IC_{50} ranging from 0.006 to 0.012 µM) than both reference drugs, *i.e.* amodiaquine and chloroquine. In fact, these compounds were 2- to 5-fold more active than amodiaquine, and 3- to 6-fold more active than chloroquine, while compounds **3.10b-c** had comparable activity to these reference drugs. The least active compound in this series against the K1 strain was **3.10a** (IC_{50} = 2.979 µM), which was about 80-fold less active than both drugs. Furthermore, compounds **3.9a-f**, **3.9k** and **3.10c** were more active than amodiaquine in the W2-resistant

strain, while only compound **3.9k** was more active than chloroquine in this strain. In addition, compound **3.10b** had comparable activity to that of amodiaquine but was less active than chloroquine on the W2 strain.

The differences in these antiplasmodial results between these two resistant strains (K1 and W2), although not too significant, might be due to the assay conditions used in the two experiments which were carried out at two independent laboratories. For instance, in the K1 assays, only 0.5% parasitemia and 2.5% hematocrit were used, whereas in the W2 assays, 1% parasitemia and 2% hematocrit were used. Thus, the parasitemia load in the W2 assays was two times higher than the one used in the K1 assays. This might in some way explain why the tested compounds appeared to be more active in the K1 assays than they were in the W2 assays.

Generally, the reference drugs were more active than all the deoxyamodiaquine analogues in the 3D7-sensitive strain, the most active compound identified against this strain is **3.9c** (IC_{50} = 0.10 µM), which was 2-fold less active than chloroquine and 12-fold less active than amodiaquine. From the structural point of view, the *para*-compound **3.9k** (IC_{50} values of 0.012 and 0.040 µM on K1 and W2, respectively) exhibited superior activity than both the *meta*- **3.9a** (IC_{50} values of 0.150 and 0.0227 µM on K1 and W2, respectively) and *ortho*- **3.9j** (IC_{50} values of 3.51and 3.51 µM on K1 and W2, respectively) analogues on both resistant strains. Furthermore, on close inspection of the data in Table 3.7, there is no obvious trend in terms of the nature of the tertiary amine of each compound, but it appears that the majority of compounds that have an acyclic tertiary amine are generally more active than the corresponding ones containing cyclic amines.

Table 3.9: *In vitro* antiplasmodial activity of deoxyamodiaquine-based compounds.

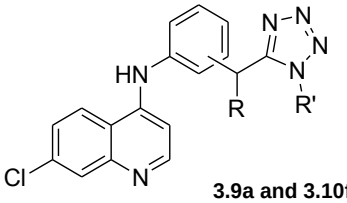

3.9a and 3.10f

R'	Position	Code	Product	R	*P. falciparum* IC_{50} (µM)			Cytotox. (µM)
					3D7	K1	W2	
	*meta*	**TK1**	**3.9a**		0.052	0.150	**0.227**	64.8[a]
	"	**TK2**	**3.9b**	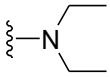	0.100	**0.006**	**0.066**	110.8[b]
	"	**TK3**	**3.9c**	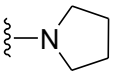	0.010	**0.0096**	**0.077**	116.6[b]
	"	**TK4**	**3.9d**	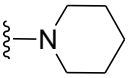	0.050	0.170	**0.082**	90.4[a]
	"	**TK6**	**3.9f**	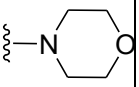	0.099	1.29	**0.195**	46.8[a]
	ortho	**TK10**	**3.9j**		3.51	3.51	3.385	ND*
	para	**TK11**	**3.9k**		0.012	**0.012**	**0.040**	ND
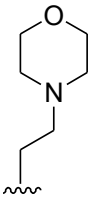	*meta*	**TK7**	**3.9g**		0.379	1.288	**0.195**	ND
	"	**TK8**	**3.9h**	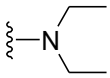	0.030	0.245	**0.194**	ND
	"	**TK9**	**3.9i**	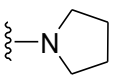	0.220	0.310	3.39	ND
H	"	**TK1B3**	**3.10a**		0.487	2.979	1.168	ND
	"	**TK2B3**	**3.10b**	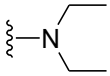	0.164	0.054	0.475	ND
	"	**TK3B3**	**3.10c**	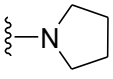	1.097	0.049	**0.181**	ND
	"	**TK4B3**	**3.10d**	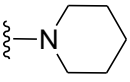	0.286	1.264	0.487	ND
	"	**TK6B3**	**3.10f**	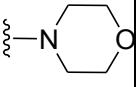	2.07	1.968	1.394	ND
-		**Amodiaquine**		-	0.000	0.0268	0.4007	ND
		Chloroquine			0.005	0.0360	0.0591	ND
		Emertine			-	-	-	0.129[b]

[a] Vero cells; [b] Chinese Hamster Ovarian (CHO) cells; * ND= not determined

The *in vitro* cytotoxicity studies were conducted on the few selected compounds using Vero and Chinese Hamster Ovarian (CHO) mammalian cell-lines. Among the five compounds tested, compounds **3.9a** (IC_{50} = 64.8 µM) and **3.9f** (IC_{50} = 46.8 µM) were moderately cytotoxic while the other compounds exhibited no cytotoxicity with IC_{50} values greater than 100 µM. However, the selective indices of all these compounds [**3.9a** (1246), **3.9b** (1108), **3.9c** (11660) **3.9d** (1808) and **3.9f** (472), calculated from the IC_{50} (mammalian cell-line)/ IC_{50} (3D7)] suggest that they are more selective towards the chloroquine-sensitive parasite than the mammalian cell-lines. Similar, selective indices on the two resistant strains (not shown) are also acceptable, suggesting that these compounds had overall acceptable cytotoxicity when viewed in terms of their selective indices.

3.7.1.2 Antiplasmodial activity of chloroquine-based compounds

The chloroquine-based compounds were also evaluated for antiplasmodial activity against the 3D7, K1 and W2 strains, and were further assessed for cytotoxicity against L6 and CHO mammalian cell-lines (Table 3.10). It is important to note that the results for K1-resistant strain were obtained from two independent experiments (LSHTM and STPH), the chloroquine IC_{50} ranged from 0.036 to 0.220 µM, and these are indicated as such in Table 3.10. The *tert*-butylated compounds **3.15a3-3.15c** (highlighted in bold) were all more active than chloroquine on all tested strains of the parasite. More specifically, 6 out of the 7 compounds tested against the 3D7 strain possessed greater activity than chloroquine, with compound **3.15a4** being the most potent while **3.15a2** was the least active. None of the de-*tert*-butylated compounds were tested against the 3D7 strain. On the other hand, 6 (**3.15a1**, **3.12a3**- **3.15a7**) out of the 14 compounds tested against K1 strain showed greater activity than chloroquine. Among the protected compounds, **3.15a5** (IC_{50} = 0.001 µM) was the most active on this strain, exhibiting 36-fold improvement in activity over chloroquine, while the least active compound, **3.15a2** (IC_{50} = 0.155 µM), was 4 times less active than chloroquine.

Table 3.10: *In vitro* antiplasmodial activity of chloroquine-based compounds.

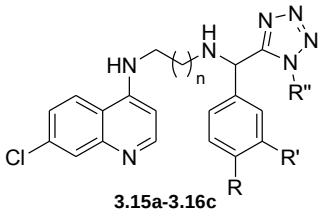

3.15a-3.16c

Product	Code	n	R''	R'	R	*P. falciparum* IC_{50} [µM (µg/mL)]			Cytotox. [µM (µg/mL)]
						3D7	K1	W2	
3.15a1	**TK900A**	1	^{t}Bu	H	H	**0.005**	**0.038**	0.069	7.54 (3.28)[a]
3.15a2	**TK900B**	1	^{t}Bu	H	OCH_3	3.821	0.155	**0.046**	ND
3.15a3	**TK900C**	1	^{t}Bu	H	CH_3	**0.001**	**0.002**	**0.0311**	185.1 (83.3)[b]
3.15a4	**TK900D**	1	^{t}Bu	Cl	Cl	**0.0004**	**0.008**	**0.0305**	10.5 (5.30)[b]
3.15a5	**TK900E**	1	^{t}Bu	H	Cl	**0.002**	**0.001**	**0.0255**	97.8 (46.0)[b]
3.15b	**TK910**	2	^{t}Bu	H	H	**0.002**	**0.027**	**0.039**	ND
3.15c	**TK920**	3	^{t}Bu	H	H	**0.002**	**0.008**	**0.020**	ND
3.16a1	**TK900AB3**	1	H	H	H	ND	14.9 (5.67)[‡]	ND	132.16 (50.2)[a]
3.16a2	**TK900BB3**	1	H	H	OCH_3	ND	13.2 (5.42)[‡]	ND	150.29 (61.6)[a]
3.16a3	**TK900CB3**	1	H	H	CH_3	ND	17.4 (6.86)[‡]	ND	155.38 (61.2)[a]
3.16a4	**TK900DB3**	1	H	Cl	Cl	ND	4.39 (1.97)[‡]	ND	155.10 (69.6)[a]
3.16a5	**TK900EB3**	1	H	H	Cl	ND	2.38 (0.987)[‡]	ND	234.86 (97.3)[a]
3.16b	**TK910B3**	2	H	H	H	ND	14.26 (5.62)[‡]	ND	167.31 (65.9)[a]
3.16c	**TK920B3**	3	H	H	H	ND	6.849 (2.79)[‡]	ND	142.43 (58.1)[a]
Chloroquine			-			0.0052	0.036	0.059	-
Chloroquine[‡]			-			-	0.220 (0.11)[‡]	-	-
Amodiaquine			-			0.0086	0.0262	0.401	-
Podophyllotoxin			-			-	-	-	0.0193 (0.008)
Emertine						-	-	-	0.129[b]

[‡]Antiplasmodial testing done at STPH; [a]L6 mammalian cell-lines; [b]CHO mammalian cell-lines.

The de-*tert*-butylated compounds were all less efficacious than chloroquine on this strain, their activities ranging from 10 to 80-fold less active than chloroquine. Against the W2-resistant strain, almost all the compounds were more active than chloroquine, except compound **3.15a1** (IC_{50} = 0.069 µM) which was 1.2 times less active than chloroquine. Compound **3.15c** (IC_{50} = 0.020 µM) was the most active with 3-fold superior activity than

chloroquine. In terms of structure-activity relationships, the compound with the shortest ethylene spacer, **3.15a1**, was less efficacious than compounds **3.15b** (IC_{50} = 0.039 µM) and **3.15c** with longer carbon spacers on all strains tested. There is no obvious trend in terms antiplasmodial activity based on the nature of the substituents on the phenyl ring. However, a substituted phenyl ring appears to be favoured relative to the unsubstituted one.

Almost all the compounds showed acceptable cytotoxicity on mammalian cell-lines, most having cytotoxicity values closer to or greater than 100 µM, except for compounds **3.15a1** (IC_{50} = 7.54 µM) and **3.15a4** (IC_{50} = 10.5 µM). Furthermore, all these compounds have favourable selectivity indices (Table 3.11), indicating that these compounds are much more cytotoxic towards the parasite than the mammalian cell-lines.

Table 3.11: Resistance indices of some chloroquine-based compounds.

Product	Code	Resistance indices		Selective index		
		A[γ]	B[§]	3D7	K1	W2
3.15a1	**TK900A**	7.6	13.8	1508	198	109
3.15a2	**TK900B**	**0.041**	**0.012**	-	-	-
3.15a3	**TK900C**	**2**	31	185000	92550	5951
3.15a4	**TK900D**	20	75	26250	1275	344
3.15a5	**TK900E**	**0.5**	12.5	48900	97800	3835
3.15b	**TK910**	13.5	19.5		-	-
3.15c	**TK920**	**4**	**10**		-	-
-	**Chloroquine**	6.9	11.3		-	-

[γ]Resistance index IC_{50}(KI)/IC_{50} (3D7); [§] Resistance index IC_{50}(W2)/IC_{50}(3D7)

Resistance indices of these chloroquine-based compounds are shown in Table 3.11. Resistance index is defined as the IC_{50} ratio of the chloroquine-resistant and chloroquine-sensitive strains. This serves as an indication of the difference in activity of the synthesized compounds in sensitive and resistant strains of *P. falciparum*, and is used to evaluate whether

(or not) those compounds have potential to develop cross-resistance with chloroquine. Ideally, for favourable antimalarial compounds, resistance indices should be unity or closer. From the table, it is apparent that the majority of these compounds have high resistance indices, many of them higher than that of chloroquine. In this regard the most favourable compounds were **3.15a2**, **3.15a3**, **3.15a5**, and **3.15c** against the K1 strain, while for W2 strain only compounds **3.15a2** and **3.15c** were favourable. Compounds **3.15a4** and **3.15b** had the least favourable resistance index, suggesting that these have a potential to develop cross-resistance with chloroquine.

3.7.1.3 Antiprotozoan activity of primaquine-based compounds

Table 3.12 shows the results obtained for primaquine-based compounds against chloroquine-resistant strain (K1) and against cultured *T. b. brucei* parasite. Briefly, *T. b. brucei* is an extracellular protozoan parasite and a causative agent for Human African Trypanosomiases (HAT), or sleeping sickness, in about 300 000 to 500 000 people in Sub-Saharan Africa.[74] A person becomes infected when bitten by an infected vector, a tsetse fly, and if this remains untreated it can lead to a coma or worse, death. The parasite multiplies in the skin before invading the hemolymphatic system where it develops into elongated trypomastigotes.[75] Currently there is no vaccine for treating HAT, and there are two strategies that are employed in combating the disease; (i) vector control through use of insecticides, and (ii) prophylactic and therapeutic measures.[76] However, drugs (e.g. melarsoprol) used for treating HAT are generally associated with toxic episodes. Thus, there is an urgent need for the development of novel drugs that will urgently address this disease.

Reference drugs used for comparison purposes were primaquine for antiplasmodial and melarsoprol for *T. b. brucei*, and their *in vitro* IC_{50} values are shown in Table 3.12. All the compounds had modest activity against *P. falciparum* K1 strain, but none possessed greater

activity than primaquine. The most active compound in this series was **3.19d** (IC_{50} = 1.311 µM), which was 2-fold less active than primaquine. In addition, these compounds did not exhibit appreciable activity against *T. b. brucei*, the most active compound, **3.19b** (IC_{50} = 14.16 µM), was 1880-fold less active than melasorprol. Furthermore, these compounds showed unfavourable cytotoxicity profile towards the L6 mammalian cells, with **3.19a** (IC_{50} = 10.77 µM), **3.19c** (IC_{50} = 12.94 µM), and **3.19e** (IC_{50} = 31.30 µM) being the most cytotoxic.

Table 3.12: *In vitro* antiprotozoan activity of primaquine-based compounds.

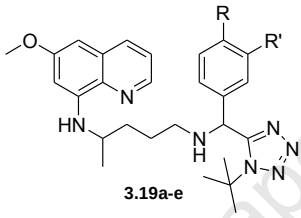

3.19a-e

Entry	Code	R''	R'	R	*P. falciparum* IC_{50} µM (µg/mL) K1	*T. b. rhod* IC_{50} [µM (µg/mL)]	Cytotox. L6 IC_{50} [µM (µg/mL)]
3.19a	**TK1000A**	^{t}Bu	H	H	2.470 (1.17)	18.10 (8.57)	10.77 (5.10)
3.19b	**TK1000B**	^{t}Bu	H	OCH_3	1.979 (0.997)	14.16 (7.13)	75.45 (38)
3.19c	**TK1000C**	^{t}Bu	H	CH_3	1.573 (0.767)	18.54 (9.04)	12.94 (6.31)
3.19d	**TK1000D**	^{t}Bu	Cl	Cl	1.311 (0.711)	18.30 (9.93)	87.93 (47.70)
3.19e	**TK1000E**	^{t}Bu	H	Cl	1.799 (0.914)	21.45 (10.9)	31.30 (15.9)
Primaquine			-		0.615 (0.280)	-	-
Melarsoprol			-		-	0.0075 (0.003)	-
Podophyllotoxin			-		-	-	0.0193 (0.008)

3.7.2 *In vitro* Antimycobacterial evaluation of the target compounds

All the synthesized compounds were screened against drug-sensitive *M. tuberculosis* H_{37}Rv strain using the MABA[78] and LORA[79] assays. MABA is non-toxic, uses a thermally stable reagent and shows good correlation with the radiometric BACTEC method.[80] Briefly, MABA is a non-radiometric assay which uses an Alamar blue dye as an indicator of cellular growth. The oxidized blue non-fluorescent form undergoes reduction to the pink florescent form, thus

allowing for growth measurements to be made. On the other hand, LORA is a luminescence-based low oxygen adapted culture of recombinant *M. tuberculosis* H_{37}Rv. This technique is used to evaluate the non-replicating persistent phenotype. In this section, MABA experiments were carried out at the Institute of Infectious Diseases and Molecular Medicine (UCT) and at the Tuberculosis Research Institute, (UIC).

3.7.2.1 Antimycobacterial activity of deoxyamodiaquine-based compounds

In vitro activities of the final compounds are shown in Table 3.13, and several compounds were found to inhibit the growth of both the replicating and non-replicating *M. tuberculosis* after 7 days of incubation. Compounds **3.9a**, **3.9c-f** inhibited over 90% of the replicating bacteria with MABA MICs ranging from 14.1 to 63.7 µM, with compound **3.9d** (MIC_{90} 14.1 µM) being the most active among these. However, the most potent of all these compounds, **3.9k** (MIC_{90} = 7.6 µM), inhibited only 10% of the replicating bacteria. For comparison purposes, two of these deoxyamodiaquine compounds, **3.9d** and **3.9k**, had greater MICs than amodiaquine (MIC_{90} 56.9 µM). The MICs of all the de-protected analogues were above the highest concentration (MIC_{90} > 128 µM) tested.

Compounds **3.9a**, **3.9c** and **3.9k** seemed to retain their activity in the LORA assay, and all had over 70% inhibitory effect on the non-replicating bacteria. Compound **3.9k**, the most potent on LORA, inhibited about 96% of the non-replicating bacteria with a MIC_{90} value of 15.1 µM. In addition, three compounds [**3.9a** (MIC_{90} = 118.7 µM), **3.9c** (MIC_{90} = 74.0 µM) and **3.9k** (MIC_{90} = 15.1 µM)] had MICs greater than that of a standard drug isoniazid (MIC_{90} >128 µM) and amodiaquine (MIC_{90} = 125 µM) in the LORA assay. In summation, three compounds (**3.9a**, **3.9c** and **3.9k**) exhibited activity against both forms of the bacteria, while none of the deprotected analogues showed any activity at the highest concentration tested (MIC_{90} > 128 µM).

Table 3.13: *In vitro* antimycobacterial activity of compounds **3.9a-3.10f**

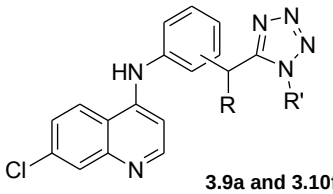

3.9a and 3.10f

R'	Position	Code	Product	R	MABA (µM)		LORA (µM)	
					%Inh	MIC_{90}	%Inh	MIC_{90}
	*meta*	**TK1**	**3.9a**		**97**	**63.7**	**79**	**118.7**
	"	**TK2**	**3.9b**	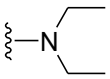	58	>128	37	>128
	"	**TK3**	**3.9c**	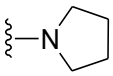	**99**	**59.3**	**91**	**74.0**
	"	**TK4**	**3.9d**	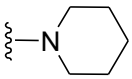	**98**	**14.1**	65	>128
	"	**TK6**	**3.9f**	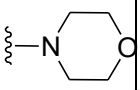	**97**	**59.1**	72	>128
	ortho	**TK10**	**3.9j**		27	>128	26	>128
	para	**TK11**	**3.9k**		**10**	**7.6**	**96**	**15.1**
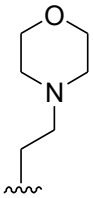	*meta*	**TK7**	**3.9g**		4	>128	-27	>128
	"	**TK8**	**3.9h**	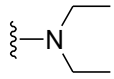	62	>128	40	>128
	"	**TK9**	**3.9i**	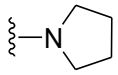	70	>128	21	>128
H	"	**TK1B3**	**3.10a**		-5	>128	9	>128
	"	**TK2B3**	**3.10b**	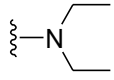	13	>128	23	>128
	"	**TK3B3**	**3.10c**	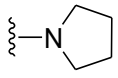	10	>128	13	>128
	"	**TK4B3**	**3.10d**	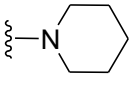	6	>128	7	>128
	"	**TK6B3**	**3.10f**	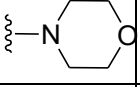	10	>128	18	>128
-	**Amodiaquine**			-	**99**	**56.9**	**92**	**125**
	RMP				100	0.05	98	1.93
	INH				92	0.23	64	>128
	PA-824				99	0.12	100	3.78

The observable trends that could be delineated from these results are; (i) the *para*-substituted compound **3.9k** (MABA and LORA MIC_{90} = 7.6 and 15.1 µM, respectively) possessed superior efficacy than the *meta* **3.9a** (MABA and LORA MIC_{90} = 63.7 and 118.7 µM, respectively) and *ortho* **3.9j** (both MABA and LORA MIC_{90} > 128) analogues on both the MABA and LORA assays; (ii) the *t*-butyl substitution on the tetrazole ring appears to be highly favoured compared to the ethylmorpholine moiety and when there is no substitution. Lastly, antimycobacterial activity is greatly influenced by solubility, similar to the antiplasmodial activity. Compounds that are less soluble (protected analogues) are substantially more active than the highly soluble (de-*tert*-butylated) analogues on both the replicating and non-replicating bacteria.

3.7.2.2 Antimycobacterial activity of chloroquine-based compounds

The *in vitro* MABA assays used to screen these chloroquine-based compounds were conducted at two different laboratories. The 7 day MABA (and LORA) experiments were conducted at the Tuberculosis Research Institute, University of Illinois at Chicago, while the 7 and 14 day experiments were performed at the Institute of Infectious Disease and Molecular Medicine (IIDMM), University of Cape Town. Several compounds were found to effectively inhibit the growth of both replicating and non-replicating *M. tuberculosis* with reasonable MICs (Table 3.14). The *para*-substituted phenyl ring is highly preferred in the MABA assay; compounds **3.15a3-a5**, all *para*-substituted, completely inhibited the growth of the bacteria, with MICs in the low micromolar range (5.6 to 14.3 µM). In addition, another *para*-substituted phenyl-based compound, **3.15a2**, possessed an MIC_{90} of 40.4 µM. Furthermore, the disubstituted phenyl ring was more efficacious than the mono- and the un-substituted rings. Elongation of the alkyl side-chain, going from n=1 to n=3, reduced the activity by 2-fold; **3.15a1** (n=1, MIC_{90} = 20.9 µM), **3.15b** (n=2, MIC_{90} = 29.0 µM) and **3.15c** (n=3, MIC_{90} = 47.8 µM). Compound **3.15a1** had a two-fold decrease in activity on the 14^{th} day (MIC_{90} =

80 µM) of incubation compared to the 7th day (MIC_{90} = 40 µM), possibly due to degradation. Similar to the trend observed with deoxyamodiaquines, the deprotected tetrazoles did not exhibit any activity at the highest tested concentration (MIC_{90} >160 µM) on both the 7th and the 14th day experiments.

Table 3.14: *In vitro* antimycobacterial activity of compounds **3.15a1-3.16c**

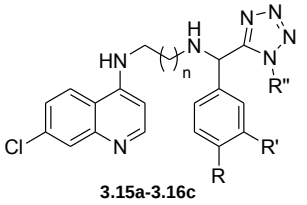

3.15a-3.16c

Product	Code	n	R''	R'	R	MABA‡ (µM)		LORA‡ (µM)		$H_{37}R_v$ (MIC_{90})§ (µM)	
						%Inh	MIC_{90}	%Inh	MIC_{90}	7days	14days
3.15a1	**TK900A**	1	^{t}Bu	H	H	10	**20.9**	**99**	**57.6**	**40**	**80**
3.15a2	**TK900B**	1	^{t}Bu	H	OCH_3	10	**40.4**	**100**	**57.2**	ND	ND
3.15a3	**TK900C**	1	^{t}Bu	H	CH_3	**99**	**14.3**	**100**	**29.7**	ND	ND
3.15a4	**TK900D**	1	^{t}Bu	Cl	Cl	**100**	**5.6**	**99**	**13.5**	ND	ND
3.15a5	**TK900E**	1	^{t}Bu	H	Cl	**100**	**6.7**	**100**	**24.0**	ND	ND
3.15b	**TK910**	2	^{t}Bu	H	H	**100**	**29.0**	**100**	**52.1**	ND	ND
3.15c	**TK920**	3	^{t}Bu	H	H	**99**	**47.8**	**100**	**60.2**	ND	ND
3.16a1	**TK900AB3**	1	H	H	H	ND	ND	ND	ND	>160	>160
3.16a2	**TK900BB3**	1	H	H	OCH_3	ND	ND	ND	ND	>160	>160
3.16a3	**TK900CB3**	1	H	H	CH_3	ND	ND	ND	ND	>160	>160
3.16a4	**TK900DB3**	1	H	Cl	Cl	ND	ND	ND	ND	>160	>160
3.16a5	**TK900EB3**	1	H	H	Cl	ND	ND	ND	ND	>160	>160
3.16b	**TK910B3**	2	H	H	H	ND	ND	ND	ND	>160	>160
3.16c	**TK920B3**	3	H	H	H	ND	ND	ND	ND	>160	>160
RMP		-				100	0.05	98	1.93	0.002	ND
INH		-				92	0.23	64	>128	-	-
PA-824		-				99	0.12	100	3.78	-	-
Moxifloxacin						100	0.29	88	31.1		
Kanamycin						-	-	-	-	3.125	3.125
Streptomycin						-	-	-	-	0.4	0.4

‡ Experiments conducted at Tuberculosis Research institute (UIC); § at the University of Cape Town (IIDMM).

Regarding the LORA results, the *para*-substituted phenyl-based compounds also exhibited superior antimycobacterial activity than the unsubstituted analogues, as in the MABA assay. There is no clear trend that could be deduced from these results regarding the elongation of the alkyl side-chain. Compounds **3.15a3** (MIC_{90} = 13.5 µM) and **3.15a4** (MIC_{90} = 24.0 µM) were more potent than the two standard drugs isoniazid (MIC_{90} >128 µM) and moxifloxacin (MIC_{90} = 31.1 µM). Furthermore, compound **3.15a4** was the most active in this series with significant MICs (MABA, 5.6 µM and LORA, 13.5 µM) on both bacterial forms.

Similar to the deoxyamodiaquine series, compounds that were experimentally determined to be less soluble (protected analogues) were more active than the highly soluble (de-*tert*-butylated) analogues on both bacterial forms.

3.7.2.3 Antimycobacterial activity of primaquine-based compounds

Table 3.15: *In vitro* antimycobacterial activity of compounds **3.19a-e.**

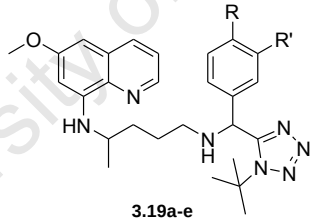

3.19a-e

Entry	Code	R''	R'	R	$H_{37}R_v$ (MIC_{90}) (µM)	
					7days	14days
3.19a	**TK1000A**	^{t}Bu	H	H	>160	>160
3.19b	**TK1000B**	^{t}Bu	H	OCH_3	>160	>160
3.19c	**TK1000C**	^{t}Bu	H	CH_3	>160	>160
3.19d	**TK1000D**	^{t}Bu	Cl	Cl	>160	>160
3.19e	**TK1000E**	^{t}Bu	H	Cl	>160	>160
Primaquine			-		80	80
RMP			-		0.002	ND
Kanamycin			-		3.125	3.125
Streptomycin			-		0.4	0.4

These 7 and 14 day *in vitro* antimycobacterial assays were conducted at the Institute of Infectious Disease and Molecular Medicine (IIDMM), University of Cape Town. All the primaquine-based compounds were tested as (1:1) diastereomeric mixture and the results are shown in Table 3.15. None of these compounds showed any antimycobacterial activity at the highest tested concentration (MIC_{90} >160 µM), while primaquine exhibited modest activity with an MIC_{90} value of 80 µM on both the 7 and 14 day assay. The complete loss of activity observed on these primaquine derivatives was unexpected, however, the antimycobacterial activity of primaquine confirms the observation of Lougheed and co-workers.[72]

3.7.3 Conclusion

In conclusion, a focused small library of compounds based on the deoxyamodiaquine, chloroquine and primaquine scaffolds were evaluated for their antiplasmodial and antimycobacterial activity. In the deoxyamodiaquine series, protected-tetrazole based compounds **3.9b-c** and **3.9k** (IC_{50} ranging from 0.006 to 0.012 µM) showed superior antiplasmodial activity than both amodiaquine (IC_{50} = 0.02689 µM) and chloroquine (IC_{50} = 0.0360 µM) in the K1-resistant strain. In addition, two deprotected compounds **3.10b** (IC_{50} = 0.054µM) and **3.10c** (IC_{50} = 0.049 µM) exhibited comparable activities to those of the reference drugs. Similarly, compounds **3.9a-f**, **3.9k** and **3.10c** (IC_{50} ranging from 0.040 to 0.194 µM) were all more potent than amodiaquine (IC_{50} = 0.4007 µM) in the W2-resistant strain, while only compound **3.9k** (IC_{50} = 0.040 µM) was more active than chloroquine (IC_{50} = 0.0591 µM) on the same strain. In the chloroquine-sensitive strain (3D7), none of the synthesized compounds were more potent than the reference drugs. Compound **3.9c** (IC_{50} = 0.10 µM) was the most active, but was 2-fold less active than chloroquine and 12-fold less active than amodiaquine.

Similarly, some of these compounds also exhibited encouraging activity against drug-sensitive $H_{37}R_v$ *M. tuberculosis* strain. Compounds **3.9a**, **3.9c-f** inhibited over 90% of the replicating bacteria (MICs ranging from 14.1 to 63.7 µM), with compound **3.9d** (MIC_{90} = 14.1 µM) being the most active among these. The most potent compound of all the deoxyamodiaquines was **3.9k** with a MIC_{90} value of 7.6 µM, but this compound barely inhibited (10%) the replicating bacteria. In addition, compounds **3.9d** and **3.9k** were more efficacious than amodiaquine (MIC_{90} = 56.9 µM), while the de-protected analogues did not exhibit any activity. Against the non-replicating bacteria, compounds **3.9a** (MIC_{90} = 118.7 µM), **3.9c** (MIC_{90} = 74 µM) and **3.9k** (MIC_{90} = 15.1 µM) were the most active, and all had over 70% inhibitory effect on the bacteria. Compound **3.9k** was the most potent against the non-replicating bacteria, with 96% inhibition and an MIC_{90} of 15.1 µM. Furthermore, compounds **3.9c** and **3.9k** possessed MICs greater than that of a standard drug isoniazid (MIC_{90} >128 µM), and in addition to **3.9a**, they had superior efficacy than amodiaquine. Lastly, all these compounds showed acceptable cytotoxicity profiles, indicating that they are more selective towards the parasite or bacteria than they are towards the mammalian cells evaluated.

The chloroquine-based compounds were also assessed for antiplasmodial activity; 6 out of the 7 compounds tested against the 3D7 strain possessed activity greater than that of chloroquine. Compound **3.15a4** (IC_{50} = 0.0004 µM), the most potent, was 13-fold more active than chloroquine (IC_{50} = 0.0052 µM), while **3.15a2** (IC_{50} = 3.821 µM) was the least active and was 732-fold less active than chloroquine. Of the 14 compounds tested against K1-strain 6 compounds showed greater activity than chloroquine. Compound **3.15a5** (IC_{50} = 0.001 µM) was the most active exhibiting a 36-fold improved activity over chloroquine (IC_{50} = 0.036 µM), and the least active was **3.15a2** (IC_{50} = 0.155 µM). Against the W2 strain, almost all the compounds tested were more active than chloroquine (IC_{50} = 0.059 µM),

except compound **3.15a1** (IC_{50} = 0.069 µM) which was 1.2 times less active. Compound **3.15c** (IC_{50} = 0.020 µM) was the most active with a 3-fold superior activity over chloroquine. In addition, the compound with the shortest ethylene spacer, **3.15a1**, was less efficacious than those with the longer carbon spacers, **3.15b** and **3.15c**, on all strains tested.

Furthermore, compounds **3.15a3-a5** completely inhibited the growth of the replicating bacteria, with MICs in the range 5.6 to 14.3 µM, and the most active being **3.15a4** (MIC_{90} = 5.6 µM). Structurally, the *para*-substituted phenyl-based compound were more efficacious than the mono- and the un-substituted. Contrary to antiplasmodial evaluation, the elongation of the alkyl side-chain had detrimental effect on activity, reducing it by 2-fold going from n=1 to n=3. With regards to the non-replicating bacteria, the *para*-substituted phenyl-based compounds also demonstrated superior activity when compared to the unsubstituted variants. Compounds **3.15a3** (MIC_{90} = 13.5 µM) and **3.15a4** (MIC_{90} = 24.0 µM) were the most potent in this assay and they were also more active than the two standard drugs used, isoniazid (MIC_{90} >128 µM) and moxifloxacin (MIC_{90} = 31.1 µM). In addition, compound **3.15a4** showed encouraging MICs (MABA, 5.6 µM and LORA, 13.5 µM) on both mycobacterial forms. All the synthesized compounds showed acceptable cytotoxicity on the Vero and CHO cell lines, the majority having cytotoxicity values closer to or greater than 100 and excellent selective indices.

The primaquine-based compounds also possessed antiplasmodial activity albeit not as good as the reference drug, primaquine. The most active compound in this series was **3.19d** (IC_{50} = 1.311 µM), which was 2-fold less active than primaquine (IC_{50} = 0.615 µM), while the least active, **3.19a** (IC_{50} = 2.470 µM), was 4-fold less active than primaquine. In addition, none of these compounds showed any activity against the *M. tuberculosis* $H_{37}R_v$ strain as revealed by

the MIC_{90} values. Furthermore, these compounds showed unfavourable cytotoxicity profile towards the L6 mammalian cells.

3.8 References

1. Biagini, G. A.; O'Neill, P. M.; Nzila, A.; Ward, S. A.; Bray, P. G., *Trends Parasitol.*, **2003**, *19*, 479.

2. Burrows, J. N., Chibale, K.; Wells, T. N. C., *Curr. Topics Med. Chem.*, **2011**, *11*, 1226.

3. Egan, T. J.; Hunter, R.; Kaschula, C. H.; Marques, H. M.; Misplon, A.; Walden, J., *J. Med. Chem*., **2000**, *43*, 283.

4. Choi, S-R.; Mukherjee, P.; Avery, M. A., *Curr. Med. Chem.*, **2008**, *15*, 161.

5. Biot, C.; Chibale, K., *Infect. Disord. Drug Targets*, **2006**, *6*, 173. 6.

6. Kassel, D. B., *Curr. Opinion Chem. Biol*., **2004**, *8*, 3389.

7. Diana, G. D.; Cutcliffe, D.; Volkots, D. L.; Mallano, J. P.; Bailey, T. R.; Vescio, N.; Oglesby, R. C.; Nits, T. J.; Wetzel, J.; Giranda, V.; Pevear, D. L.; Dukto, F. J., *J. Med. Chem*., **1993**, *36*, 3240.

8.Watchter, G. A.; Davis, M. C.; Martin, A. R.; Franzblau, S. G., *J. Med. Chem.*, **1998**, *41*, 2436.

9. Biot, C.; Bauer, H.; Schirmer, R. H.; Davioud-Charvet, E., *J. Med. Chem.*, **2004**, *47*, 5972.

10. Zhau, P.; Liu, H.; Liu, X.; Wang, Y.; Pannecouque, L.; Witvrouw, M.; De Clerq, E., *Med. Chem. Res.*, **2010**, *19*, 652.

11. Burckhalter, J. H.; Tendwick, J. H.; Jones, F. H.; Holcombe, W. F.; Rawlins, A. L., *J. Am. Chem. Soc*., **1948**, *70*, 1363.

12. O'Neill, P. M.; Bray, P. G.; Hawley, S. R.; Ward, S. A.; Park, B. K., *Pharmacol. Ther*., **1998**, *77*, 29.

13. Neftel, K. A.; Woodtly, W., *Br. Med. J*., **1986**, *292*, 721.

14. Kerb, R.; Fux, R.; Mörike, K.; Kremsner, P. G.; Gil, J. G.; Gleiter, C. H.; Schwab, M., *Lancet Infect. Dis*., **2009**, *9*, 760.

15. Vangapandu, S.; Jain, M.; Kaur, K.; Patil, P.; Patel, S. R.; Jain, R., *Med. Chem. Rev*., **2007**, *27*, 65.

16. Schlitzer, M., *ChemMedChem.*, **2007**, *2*, 944.

17. O'Neill, P. M.; Mukhtar, A.; Stocks, P. A.; Randle, L. E.; Hindley, S.; Ward, S. A.; Storr, R. C.; Bickley, J. F.; Hughes, K. H.; Winstanley, P. A.; Bray, P. G.; Park, B. K., *J. Med. Chem*., **2003**, *46*, 4933.

18. (a) Johansson, T.; Jurva, U.; Grönberg, G.; Weidolf, L.; Masimirembwa, C., *Drug Metab. Dispos.*, **2009**, *37*, 571.

(b) Jurva, U.; Holmén, A.; Grönberg, G.; Masimirembwa, C.; Weidolf, L., *Chem. Res. Toxicol.*, **2008**, *21*, 928.

19. O'Neill, P. M.; Park, B. K., WO0014070, **2000**.

20. O'Neill, P. M.; Harrison, A. C.; Storr, R. C.; Hawley, S. R.; Ward, S. A.; Park, B. K., *J. Med. Chem.*, **1994**, *37*, 1362.

21. O'Neill, P. M.; Willock, D. J.; Hawley, S. R.; Bray, P. G.; Storr, R. C.; Ward, S. A.; Park, B. K., *J. Med. Chem*., **1997**, *40*, 437.

22. Casagrande, M.; Basilico, N.; Parapini, S.; Romeo, S.; Taramelli, D.; Sparatore, A., *Bioorg. Med. Chem*., **2008**, *16*, 6813.

23. O'Neill, P. M.; Park, B. K.; Shone, A. E.; Maggs, J. L.; Roberts, P.; Stocks, P. A.; Biagini, G. A.; Bray, P. G.; Gibbons, P.; Berry, N.; Winstanley, P. A.; Mukhtar, A.; Bonar-Law, R.; Hindley, S.; Bambal, R. M.; Davis, C. B.; Bates, M.; Hart, T. K.; Gresham, S. L.; Lawrence, R. M.; Brigandi, R. A.; Gomez-delas-Heras, F. M.; Gargallo, D. V.; Ward, S. A.; *J. Med. Chem*., **2009**, *52*, 1408.

24. Graebin, C. S.; Uchoa, F. D.; Bernardes, L. S. C.; Campo, V. L.; Carvalho, I.; Eiffer-Lima, V. L., *Anti-Infect. Agents Med. Chem*., **2009**, *8*, 345.

25. Hawley, S. R.; Bray, P. G.; O'Neill, P. M.; Naisbitt, D. J.; Park, B. K.; Ward, S. A., *Antimicrob. Agents Chemother*., **1996**, *40*, 2345.

26. Medlen, C. E.; Soares de Melo, C.; Chibale, K.; *PCT Int. Appl*. (**2009**), WO 2008135886

27.Hecht, D.; Fogel, G. B., *Frontiers Drug Des. Disc*., **2009**, *4*, 351.

28. van de Waterbeemd, H.; Gifford, E., *Nature Rev*., **2003**, *2*, 192.

29. Kerns, C. H., *J. Pharm. Sci*., **2001**, *90*, 1838.

30. Shearer, T. W.; Smith, K. S.; Diaz, D.; Asher, C.; Ramirez, J., *Comb. Chem. High Throughput Screening*, **2005**, *8*, 89.

31. Yu, H.; Adedoyin, A., *Drug Disc. Today*., **2003**, *8*, 852.

32. Eddershaw, P. J.; Bereford, A. P.; Baylis, M. K., *Drug Disc. Today*, **2000**, *5*, 409.

33. Butina, D.; Segall, M. D.; Frankcombe, K., *Drug Disc. Today*, **2002**, *7*, 583.

34. Roncaglioni, A.; Benfenati, E., *Chem. Soc. Rev*., **2008**, *37*, 441.

35. Wold, S.; Esbensen, K.; Galadi, P., *Chemon. Intell. Lab. Syst*., **1987**, 2, 37.

36.Doddareddy, M.; Cho, Y. S.; Koh, H. Y.; Kim, D. Y.; Pae, A. N., *J. Chem. Inf. Model*, **2006**, *46*, 1312.

37. Cruciani, G.; Crivori, P.; Carrupt, P. A.; Testa, B., *J. Mol. Struct. (Theochem)*, **2000**, *503*, 17.

38. Cruciani, G.; Pastor, M.; Guba, W., *Eur. J. Pharm. Sci*., **2000**, *11*, S29.

39. Zamora, I.; Oprea, T.; Cruciani, G.; Pastor, M., Ungel, A. L., *J. Med. Chem*., **2003**, *46*, 25.

40. Kerns, E. H., Di, L., *Drug-like properties: Concepts, Structure, Design and Methods: From ADME to Toxicity Optimization*, 1st Ed., Academic Press/Elsevier: Amsterdam, the Netherlands (**2008**).

41. Guantai, E. M.; Ncokazi, K. K.; Egan, T. J.; Gut, J.; Rosenthal, P. J.; Bhampidipati, R.; Kopinathan, A.; Smith, P. J.; Chibale, K., *J. Med. Chem*., **2011**, *54*, 3637.

42. Ostrovskii, V. A.; Koren, A. O., *Heterocycles*, **2000**, *53*, 1421.

43. Zamora, I.; Afzelius, L.; Cruciani, G., *J. Med. Chem*., **2003**, *46*, 2313.

44. Cruciami, G.; Carosati, E.; De Boeck, B.; Ethirajulu, K.; Mackie, C.; Howe, T.; Vianello, R.; *J. Med. Chem*., **2005**, *48*, 6970.

45. Winstanley, P. A.; Simooya, O.; Kofi-Ekue, J. M.; Walker, O.; Salako, L. A.; Edwards, G., *Brit. J. Clin. Pharmacol*., **1990**, 29, 695.

46. Feng, T-S, *PhD Thesis*, University of Cape Town, **2009**.

47. Nguyen, M. T.; Diaz, A. F., *Macromolecules*, **1994**, *27*, 7003.

48. Parikh, J. R.; Doering, W. E., *J. Am. Chem. Soc*., 1**967**, *89*, 5505.

49. Mancuso, A. J.; Huang, S-L.; Swern, D., *J. Org. Chem*., **1978**, *43*, 2480.

50. Dömling, A.; Beck, B.; Magnin-Lachaux, M., *Tetrahedron Lett*., **2006**, *47*, 4289.

51. Mayer, J .; Umkehrer, M.; Kalinski, C.; Ross, G.; Kolb, J.; Burdack, C.; Hiller, W., *Tetrahedron Lett*., **2005**, *46*, 7393.

52. Nixely, T.; Kelly, M.; Semin, D.; Hulme, C., *Tetrahedron Lett*., **2002**, *43*, 3681.

53. Daumas, M.; *Fr. Dremande, 2716196, 18/08/**1995***.

54. Kanno, H.; Yamaguchi, H.; Ichikawa, Y.; Isoda, S.; *Chem. Pharm. Bull*., **1991**, *35*, 1105

55. Elodah, H. M.; Friedrichs, G. S.; Chai, S.; Harrison, B. L.; Primeau, J.; Chlenov, M.; Crandall, D. L., *Bioorg. Med. Chem. Lett.*, **2002**, *12*, 1967.

56. Gaponik, P. N.; Voitekhovich, S. V.; Lyakhov, A. S., *Chem. Heterocycl. Compd.*, **2000**, *36*, 326.

57. Mason, T. J.; Lorimer, J. P.; Mistry, B. P., *Tetrahedron.*, **1985**, *41*, 5201.

58. Cysewsky, P.; Gackowska, A.; Gaca, J., *Chemosphere.*, **2006**, *63*, 165.

59. Vennestrom, J. L.; Ellis, W. Y.; Ager Jr, A. L.; Andersen, S. L.; Genera, L.; Milhous, W. K., *J. Med. Chem.*, **1992**, *35*, 2129.

60. Natarajan, J. K.; Alumasa, J. N.; Yearick, K.; Ekoue-Kovi, A. C.; Wolf, C.; Roepe, P. D., *J. Med. Chem*., **2008**, *51*, 3466.

61. Bray, P. G.; Hawley, S. R.; Mungthin, M.; Ward, S. A.; *Mol. Pharmacol.*, **1996**, *50*, 1559.

62. Stocks, P. A.; Raynes, K. J.; Bray, P. G.; Park, B. K.; O'Neill, P. M.; Ward, S. A., *J. Med. Chem.*, **2002**, *45*, 4975.

63. Madrid, P. B.; Wilson, N. T.; DeRisi, J. L.; Guy, R. K., *J. Comb. Chem.*, **2004**, *6*, 437.

64. (a) Egan, T. J.; Mavuso, W. W.; Ncokazi, K. K., *Biochemistry.*, **2001**, *40*, 204.

(b) Egan, T. J.; Hunter, R.; Kaschula, C. H.; Marques, H. M.; Misplon, A.; Walden, J., J. Med. Chem., 2000, 43, 283.

65. Deng, H.; Liu, H.; Krogstad, F. M.; Krogstad, D. L., *J. Chromatogr. B*, **2006**, *833*, 122.

66. Projean, D.; Baune, B.; Farinotti, R.; Flinois, J-P.; Baune, P.; Tuburet, A-M.; Ducharme, J., *Drug Metab. Dispos*., **2003**, *31*, 748.

67. De, D.; Byers, L. D.; Krogstad, D. J., *J. Heterocycl. Chem*., **1997**, *34*, 315.

68. Peck, R. M.; Preston, R. K.; Creech, H. J., *J. Am. Chem. Soc*., **1959**, *81*, 3984.

69. Musonda, C. C.; Ncokazi, K.; Egan, T. J.; Yardley, V.; Carvalho de Souza, R.; Chibale, K., *Org. Biomol. Chem.*, **2008**, *6*, 4446.

70. Musonda, C. C., *PhD Thesis*, University of Cape Town, **2005**.

71. Gomes, P.; Araújo, M. J.; Rodrigues, M.' Vale, N.; Azevedo, Z.; Iley, J.; Chambel, P.; Morais, J.; Moreira, R., *Tetrahedron.*, **2004**, *60*, 5551.

72. Araújo, M. J.; Bom, J.; Capela, R.; Casimiro, C.; Chambel, P.; Gomes, P.; Iley, J.; Lopes, F.; Morais, J.; Moreira, R.; de oliveira, E.; do Rosario, V.; Vale, N., *J. Med. Chem.*, **2005**, *48*, 888.

73. Loughheed, K. E. A.; Taylor, D. L.; Osborne, S. A.; Bryans, J. S.; Buxton, R. S., *Tuberculosis(Edinb)*, **2009**, *89*, 364.

74. Vale, N.; Moriera, R.; Gomes, P., *Eur. J. Med. Chem*., **2009**, *44*, 937.

75. Nkemngu, N. J.; Grande, R.; Hansell, E.; McKerrow, J. H.; Caffrey, C. R.; Steverding, D., *Int. J. Antimicrob. Agents*, **2003**, *22*, 155.

76. Chung, M. C.; Ferreira, E. I.; Santos, J. L.; Giarolla, J.; Rando, D. G., Almeida, A. E.; Bosquesi, P. L.; Menegon, R. F.; Blau, L., *Molecules*, **2008**, *13*, 616.

77. Das, B. P.; Boykin, D. W., *J. Med. Chem*., **1977**, *20*, 531.

78. Franzblau, S. G.; Witzig, R. S.; McLaighlin, J. C.; Torres, P.; Madico, G.; Hernandez, A.; Degnan, M. T.; Cook, M. B.; Quenzer, V. K.; Ferguson, R. M.; Gilman, R. H., *J. Clin. Microbiol.*, **1998**, *36*, 362.

79. Cho, S. H.; Warit, S.; Wan, B.; Hwang, C. H.; Pauli, G. F.; Franzblau, S. G., *Antimicrob. Agents Chemother.*, **2007**, *51*, 1380.

80. de Souza, M. V. N.; Pais, K. C.; Kaiser, C. R.; Peralta, M. A.; Ferreira, M. de L.; Lourenço, M. C. S., *Bioorg. Med. Chem*., **2009**, *17*, 1474.

Chapter Four

Synthesis and biological evaluation of 4-arylamino quinoline- and PA-824-tetrazoles, and *β*-Lactams

4.1 Preface

Encouraged by some of the results obtained from the deoxyamodiaquine and chloroquinoline tetrazoles (Chapter 3), the 4-arylamino quinoline and PA-824 scaffolds were utilized in designing the next series of compounds. The main objective of this undertaking was to generate compounds that will possess improved biological activity and physico-chemical properties compared to the parent drugs. Thus, this chapter will describe the synthesis and biological evaluation of tetrazoles based on the quinine-, mefloquine- and PA-824 scaffolds. In addition, a limited series of *β*-lactams is also described. In line with our overall goal in this project, *in silico* prediction tools were used in profiling the designed target compounds, synthesis of which was achieved through the use of the multi-component and Staudinger reactions. Lastly, *in vitro* antiplasmodial and antimycobacterial activity of the synthesized compounds is also disclosed.

4.2 4-Arylamino quinolines

The arylamino alcohol family of compounds include the 4-quinoline methanols, *i.e.* quinine and mefloquine, and their derivatives (Chapter 1, section 1.4.1.4.1A). About 400 years ago quinine's effectiveness was first documented. However, this drug is still an important antimalarial drug today.[1] Quinine (**4.1**) (Fig. 4.1) was one of the commonly used antimalarial drugs in the 1940s, and it was the first to be used for effectively treating malaria caused by *P. falciparum*.[2] Since that time, however, quinine has been replaced by other quinoline-based antimalarial drugs such as chloroquine, amodiaquine and mefloquine. Despite its limited use, quinine is still the drug of choice for the treatment of severe malaria. The mechanism of

action of quinine is unknown but is believed to exert its effectiveness against the asexual blood stage of the parasite because of its interference with the detoxification process of haematin.[3] One drawback of quinine and its stereoisomer, quinidine, is their implication in the inhibition of CYP2D6, an essential enzyme in the metabolism of a number of well known and important drugs.[4]

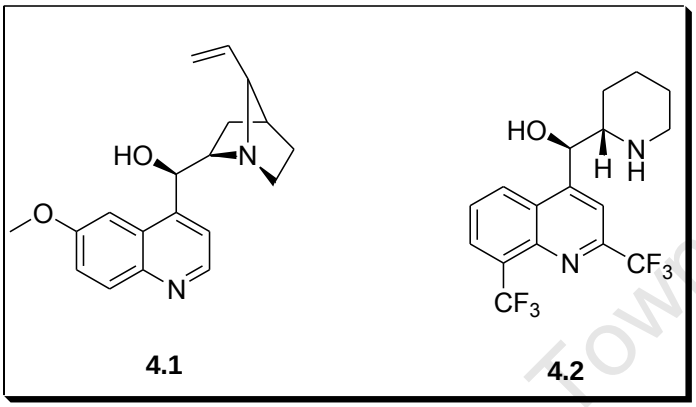

Figure 4.1: Quinine and Mefloquine, anti-malarial drugs.

Mefloquine (**4.2**) (Fig. 4.1) was discovered by the Walter Reed Army Institute of Research (WRAIR) in the 1960s following widespread resistance to quinine.[5] Mefloquine is a long-acting blood schizontocide, which is highly effective against the multi-drug resistant *P. falciparum*.[6] Mefloquine is also effective against all human malaria causing species, including *P. Knowles*.[7] The mode of action of mefloquine is not clearly understood but is believed to act in a similar way as quinine.[8] As effective as mefloquine is, its use is limited by adverse events such as neuropsychiatric adverse reactions, gastro-intestinal intolerability, and in rare instances cardiovascular effects.[7,8]

As already mentioned, the exact mechanism of action for this class of antimalarial drugs is not clearly understood. However, recent studies have proposed that these compounds exert their activity through (i) π-stacking with the porphyrin ring of the haeme moiety, (ii) coordination with the iron centre of the heme *via* the alkoxide formation on the benzylic alcohol, and (iii) intermolecular hydrogen-bonding interactions with the propionate side-

chain of the haeme.[9,10,11] Furthermore, the most convincing evidence in support of this proposed mode of action came from the crystal structure of the complex between halofantrine and ferriprotoporphyrin IX [Fe(III)PPIX] disclosed by Egan and co-workers (Fig 4.2).[9a]

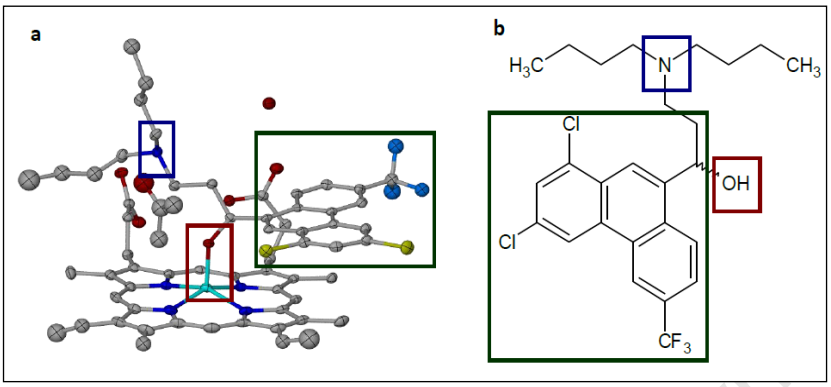

Figure 4.2: (**a**) Crystal structure of the haeme-halofantrine complex; (**b**) Highlighted halofantrine structural features responsible for the interaction with the haeme (reproduced from references 9a and 10).

In the crystal structure, in addition to the π-stacking with the porphyrin ring (green), halofantrine is depicted coordinating with the iron centre of the haeme through its benzyl alcohol moiety (red), and forming intermolecular hydrogen-bonding with the propionate side-chain of the haeme through its tertiary amine of the alkyl side-chain (blue). The same group expanded the scope of this study by further investigating the coordinating ability of various nitrogen donor ligands such as imidazoles, pyridines and amines with the haeme.[9b,10] From this study they discovered that nitrogen donor ligands containing sp^2 hybridised nitrogen, *i.e.* imidazoles and pyridine ligands, formed strong coordination with the iron centre of the haeme.

In our study, we hypothesized that incorporating the tetrazole ring that contains sp^2 hybridised nitrogen atoms, and the tertiary amine moiety in the arylamino quinoline core should potentially satisfy the three key requirement for activity of this class of compounds. The ability of the tetrazole ring to coordinate with the iron centre of the haeme has been

exploited by Roman *et al.*,[12] in the design of haeme oxygenase inhibitors, and by Adachi *et al*.,[13] in ligand binding studies of tetrazole-myoglobin complex. As such, in the design of our new analogues, the *O*-donor hydroxyl group is replaced with the *N*-donor tetrazole moiety, while the bridged six membered heterocyclic ring in quinine (Fig. 4.3A) or the piperidine ring in mefloquine (Fig. 4.3B) were in turn replaced by various tertiary amines.

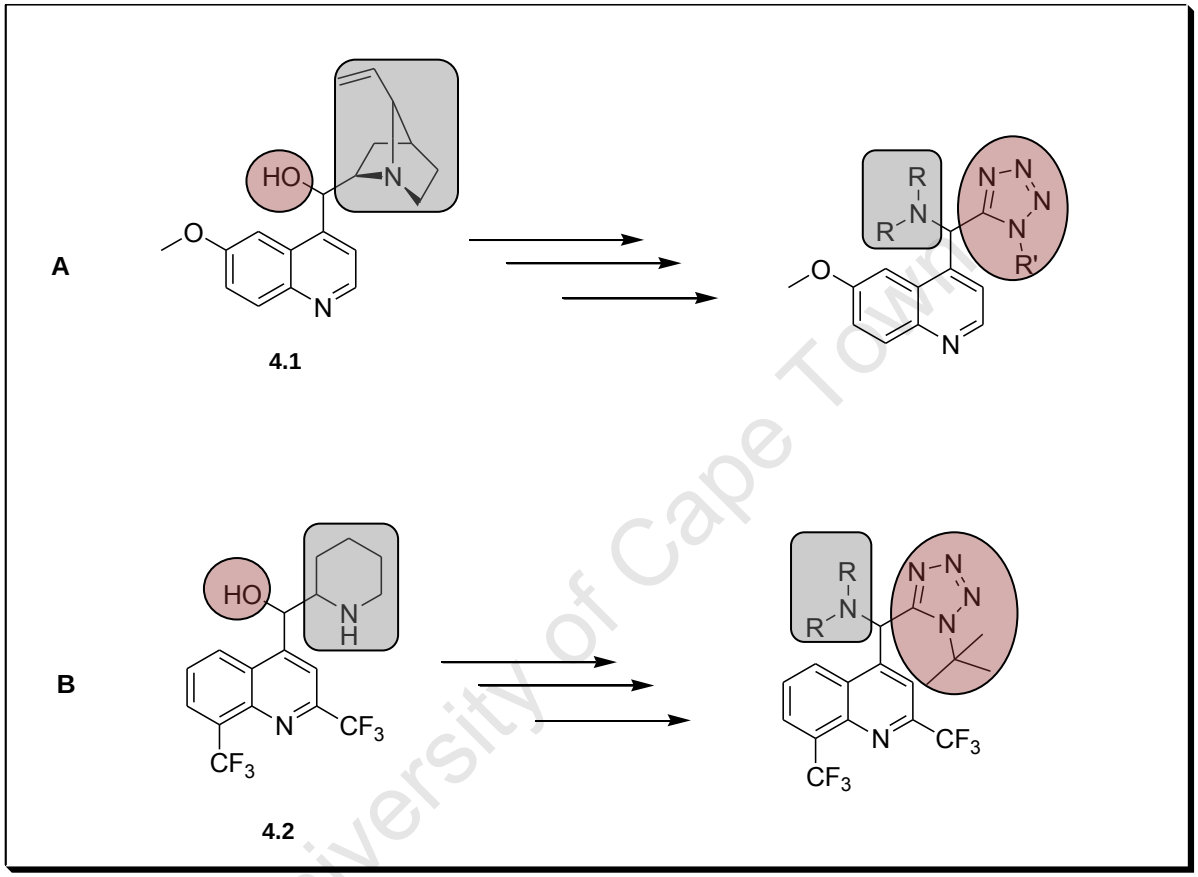

Figure 4.3: Substructure replacement in the design of quinine- and mefloquine-based target compounds.

4.2.1 In silico Profiling

The arylamino quinolines that were profiled *in silico* for aqueous solubility, metabolic stability, and blood-brain barrier (BBB) penetration are shown in Figure 4.4. The inclusion of the blood-brain barrier model was due to the fact the mefloquine and its derivatives tend to accumulate in the central nervous system (CNS).[14] Moreover, quinine has also been shown to have dose-related CNS effects following excessive infusion or from accumulation following

oral administration.[15] Thus, designing compounds with reduced permeation through the blood-brain barrier is of critical importance in avoiding adverse CNS effects.

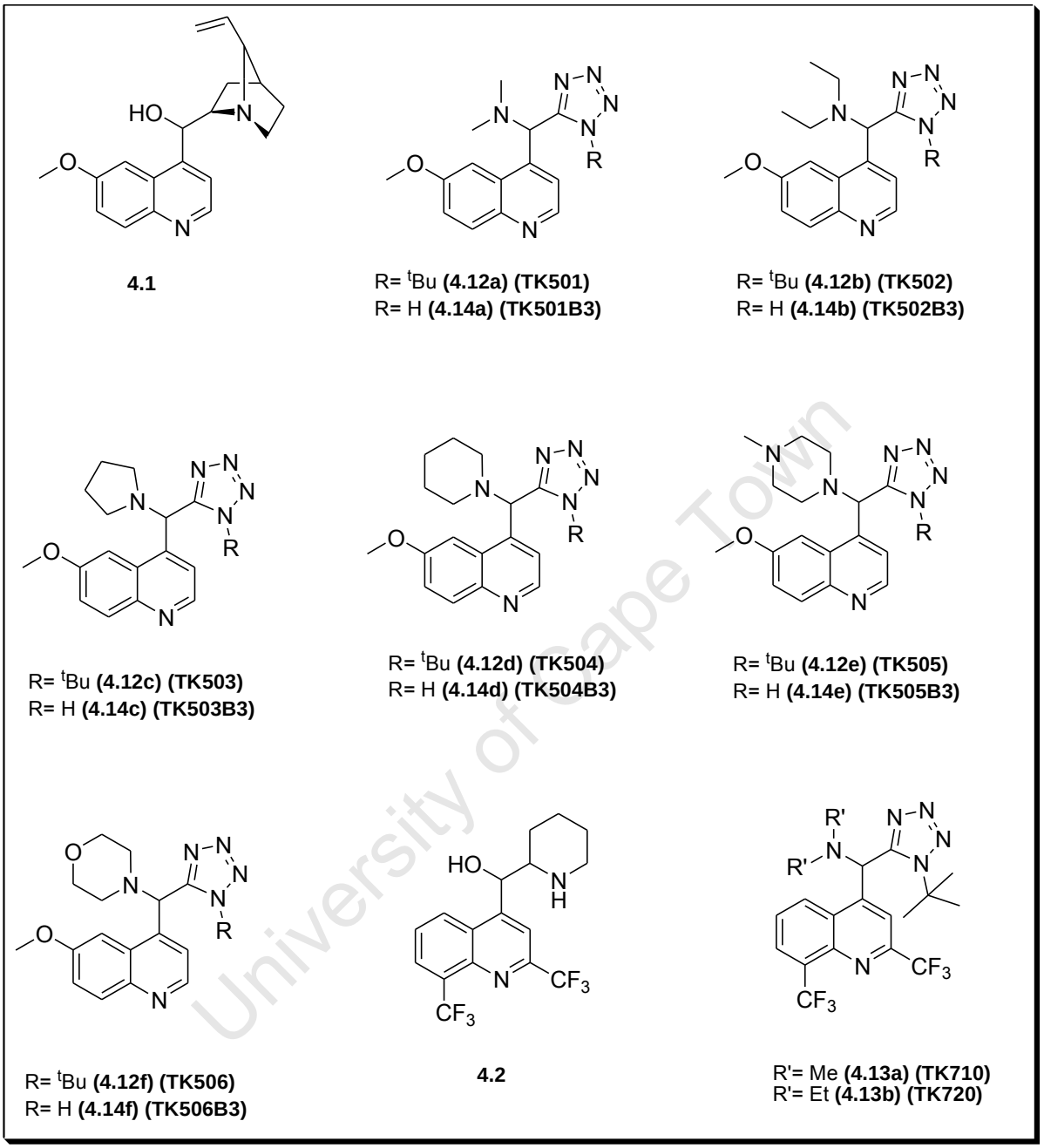

Figure 4.4: Structures of quinine- and mefloquine derivatives for *in silico* profiling.

At both pHs 5.0 and 7.5, the designed target compounds exhibited comparable and in some instances better predicted aqueous solubility than both reference drugs, quinine and mefloquine (Fig. 4.5). At pH 5, the majority of the deprotected quinine derivatives were predicted to be more soluble than quinine, with compounds **3.14a** and **3.14f** being the most

soluble. The *t*-butyl protected quinine derivatives showed reduced solubility compared to quinine, the least soluble compound in this series being **4.12e**. Mefloquine was predicted to be more soluble than its derivatives (**4.13a** and **4.13b**) but less soluble than quinine at pH 5. This was expected since mefloquine and its derivatives are known to be more lipophilic than quinine.

A similar trend to the one observed at pH 5 was also displayed by these target compounds at pH 7.5. The deprotected quinine derivatives were predicted to be about 100-fold more soluble than quinine, while the *t*-butyl protected derivatives had similar solubilities to quinine. This was also anticipated since the free tetrazoles are known to have strong acidic characteristics, hence they are easily ionised in basic conditions. Mefloquine on the other hand was again predicted to be more soluble than its analogues. The log D values of these compounds appeared to be highly influenced by the different pHs. The *t*-butyl protected quinine derivatives had lower log D values at pH 5 (ranging from 0 to 0.75) than at pH 7.5 (ranging from 1.8 to 2.8), while log D variations for the deprotected compounds was not as significant.

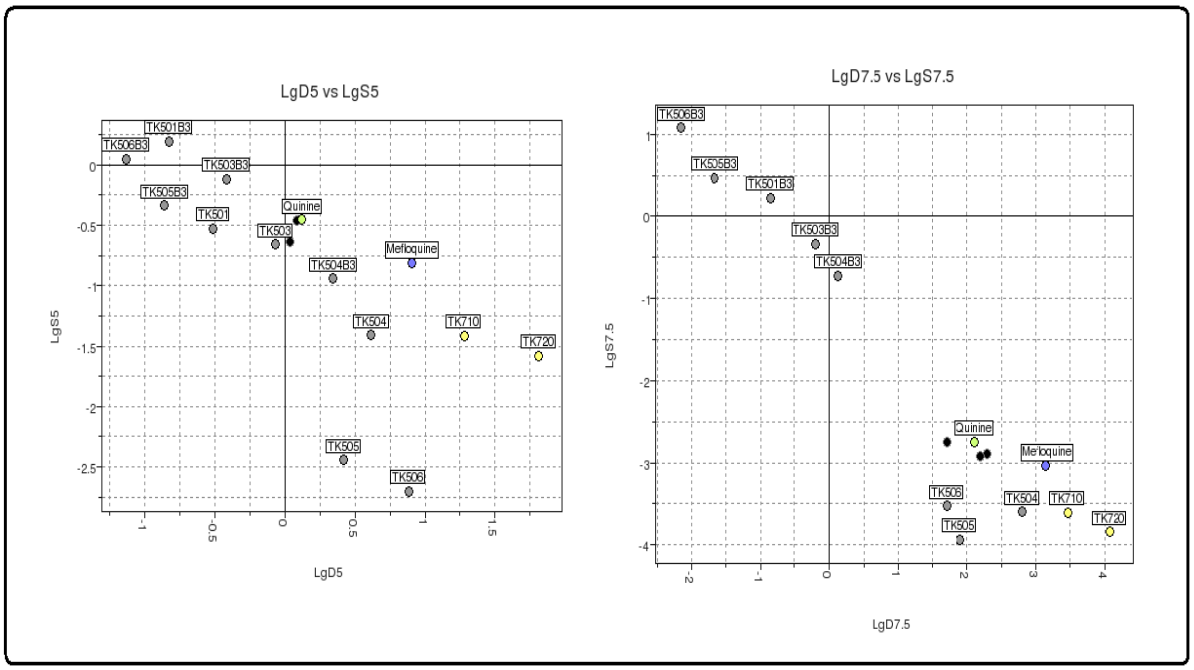

Figure 4.5: Plots of predicted aqueous solubility (log S) against *n*-octanol-water partition coefficient (log D) at pH 5.0 and 7.5.

Quinine and its derivatives were predicted to have acceptable metabolic stability (they all fall in the blue region) (Fig. 4.6). The deprotected derivatives were predicted to be more stable than quinine and the *t*-butyl protected analogues. Metabolic stability of mefloquine and its derivatives fell outside the 99% confidence interval, *i.e.* outside the solid ellipsoid, thus these compounds could not be reliably quantified.

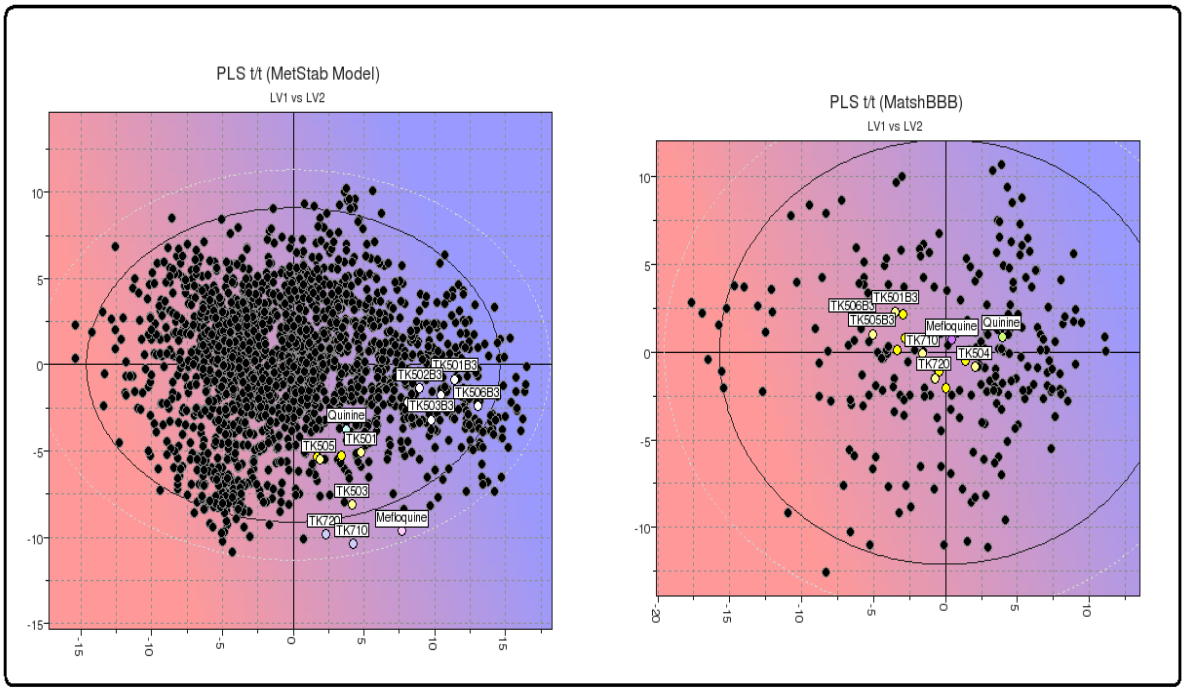

Figure 4.6: Plots showing the designed target compounds projected onto PLS models used to predict metabolic stability and blood-brain barrier permeation.

In addition, quinine and its *t*-butyl protected derivatives were predicted to have higher permeation through the blood-brain barrier, while the deprotected derivatives were not (Fig. 4.6). This observation to some extent lends support to the observed dose-related CNS effects caused by quinine. Mefloquine was also predicted to cross the blood-brain barrier as expected since this drug accumulates in the CNS. However, its two derivatives were predicted to have a reduced affinity for crossing the blood-brain barrier. It is important to note that these models were merely used as guide and indicator of potential physico-chemical properties inherent in the designed target compounds.

4.2.2 Synthesis of quinine and mefloquine derivatives

4.2.2.1 Synthesis of quinine and mefloquine nuclei

The first step in the synthesis of quinine and mefloquine derivatives involved the synthesis of quinine and mefloquine nuclei, *i.e.* 6-methoxyquinoline-4-carbaldehyde (**4.8**) and 2,8-bis(trifluoromethyl)quinoline-4-carbaldehyde (**4.11**). In synthesizing the quinine nucleus, procedures described by Daines *et al*.,[16] and Mao *et al*.,[17] were followed. Initially, the Meldrum's acid (**4.4**) was refluxed in ethanol with triethyl orthorformate to give an intermediate, methoxyethylene Meldrum's acid, *in situ*. This intermediate was then condensed with *p*-anisidine (**4.3**) *via* the addition-elimination reaction to yield an ene-amine intermediate **4.5**, which was subsequently used without further purification (Scheme 4.1).[18] Intermediate **4.5** undergoes intramolecular thermal cyclisation when refluxed in Dowtherm A to form the 6-methoxyquinolin-4-ol (**4.6**) in good yields upon cooling and subsequent precipitation with diethyl ether. Thereafter, the 6-methoxyquinolin-4-ol was brominated at room temperature by the slow addition of phosphorus tribromide under inert nitrogen atmosphere to give the 4-bromo-6-methoxyquinoline (**4.6**) in reasonable yields. The quinine nucleus then formed *via* the *n*-BuLi mediated formylation of 4-bromoquinoline in good yields.

The mefloquine nucleus was synthesized following a procedure described by Milner *et al*.[14] The commercially available 2,8-*bis*(trifluoromethyl)quinoline-4-ol (**4.9**) was melted with phosphorus oxybromide at 75 to 150 °C to give rise to the 4-bromo-2, 8-*bis*(trifluoromethyl)quinoline (**4.10**) in reasonable yields (Scheme 4.2). The mefloquine nucleus, 2,8-*bis*(trifluoromethyl)quinoline-4-carbaldehyde (**4.11**), was also obtained *via* the *n*-BuLi mediated formylation of 4-bromo-2,8-*bis*(trifluoromethyl)quinoline in low yields, and as such was used in the next step without any further purification.

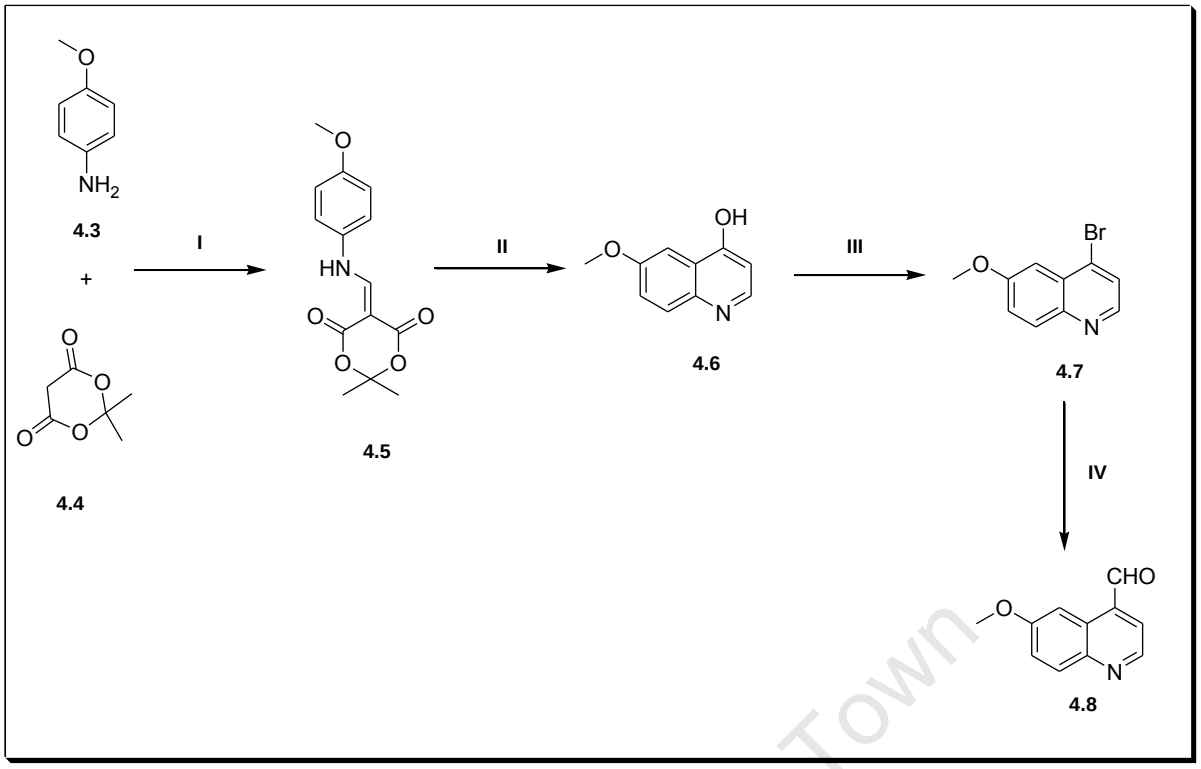

Scheme 4.1: *Reagents and conditions*: (i) triethyl orthorformate (1.0 eq), EtOH, reflux, 4 hrs, **80%**; (ii) Dowtherm A, 250 °C, 20 min, **90 %**; (iii) PBr_3 (1.2 eq), DMF, N_2, 2 hrs, rt, **55%**; (iv) Et_2O, *n*-BuLi (0.5 eq), DMF, -78 °C, 3 hrs, **86%**.

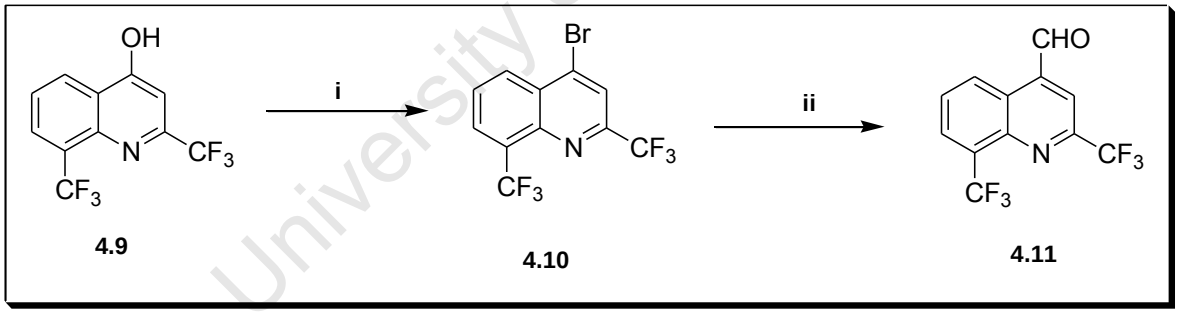

Scheme 4.2: *Reagents and conditions*: (i) $POBr_3$ (8.0 eq), 75 ^oC to 150 ^oC, 2 hrs, **65%**; (ii) THF, *n*-BuLi (3.0 eq), DMF, -78 °C, 3 hrs, **29%** (crude yield).

4.2.2.2 Mechanistic comments on the synthesis of 6-methoxyquinolin-4-ol (4.6)

Meldrum's acid is a highly acidic (pKa 4.97) and versatile synthetic reagent that readily undergoes *mono*- or *di*-functionalisation at the 5 or (β) position due to its propensity to enolize.[19,20] The mechanism begins when triethyl orthoformate first expels an ethoxide ion (**A**) *in situ*, which will deprotonate Meldrum's acid (**4.4**) to form an enolate (**I**), resulting in

the formation of electrophilic oxonium ion (**B**).[21] This oxonium ion is then attacked by the enolate to give rise to intermediate **II** (Scheme 4.3). Abstraction of the second acidic proton in **II** results in ethoxymethylene Meldrum's acid intermediate **III**, which undergoes a Michael addition reaction with the *p*-anisidine **4.3** to give intermediate **IV** that rearranges into intermediate **V**, which then form an ene-amine intermediate **4.5**.[18] The nitrogen lone-pair of electrons then activates the *ortho* position of the ring (**VI**),[22] and this activated intermediate then undergoes intramolecular cyclisation *via* the elimination of acetone to give intermediate **VII**. Subsequent thermal decarboxylation and proton transfer of intermediate **VII** results in the desired 6-methoxyquinolin-4-ol (**4.6**).

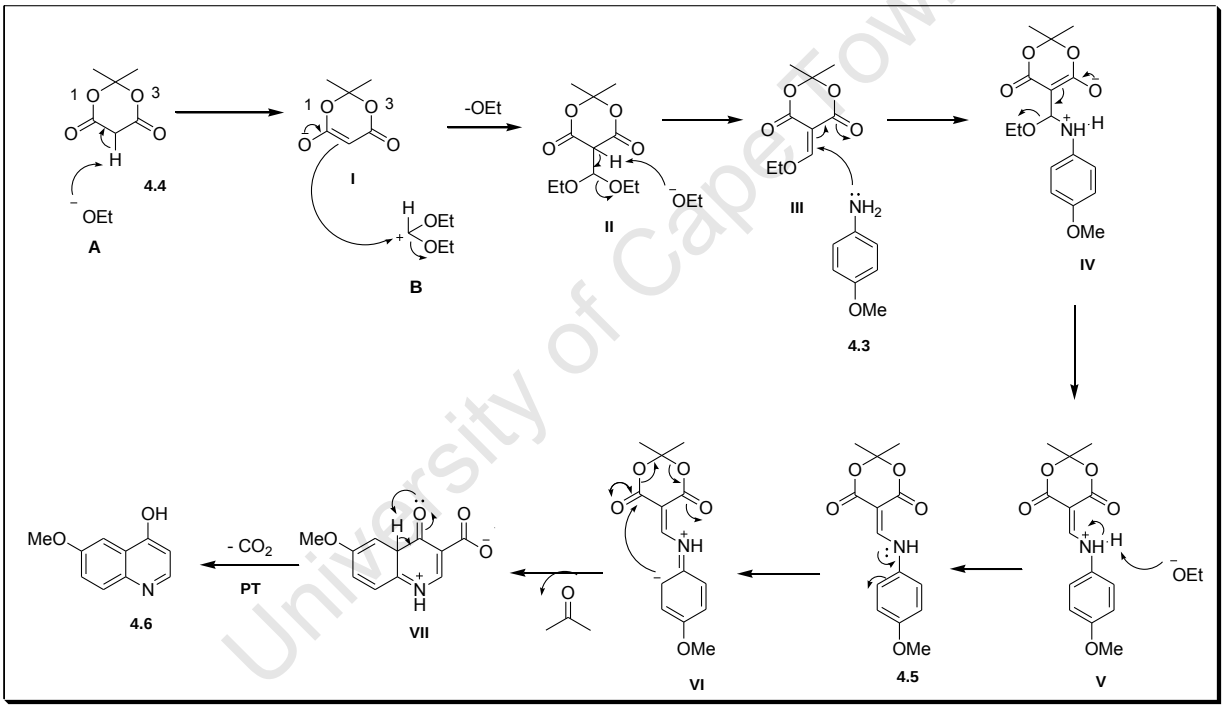

Scheme 4.3: Proposed mechanism for the formation of 6-methoxyquinolin-4-ol (**4.6**).

4.2.2.3 Synthesis of quinine- and mefloquine-based tetrazoles

With the desired nuclei (**4.8** and **4.11**) in hand, the modified $TMSN_3$-Ugi MCR procedure described in chapter 3, was followed to give the desired target compounds, **4.12a-f** and **4.13a-b**, in low to excellent yields after column chromatography purification (Scheme 4.4 and

Table 4.1). Furthermore, HPLC purity check of the synthesized compounds confirmed purity greater than 95%.

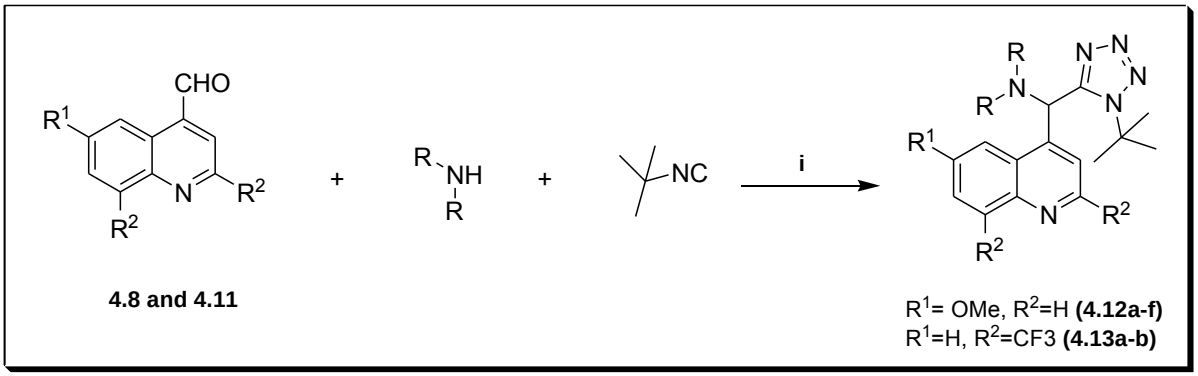

Scheme 4.4: *Reagents and conditions*: (i) $TMSN_3$ (1.0 eq), MeOH, 26 °C, 24 hrs.

Table 4.1: Yields and melting points of the target compounds.

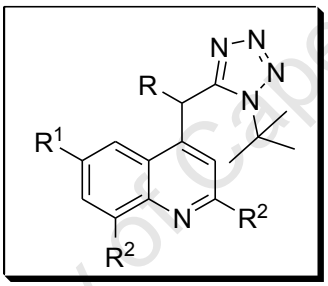

Code	Product	R	R^1	R^2	Yield/ [%]	HPLC Purity/ [%]	Melting point/ [°C]
4.12a	**TK501**		OMe	H	65	95.2	101-103
4.12b	**TK502**	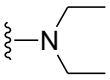	OMe	H	80	99	118-121
4.12c	**TK503**	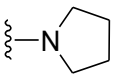	OMe	H	46	96.6	-
4.12d	**TK504**	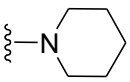	OMe	H	87	95.5	117-119
4.12e	**TK505**	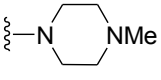	OMe	H	56	98.9	140-144
4.12f	**TK506**	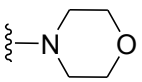	OMe	H	75	93.8	110-112
4.13a	**TK710**		H	CF_3	22	98.9	171-173
4.13b	**TK720**	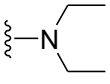	H	CF_3	12	95.3	76-78

Figure 4.7 shows superimposed ^{1}H NMR spectra of the representative compounds **4.12a** and **4.13a**. Singlets at 1.56, 2.48, 3.99 and 6.12 ppm in the spectrum of **4.12a** are due to the nine protons of the *t*-butyl group (H11), six protons of the two methyl groups (H10), methoxy protons, and H9 methine proton, respectively. Similarly, in the spectrum of **4.13a**, singlets at 1.60, 2.43, and 6.29 ppm are due to the nine protons of the *t*-butyl group (H10), six protons of the two methyl groups (H9), and H8 methine proton, respectively. Moreover, in both compounds protons in the aromatic regions are accounted for, thus these in addition to the mass spectrometry confirm the formation of the desired target compounds.

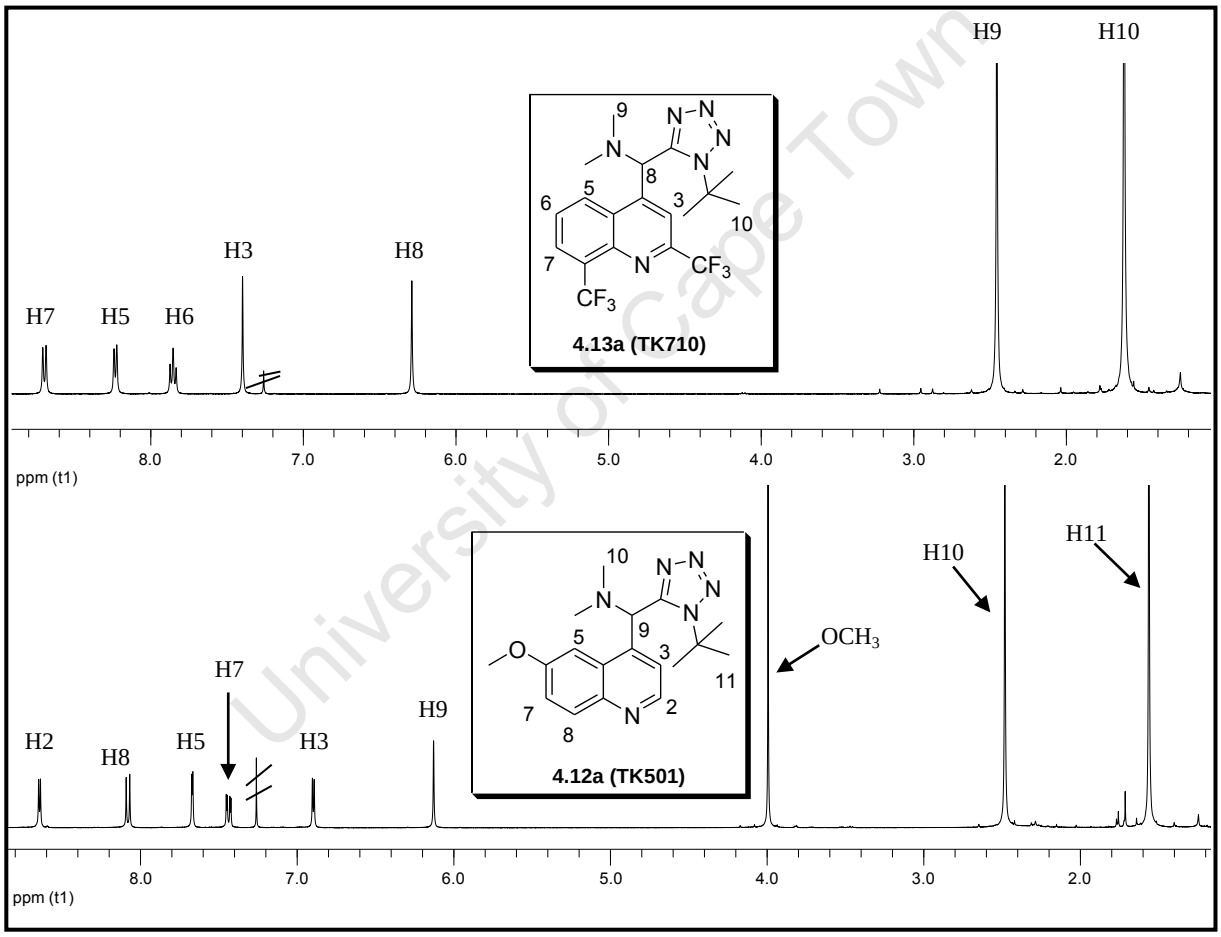

Figure 4.7: Superimposed 400 MHz ^{1}H NMR spectra of products **4.12a** and **4.13a** in $CDCl_3$.

4.2.2.4 De-*tert*-butylation of quinine-based tetrazole compounds

The de-*tert*-butylation procedure disclosed in chapter 3 was followed in the synthesis of de-*tert*-butylated quinine derivatives **4.14a-f** (Scheme 4.5**,** Table 4.2). It is also worth

mentioning that de-*tert*-butylation of the mefloquine derivatives was not attempted due to the insufficient amounts obtained in the synthesis of compounds **4.13a** and **4.13b**.

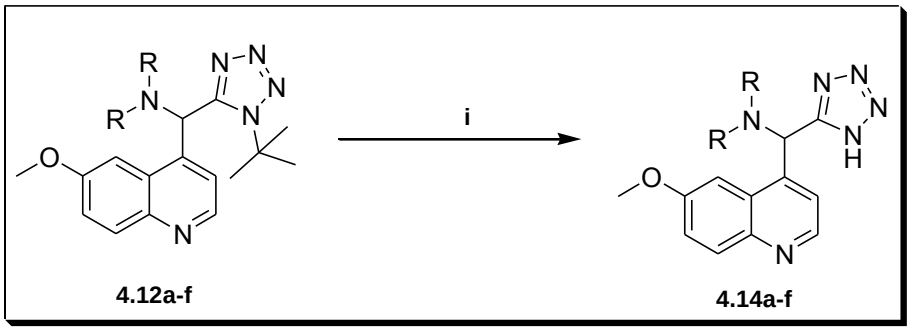

Scheme 4.5: *Reagents and conditions*: (i) neat 32% HCl, 120 °C, 8-12 hrs.

Table 4.2: Yields of the Quinine-based target compounds

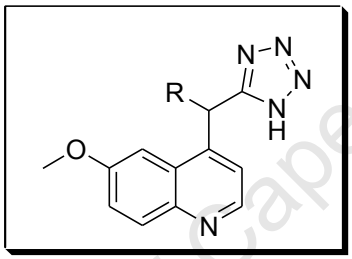

Code	Product	R	Yield/ [%]	HPLC Purity/ [%]	Melting point/ [°C]
4.14a	**TK501B3**		33	95.8	159-162
4.14b	**TK502B3**	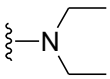	15	96.7	168-171
4.14c	**TK503B3**	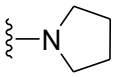	13	95.1	211-214
4.14d	**TK504B3**	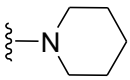	28	95.2	131-134
4.14e	**TK505B3**	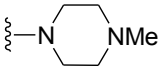	34	95.6	176-179
4.14f	**TK506B3**	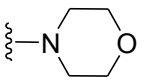	21	99.1	137-140

The presence of the desired de-*tert*-butylated compounds was confirmed by NMR spectroscopy (^{1}H and ^{13}C) and mass spectrometry. Figure 4.8 shows superimposed ^{1}H NMR spectra of products **4.14b**, the desired de-*tert*-butylated product, and **4.12b**, the parent

compound. The main differences between the spectra of the two compounds is the absence of a singlet at 1.56 ppm that corresponds to the nine protons of the *tert*-butyl group (H12) and the downfield shift of H3 signal in the spectrum of compound **4.14b** when compared to that of compound **4.12b**.

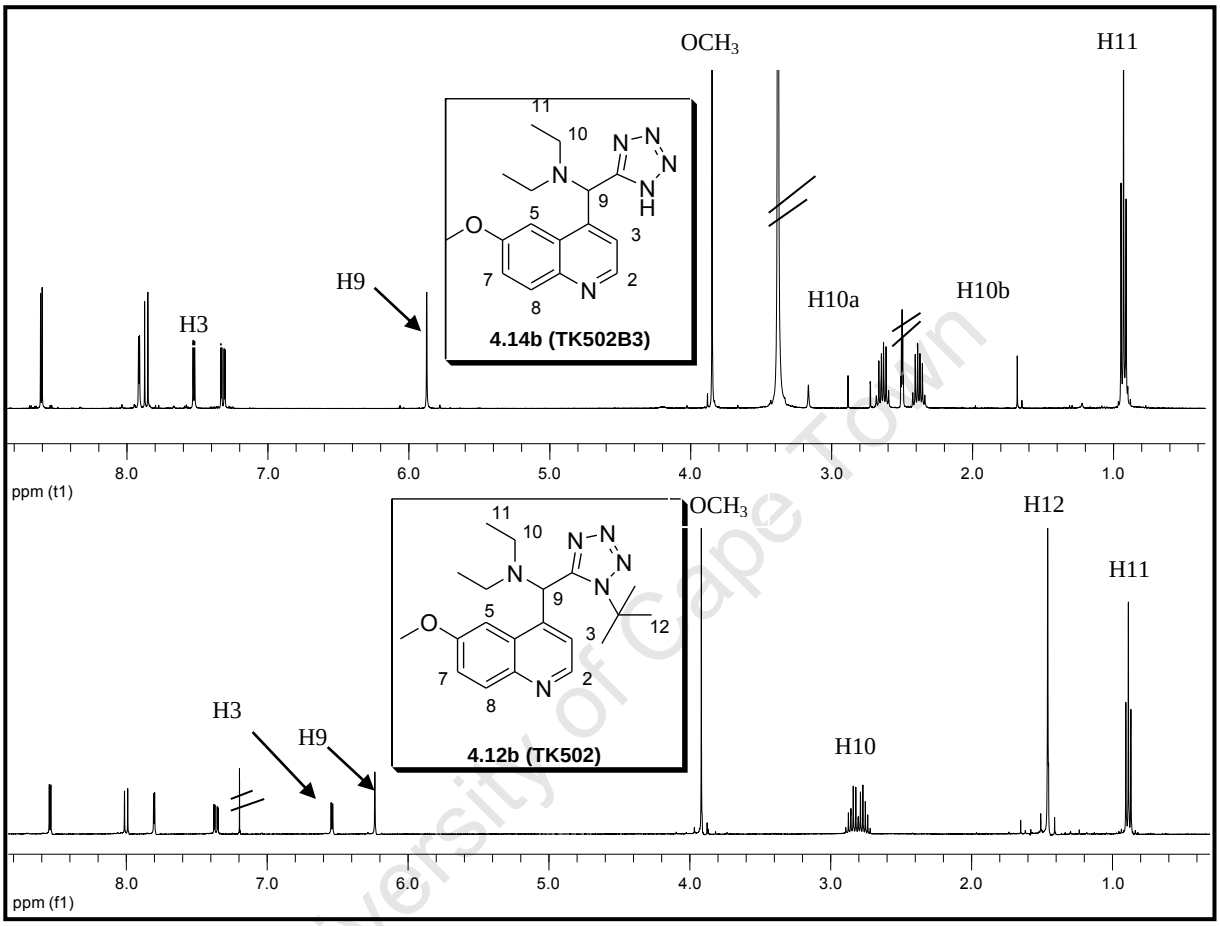

Figure 4.8: Superimposed 400 MHz ^{1}H NMR spectra of products **4.12b** in $CDCl_3$ and **4.14b** in DMSO-d_6.

4.2.3 Experimental determination of solubility

Experimentally determined kinetic solubility results of the selected arylamino quinoline derivatives at pH 7.4 are shown in Table 4.3. It is important to note that for comparison purposes only one of the de-*tert*-butylated compounds was assayed for solubility. From Table 4.3 it is clearly evident that all these compounds exhibited high solubility, with values greater than 100 μM. Also, as was in the *in silico* predictions, the de-*tert*-butylated compound **4.14f** (201.86 μM) was found to be more soluble than the protected analogues, **412f** (178.54 μM).

Furthermore, quinine (186.68 μM) was more soluble than these compounds except for compounds **4.12a** (189.45 μM) and **4.14f** (201.86 μM), confirming the results of the *in silico* predictions.

Table 4.3: Results for experimentally determined kinetic solubility at pH 7.4

Code	Product	Solubility at pH 7.4 (μM)	Conclusion
TK501	**4.12a**	189.45	Highly soluble
TK502	**4.12b**	136.84	Highly soluble
TK504	**4.12d**	114.44	Highly soluble
TK506	**4.12f**	178.54	Highly soluble
TK506B3	**4.14f**	201.86	Highly soluble
Quinine sulfate		186.68	Highly soluble

4.3 Nitroimidazoles

4.3.1 Brief background on nitroimidazooxazines

Imidazole, a privileged scaffold, is a five-membered heterocyclic system that has a wide spectrum of biological activity such as antifungal,[23] antibacterial and antitubecular,[24] anti-inflammatory,[25] anticancer,[26] and antiviral activity[27] among others. Nitroimidazoles are a special class of compounds that are widely used in the management of anaerobic bacterial and protozoan infections.[28] In addition, nitroimidazoles have been shown to possess activity against the HIV-1 recombinant reverse transcriptase enzyme.[29]

Nitroimidazooxazines are pro-drugs that are highly effective against both the replicating and non-replicating persistent forms of *M. tuberculosis*, a causative agent of TB.[30,31] Their activity is believed to arise as a result of metabolic activation of the nitroimidazole ring, which leads to the generation of nitric oxide as an active species.[32] An example of a nitroimidazooxazine-based antitubercular drug is PA-824. This drug is active against the multi-drug resistant form of TB and its use is aimed at shortening the current six-month TB

therapy.[30] PA-824 is being developed by the Global Alliance for TB Drug Development and is currently undergoing phase III clinical trials. From the SAR studies, the key structural features that have been identified to be responsible for the activity of PA-824 are the nitro group at the 4-position of the imidazole ring, the conformationally rigid bicyclic system, the *S*-configuration of the stereogenic centre, and the lipophilic group at the *para*-position of the phenyl ring (Fig. 4.9).[32,33,34] Interestingly, the *S*-enantiomer of PA-824 is at least 100-fold more active than the *R*-enantiomer.[31] The main drawbacks of this drug are its poor aqueous solubility and its propensity to bind to proteins in human plasma.[35,36] Various strategies have been utilized in attempts to address these shortcomings. These include the synthesis of biphenyl analogues of PA-824,[37] the incorporation of the five-membered heterocyclic systems in PA-824,[34] the use of urea, carbamate and amide linkers in the place of the benzyl ether,[30] and hybridisation of PA-824 with oxazolidinone[38] among others. However, very few of these studies managed to improve these shortcomings while simultaneously retaining a similar or improved activity than PA-824. Thus, the aim of this study was to design and synthesize tetrazole derivatives of PA-824 that would possess improved physico-chemical properties and/or biological activity than the parent drug.

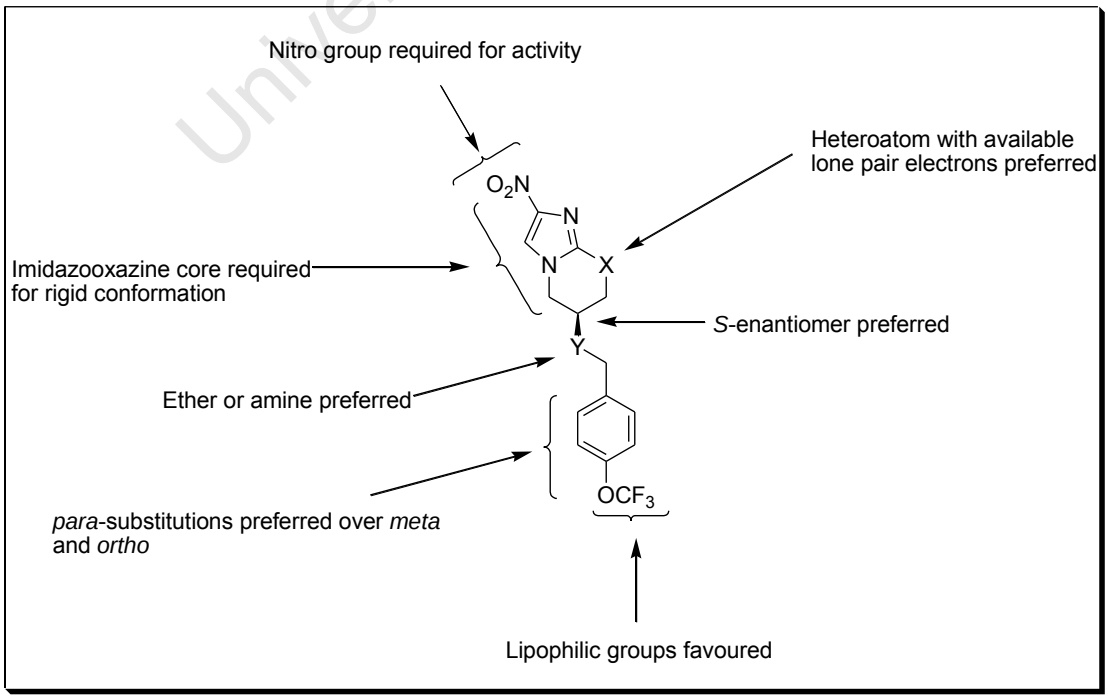

Figure 4.9: Structure-activity relationships of PA-824 (adapted from reference 31).

4.3.2 Rationale behind the design of PA-824 tetrazoles

The focus of the PA-824-oxazolidinone hybrids mentioned above was to investigate the effects of substituting the terminal lipophilic trifluoromethyl ether group in PA-824 (Fig. 4.10). From these studies, Ding *et al.*,[38] discovered that a number of these hybrids had improved activity compared to PA-824, and they also possessed a broad spectrum of activity. In an analogous manner to these hybrids, our rationale behind the design of PA-824-tetrazole derivatives is also depicted in Figure 4.10. It involved replacing the hydrophobic trifluoromethyl ether group with a tetrazole moiety and various ionisable tertiary or secondary amines.

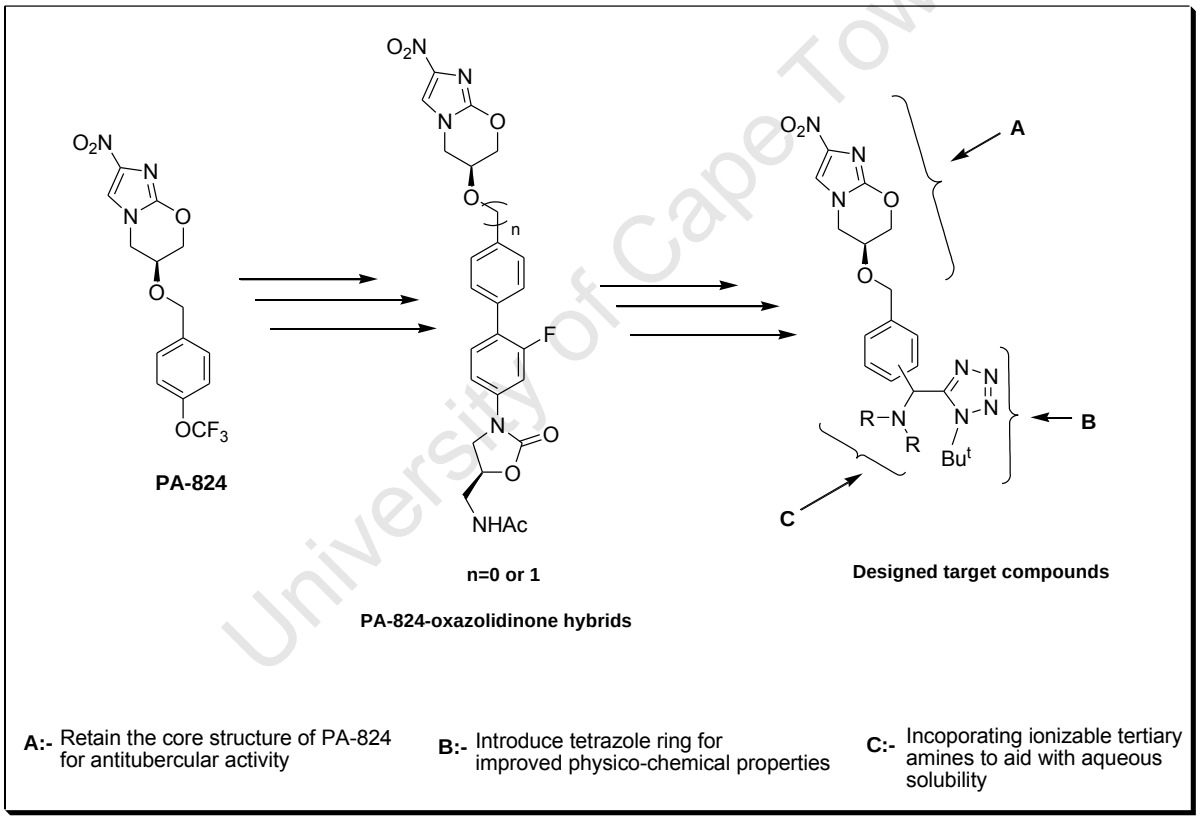

Figure 4.10: Rationale for the design of PA-824-tetrazole derivatives.

4.3.2.1 *In silico* profiling

As already mentioned above, the objective of our work on the nitroimidazooxazine was to design PA-824 derivatives that would be able to address the shortcomings of the PA-824 (*i.e.* improved aqueous solubility and reduced plasma protein binding). Figure 4.11 shows the

proposed series of PA-824 derivatives that were profiled *in silico* for aqueous solubility, permeability, metabolic stability, Protein_Binding (PB), and volume of distribution (VD). Hu *et al.*,[36] showed that 94% of PA-824 was protein bound in human plasma when given orally, thus this coupled with poor aqueous solubility of PA-824 have a negative impact on the oral bioavailability of this drug. Hence, this necessitated the inclusion of PB and VD models in the *in silico* predictions of the physico-chemical properties of the target PA-824 derivatives.

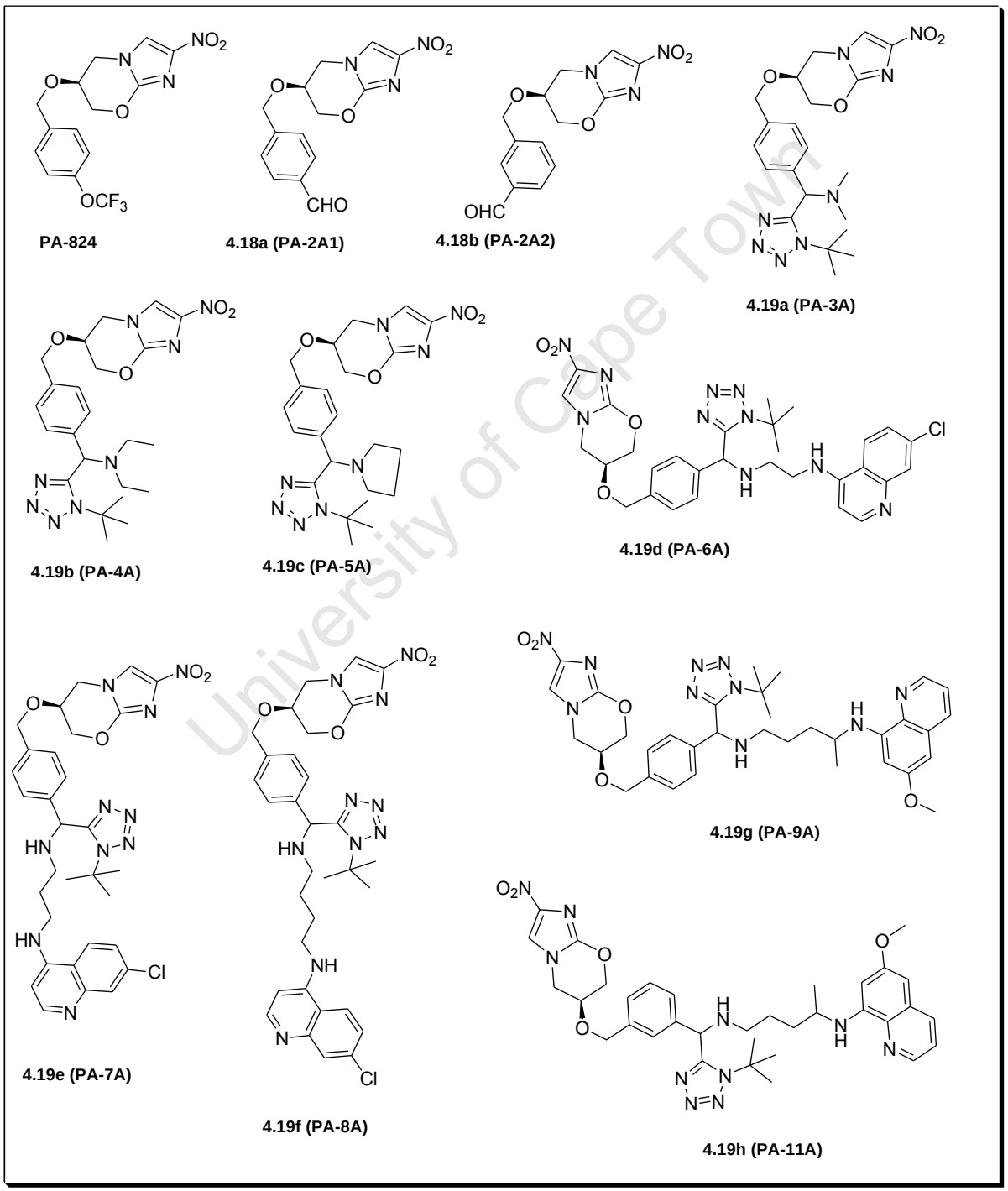

Figure 4.11: A series of tetrazole-based PA-824 derivatives for *in silico* profiling.

At pH 5, eight of the ten designed target compounds exhibited improved predicted aqueous solubilities than PA-824, the most soluble being compound **4.19e** (Fig. 4.12). This was anticipated since most of these new compounds contain ionisable centres and would exist predominantly in their ionized state at low pH levels. Primaquine-based PA-824 derivatives (**4.19g** and **4.19h**) were predicted to be the least soluble at this pH. Similarly at pH 7.5, compounds **4.18a-b** and **4.19a-c** showed superior solubility compared to PA-824, while compounds **4.19d-f** had comparable solubilities to that of the parent drug. Just like at pH 5, primaquine-based PA-824 derivatives (**4.19g** and **4.19h**) were less soluble than PA-824.

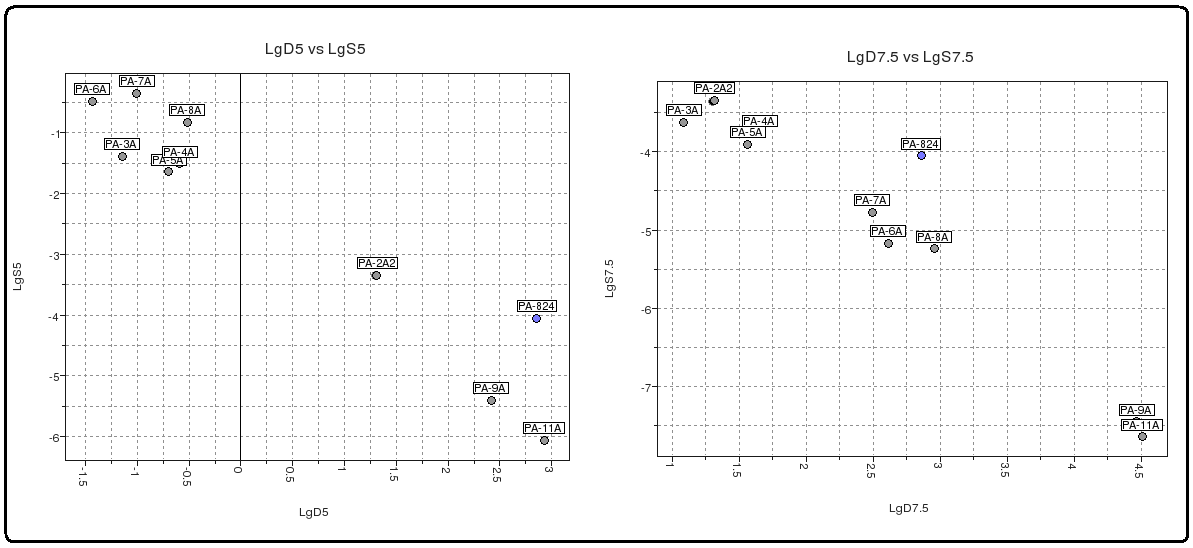

Figure 4.12: Plots of predicted aqueous solubility (log S) against *n*-octanol-water partition coefficient (log D) at pH 5.0 and 7.5.

Prediction of Caco-2 permeability, metabolic stability, PB and VD were all qualitative. All the designed compounds and PA-824 were predicted to have acceptable Caco-2 permeation (Fig. 4.13A). Compounds **4.18a-b** and **4.19a-c** were predicted to have comparable metabolic stability to PA-824, while compounds **4.19d-h** had relatively poor metabolic stabilities (Fig. 4.13B).

Volsurf+ Protein_Binding model reports mainly albumin protein binding values and the model contains 500 related, but structurally different database compounds partially collected

from literature and laboratories connected to the creators of the software. When these novel PA-824 derivatives were projected onto the two dimensional PLS plot of the database compounds used to generate the PB model, compounds **4.18a-b** and **4.19a-c** showed intermediate protein binding similar to PA-824, while compounds **4.19d-h** fell outside the quantifiable range, thus could not be assigned whether they are protein bound or not (Fig. 413C). However, due to the lipophilic nature of compounds **4.19d-h**, possibly they would bind to proteins in human plasma.

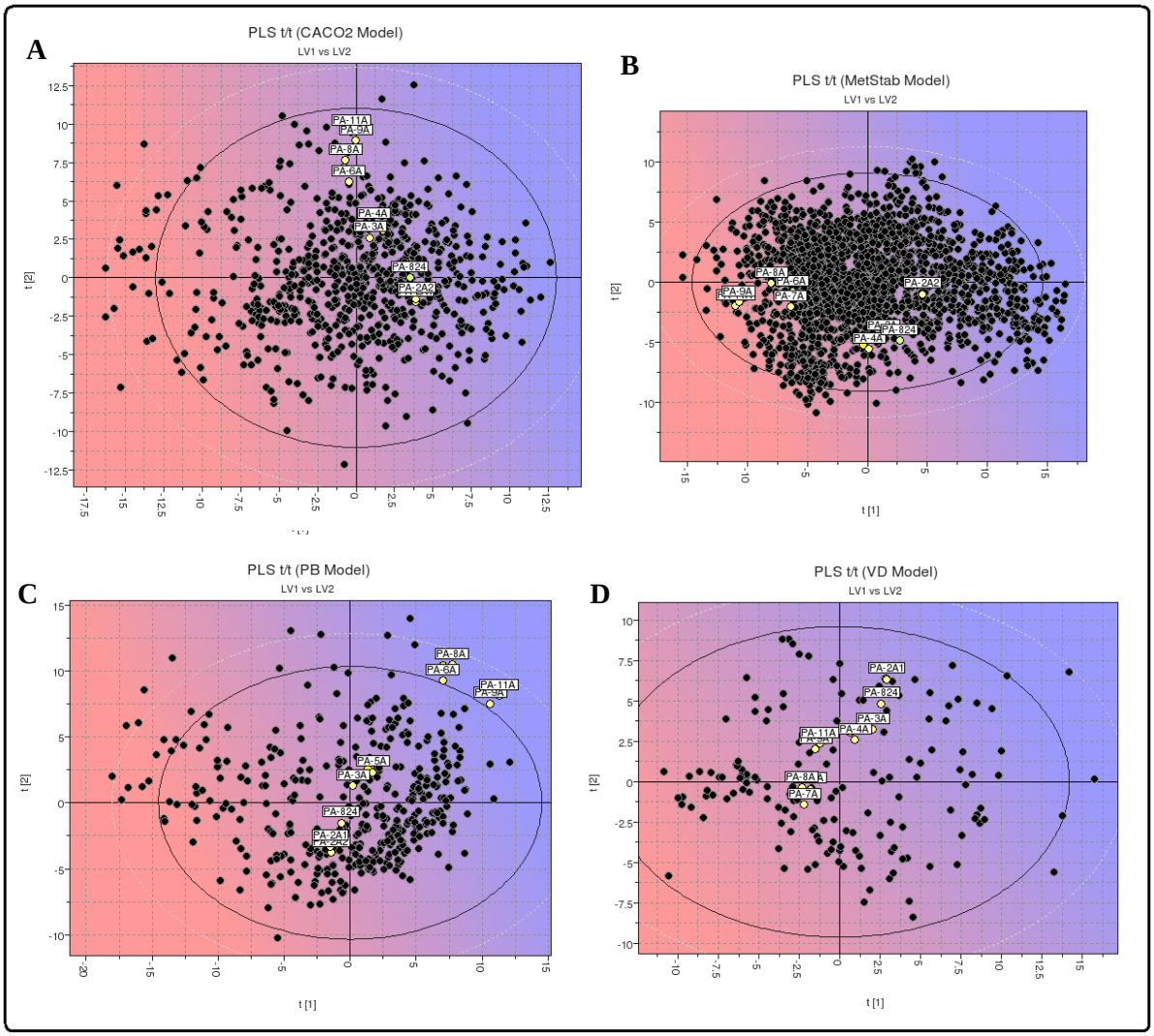

Figure 4.13: Plots showing the designed target compounds projected onto PLS models used to predict Caco-2 permeability, metabolic stability, protein binding (PB), and volume of distribution (VD).

In an attempt to get an idea on the distribution profile of these new PA-824 derivatives in the body, Volsurf+ volume of distribution model was utilized. This model consists of an inbuilt collection of more than 600 compounds from literature. Low VD values indicate low distribution to tissues while high VD values mean high distribution to tissues. When these new PA-824 derivatives were projected on this model it was found that compounds **4.18a-b** and **4.19a-c** were predicted to be highly distributed to tissues in the plasma, falling within the blue region, while compounds **4.19d-h** were less distributed to tissues, falling in the red zone. The fact that compounds **4.19d-h** were predicted to have less distribution to tissues corroborates the observation of the PB model, which indicated that these compounds have a slight affinity for binding to tissues.

In summary, a number of these novel compounds were predicted to have superior aqueous solubility than PA-824 at both physiological pHs. However, some of these appeared to have an affinity for binding to proteins and were susceptible to hepatic metabolic degradation.

4.3.2.2 Synthesis of target compounds

4.3.2.2.1 Retrosynthesis

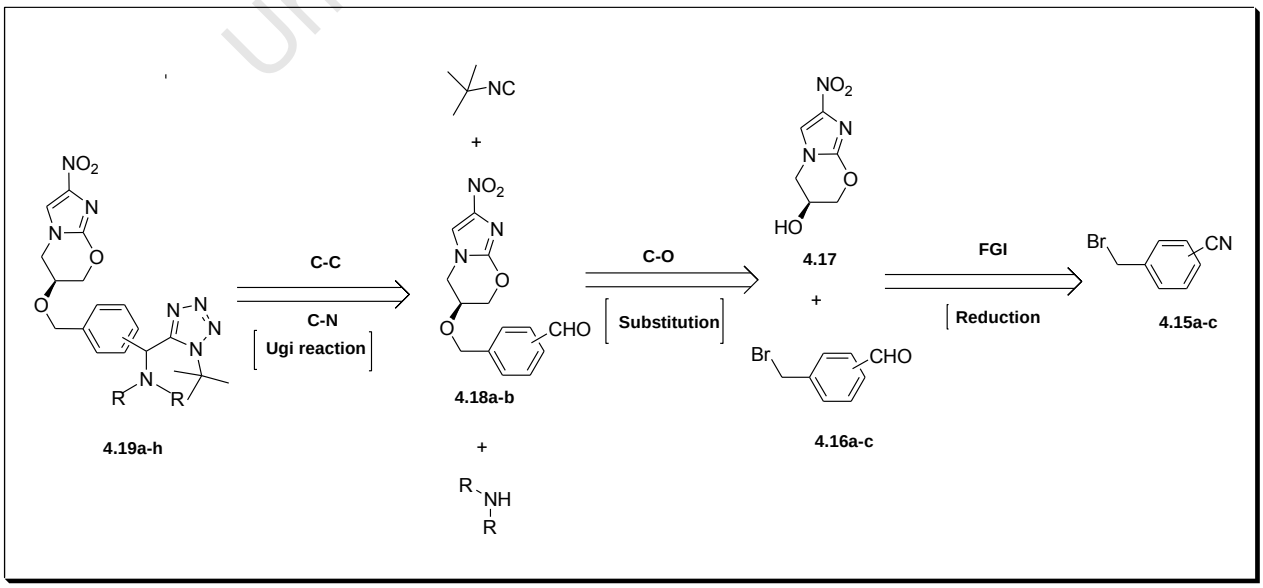

Scheme 4.6: Retrosynthetic pathway towards the PA-824-tetrazole analogues.

The retrosynthetic pathway towards the PA-824 derived target compounds is illustrated in Scheme 4.6. The key intermediates (**4.18a-b**) in the synthesis of the target compounds were obtained from the nucleophilic substitution reaction of alkyl halides (**4.16a-c**) and the commercially available nitroimidazooxazine alcohol (**4.17**). The benzylbromide aldehydes (**4.16a-c**) were in turn obtained from diisobutyl aluminium hydride (DIBAL-H) mediated reduction of the nitrile group.

4.3.2.2.2 Synthesis

The first step in the synthesis of the target compounds involved synthesizing alky halides (**4.16a-c**) using a known literature method.[39] The synthesized alkyl halides were then reacted with the commercially available nitroimidazooxazine-alcohol (**4.17**) in the presence of sodium hydride to afford the nitroimidazooxazine-aldehydes (**4.18a-b**) (*meta* and *para*) in modest to excellent yields (Scheme 4.7).[40] The *ortho* nitroimidazooxazine-aldehyde was not obtained as evidenced by the recovery of unreacted starting materials from the reaction mixture. The failure of the formation of the *ortho* nitroimidazooxazine-aldehyde is postulated to be the result of steric hindrance. The desired target compounds (**4.19a-h**) were then obtained from the MCR in moderate to excellent yields, with complete diastereoselectivity (Scheme 4.7 and Fig. 4.14).

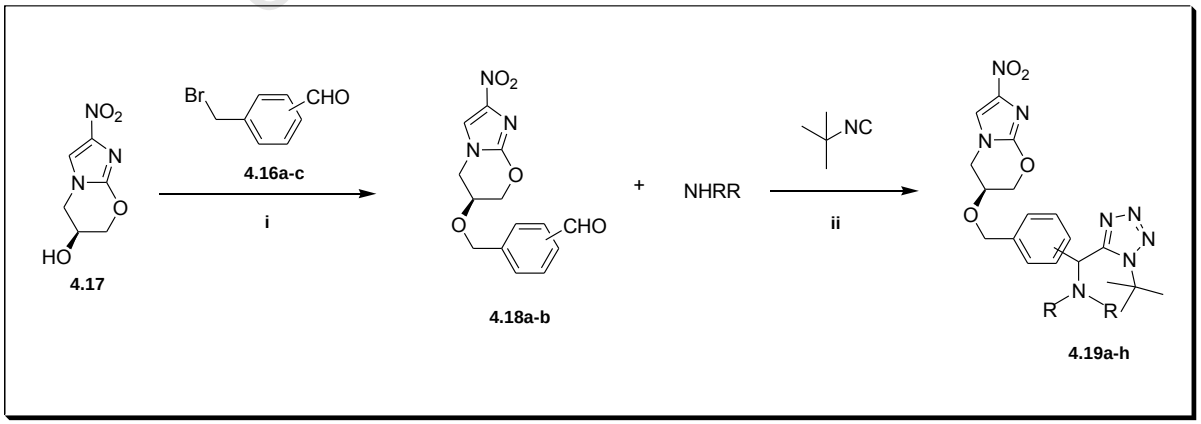

Scheme 4.7: *Reagents and conditions*: (i) NaH (1.3 eq), DMF, N_2, O°C to rt, 12 hrs; (ii) MeOH, 40°C, 12 hrs. (in the case of HCl protected amines, diisopropyl ethylamine (2.0 eq) was used to neutralize such salts).

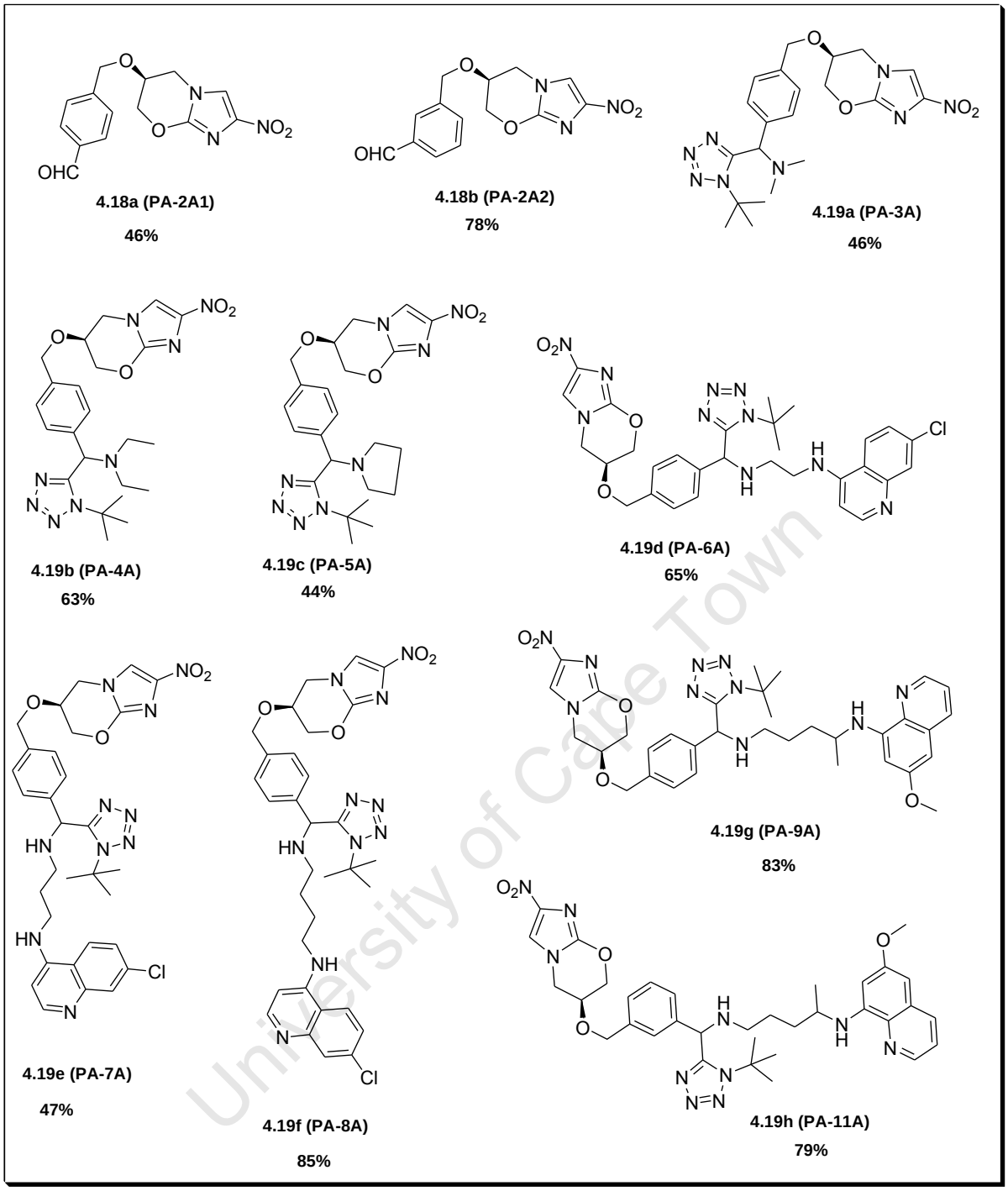

Figure 4.14: Yields and structures of the final PA-824 tetrazole derivatives.

Based on the ^{1}H NMR, six (**4.19a-f**) of the eight target compounds were obtained exclusively as single diastereomers, while compounds **4.19g** and **4.19h** were obtained as 1:1 diastereomeric mixtures. This may suggest that the newly created stereogenic centre favours one configuration over the other, *i.e.* stereochemical discrimination (it is important to note that the relative stereochemistry of this new stereogenic centre was not assigned). However,

this is surprising considering the fact that the $TMSN_3$-Ugi MCR is known for its poor diastereoselectivity.[41] Thus, this observed complete diastereoselectivity of this reaction is unprecedented. In addition, the obtained 1:1 diastereomeric mixtures of compounds **4.19g** and **4.19h** is not surprising given the fact that the primaquine salt used in this study is racemic.

A typical ^{1}H NMR spectrum of the precursor nitroimidazooxazine aldehyde (**4.18a**) is showed in Figure 4.15. All the signals are accounted for, and the important ones to highlight here are the singlets at 9.99 and 8.02 ppm which are due to the characteristic aldehyde proton and the H1 methine proton of the nitroimidazole ring, respectively. The doublet of doublets resonating at roughly 4.77 ppm is due to the H5 diastereotopic methylene protons, while the two signals at 2.73 and 2.89 ppm are due to the traces of the residual reaction solvent, *i.e.* dimethylformamide (DMF).

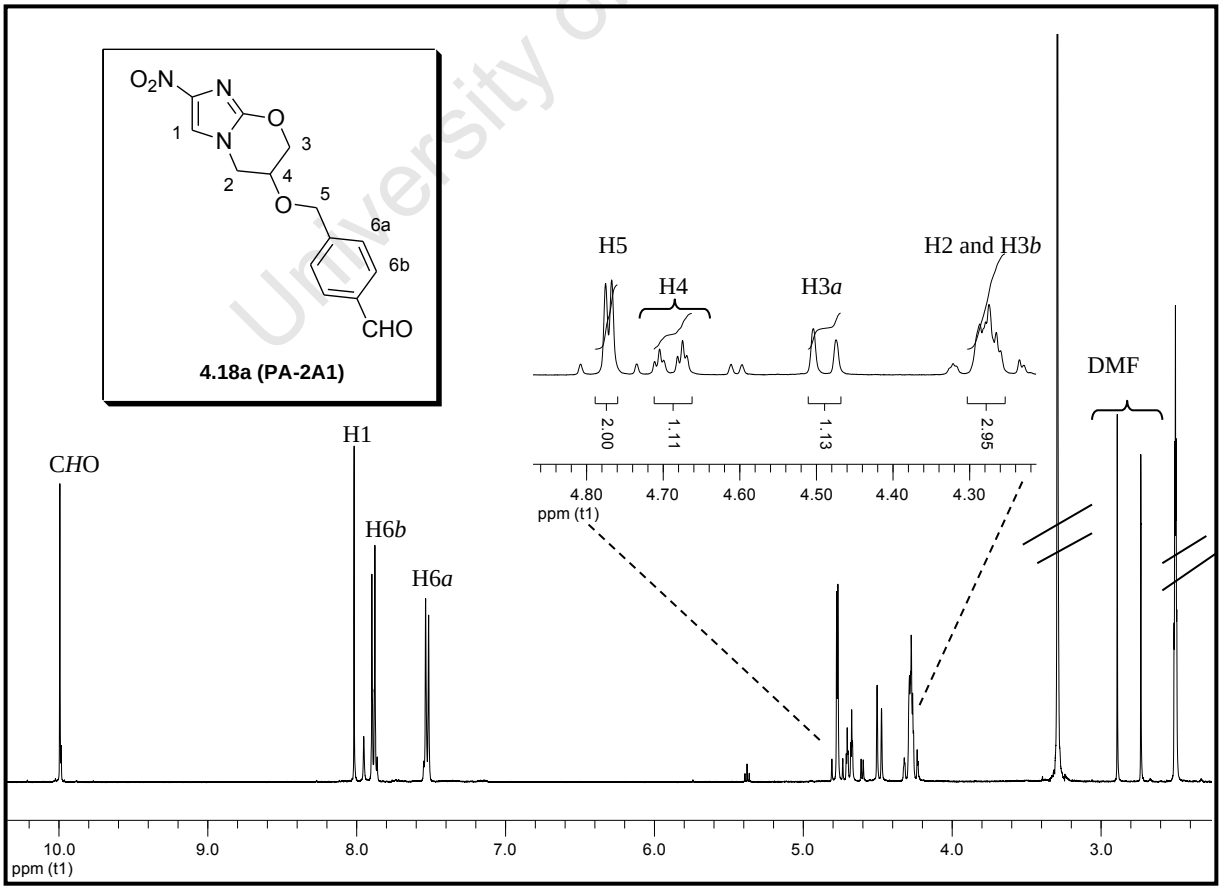

Figure 4.15: 400 MHz ^{1}H NMR spectrum of product **4.18a** in DMSO-d_6.

Figures 4.16 and 4.17 show ^{1}H NMR spectra of products **4.19c** and **4.19e**, a nitroimidazooxazine-quinoline hybrid compound, respectively. In Figure 4.16, the presence of the desired product **4.19c** was confirmed by the appearance of two singlets resonating at 1.69 and 5.20 ppm, which are due to the *t*-butyl group protons and H7 methine proton, respectively. Furthermore, signals resonating at 1.76 and 2.35-2.60 ppm are due to the pyrrolidine protons, while the rest of the signals are due to the nitroimidazooxazine scaffold. Similarly, Figure 4.17 confirms the presence of compound **4.19e**. Signals resonating at 1.57 and 5.30 ppm are due to the *t*-butyl group and H7 methine protons. Also, signals at 1.92, 2.75-2.93, and 3.41 ppm are due to the methylene H9, H10 and H8 protons, respectively, while the quinoline aromatic protons resonate in the region 6.29 to 8.46 ppm. The rest of the signals in figure 4.16 are due to the nitroimidazooxazine scaffold. In Figure 4.18, all the carbon signals are duplicated and off equal intensity, an indication of a 1:1 diastereomeric mixture of compound **4.19h**.

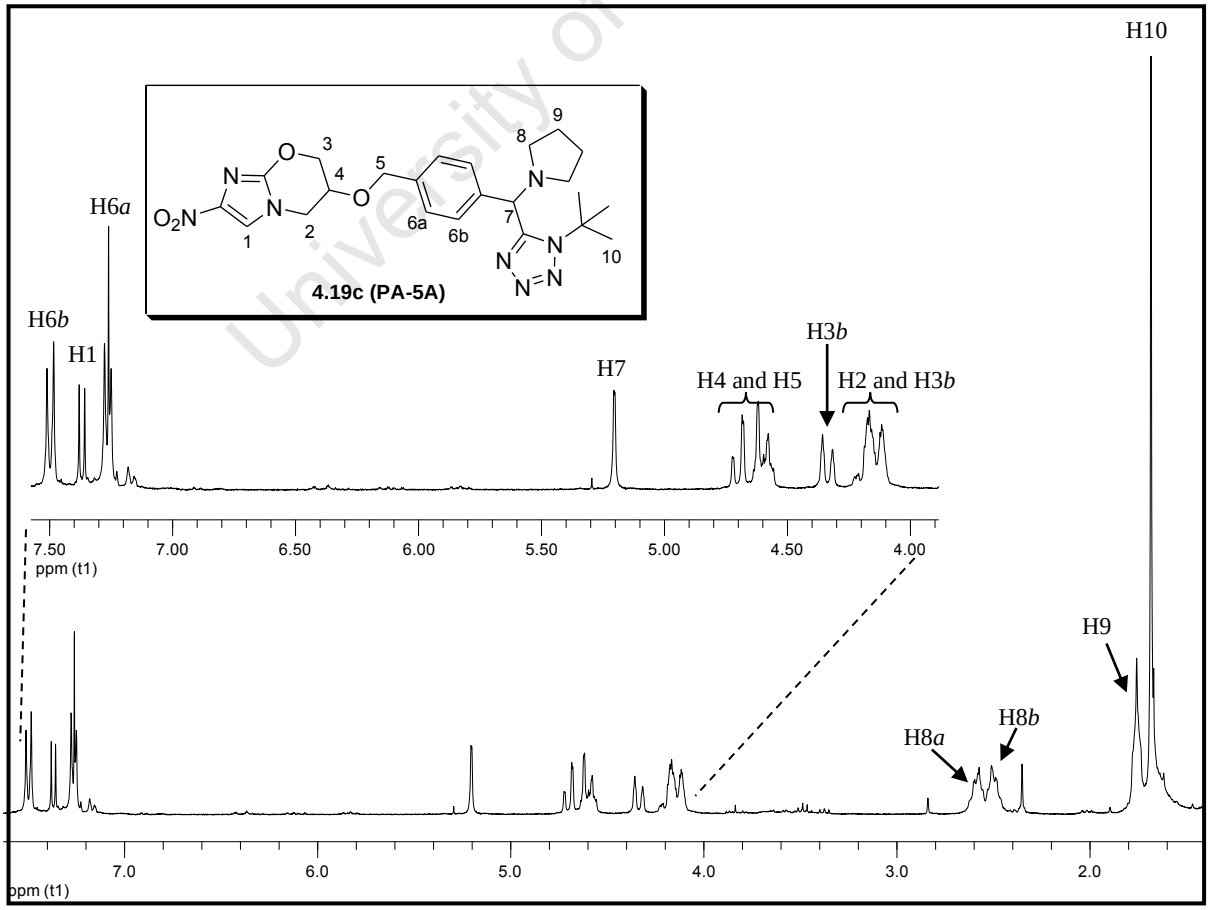

Figure 4.16: 400 MHz ^{1}H NMR spectrum of product **4.19c** in $CDCl_3$.

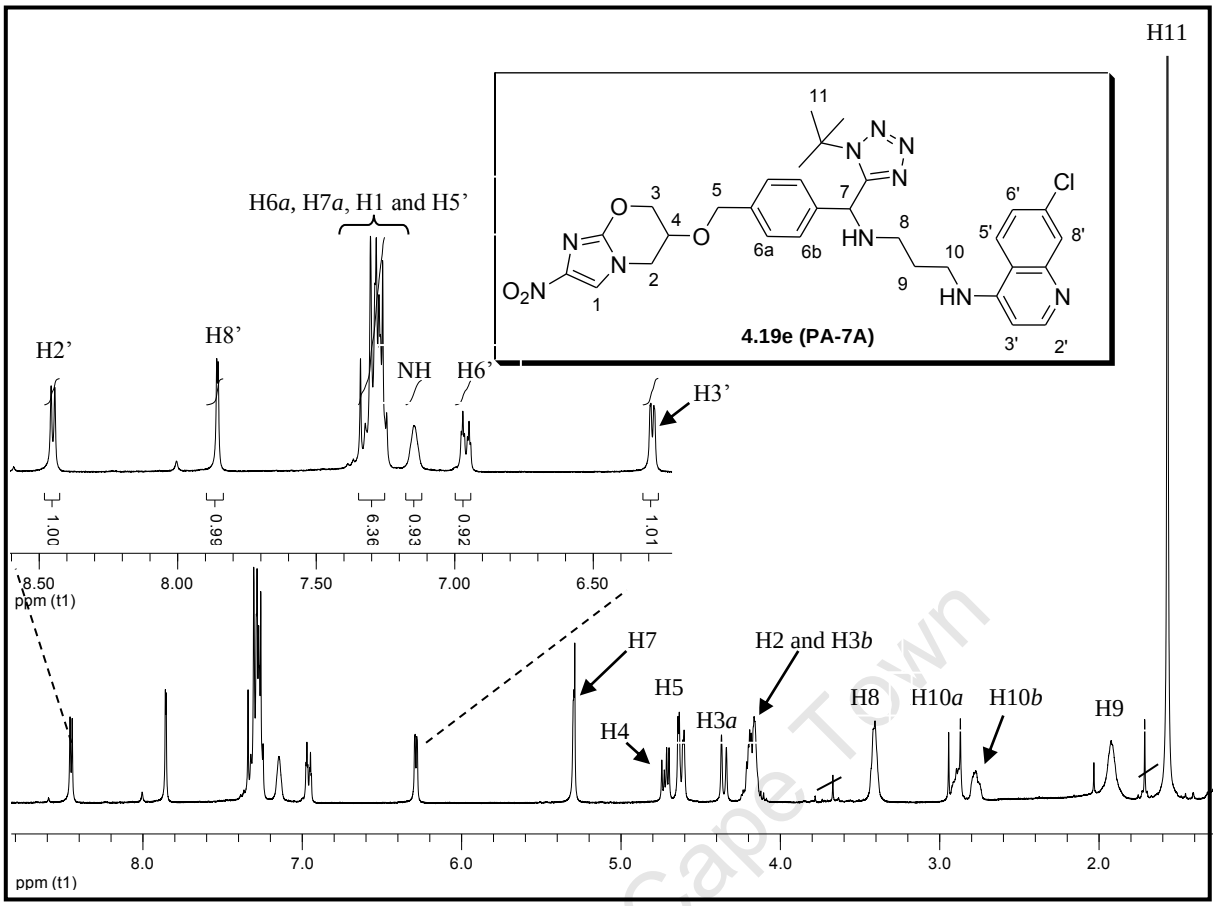

Figure 4.17: 400 MHz ^{1}H NMR spectrum of products **4.19e** in $CDCl_3$.

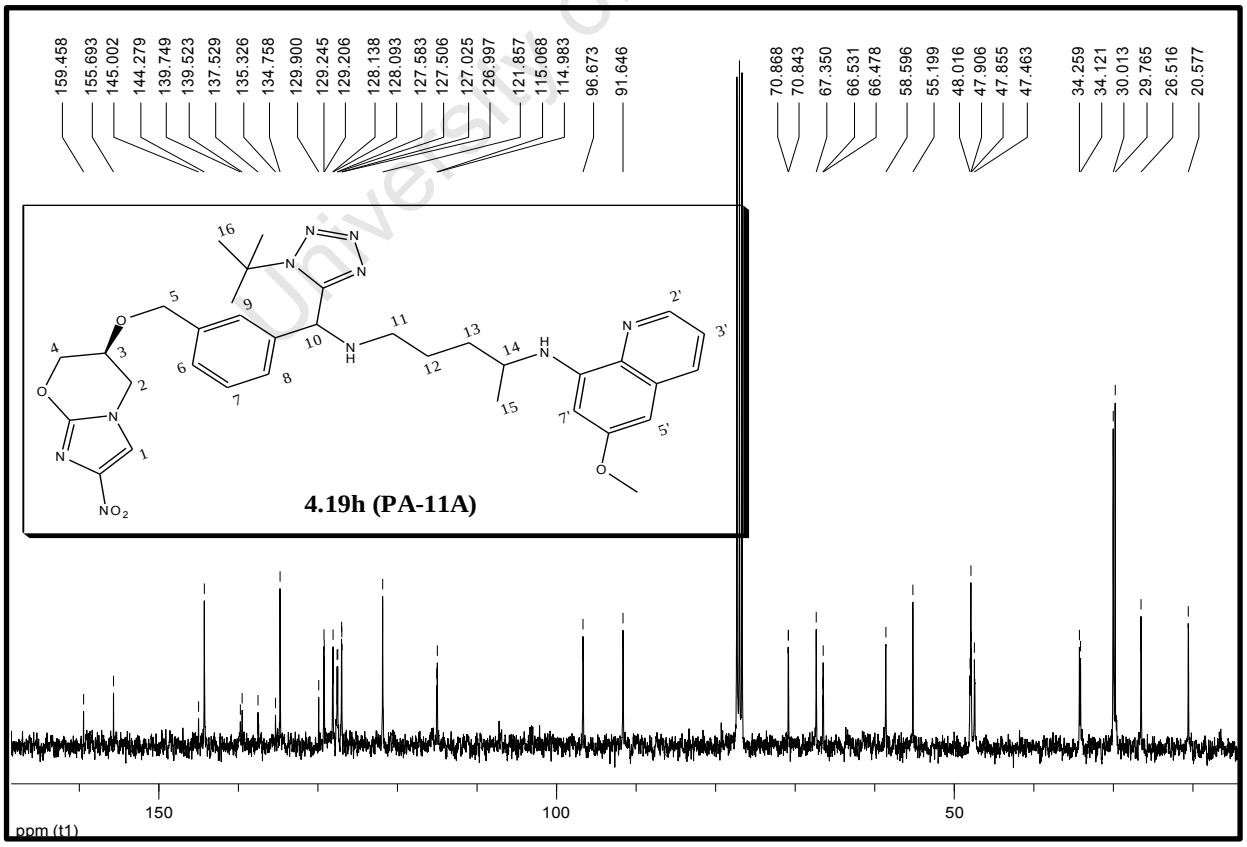

Figure 4.18: 101 MHz ^{13}C NMR spectrum of products **4.19h** in $CDCl_3$.

4.3.3 Experimental determination of solubility

As was in the *in silico* predictions, compounds with commercial amines (**4.19a**) were more soluble than the hybrids (Table 4.4).

Table 4.4: Results for experimentally determined kinetic solubility at pH 7.0 and 7.4.

Code	Product	Solubility at pH 7.0 and 7.4 (μM)	Conclusion
PA-3A	**4.19a**	195.79[a]	Highly soluble
PA-6A	**4.19d**	62.9 ± 0.66[b]	soluble
PA-7A	**4.19e**	59.9 ± 1.35[b]	soluble
PA-8A	**4.19f**	<5[a]	Insoluble
PA-9A	**4.19g**	<5[a]	Insoluble
PA-11A	**4.19h**	<5[b]	Insoluble

[a]Kinetic solubility performed at pH 7.4; and [b]Performed at pH 7.0

Among the hybrids, the PA-824-primaquine hybrids (**4.19g** and **4.19h**) were found to be insoluble, with values < 5 μM. On the other hand, solubility of the PA-824-quinoline hybrids decreased with an increase in chain length of the alkyl side-chain, with the 2-carbon spacer analogue, **4.19d** (62.9 μM); being slightly more soluble than the 3-carbon spacer, **4.19e** (59.9 μM), while solubility of the 4-carbon spacer analogue, **4.19f** (<5 μM) was completely abolished.

4.4 *β*-lactams

4.4.1 Brief background on *β*-lactams and Staudinger reaction

A *β*-lactam is a four-membered cyclic amide system found mostly in antibiotics such as penicillin and cephalosporin. *β*-lactam antibiotics are potent non-toxic broad-spectrum agents that have been a powerful first-line of defence against bacterial infections since their discovery.[42] The biological activity of most antibiotics is largely due to the presence of the *β*-lactam ring, of which once open, the antibiotic loses its antibacterial activity.[43] The heavy use of antibiotics over the years led to the emergence of bacteria that are resistant to *β*-lactams.[41] The most common and

relevant bacterial mechanism of resistance to *β*-lactams is the production of *β*-lactamase, a bacterial enzyme. This enzyme functions by hydrolyzing the *β*-lactam into the ring-opened *β*-amino acid, and as such inactivating antibiotics or compounds containing the *β*-lactam ring.[43] There are, however, various *β*-lactam derivatives that are known for inhibiting this enzyme. An example of this is the naturally occurring clavulanic acid (**4.20**) (Fig. 4.19).[44,45] Apart from their use as antibiotics, a number of compounds that contain the *β*-lactam nucleus are known to possess anti-HIV,[46] anti-cancer,[47] anti-malarial[48] and anti-TB[49,50] activity among others.

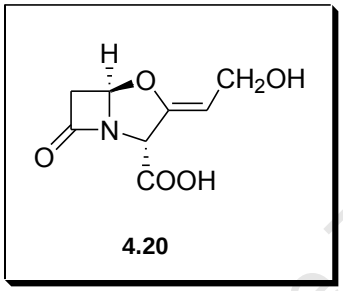

4.20

Figure 4.19: Clavulanic acid, a naturally occurring *β*-lactamase inhibitor.

A number of methods used to synthesize *β*-lactams are described in literature. However, the Staudinger[51] reaction is generally accepted as a method of choice.[52] The Staudinger reaction, named after its inventor, is a [2+2] imine-ketene cycloaddition reaction that results in the creation of a *β*-lactam ring bearing two stereogenic centres. This reaction was discovered in 1907, and to date its exact reaction mechanism is still a matter of debate.[53] However, it is generally acknowledged that this [2+2]-cycloaddition reaction is a stepwise reaction rather than a concerted one, and the key intermediate is a zwitterionic species that undergoes ring closure to give a final product as a *cis*-, *trans*- or a mixture of the two.[54,55] In this study this reaction was chosen in synthesizing a limited number of *β*-lactams mainly due to its simplicity.

4.4.2 Rationale for the design

Due to the broad spectrum of biological activity of *β*-lactams, the rationale behind this section of the project involved hybridizing the *β*-lactam ring with the 4-amino-7-chloroquinoline analogues (Fig. 4.20).

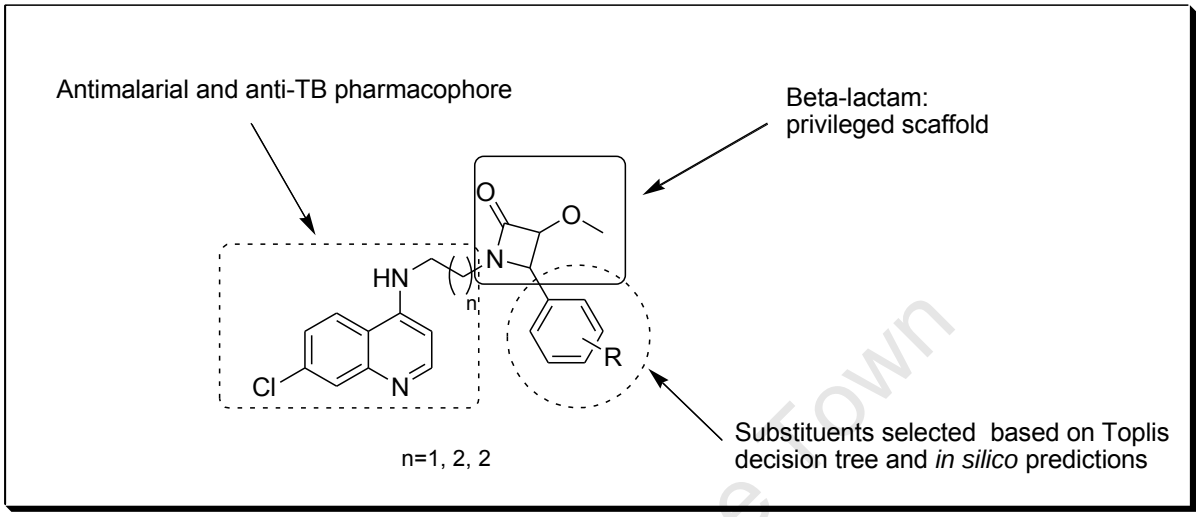

Figure 4.20: Rationale behind the *β*-lactam-quinoline hybrids.

The quinoline scaffold is found in a number of potent antimalarial drugs and is also known for possessing antitubecular activity.[53] Furthermore, *β*-lactam-quinolone hybrids have been shown by Miller and co-workers to have potent antitubercular activity.[49] Thus, it was envisaged that hybrid compounds containing these two scaffolds will not only possess a novel mechanism of action but will also circumvent metabolic *N*-dealkylation of the terminal alkyl side-chain of the 4-aminoquinolines, hence reducing the potential for resistance development.

4.4.3 *In silico* predictions

These *β*-lactam-quinoline hybrids were profiled *in silico* for aqueous solubility, permeability and metabolic stability in relation to chloroquine. At both pH 5.0 and 7.5 chloroquine showed significantly superior aqueous solubility than the hybrids (Fig. 4.21). This is expected since these *β*-lactam-quinoline hybrids are more hydrophobic than chloroquine. Furthermore, chloroquine has an added protonatable nitrogen on the alkyl side-chain which is absent in these hybrids.

Also, these *β*-lactam-quinoline hybrids showed acceptable predicted Caco-2 permeation that is comparable to that of chloroquine (Fig. 4.22). However, these hybrids were predicted to have intermediate metabolic stability, similar to that of chloroquine. The compound with the 3,4-*di*-chloro substituents on the phenyl ring was predicted to be the least stable in this series.

In summary, these *β*-lactam-quinoline hybrids were predicted to have *in silico* physico-chemical properties that were comparable but not better than chloroquine. Low aqueous solubility at both physiological pHs was identified to be major limitation of these hybrids.

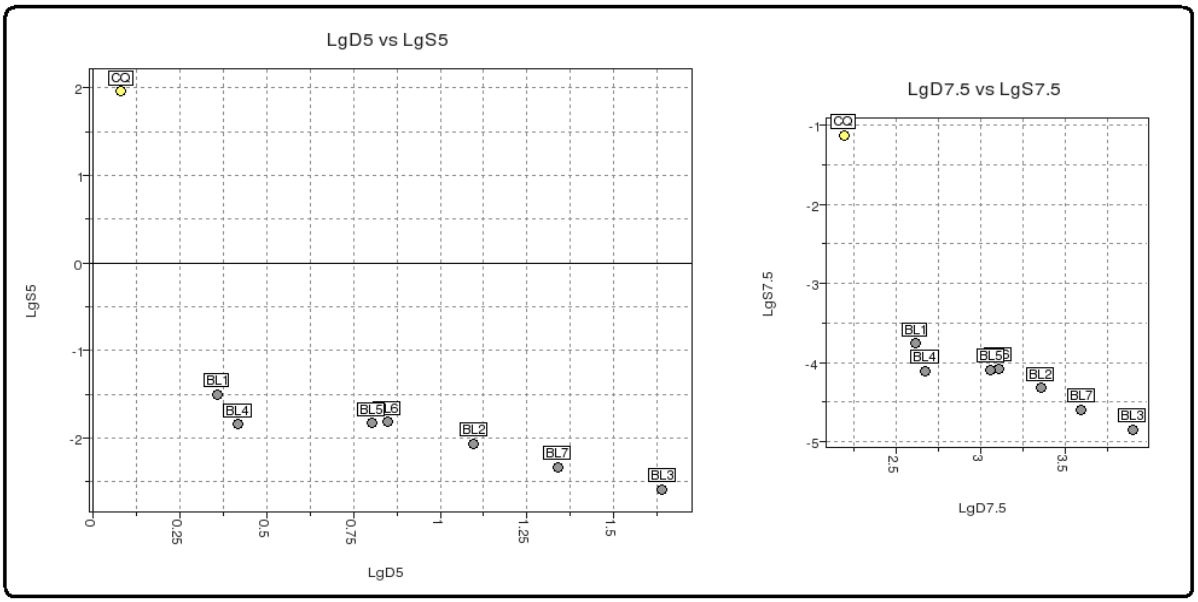

Figure 4.21: Plots of predicted aqueous solubility (log S) against *n*-octanol-water partition coefficient (log D) at pH 5.0 and 7.5, of *β*-lactam-quinoline hybrids.

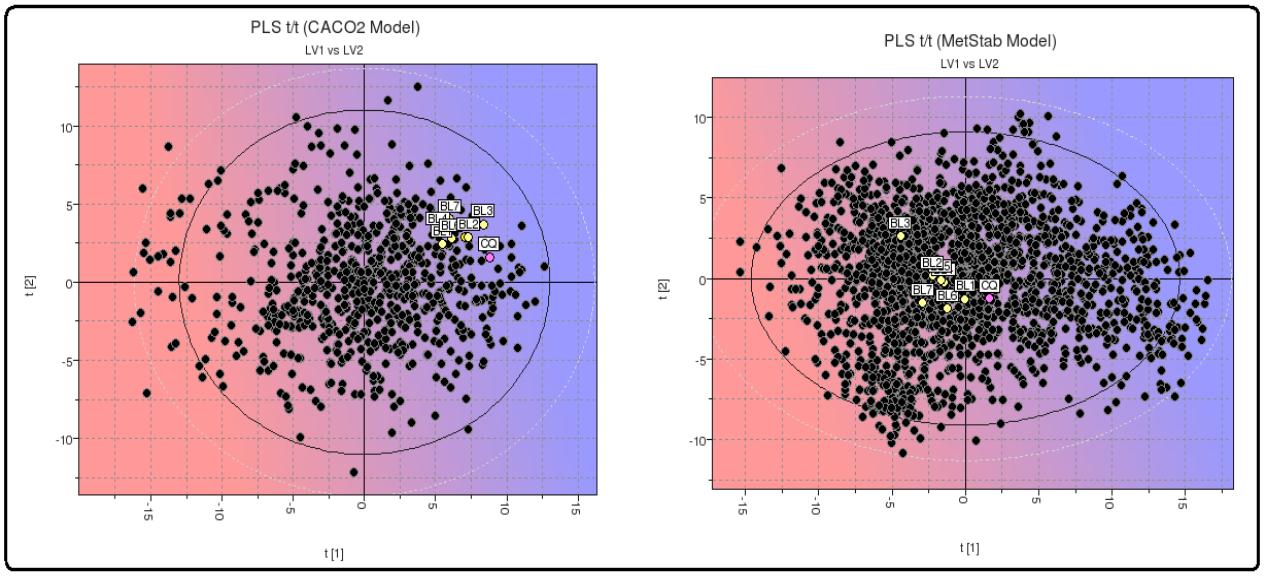

Figure 4.22: Plots showing the designed *β*-lactam-quinoline hybrids projected onto PLS models used to predict Caco-2 permeability and metabolic stability.

4.4.4 Synthesis of *β*-lactam-aminoquinoline hybrids

The synthesis of these hybrids began with the synthesis of key intermediates, quinoline amines **3.13a-c**, that were described in chapter 3, section 3.5.2.1. These intermediates were subsequently reacted at room temperature with various aromatic aldehydes (**3.14**) over a period of 24 hours to give imines **4.21a-g** in reasonable crude yields after being dried on the vacuum line for 4 hours (Scheme 4.8). No attempt was made in purifying these imines because of their known instability properties, hence they were used as such in the next step. The last step in the synthesis of these hybrids involved reacting these crude imines with the methoxyacetyl chloride under Staudinger reaction conditions to afford exclusively the *cis β*-lactams (**4.22a-g**) based on the ^{1}H NMR spectroscopy (Scheme 4.8). The configurations of these *β*-lactams were assigned following a model proposed by Jiao and co-workers.[56] The model suggests that when the *J*-coupling constant between the two protons on the adjacent chiral carbon is between 4-6 ppm then the configuration of the *β*-lactam is *cis*, while between 2-3 ppm indicates *trans*. The desired compounds were obtained in low yields, and were confirmed and fully characterized by NMR (^{1}H and ^{13}C) and mass spectroscopy. In addition, their purity was established by HPLC to be greater than 94% (Table 4.5). The reason for the relatively low yields is probably due to the fact that almost all the imines used were partially soluble in DCM, thus only a small percentage of these imines were available *in situ* to react with the methoxy acetyl chloride.

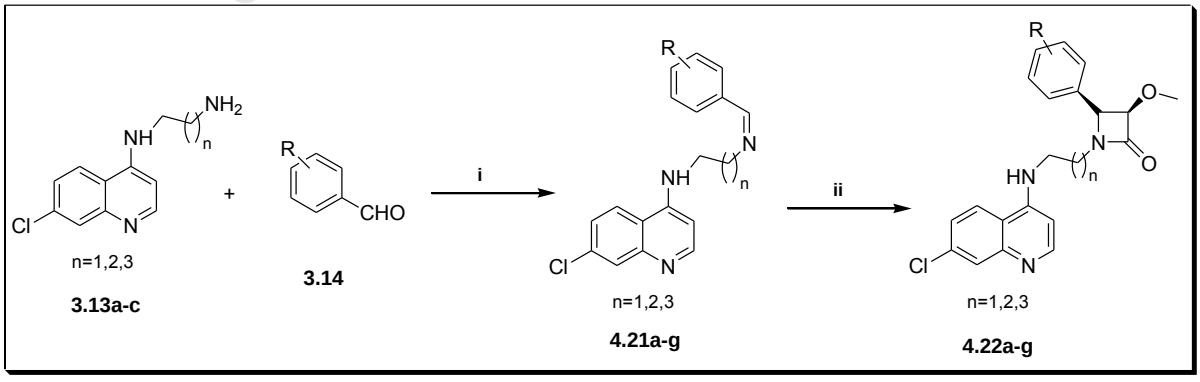

Scheme 4.8: *Reagents and conditions*: (i) MeOH, rt, 24 hrs; (ii) methoxy acetyl chloride (1.5 eq), Et_3N (3.0 eq), DCM, N_2, -78 °C to rt, overnight

Table 4.5: Yields, melting points and HPLC purity of *β*-lactam-quinoline hybrids.

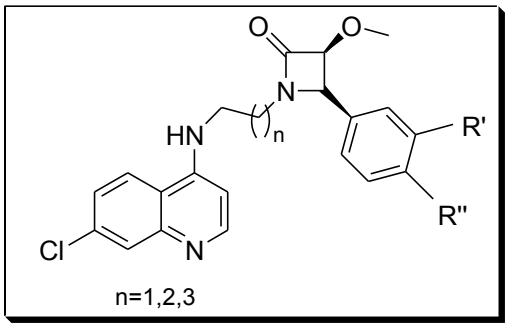

Code	Product	n	R'	R''	Yield/[%]	Melting points/[°C]	HPLC Purity/[%]
4.22a	**BL1**	1	H	H	30	142-146	95.6
4.22b	**BL2**	1	H	Cl	14	135-138	99.2
4.22c	**BL3**	1	Cl	Cl	4	152-156	99.5
4.22d	**BL4**	1	H	OCH_3	9	144-147	95.6
4.22e	**BL5**	1	H	Me	6	78-82	94.6
4.22f	**BL6**	2	H	H	5	-	97.2
4.22g	**BL7**	3	H	H	9	86-89	98

4.4.4.1 Reaction pathways towards *cis*- and *trans*-*β*-lactams

As mentioned earlier there is still no consensus among researchers with regards to the exact mechanism of this reaction. However, the pathway for the formation of the *cis*- or *trans*-*β*-lactams is shown in Scheme 4.9.[56] The relative stereochemistry of the *β*-lactam is decided by the initial approach of the imine (**B**) to the ketene (**A**), and by the competition between direct ring closure and the isomerisation of the imine in the zwitterionic intermediate.[56,57] Furthermore, this stereochemistry is also influenced by electronic effects of the substitutents on the imine. The initial *exo* attack of the imine to the ketene generates intermediate **C**. Subsequent direct ring closure of this intermediate forms a *cis*-*β*-lactam (**a** to **b**). However, isomerisation of intermediate **C** to **D**, followed by direct ring closure gives rise to the *trans*-*β*-lactam (**a** to **c** and then **d**). Also note that the use of Bose-Evans Ketenes in the *β*-lactam synthesis always results in formation of *cis*-*β*-lactam.[56]

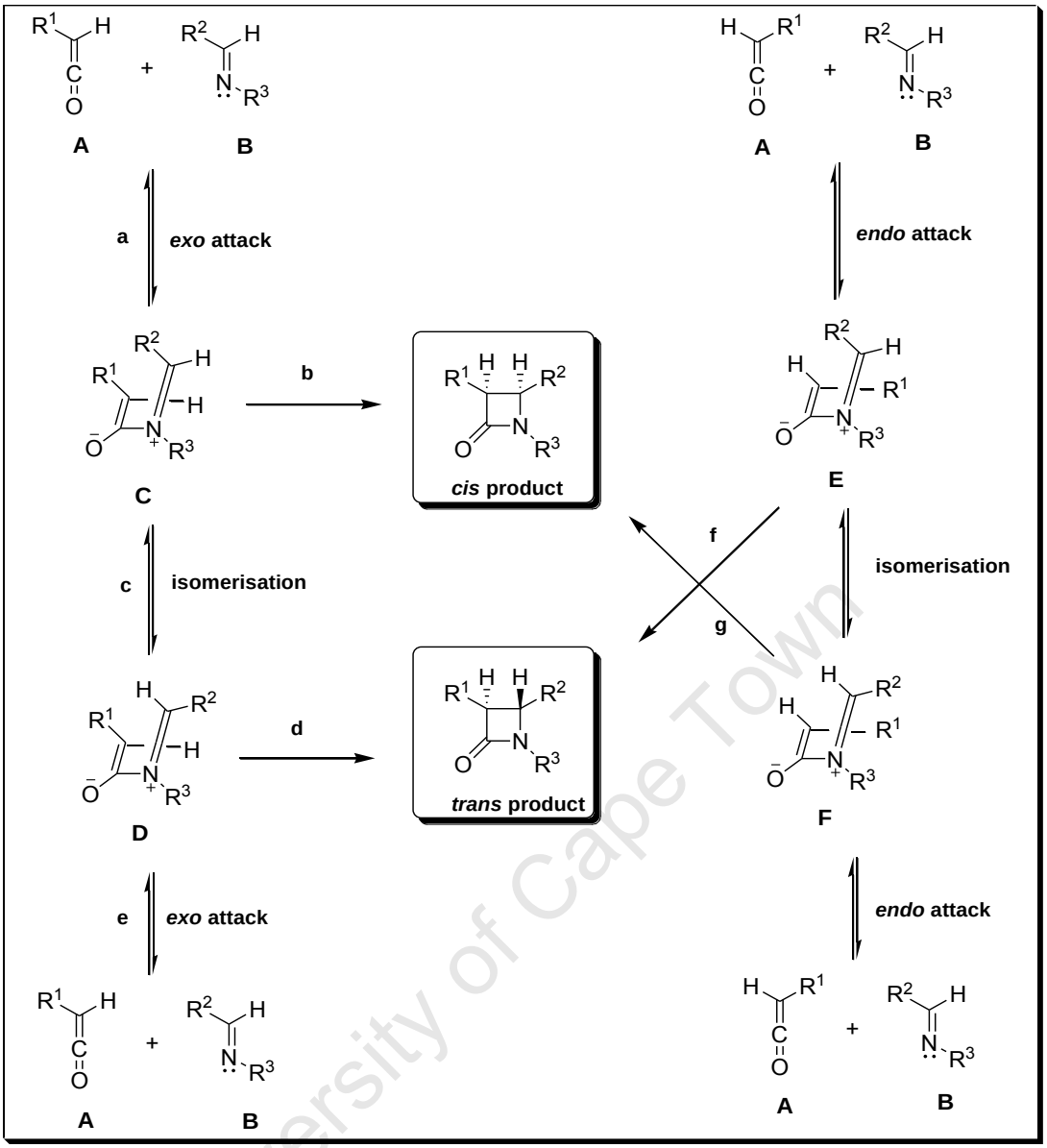

Scheme 4.9: Pathway for the formation of *cis*- and *trans*-isomers, only one enantiomer is shown (adapted from reference 55).

Confirmation of the *cis*-*β*-lactam-quinoline hybrids was by the presence of the two distinct coupling (^3J 4.3-4.5 Hz) doublets in ^{1}H NMR spectra, each integrating for one proton, resonating in the region 4.3-4.7 ppm. As mentioned previously, based on the model proposed by Jiao *et al*.,[56] these ^3J-coupling constant values indicate the formation of the *cis*-*β*-lactams. Also apparent in the spectra of these compounds are singlets resonating in the region 3.10-3.45 ppm, which correspond to the methoxy group of the acetyl chloride input. This is exemplified by Figure 4.23, ^{1}H NMR spectrum of compound **4.22b**.

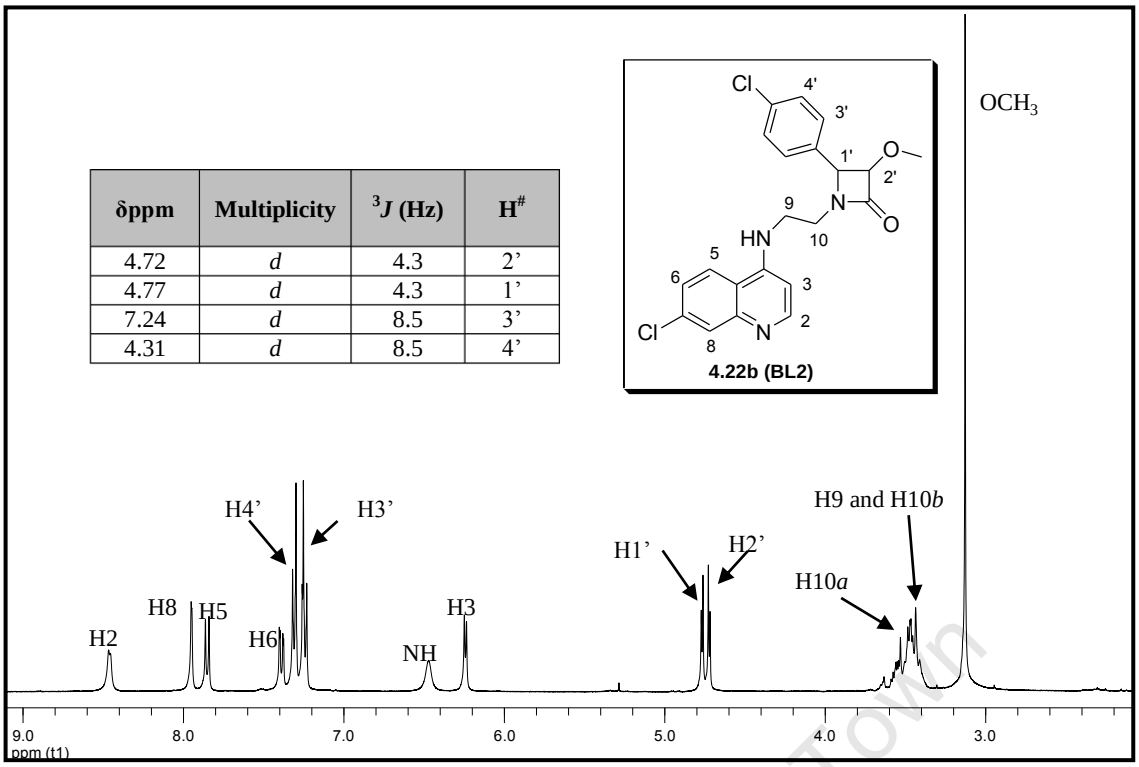

Figure 4.23: 400 MHz ^{1}H NMR spectra of products **4.22b** in $CDCl_3$.

4.4.5 Experimental determination of solubility

Three of these new *β*-lactam derivatives were profiled *in vitro* for aqueous solubility (Table 4.6). All the tested *β*-lactam derivatives were found to be highly soluble while the commercially available chloroquine diphosphate could not be determined due to it being insoluble in DMSO.

Table 4.6: Results for experimentally determined kinetic solubility at pH 7.0.

Code	Product	Solubility at pH 7.0 (µM)	Conclusion
BL1	**4.22a**	221	Highly soluble
BL2	**4.22b**	222 ± 1.30	Highly soluble
BL7	**4.22g**	215 ± 1.87	Highly soluble
Chloroquine diphosphate		Did not dissolve in DMSO	-

4.5 Biological results and discussion

Biological evaluation of compounds in this chapter were conducted in the same laboratories mentioned in chapter 3, section 3.7.

4.5.1 *In vitro* antiplasmodial evaluation of the target compounds

4.5.1.1. Antiplasmodial activity of 4-Arylamino quinolines

Table 4.7: *In vitro* antiplasmodial activity of 4-arylamino quinolines.

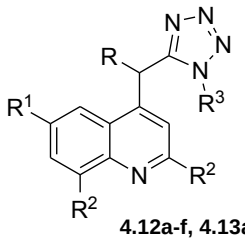

4.12a-f, 4.13a-b

Code	Product	R	R^1	R^2	R^3	*P. falciparum* IC_{50} [µM (µg/mL)]		
						3D7	K1	W2
4.12a	**TK501**		OMe	H	^{t}Bu	1.310	**1.310**	>10
4.12b	**TK502**	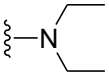	OMe	H	^{t}Bu	2.393	2.393	>10
4.12c	**TK503**	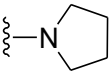	OMe	H	^{t}Bu	13.84	13.80	>10
4.12d	**TK504**	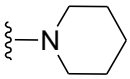	OMe	H	^{t}Bu	**0.647**	2.633	>10
4.12e	**TK505**	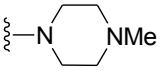	OMe	H	^{t}Bu	16.790	7.947	8.393
4.12f	**TK506**	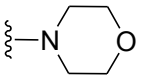	OMe	H	^{t}Bu	**0.980**	**1.228**	>10
4.14f	**TK506B3**	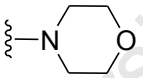	OMe	H	H	8.625	6.737	>10
4.13a	**TK710**		H	CF_3	^{t}Bu	ND	4.525‡ (2.02)	ND
4.13b	**TK720**	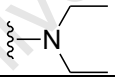	H	CF_3	^{t}Bu	ND	2.318‡ (1.1)	ND
Quinine		-				0.0007	0.0204	0.0187

‡Antiplasmodial testing done at STPH.

As clearly evident from Table 4.7, the most active compound [**4.12f** (IC_{50} = 1.228 µM)] in this series was 60 times less efficacious than quinine in the resistant K1 strain. Also, quinine derivatives were more active than the two mefloquine derivatives (**4.13a-b**). In addition, none of the tested compounds exhibited any significant activity against the W2 strain. Furthermore, these compounds were more active in the sensitive 3D7 strain than in the two resistant strains, the most active compound **4.12d** (IC_{50} = 0.647 µM) being 924-fold less active than

quinine. Unfortunately comparison between mefloquine and its derivatives cannot be made since the former was not tested.

4.5.1.2. Antiprotozoan activity of PA-824 derivatives

Based on the results in Table 4.8, the PA-824-aminoquinoline hybrids were the most active against the K1 strain in this series. Hybrids **4.19d** (IC_{50} = 0.100 µM) and **4.19f** (IC_{50} = 0.164 µM) exhibited at least 1- and 4-fold superior activity than both chloroquine (IC_{50} = 0.213 µM) and primaquine (IC_{50} = 0.643 µM), respectively. Also, **4.19d** (IC_{50} = 0.100 µM) showed 3-fold improved activity than its intermediates **3.13a** (IC_{50} = 0.298 µM) and the 1:1 molar combination of the parent compounds (**4.18a**:**3.13a**) (IC_{50} = 0.303 µM). However, the second intermediate (**4.18a**) of this hybrid was unfortunately not tested. This improved activity of **4.19d** over one of its intermediate (**3.13a**) and the equimolar combination of the individual components highlights the benefit of the covalent linkage (hybridization), indicating an additive effect. Moreover, the equimolar combination **4.18a:3.13a** (IC_{50} = 0.303 µM) also possessed better activity than primaquine. In terms of the SAR, there was no clear trend that could be delineated from these results based on the length of the alkyl side-chain of these hybrids. However, the 2- and 4-carbon spacers appear to be more favoured.

The two PA-824-primaquine hybrids [**4.19g** (IC_{50} = 2.042 µM) and **4.19h** (IC_{50} = 0.985 µM)], which were tested as 1:1 diastereomeric mixtures, were less active than both primaquine (IC_{50} = 0.643 µM) and chloroquine (IC_{50} = 0.213 µM) on the K1 strain. Compound **4.19h**, the most active of the two, showed 1- to 4.6-fold less activity than both reference drugs. Furthermore, **4.19h** (IC_{50} = 0.985 µM) was significantly more active than one of its intermediate, **4.18b** (IC_{50} = 62.62 µM), but comparable to the 1:1 combination of the individual components, **4.18b:Primaquine** (IC_{50} = 0.721 µM). Since the activity of the hybrid (**4.19h**) is less than one of its intermediates, primaquine (IC_{50} = 0.643 µM), an

antagonistic effect is suggested. Lastly, the PA-824 derivatives with commercial amines [**4.19a** (IC_{50} = 15.79 µM), **4.19b** (IC_{50} = 7.95 µM), and **4.19c** (IC_{50} = 8.70 µM)] did not show any significant activity against the K1 strain.

Table 4.8: *In vitro* antiprotozoan activity of PA-824 derivatives.

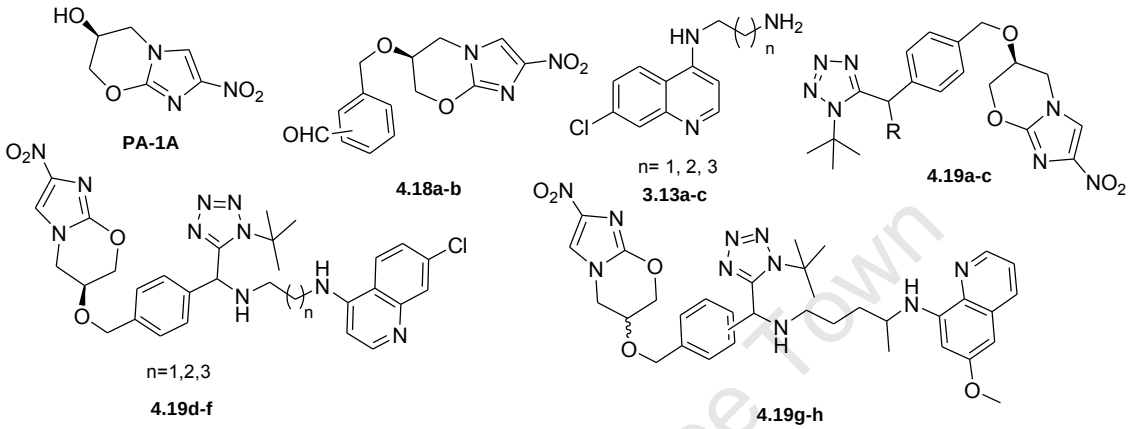

Code	Product	R	Position	n	K1 IC_{50} [µM (µg/mL)]	*T. b. rhod* IC_{50} [µM (µg/mL)]	Cytotox. L6 IC_{50} [µM (µg/mL)]	SI[a]
4.17	**PA-1A**	-	-	-	>270 (>50)	>540 (>100)	330.6 (61.2)	-
4.18a	**PA-2A1**	-	*para*	-	ND	ND	ND	-
4.18b	**PA-2A2**	-	*meta*	-	62.62 (19)	102.6 (31.1)	34.293 (10.4)	0.54
4.19a	**PA-3A**	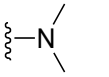	*para*	-	15.79 (7.21)	69.66 (31.8)	176.9 (80.8)	11.21
4.19b	**PA-4A**	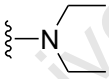	"	-	7.95 (3.85)	34.27 (16.6)	112.7 (54.6)	14.18
4.19c	**PA-5A**	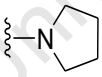	"	-	8.70 (4.20)	41.65 (20.1)	75.23 (36.3)	8.65
4.19d	**PA-6A**	-	"	1	**0.100 (0.064)**	**3.850 (2.44)**	24.64 (15.6)	**246**
4.19e	**PA-7A**	-	"	2	**0.485 (0.314)**	**4.064 (2.63)**	41.52 (26.9)	**85**
4.19f	**PA-8A**	-	"	3	**0.164 (0.109)**	**6.76 (4.47)**	29.34 (19.4)	**178**
4.19g	**PA-9A**	-	"	-	2.042 (1.37)	11.73 (7.87)	75.88 (50.9)	37
4.19h	**PA-11A**	-	*meta*	-	**0.985 (0.661)**	9.929 (6.66)	142.83 (95.8)	**145**
3.13a		-		1	0.298 (0.066)	10.49 (2.32)	21.22 (4.69)	71.2
4.18a:3.13a		-		1	**0.303 (0.159)**	4.615 (2.42)	20.41 (10.7)	67.4
4.18a:3.13b		-		2	1.874 (1.01)	3.377 (1.82)	21.89 (11.8)	11.7
4.18a:3.13c		-		3	2.514 (1.39)	3.562 (1.97)	11.81 (6.53)	4.69
4.18a:Primaquine		-		-	0.900 (0.683)	2.557 (1.94)	29 (22)	32.2
4.18b:Primaquine		-		-	0.721 (0.547)	2.992 (2.27)	22.94 (17.4)	31.8
Chloroquine		-			0.213 (0.110)	-	-	-
Primaquine		-			0.643 (0.280)	-	-	-
Melarsoprol		-			-	0.0075 (0.003)	-	-
Podophyllotoxin		-			-	-	0.0193 (0.008)	-

[a] Selective indices [(IC_{50} mammalian cell-line)/IC_{50} (K1)]

Most of the compounds in this series showed poor activity against the cultured *T. b. brucei* parasite, only the two PA-824-aminoquinoline hybrids [**4.19d** (IC_{50} = 3.850 μM) and **4.19e** (IC_{50} = 4.064 μM)] exhibited some notable activity, which decreased with an increase in length of the alkyl side-chain. The selective indices of the most active compounds in this series were closer to or greater than 100, suggesting that these compounds are more selective towards the chloroquine-resistant parasite.

Aqueous solubility of these compounds does not seem to be playing a significant role on antiplasmodial activity. This appears so because the two most active compounds in this series exhibit contrasting solubilities, with one being highly soluble [**4.19d** (62.9 ± 0.66 μM)] while the other was insoluble [**4.19h** (< 5 μM)]. Moreover, both the PA-824-primaquine hybrids were found to be insoluble (< 5 μM) but one of them possessed potent antiplasmodial activity while the other did not.

4.5.1.3. Antiprotozoan activity of *β*-lactam-aminoquinoline hybrids

The desired *β*-lactams were all active against the K1 strain, exhibiting IC_{50} values in the low micromolar range (Table 4.9). Compounds containing chloro substituted phenyl rings [*di*-chloro substituted **4.22c** (IC_{50} = 0.209 μM) and *mono*-chloro substituted **4.22b** (IC_{50} = 0.304 μM)] showed comparable activity to chloroquine (IC_{50} = 0.213 μM) and intermediate **3.13a** (IC_{50} = 0.298 μM). On the other hand, the least active compound in this series, **4.22d** (IC_{50} = 0.617 μM), was 3-fold less active than the reference drug. In terms of SAR, there was no obvious trend with regards to the length of the alkyl side-chain on antiplasmodial activity. However, similar to the PA-824-aminoquinoline hybrids, compounds with the 2- and 4-carbon spacer showed superior activity to the corresponding analogue with a 3-carbon methylene spacer.

However, none of these *β*-lactams showed any significant inhibitory activity against the cultured *T. b. brucei* parasite. The most active compound **4.22b** (IC_{50} = 7.005 µM) in this series was 934 times less active than melarsoprol (IC_{50} = 0.0075 µM), a reference drug.

All these compounds except **4.22a** and **4.22e** showed notable cytotoxicity against the L6 mammalian cell-line. Compound **4.22g** (IC_{50} = 2.87 µM) was the most cytotoxic in this series, followed by compound **4.22c** (IC_{50} = 8.54 µM). This cytotoxicity profile exhibited by these *β*-lactams potentially limits their chances for further development.

Table 4.9: *In vitro* antiprotozoan activity of *β*-lactam-aminoquinoline hybrids.

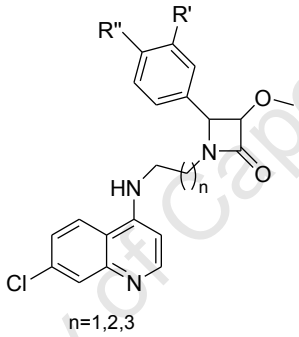

4.22a-g

code	Product	n	R'	R''	K1 IC_{50} [µM (µg/mL)]	*T. b. rhod* IC_{50} [µM (µg/mL)]	Cytotox. L6 IC_{50} [µM (µg/mL)]
4.22a	**BL1**	1	H	H	0.466 (0.178)	53.16 (20.3)	98.47 (37.6)
4.22b	**BL2**	1	H	Cl	**0.304** (0.127)	7.005 (2.94)	11.62 (4.84)
4.22c	**BL3**	1	Cl	Cl	**0.209** (0.094)	18.99 (8.54)	8.54 (3.85)
4.22d	**BL4**	1	H	OMe	0.617 (0.254)	52.93 (21.8)	20.37 (8.39)
4.22e	**BL5**	1	H	Me	0.581 (0.23)	52.54 (20.8)	92.70 (36.7)
4.22f	**BL6**	2	H	H	0.568 (0.225)	16.09 (6.37)	14.40 (5.7)
4.22g	**BL7**	3	H	H	**0.309** (0.127)	20.00 (8.2)	2.87 (1.18)
3.13a		1	-		0.298 (0.066)	10.49 (2.32)	21.22 (4.69)
Chloroquine			-		0.220 (0.100)	-	-
Melarsoprol			-		-	0.0075 (0.003)	-
Podophyllotoxin			-		-	-	0.0193 (0.008)

4.5.2 *In vitro* Antimycobacterial evaluation of the target compounds

4.5.2.1 Antimycobacterial activity of 4-Arylamino quinolines

Table 4.10: *In vitro* antimycobacterial activity of 4-aryamino quinolines

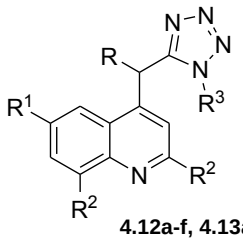

4.12a-f, 4.13a-b

Code	Product	R	R^1	R^2	R^3	MABA (µM)		LORA (µM)		$H_{37}R_v$ MIC_{90} (µM)	
						%Inh	MIC_{90}	%Inh	MIC_{90}	7 days	14 days
4.12a	**TK501**		OMe	H	^{t}Bu	16	>128	42	>128	-	-
4.12b	**TK502**	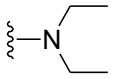	OMe	H	^{t}Bu	**83**	>128	**94**	**123.2**	-	-
4.12c	**TK503**	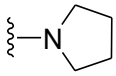	OMe	H	^{t}Bu	24	>128	30	>128	-	-
4.12d	**TK504**	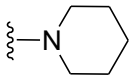	OMe	H	^{t}Bu	**98**	**92.5**	64	>128	-	-
4.12e	**TK505**	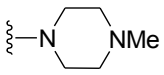	OMe	H	^{t}Bu	0	>128	0	>128	-	-
4.12f	**TK506**	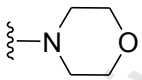	OMe	H	^{t}Bu	o	>128	32	>128	-	-
4.14f	**TK506B3**	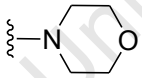	OMe	H	H	0	>128	1	>128	-	-
4.13a	**TK710**		H	CF_3	^{t}Bu	-	-	-	-	>160	>160
4.13b	**TK720**	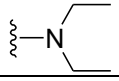	H	CF_3	^{t}Bu	-	-	-	-	>160	>160
Quinine			-			95	119.7	98	122.0	-	-
Mefloquine						-	-	-	-	10	20
RMP			-			100	0.05	98	1.93	-	-
INH			-			92	0.23	64	>128	-	-
PA-824			-			99	0.12	100	3.78	-	-
Kanamycin			-			-	-	-	-	3.125	3.125
Streptomycin			-			-	-	-	-	0.4	0.4

Generally, the target compounds (Table 4.10) had MICs greater than the highest tested concentrations (MIC_{90} >128 and >160) against both the replicating and slow-growing

bacteria, with the exception of two compounds, **412b** and **4.12d**. Compound **4.12b** inhibited 83 and 94% bacterial growth of the replicating and non-replicating bacteria, respectively. Also, this compound had an MIC_{90} of 123.2 μM against the non-replicating bacteria. In addition, compound **4.12d** (MIC_{90} = 92.5 μM) inhibited 98% of the replicating bacteria However, this compound only showed weak inhibition of the non-replicating bacteria. This lack of activity exhibited by the majority of these compounds is not surprising considering the fact that Kozikowski *et al*.,[58] observed in their SAR studies that the replacement of the hydroxyl group of the 4-quinoline methanols was accompanied by the complete loss of activity. Thus, it maybe postulated that perhaps the abolished activity of these target compounds was largely due to the replacement of the hydroxyl group.

4.5.2.2 Antimycobacterial activity of PA-824 derivatives

All the PA-824 derivatives showed potent antimycobacterial activity against the replicating *M. tuberculosis* drug sensitive H_{37}Rv strain during the 7 and 14 day assays (Table 4.11). The MICs of all the target compounds ranged between 0.25 and 1.25 μM, except for the PA-824-primaquine diastereomeric mixture **4.19h**. All these compounds were more active than the standard TB drug, Kanamycin (MIC_{90} = 3.125 μM), and the two antimalarial drugs, chloroquine (MIC_{90} > 160 μM) and primaquine (MIC_{90} = 80 μM). In addition, the three equimolar combinations [**4.18a:3.13a**, **4.18a:3.13b** and **4.18a:3.13c**, all had MIC_{90} of 0.25 μM] were more efficacious than Streptomycin (MIC_{90} = 0.4 μM), while four compounds, **4.18a** (MIC_{90} = 0.25 μM), **4.19b** (MIC_{90} = 0.313 μM), **4.19c** (MIC_{90} = 0.313 μM) and **4.19d** (MIC_{90} = 0.4 μM), had comparable activity to this standard TB drug in the 7 day assay. Intermediate **4.18a** showed superior activity than all the target compounds in the 7 day assay, while it had the same activity as both **4.19b** and **4.19d** in the 14 day experiment. However, the majority of these compounds appeared to lose their 7 day efficacy when incubated for longer periods except compound **4.19d**, which exhibited a slight improvement in activity.

Reasons for this loss in activity are unknown at this stage, perhaps degradation and precipitation in the assay media might have potentially influenced this observation. However, this postulation will have to be verified experimentally.

Table 4.11: *In vitro* antimycobacterial activity of PA-824 derivatives

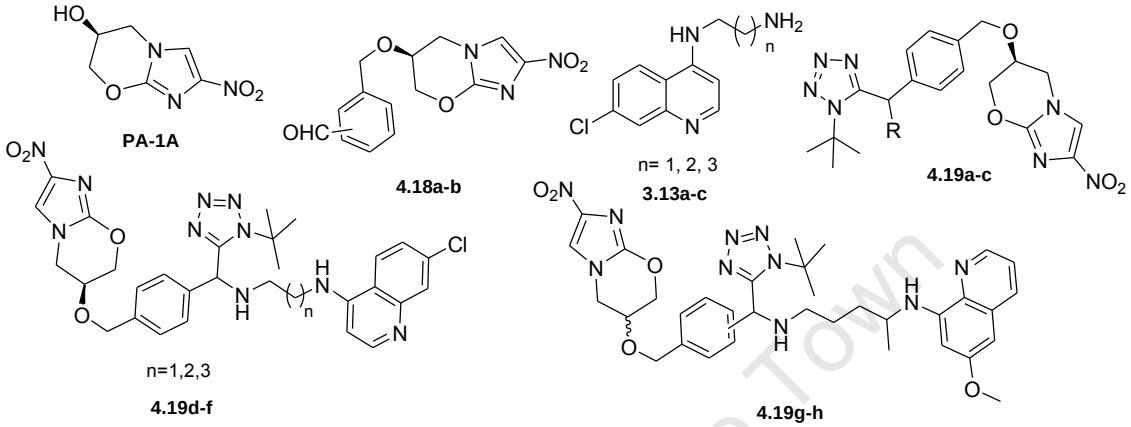

Code	Product	R	Position	n	$H_{37}R_v$ MIC$_{90}$ (µM)	
					7 days	14 days
4.17	**PA-1A**	-	-	-	40	40
4.18a	**PA-2A1**	-	*para*	-	**0.25**	**0.313**
4.18b	**PA-2A2**	-	*meta*	-	**0.625**	**1.25**
4.19a	**PA-3A**	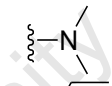	*para*	-	**0.625**	**1.25**
4.19b	**PA-4A**	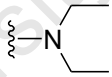	"	-	**0.313**	**0.313**
4.19c	**PA-5A**	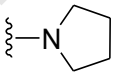	"	-	**0.313**	**0.625**
4.19d	**PA-6A**	-	"	1	**0.4**	**0.313**
4.19e	**PA-7A**	-	"	2	ND	ND
4.19f	**PA-8A**	-	"	3	**0.625**	1.25
4.19g	**PA-9A**	-	"	-	**0.625**	1.25
4.19h	**PA-11A**	-	*meta*	-	5	20
3.13a		-		1	160	>160
3.13b		-		2	>160	>160
3.13c		-		3	>160	>160
4.18a:3.13a		-		1	0.25	<0.156
4.18a:3.13b		-		2	0.25	<0.156
4.18a:3.13c		-		3	0.25	<0.156
4.18a:Primaquine		-		-	0.4	<0.156
4.18b:Primaquine		-		-	0.625	0.625
Chloroquine		-			>160	>160
Primaquine		-			80	80
Kanamycin		-			3.125	3.125
Streptomycin		-			0.4	0.4

Contrary to the antiplasmodial data, compounds containing commercial amines (**4.19a**, **4.19b**, and **4.19c**) possessed better antimycobacterial activity than the PA-824-aminoquinoline hybrids, with compounds **4.19b** and **4.19c** having MICs in the range of 0.313-0.625 μM. An increase in the length of the alkyl side-chain of the PA-824-aminoquinoline hybrids was accompanied by reduction in activity in both assays. Also apparent from this data was that the *para*-analogues were more active than their *meta* counterparts. This is exemplified by intermediate **4.18a** compared to **4.18b**, and by the primaquine-based diastereomeric mixtures **4.19g** and **4.19h**.

From the data it appears that the MICs of the physically mixed equimolar combinations are approximately equal to the MIC_{90} of the most active corresponding parent compound. This is to be expected since the 4-aminoquinolines (**3.13a-c**) completely lack activity at the highest tested concentration (MIC > 160 μM). Also, all the equimolar combinations were more active than the corresponding hybrids in both assays. The PA-824-aminoquinoline hybrids (**4.19d-f**) were less active than the nitroimidazooxazine **4.18a** intermediate while they were significantly more active than their corresponding 4-aminoquinoline (MIC90 > 160 μM) intermediate. Similarly, the PA-824-primaquine (**4.19g-h**) hybrids showed the same trend, where the nitroimidazooxazine **4.18a-b** intermediates showed superior activity to the corresponding hybrids while the primaquine (MIC_{90} = 80 μM) intermediate was less so. Thus, hybridisation in both cases indicates an antagonistic effect, suggesting that administering these intermediates in equimolar combinations is much more advantageous than covalently linking them.

Unlike in the antiplasmodial data, aqueous solubility appears to be playing a minor role on antimycobacterial activity. Among the PA-824-aminoquinoline hybrids, antimycobacterial activity correlates with solubility. In fact, the most active of these hybrids **4.19d** exhibited

better solubility (62.9 ± 0.66 μM) than the other hybrid **4.19f** (< 5 μM). Furthermore, compounds with commercial amines had better activity and solubility than the hybrids. However, the role of solubility on the PA-824-primaquine hybrids is less clear because one of these hybrids is significantly more active than the other although both of them had similar solubilities (< 5 μM).

4.5.2.3 Antimycobacterial activity of *β*-lactam-aminoquinoline hybrids

Table 4.12: *In vitro* antimycobacterial activity of *β*-lactam-aminoquinoline hybrids

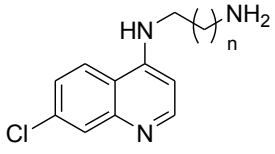

n= 1, 2, 3

3.13a-c

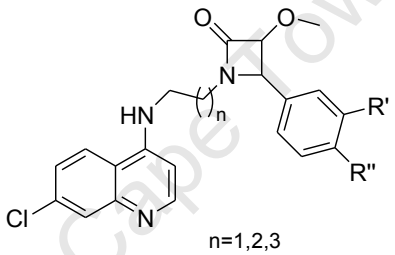

n=1,2,3

4.22a-g

code	Product	n	R'	R''	$H_{37}R_v$ MIC$_{90}$ (μM)	
					7 days	14 days
4.22a	**BL1**	1	H	H	>160	>160
4.22b	**BL2**	1	H	Cl	160	>160
4.22c	**BL3**	1	Cl	Cl	**80**	160
4.22d	**BL4**	1	H	OCH_3	>160	>160
4.22e	**BL5**	1	H	Me	>160	>160
4.22f	**BL6**	2	H	H	>160	>160
4.22g	**BL7**	3	H	H	>160	>160
3.13a		1	-		160	>160
3.13b		2	-		>160	>160
3.13c		3	-		>160	>160
Chloroquine			-		>160	>160
Kanamycin			-		3.125	3.125
Streptomycin			-		0.4	0.4

Almost all the tested compounds were inactive against the replicating bacteria in both assays at the highest concentration (MIC$_{90}$ > 160 μM) tested, the exception being **4.22c** which had an MIC of 80 μM in the 7 day assay (Table 4.12). Similar, the intermediates (**3.13a-c**) of these *β*-lactams also lack activity in both assays at the highest tested concentration (MIC$_{90}$ >

160 µM). The lack of activity observed in these *β*-lactam-aminoquinoline hybrids is in stark contrast to the documented antitubercular activity of *β*-lactams and quinoline-based[53,54] compounds. This may suggest an antagonistic effect when these respective scaffolds are covalently linked.

4.5.3 Conclusion

In conclusion a number of the synthesized target compounds exhibited better antiplasmodial and antimycobacterial activity than the used reference drugs. Most notable, the two PA-824-aminoquinoline hybrids **4.19d** (IC_{50} = 0.100 µM) and **4.19f** (IC_{50} = 0.164 µM) were slightly more active than chloroquine (IC_{50} = 0.213 µM), while all compounds in this series were more potent than primaquine (IC_{50} = 0.643 µM). Moreover, the PA-824-aminoquinoline hybrids exhibited additive antiplasmodial activity while the PA-824-primaquine hybrids showed antagonism. Also, these derivatives were more active in the TB assays than the standard drugs, kanamycin, chloroquine and primaquine, while three of them were more efficacious than streptomycin, another standard TB drug. In the antimycobacterial evaluation, both the PA-824-aminoquinoline and PA-824-primaquine hybrids showed antagonistic effect. More interestingly, these compounds appear to be more selective towards the parasite and bacteria than the mammalian cell-lines used.

Also, the *β*-lactams showed IC_{50} values in the low micromolar range against K1 strain, with compound **4.22c** (IC_{50} = 0.209 µM), the most active in this series, showing comparable activity to chloroquine (IC_{50} = 0.213 µM). The one limitation of these *β*-lactams was their unfavourable cytotoxicity profile against the mammalian cell-lines..

4.6 References

1. Achan, J.; Talisuna, A. O.; Erhart, A.; Yeka, A.; Tibenderana, J. K.; Buliraine, F. N.; Rosenthal, P. J.; D'Alessandro, U., *Malaria J*., **2011**, *10*, 144.

2. Kumar, V.; Mahajan, A.; Chibale, K., *Bioorg. Med. Chem*., **2009,** *17*, 2236.

3. Frosch, T.; Schmitt, M.; Popp, J., *J. Phy. Chem. B*, **2007**, *111*, 4171.

4. Hutzler, J. M.; Walker, G. S.; Wienkers, L. C., *Chem. Res. Toxicol.*, **2003**, *16*, 450.

5. Cravo, P.; Culleton, R.; Afonso, A.; Ferreira, I. D.; Rosário, V. E., *Anti Infect. Agents Med. Chem*., **2006**, *5*, 65.

6. Burrows, J. N.; Chibale, K.; Wells, T. N. C., *Curr. Topics Med. Chem.*, **2011**, *11*, 1226.

7. Schlagenhauf, P.; Adamcosa, M.; Regep, L.; Schaerer, M. T.; Rhein. H-G.; *Malaria J.*, **2010**, *9*, 357.

8. Choi, S-R.; Mukherjee, P.; Avery, M. A., *Curr. Med. Chem.*, **2008**, *15*, 161.

9.(a) de Villiers, K. A.; Marques, H. M.; Egan, T. J., *J. Inorg. Biochem*., **2008**, *102*, 1660.

(b) Kuter, D.; Chibale, K.; Egan, T. J., *J. Inorg. Biochem*., **2011**, *105*, 684.

10. Kuter, D., *MSc Thesis*, University of Cape Town, **2009**.

11. Behere, D. V.; Goff, H. M., *J. Am. Chem. Soc*., **1984**, *106*, 4945.

12. Roman, G.; Rahman, M. N.; Vukomanovic, D.; Jia, Z.; Nakatsu, K.; Szarek, W. A., *Chem. Biol. Drug Des.*, **2010**, *75*, 68.

13. Adachi, S-I.; Morishima, I., *Biochemistry*, **1992**, *31*, 8613.

14. Milner, E.; McCalmont, W.; Bhonsle, J.; Caridha, D.; Cobar, J.; Gardner, S.; Gerena, L.; Goodine, D.; Lanteri, C.; Melendez, V.; Roncal, N.; Sousa, J.; Wipf, P.; Dow, G. S., *Malaria J*., **2010**, *9*, 51.

15. Alkadi, H. O., *Chemother*., **2007**, *53*, 385.

16. Daines, R and Price, A. T., WO**2007**/016610A2.

17. Mao, J.; Yuan, H.; Wang,Y.; Wan, B.; Pieroni, M.; Huang, Q.; van Breemen, R. B.;. Kozikowski, A. P.;Franzblau, S. G., *J. Med. Chem*., **2009**, *52*, 6966.

18. Ghosh, B.; Antonio, T.; Reith, M. E. A.; Dutta, A. K., *J. Med. Chem*., **2010**, *53*, 2114.

19. McNab, H., *Chem. Soc. Rev*., **1978**, *7*, 345.

20. Kore, A. R.; Mane, R. B.; Salunkhe, M. M., *Bull. Soc. Chim. Belg*., **1995**, *104*, 643.

21. Pindur, U.; Witzel, H., *Monatshefte für Chemie*, **1990**, *121*, 77.

22. Clayden, J.; Greeves, N.; Warren, S.; Wothers, P., *Organic Chemistry*, Oxford University Press, NY, **2001**.

23. Shingalapur, R. V.; Hossamani, K. M.; Keri, R. S., *Eur. J. Med. Chem*., **2009**, *44*, 4244.

24. Gupta, P.; Hameed, S.; Jain, R., *Eur. J. Med. Chem*., **2004**, *39*, 805.

25. Puratchikodya, A.; Doble, M., *Bioorg. Med. Chem.*, **2007**, *15*, 1083.

26. Rafaet, H. M., *Eur. J. Med. Chem.*, **2010**, *45*, 2949.

27. Tonelli, M.; Simone, M.; Tosso, B.; Novelli, F.; Biodo, V., *Bioorg. Med. Chem.*, **2010**, *18*, 2937.

28. Mital, A., *Sci. Pharm*., **2009**, *77*, 497.

29. Silvestri, R.; Artico, M.; De Martino, G.; Ragno, K.; Massa, S.; Loddo, K.; Murgioni, C.; Loi, A. G.; LaColla, P.; Pani, A., *J. Med. Chem*., **2002**, *45*, 1587.

30. Denny, W. A.; Palmer, B. D., *Future Med. Chem*., **2010**, *2*, 1295.

31. Marriner, G. A.; Nayyar, A.; Uh, E.; Wang, S. Y.; Mukherjee, T.; Via, L. E.; Carroll, M.; Edwards, R. L.; Gruber, T. D.; Choi, I.; Lee, J.; Arora, K.; England, K. D.; Boshoff, H. I. M.; Barry III, C. E., *Top Med. Chem*., **2011**, *7*, 47.

32. Ginsberg, A. M.; Laurenzi, M. W.; Rouse, D. J.; Whitney, K. D.; Spigelman, M. K., *Antimicrob. Agents Chemother*., **2009**, *53*, 3720.

33. Kim, P.; Manjunatha, U. H.; Singh, R.; Patel, S.; Jiricek, J.; Keller, T. H.; Boshoff, H. I. M.; Barry III, C. E.; Dowd, C. S., *J. Med. Chem*., **2009**, *52*, 1317.

34. Sutherland, H. S.; Blaser, A.; Kmentova, I.; Franzblau, S. G.; Wan, B.; Wang, Y.; Ma, Z.; Palmer, B. D.; Denny, W. A.; Thompson, A. M., *J. Med. Chem*., **2010**, *53*, 855.

35. Burman, W. J., *Clin. Infect Dis*., **2010**, *50*, S165.

36. Hu, Y.; Coates, A. R. M.; Mitchison, D. A., *Int. J. Tuberculosis Lung Dis*., **2008**, *12*, 69.

37. Palmer, B. D.; Thompson, A. M.; Sunderland, H. S.; Blaser, A.; Kmentova, I.; Franzblau, S. G.; Wan, B.; Wang, Y.; Ma, Z.; Denny, W. A., *J. Med. Chem*., **2010**, *53*, 282.

38. Ding, Z. C.; Genliang, L.; Combrink, K.; Chen, D. D.; Song, M.; Wang, J.; Ma, Z.; Palmer, B. D.; Blaser, A.; Thompson, A. M.; Kmentova, I.; Sunderland, H. S.; Denny, W. A., *PCT Int. Appl*. (**2009**), WO2009120789.

39. Illiashevsky, O.; Amir, L.; Glaser, R.; Marks, R. S.; Lemcoff, N. G., *J. Meter. Chem*., **2009**, *16*, 6616.

40. Jiricek, J.; Patel, S.; Keller, T. H.; Barry III, C. E.; Dowd, C. S., *PCT Int. Appl*. (**2008**), WO20080275035.

41. Banfi, L.; Basso, A.; Cerulli, V.; Roca, V.; Riva, R., *Beilstein J. Org. Chem*., **2011**, *7*, 976.

42. Brocollo, F.; Gainelli, G.; Caltabiano, G.; Cocuzza, C. E. A.; Fortuna, C. G.; Galletti, P.; Giacomini, D.; Musumara, G.; Musumeni, R and Quintavalla, A., *J. Med. Chem*., **2006**, 4*9*, 2804.

43. Venturalli, A.; Tondi, D., Canciani, , L.; Morandi, F.; Cannazza, G.; Segatore, B.; Prati, F.; Amicosante, G., Shoichet, B. K and Costi, M. P., *J. Med. Chem*., **2007**, *50*, 5644.

44. Howarth, T. T.; Brown, A. G.; King, T. J., *J. Am. Chem. Soc.*, **1976**, 266.

45. Khaleeli, N.; Li, R.; Townsend, C. A., *J. Am. Chem. Soc.*, **1999**, *121*, 9223.

46. Sperka, T.; Pillik, J.; Bagossi, P and Tozser, J., *Bioorg. Med. Chem. Lett.*, **2005**, *15*, 3086.

47. Banik, B. K.; Becker, F. F and Banik, I., *Bioorg. Med. Chem. Lett.*, **2004**, *12*, 2523.

48. Nivsarkar, M.; Thavalsevam, D.; Prasanna, S.; Sharma, M and Kaushik, M. P., *Bioorg. Med. Chem. Lett.*, **2005**, *15*, 1371.

49. Zhao, G.; Miller, M. J.; Franzblau, S. G.; Wan, B and Mollman, U.; *Bioorg. Med. Chem. Lett.*, **2006**, *16*, 5534.

50. Walz, A. J.; Miller, M. J., *Tetrahedron Lett.*, **2007**, *48*, 5103.

51. Staudinger, H., *Liebigs Ann. Chem*., **1907**, *365*, 51.

52. D'hooghe, M.; Van Brabandt, W.; Dekeukeleire, S.; Dejaegher, Y.; De Kimpe, N., *Chem. Eur. J.*, **2008**, *14*, 6336.

53. Matteeli, A.; Carvalho, A. C. C.; Dooley, K. E.; Kritski, A., *Future Microbiol*., **2010**, *5*, 849.

54. Brandi, A.; Cicchi, S and Cordero, F. M., *Chem. Rev.*, **2008**, *108*, 3988.

55. Cossio, F., Arrieta, A and Sirra, M. A., *Account. Chem. Res*., **2008**, *41*, 925.

56. Jiao, L.; Liang, Y.; Xu, J., *J. Am. Chem. Soc*., **2006**, *128*, 6060.

57.(a) Brady, W. T.; Gu, Y. Q., *J. Org. Chem*., **1989**, *54*, 2838.

(b) Lecea, B.; Arrastia, I.; Arrieta, A.; Roa, G.; Lopez, X.; Arriortua, M. I.; Ugalde, J. M.; Cossío, F., *J. Org. Chem.*, **1996**, *61*, 3070.

58. (a) Jayaprakash, S.; Iso, Y.; Wan, B.; Franzblau, S. G.; Kozikowski, A. P., *ChemMedChem*., **2006**, *1*, 593.

(b) Lileinkampt, A.; Mao, J.; Wan, B.; Wang, Y.; Franzblau, S. G.; Kozikowski, A. P., *J. Med. Chem.*, **2009**, *52*, 2109.

Chapter five

Summary, Conclusions and Recommendations

5.1 Summary and Conclusions

The main objective of this study was to design a series of compounds around the tetrazole moiety utilizing known anti-malarial and anti-TB pharmacophores or bioactiphores, which possess *in vitro* and/or *in vivo* antiplasmodial and antimycobacterial potency. Specifically, these bioactiphores included deoxyamodiaquine, chloroquine-like, primaquine, 4-arylamino quinoline and PA-824 scaffolds.

A limited number of derivatives of each bioactiphore were synthesized from the modified $TMSN_3$-Ugi multi-component reaction (MCR) strategy, followed by evaluation *in vitro* for antiplasmodial and antimycobacterial activity. Furthermore, these derivatives were profiled *in silico* for solubility, permeability and metabolic stability among others. Aqueous solubility of key compounds from each series was determined experimentally to corroborate or negate these *in silico* predictions. Below is the summary of the results from each series:

(i) In the deoxyamodiaquine series, the *t*-butyl protected tetrazole compounds **3.9b-c** and **3.9k** with IC_{50} values ranging from 0.006 to 0.012 µM showed superior antiplasmodial activity than both amodiaquine (IC_{50} = 0.02689 µM) and chloroquine (IC_{50} = 0.0360 µM) in the K1 strain. In addition, two of the de-*tert*-butylated compounds **3.10b** (IC_{50} = 0.054µM) and **3.10c** (IC_{50} = 0.049 µM) exhibited comparable activities to the reference drugs. Similarly, compounds **3.9a-f**, **3.9k** and **3.10c** (IC_{50} values ranging from 0.040 to 0.194 µM) were all more potent than amodiaquine (IC_{50} = 0.4007 µM) in the W2 strain, while only one compound, **3.9k** (IC_{50} = 0.040 µM), was more active than chloroquine (IC_{50} = 0.0591 µM) on this same strain.

Moreover, these compounds also exhibited encouraging antimycobacterial activity against drug-sensitive $H_{37}Rv$ *M. tuberculosis* strain, with compounds **3.9a**, **3.9c-f** inhibiting over 90% of the replicating bacteria with MICs in the 14.1- 63.7 µM range. In addition, compounds **3.9d** (MIC_{90} = 7.6 µM) and **3.9k** (MIC_{90} = 14.1 µM) were also more efficacious than amodiaquine (MIC_{90} = 56.9 µM). Against the non-replicating bacteria, compounds **3.9a** (MIC_{90} = 118.7 µM), **3.9c** (MIC_{90} = 74 µM) and **3.9k** (MIC_{90} = 15.1 µM) were the most active, and all had over 70% inhibitory effect on the bacteria. Also, these derivatives showed acceptable cytotoxicty with selective indices greater than 1000. The experimentally determined aqueous solubility of key compounds in this series corroborated the results obtained from the *in silico* solubility predictions; that is, the de-*tert*-butylated compounds were more soluble than the *t*-butyl protected analogues.

(ii) Among the chloroquine-like compounds, **3.15a4** (IC_{50} = 0.0004 µM) was 13-times more active than chloroquine (IC_{50} = 0.0052 µM) in the 3D7 strain. On the other hand, 6 (**3.15a1**, **3.12a3**- **3.15a7**) out of the 14 compounds tested against K1 strain showed greater activity than chloroquine, with **3.15a5** (IC_{50} = 0.001 µM) exhibiting a 36-fold improved activity over chloroquine (IC_{50} = 0.036 µM). Moreover, compounds **3.15a2**, **3.15a3**, **3.15a5**, and **3.15c** showed favourable resistance index against K1, suggesting a reduced potential to develop cross-resistance with chloroquine. Against the W2 strain, almost all the compounds tested were more active than chloroquine (IC_{50} = 0.059 µM), the exception being **3.15a1** (IC_{50} = 0.069 µM) which had comparable activity to this reference drug. In terms of SAR, the compound with the shortest ethylene spacer, **3.15a1**, was less efficacious than those with the longer carbon spacers (**3.15b** and **3.15c**) on all strains tested.

In the antimycobacterial evaluation, the *para*-substituted phenyl ring was highly preferred in the MABA assay. Compounds **3.15a3-a5**, all *para*-substituted, completely inhibited the

growth of the bacteria with MICs in the low micromolar range (5.6 to 14.3 µM). In addition, the elongation of the alkyl side-chain, going from n=1 to n=3, reduced the activity by 2-fold; **3.15a1** (n=1, MIC_{90} = 20.9 µM), **3.15b** (n=2, MIC_{90} = 29.0 µM) and **3.15c** (n=3, MIC_{90} = 47.8 µM). Against the non-replicating bacteria, the *para*-substituted phenyl-based compounds also exhibited superior antimycobacterial activity than the unsubstituted analogues. However, there was no clear trend that could be deduced regarding the elongation of the alkyl side-chain. Furthermore, compounds **3.15a3** (MIC_{90} = 13.5 µM) and **3.15a4** (MIC_{90} = 24.0 µM) were more potent than moxifloxacin (MIC_{90} = 31.1 µM) in this assay, a standard TB drug. In terms of cytotoxicity, almost all the compounds in this series showed acceptable cytotoxicity on mammalian cell-lines having values closer to or greater than 100 µM.

(iii) In the primaquine series, the most active compound **3.19d** (IC_{50} = 1.311 µM) was 2-fold less active than the primaquine (IC_{50} = 0.615 µM). Also, none of these compounds showed any activity against the *M. tuberculosis* H_{37}Rv strain. Furthermore, these compounds showed unfavourable cytotoxicity profile towards mammalian cell-lines.

(iv) The 4-arylamino quinoline derivatives did not show any significant activity against both K1 and W2 strains. Against the 3D7 strain the most active compound **4.12d** (IC_{50} = 0.647 µM) was 924-fold less active than quinine. Also, quinine derivatives were significantly more active than their mefloquine counterparts. In this series there were only two compounds, **4.12b** and **4.12d** that exhibited antimycobacterial activity. Compound **4.12b** had an MIC_{90} of 123.2 µM against the non-replicating bacteria, while **4.12d** inhibited 98% of the replicating bacteria with an MIC_{90} of 92.5 µM.

(v) Among the PA-824 derivatives, the PA-824-aminoquinoline hybrids were the most active against the K1 strain, with compounds **4.19d** (IC_{50} = 0.100 µM) and **4.19f** (IC_{50} = 0.164 µM) exhibiting better activity than both chloroquine (IC_{50} = 0.213 µM) and primaquine (IC_{50} = 0.643 µM). Also, **4.19d** (IC_{50} = 0.100 µM) was more active than its parent compound **3.13a** (IC_{50} = 0.298 µM) and the equimolar combination of parent compounds (**4.18a**:**3.13a**) (IC_{50} = 0.303 µM), indicating an additive activity. Among these hybrids, compounds with 2- and 4-carbon spacer were more active than one containing a 3-carbon spacer. In contrast to the PA-824-aminoquinoline hybrids, the two PA-824-primaquine hybrids [**4.19g** (IC_{50} = 2.042 µM) and **4.19h** (IC_{50} = 0.985 µM)], which were tested as 1:1 diastereomeric mixtures, were less active than both primaquine (IC_{50} = 0.643 µM) and chloroquine (IC_{50} = 0.213 µM) on the K1 strain. Furthermore, these hybrids exhibited an antagonistic effect on antiplasmodial activity. Against the cultured *T. b. brucei* parasite, most compounds in this series showed poor activity.

Similarly, these PA-824 derivatives showed potent antimycobacterial activity against the replicating *M. tuberculosis* bacteria in the 7 and 14 day assays, with MICs ranging from 0.25 to 1.25 µM. Furthermore, all these compounds were more active than Kanamycin (MIC_{90} = 3.125 µM), a standard TB drug, and the two antimalarial drugs, chloroquine (MIC_{90} > 160 µM) and primaquine (MIC_{90} = 80 µM), in both assays. However, the majority of these compounds appeared to lose their 7 day efficacy when incubated for longer periods except compound **4.19d**, and this was postulated to be the result of degradation and precipitation in the assay media. The PA-824-aminoquinoline hybrids exhibited MICs in the range of 0.313-0.625 µM, where an increase in the length of the alkyl side-chain was accompanied by reduction in activity in both assays. Moreover, these PA-824-aminoquinoline hybrids (**4.19d-f**) were less efficacious than their parent compound, nitroimidazooxazine **4.18a**. Similarly, the PA-824-primaquine (**4.19g-h**) hybrids exhibited the same trend, where the

nitroimidazooxazine **4.18a-b** parent compounds showed superior activity than the corresponding hybrids. Thus, hybridisations in both cases of antimycobacterial evaluation indicate an antagonistic effect, suggesting that hybridisation in this instance does not yield any beneficial outcome. The selective indices of the most active compounds in this series were closer to or greater than 100, indicating that these compounds are more selective towards the pathogens. Aqueous solubility of these compounds did not appear to be playing a significant role on antiplasmodial activity. However, on the antimycobacterial activity, good solubility was accompanied by improved activity.

(vi) The *β*-lactam series possessed antiplasmodial activity against the K1 strain with IC_{50} values in the low micro-molar range. Compound **4.22c** (IC_{50} = 0.209 µM) was the most active in this series and had comparable activity to chloroquine (IC_{50} = 0.213 µM). However, none of these *β*-lactams showed any significant inhibitory activity against the *T. b. brucei* parasite and against the drug sensitive *M. tuberculosis* H_{37}Rv strain. Furthermore, these compounds showed notable cytotoxicity against mammalian cell-lines..

In conclusion, a number of new derivatives that possessed potent antiplasmodial and/or antimycobacterial activity which have a potential to be anti-malarial or antimycobacterial agents were identified from this study. These first generation compounds provide interesting starting point for further derivatization and optimization, provided their shortcomings are addressed.

5.2 Recommendations for future work

Since a number of potent compounds were identified in this study, the following future studies are proposed: (i) *In vitro* ADME profiling including metabolite identification and (ii) *in vivo* pharmacokinetic (PK) studies on key compounds, and (iii) elucidation of the

mechanistic details of these new derivatives by investigating the inhibition of the β-haematin formation amongst others.

Also, *in vitro* and *in vivo* drug metabolism and pharmacokinetic (DMPK), and *in vivo* efficacy studies should ideally be undertaken as well. The *in silico* predicted physico-chemical properties such as the Blood Brain-Barrier (BBB) penetration should also be determined experimentally to corroborate these predictions. Lastly, whenever possible, the effect of these compounds on hERG should also be studied.

Chapter Six

Experimental

6.1 Chemical reagents and Solvents

All chemical reagents used were supplied by either Sigma-Aldrich® or Merck and were used without further purification. Unless otherwise stated, all the solvents used were anhydrous and were purchased from Sigma-Aldrich, with the exception of THF and diethyl ether which were dried by appropriate techniques. Chromatographic solvents such as Ethyl acetate, dichloromethane and Hexane were purchased from Kimix or Protea Chemicals and were distilled prior to use. HPLC grade methanol, acetonitrile and formic acid (98 – 100%) were purchased from Sigma-Aldrich. Ultra filtered water was purified by a Millipore Synergy water purification system and was used as such.

6.2 Chromatography Purification

Thin layer chromatography (TLC) was carried out on a Merck PF_{254} aluminium-backed pre-coated silica gel plates and viewed under ultraviolet (UV) light or visualized using iodine vapour. Product purification on the flash column chromatography was carried out using Merck Kieselgel 60: 70 – 230 mesh.

Preparative HPLC separations were performed on a modular Waters HPLC system consisting of a 2767 sample manager, 2545 quaternary gradient pump, 1500 series column heater and a 2998 photodiode array detector (PDA) with a Prep 2998 flow-cell. Sample solutions for purification were prepared at *ca.* 100 mg/mL in 50% methanol. Injection volumes ranged between 50 μL and 1 mL, the mobile phase flow rate was 20 mL/min for all purifications and the column heater was set at 30°C. A mobile phase gradient was used, where mobile phase A,

an aqueous solution of 0.1% formic acid, was mixed on-line with mobile phase B, a 0.1% formic acid solution in methanol.

6.3 Physical and spectroscopic characterization

Melting points were determined on a Reichert-Jung Thermovar hot-stage microscope and are uncorrected. Microanalyses were determined using a Fisons EA 1180 CHNO-S instrument. Low-resolution mass spectra were obtained by flow-injection (5 mM NH_4 formate pH3 in H_2O:ACN, no column used) on a AB SCIEX 4000 QTRAP Hybrid triple quadrupole linear ion trap mass spectrometer, coupled with an Agilent 1200 Rapid Resolution (600 bar) HPLC system consisting of a binary pump, degasser, auto sampler and temperature controlled column compartment. Infra-red spectra were recorded on a PerkinElmer Spectrum 100 FT-IR spectrometer in the 4000 – 450 cm^{-1} range, with samples either as dichloromethane solution or as KBr discs.

NMR spectra were recorded on Bruker 400 MHz or Varian Unity 400 MHz and/or Varian Mercury 300 MHz spectrometers, all chemical shifts are reported in ppm and were referenced using solvent signals (2.50 and 39.4 ppm for DMSO-d_6 and 7.6 and 77.0 ppm for $CDCl_3$). Chemical shifts (δ) are recorded in parts per million (ppm). Coupling constants, *J*, are measured in Hertz (Hz) and rounded off to one decimal place. Abbreviations used in the assignment of the ^1H NMR spectra are as follows: br (broad), d (doublet), dd (doublet of doublets), m (multiplets), s (singlet) and t (triplet). ^{13}C NMR chemical shifts are listed without assignment to specific carbon atoms.

6.4 Experimental details

General procedure for the synthesis of 4-aminoquinoline-phenyl alcohols 3.7a-c.

4,7-Dichloroquinoline (1.0 eq) (**3.6**) and various aminobenzyl alcohols (1.0 eq) (**3.5a-c**) were refluxed in EtOH (25 ml) at 85-90 °C for 3 hrs. The resulting mixture was allowed to cool to room temperature, basified to pH 8 by drop-wise addition of ice-cold ammonium hydroxide solution (25%). The resulting precipitates were collected by filtration, washed with water (2 x 50 ml), ice-cold ethanol (2 x 30 ml) and allowed to further dry on standing in the fume-hood overnight to afford crude products. Product **3.7a** was purified by column chromatography eluting with 20% methanol: DCM mixture while products **3.7b** and **3.7c** were purified eluting with 5% methanol: DCM mixture.

{3-[(7-*Chloroquinolin*-4-*yl*)*amino*]*phenyl*}*methanol*, 3.7a

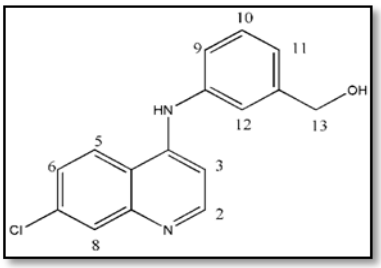

As a cream-colored powder (1.94 g, 88%); m. p. 241-243 °C (*lit.*[1] 247- 250 °C), R_f (MeOH: DCM, 20:80%) 0.19; δ_H (400 MHz; DMSO-*d6*) 9.07 (1H, s, NH), 8.47 (1H, d, *J* 5.6 Hz, H2), 8.45 (1H, d, *J* 9.2 Hz, H5), 7.89 (1H, d, *J* 2.0 Hz, H8), 7.57 (1H, dd, *J* 9.2 and 2.0 Hz, H6), 7.37 (1H, t, *J* 7.8 Hz, H10), 7.34 (1H, s, H12), 7.24 (1H, d, *J* 7.8 Hz, H11), 7.11 (1H, d, *J* 7.8 Hz, H9), 6.93 (1H, d, *J* 5.6 Hz, H3), 5.21 (1H, t, *J* 5.6 Hz, OH), 4.45 (2H, d, *J* 5.6 Hz, H13).

{2-[(7-*Chloroquinolin*-4-*yl*)*amino*]*phenyl*}*methanol*, 3.7b

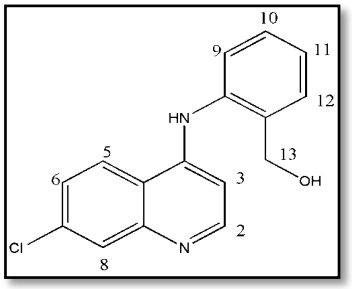

As a yellow solid (0.37 g, 25%); m. p. 185-188 °C (*lit.*[1] 194-197 °C), R_f (MeOH: DCM, 5:95%) 0.28;δ_H (300 MHz; DMSO-*d6*) 8.79 (1H, br s, NH), 8.39 (2H, m, H2 and H5), 7.89 (1H, d, *J* 2.0 Hz, H8), 7.62 (1H, m, H11), 7.57 (1H, dd, *J* 9.1 and 2.0 Hz, H6), 7.34 (3H, m, H9, H10 and H12), 6.32

(1H, d, *J* 5.3 Hz, H3), 5.23 (1H, br s, OH), 4.50 (2H, s, H13).

{4-[(7-*Chloroquinolin*-4-*yl*)*amino*]*phenyl*}*methanol*, 3.7c

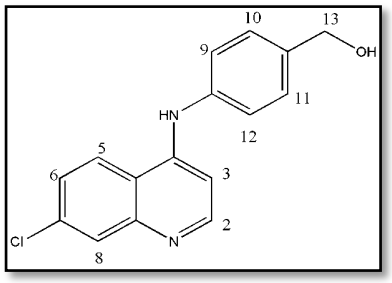

As a pale-yellow powder (0.58 g, 30%); m. p. 155-157 °C , R_f (MeOH: DCM, 5:95%) 0.33; δ_H (400 MHz; DMSO-*d6*) 9.04 (1H, s, NH), 8.45 (1H, d, *J* 5.6 Hz, H2), 8.43 (1H, d, *J* 9.2 Hz, H5), 7.89 (1H, d, *J* 2.0 Hz, H8), 7.57 (1H, dd, *J* 9.2 and 2.0 Hz, H6), 7.39 (2H, d, *J* 8.4 Hz, H10 and H11), 7.32 (2H, d, *J* 8.4 Hz, H9 and H12), 6.86 (1H, d, *J* 5.6 Hz, H3), 5.17 (1H, t, *J* 5.4 Hz, OH), 4.52 (2H, d, *J* 5.4 Hz, H13); δ_C (101 MHz; DMSO-*d6*) 152.0, 149.6, 149.4, 147.7, 143.8, 139.8, 133.5, 128.9, 127.6 (2C), 124.7 (2C), 121.9, 118.2, 101.6 and 62.5; *m*/*z* 283.63 (M^+, 100%).

General procedure for the synthesis of 4-aminoquinoline-phenyl aldehydes 3.8a-c.

SO_3.Pyr (2.0 eq) was added to a stirred solutions of benzyl alcohols **3.7a-c** (1.0 eq) and Et_3N (4.0 eq) in anhydrous DMSO (5 ml) under nitrogen at 26°C. The resulting mixtures were further stirred at this temperature for 3 days, extracted with EtOAc (5 x 50 ml). The extracts were washed with water (10 ml) and brine (10 ml), dried over $MgSO_4$ and solvent evaporated in *vacuo* and the obtained crude products purified by chromatography to give the desired products **3.8a-c** in moderate yields.

3-[(7-*Chloro*-*quinolin*-4-*yl*)*amino*]*benzaldehyde*, 3.8a

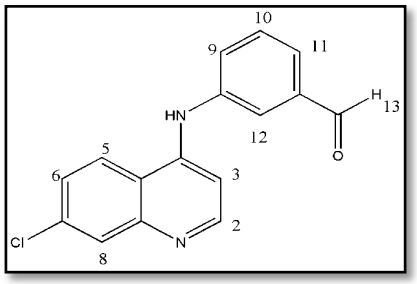

As a pale-yellow powder (0.20 g, 84.4%); m. p. 182- 184 °C (*lit*.[1] 182- 184 °C), R_f (EtOAc: Hexane, 70:30%) 0.25; δ_H (400 MHz; DMSO-*d6*) 10.03 (1H, s, H13), 9.29 (1H, s, NH), 8.54 (1H, d, *J* 5.2 Hz, H2), 8.44 (1H, d, *J*

9.2 Hz, H5), 7.94 (1H, d, *J* 1.8 Hz, H8), 7.93 (1H, s, H12), 7.70 (4H, m, H9, H10, H11 and H6), 7.07 (1H, d, *J* 5.2 Hz, H3).

2-[(7-*Chloro-quinolin*-4-*yl*)*amino*]*benzaldehyde*, 3.8b

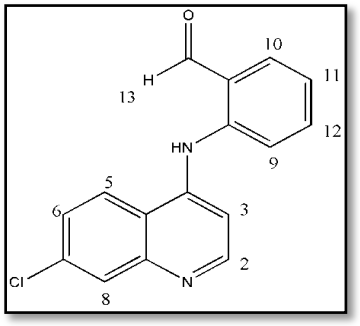

As a yellow solid (0.481 g, 87%); m. p. 158- 160 °C (*lit*.[13] 164- 166 °C), R_f (DCM: MeOH, 95:5%) 0.28; δ_H (400 MHz; DMSO-*d6*) 10.27 (1H, br s, NH), 10.10 (1H, s, H13), 8.61 (1H, d, *J* 5.2 Hz, H2), 8.31 (1H, d, *J* 9.2 Hz, H5),7.99 (1H, d, *J* 1.2 Hz, H8), 7.96 (1H, dd, *J* 9.2 and 1.2 Hz, H6), 7.57 (3H, m, H9, H10 and H12), 7.31 (1H, t, *J* 4.4 Hz, H11), 7.18 (1H, d, *J* 5.2 Hz, H3).

4-[(7-*Chloro-quinolin*-4-*yl*)*amino*]*benzaldehyde*,[1] 3.8c

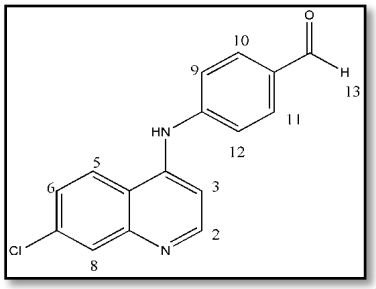

As a pale-yellow solid (0.39 g, 19%); R_f (DCM: MeOH, 95:5%) 0.31; δ_H (400 MHz; DMSO-*d6*) 11.01 (1H, br s, NH), 10.03 (1H, s, H13), 8.65 (1H, d, *J* 5.4 Hz, H2), 8.54 (1H, d, *J* 9.1 Hz, H5), 8.05 (1H, d, *J* 2.1 Hz, H8), 7.82 (2H, 2 x d, *J* 8.4 Hz, H10 and H11), 7.56 (1H, dd, *J* 9.1 and 2.1 Hz, H6), 7.32 (2H, 2 x d, *J* 8.4 Hz, H9 and H12), 6.86 (1H, d, *J* 5.5 Hz, H3).

Alternative synthesis* of the aldehyde 4c as an HCl salt.

A stirred methanolic mixture of 4,7-dichloroquinoline (1.0 eq) and 4-aminobenzaldehyde[1] (1.0 eq) was treated with 2M HCl (4 ml) and refluxed at 90 °C. After 30 minutes a thick yellow precipitate appeared and heating was continued at a low setting for 3 hrs and the resultant mixture was allowed to cool to room temperature. The yellow solid was filtered, washed with ice-cold methanol, then ether and dried on the vacuum line over a period of 6 hrs to obtain product **3.8c** as an HCl salt in quantitative yields.

General procedure[4] for the synthesis of deoxyamodiaquine-tetrazoles 3.9a-k.

Aldehydes **3.8a-c** (0.5 mmol) and an amine[‡] (1.0 mmol) were stirred in anhydrous methanol at 25 °C for 1 hr. Thereafter $TMSN_3$ (1.0 mmol) was added, followed by the addition of the *t*-butyl or ethylmorpholine isocyanide (1.0 mmol) and the resulting mixture stirred at this temperature for 24 hrs. The solvent was removed in *vacuo* to afford a crude product which was purified by column chromatography and HPLC to afford tertazoles **3.9a-k**.

N-{3-[(1-tert-*butyl*-1H-*tetrazol*-5-*yl*)(*dimethylamino*)*methyl*]*phenyl*}-7-*Chloroquinolin*-4-*amine*, 3.9a (TK1)

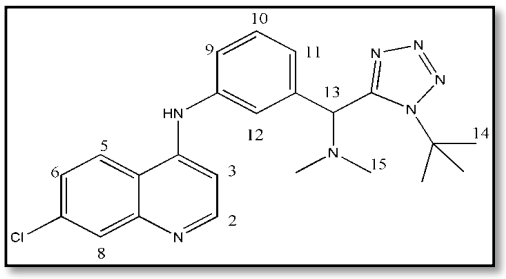

As a yellow solid (185 mg, 86%); m. p. 200- 202 °C, R_f (EtOAc, 100%) 0.46; IR ν_{max} (DCM)/cm^{-1} 3431 (N-H), 1610 (Ar C=C), 1372 (N=N), 1322 (C=N); δ_H (400 MHz; DMSO-*d6*) 9.12 (1H, s, NH), 8.46 (1H, d, *J* 5.2 Hz, H2), 8.43 (1H, d, *J* 9.0 Hz, H5), 7.90 (1H, s, H8), 7.57 (1H, d, *J* 9.0 Hz, H6), 7.49 (1H, s, H12), 7.43 (1H, t, *J* 7.8 Hz, H10), 7.33 (1H, d, *J* 7.8 Hz, H9), 7.23 (1H, d, *J* 7.8 Hz, H11), 6.87 (1H, d, *J* 5.2 Hz, H3), 5.50 (1H, s, H13), 2.27 (6H, s, 2 x H15), 1.68 (9H, s, 3 x H14); δ_C (101 MHz; DMSO-*d6*) 154.0, 151.7, 149.5, 147.7, 140.0, 137.5, 133.8, 129.0, 127.5, 125.0, 124.8, 124.3, 123.4, 122.0, 118.2, 101.7, 62.8, 61.3, 41.6 (2C) and 29.4 (3C); MS (ESI) *m/z* 435.8 (M^+) and 458.4 (M^++Na), (Found: C, 60.63, H, 6.16, N, 22.14 %; $C_{23}H_{26}ClN_7.H_2O$ Requires C, 60.57, H, 6.22, N, 21.90). HPLC purity: 99.5%; $t_{r'}$=4.47 min.

[‡] HCl protected amines were neutralized by addition of the base, diisopropyl ethylamine (2 eq)

N-{3-[(*diethylamino*)(1-tert-*butyl*-1H-*tetrazol*-5-*yl*)*methyl*]*phenyl*}-7-*Chloroquinolin*-4-*amine*, 3.9b (TK2)

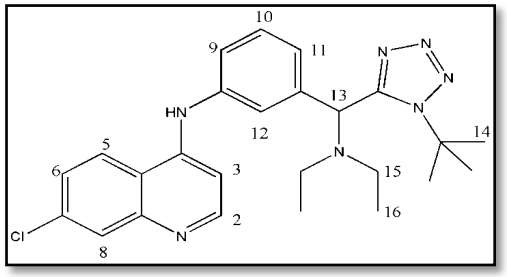

As a yellow solid (81 mg, 25%); m. p. 111- 112 °C, R_f (EtOAc: Hex, 70:30%) 0.19; IR ν_{max} (DCM)/cm^{-1} 3455 (N-H), 1606 (Ar C=C), 1374 (N=N), 1324 (C=N); δ_H (400 MHz; DMSO-*d6*) 9.10 (1H, s, NH), 8.46 (1H, d, *J* 5.2 Hz, H2), 8.41 (1H, d, *J* 9.0 Hz, H5), 7.90 (1H, d, *J* 1.6 Hz,, H8), 7.57 (1H, dd, *J* 9.0 and 1.6 Hz, H6), 7.40 (1H, t, *J* 7.9 Hz, H10), 7.32 (1H, s, H12), 7.31 (1H, d, *J* 7.9 Hz, H9), 7.08 (1H, d, *J* 7.9 Hz, H11), 6.86 (1H, d, *J* 5.2 Hz, H3), 5.74 (1H, s, H13), 2.73 (4H, 2 x q, *J* 7.0 Hz, 2 x H15), 1.68 (9H, s, 3 x H14), 0.92 (6H, t, *J* 7.0Hz, 2 x H16); δ_C (101 MHz; DMSO-*d6*) 154.5, 151.6, 149.5, 147.7, 140.0, 139.2, 133.8, 129.0, 127.5, 124.8, 124.7, 124.3, 123.2, 121.7, 118.2, 101.7, 60.0, 59.9, 44.1 (2C), 29.3 (3C) and 13.9 (2C); *m/z* 391.80 [M^+-N(CH_2CH_3)$_2$, 100%]; LCMS *m/z* 464.1 (M^+) and 486.2 (M^++Na), (Found: C, 61.75, H, 7.40, N, 19.49 %; $C_{25}H_{30}ClN_7$.1.5H_2O Requires C, 61.15, H, 6.97, N, 19.97%), HPLC purity: 98.7%; t_r=4.59 min.

N-{3-[(1-tert-*butyl*-1H-*tetrazol*-5-*yl*)(*pyrrolidin*-1-*yl*)*methyl*]*phenyl*}-7-*Chloroquinolin*-4-*amine*, 3.9c (TK3)

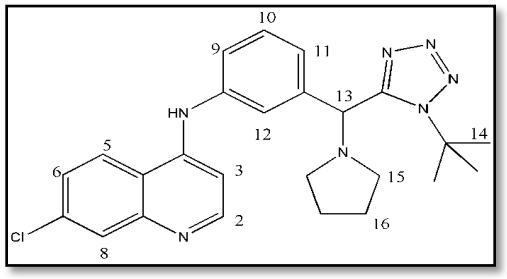

As a yellow-crystalline powder (200 mg, 87%); m. p. 90- 92 °C, R_f (EtOAc, 100%) 0.38; IR ν_{max} (DCM)/cm^{-1} 3426 (N-H), 1608 (Ar C=C), 1374 (N=N), 1329 (C=N); δ_H (400 MHz; DMSO-*d6*) 9.12 (1H, s, NH), 8.46 (1H, d, *J* 5.2 Hz, H2), 8.42 (1H, d, *J* 9.0 Hz, H5), 7.90 (1H, d, *J* 1.8 Hz, H8), 7.59 (1H, s, H12), 7.57 (1H, dd, *J* 9.0 and 1.8 Hz, H6), 7.42 (1H, t, *J* 7.8 Hz, H10), 7.31 (2H, d, *J* 7.8 Hz, H9 and H11), 6.84 (1H, d, *J* 5.2 Hz, H3), 5.50 (1H, s, H13), 2.61 (2H,

m, H*15a*), 2.45 (2H, m, H*15b*), 1.69 (9H, s, 3 x H14), 1.67 (4H, m, 2 x H16); δ_C (101 MHz; DMSO-*d6*) 154.8, 151.7, 149.5, 147.7, 140.1, 138.5, 133.8, 129.1, 127.5, 124.8, 124.7, 124.3, 123.1, 121.9, 118.2, 101.8, 61.3, 60.9, 50.1 (2C), 29.5 (3C) and 22.8 (2C); MS (ESI) *m/z* 461.9 (M^+), (Found: C, 62.26, H, 6.70, N, 20.72 %; $C_{25}H_{28}ClN_7.H_2O$ Requires C, 62.56, H, 6.30, N, 20.43%), HPLC purity: 99.0%; $t_{r'}$=4.46 min.

N-{3-[(1-tert-*butyl*-1H-*tetrazol*-5-*yl*)(*piperidin*-1-*yl*)*methyl*]*phenyl*}-7-*Chloroquinolin*-4-*amine*, 3.9d (TK4)

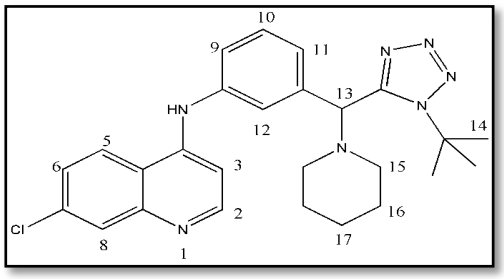

As a white solid (131 mg, 55%); m. p. 136- 138 °C, R_f (EtOAc, 100%) 0.64; IR ν_{max} (DCM)/cm^{-1} 3422 (N-H), 1608 (Ar C=C), 1374 (N=N), 1327 (C=N); δ_H (400 MHz; DMSO-*d6*) 9.12 (1H, s, NH), 8.46 (1H, d, *J* 5.6 Hz, H2), 8.43 (1H, d, *J* 9.0 Hz, H5), 7.90 (1H, d, *J* 1.8 Hz, H8), 7.57 (1H, dd, *J* 9.0 and 1.8 Hz, H6),7.52 (1H, s, H12), 7.42 (1H, t, *J* 7.8 Hz, H10), 7.32(1H, d, *J* 7.8 Hz, H9), 7.23 (1H, d, *J* 7.8 Hz, H11), 6.85 (1H, d, *J* 5.6 Hz, H3), 5.46 (1H, s, H13), 2.61 (2H, m, H*15a*), 2.33 (2H, m, H*15b*), 1.66 (9H, s, 3 x H14), 1.43 (4H, m, 2 x H16), 1.33 (2H, m, H17); δ_C (101 MHz; DMSO-*d6*) 153.9, 151.7, 149.5, 147.7, 139.9, 137.1, 133.8, 128.9, 127.5, 125.2, 124.8, 124.3, 123.5, 121.8, 101.8, 79.0, 63.2, 61.5, 50.3 (2C), 29.4 (3C), 25.7 (2C) and 23.9; MS (ESI) *m/z* 476.0 (M^+), (Found: C, 62.93, H, 6.86, N, 19.79 %; $C_{25}H_{30}ClN_7.H_2O$ Requires C, 63.21, H, 6.53, N, 19.85%), HPLC purity: 99.5%; $t_{r'}$=4.56 min.

N-{3-[(1-tert-*butyl*-1H-*tetrazol*-5-*yl*)(*piperazinn*-1-*yl*)*methyl*]*phenyl*}-7-*Chloroquinolin*-4-*amine*, 3.9e (TK5)

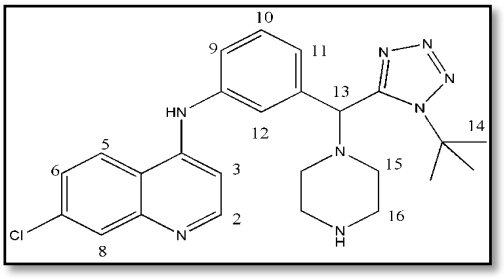

As a yellow crystalline solid (78 mg, 19%), m.p. 140- 144 °C, R_f (DCM: MeOH, 95: 05%) 0.48; IR ν_{max} (DCM)/cm^{-1} 3415 (N-H), 1609 (Ar C=C), 1374

(N=N), 1325 (C=N); δ_H (400 MHz; DMSO-*d6*) 8.57 (1H, s, NH), 8.26 (1H, d, *J* 6.3 Hz, H2), 8.21 (1H, d, *J* 9.0 Hz, H5), 7.80 (1H, d, *J* 1.6, H8), 7.64 (1H, s, H12), 7.41 (2H, m, H10 and H11), 7.35 (1H, dd, *J* 9.0 and 1.6 Hz, H6), 7.25 (1H, d, *J* 7.9 Hz, H9), 6.70 (1H, d, *J* 5.6 Hz, H3), 5.38 (1H, s, H13), 3.52 (2H, m, H*16a*), 3.37 (2H, t, J 4.9 Hz, H*16b*), 2.81 (1H, m, H*15a1)*, 2.67 (1H, m, H*15a2*), 2.46 (2H, m, H*15b*), 1.76 (9H, s, 3 x H14), δ_C (101 MHz; DMSO-*d6*) 153.4, 152.0, 145.3, 142.6, 138.8, 138.3, 136.8, 130.0, 127.2, 127.1, 124.8, 124.2, 123.6, 122.7, 116.7, 100.8, 64.4, 61.9, 50.3, 49.8, 45.7, 40.1 and 30.4 (3C); MS (ESI) *m/z* 477.5 (M^+); HPLC purity: 99.5%; $t_{r'}$=4.47 min.

N-{3-[(1-tert-*butyl*-1H-*tetrazol*-5-*yl*)(*morpholino*)*methyl*]*phenyl*}-7-*Chloroquinolin*-4-*amine*, 3.9f (TK6)

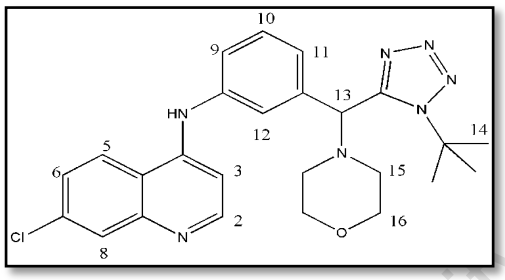

As a yellow-crystalline powder (127 mg, 53%); m. p. 166-168 °C, R_f (EtOAc, 100%) 0.29; IR ν_{max} (DCM)/cm^{-1} 3288 (N-H), 1611 (Ar C=C), 1372 (N=N), 1327 (C=N), 1112 (C-O-C); δ_H (400 MHz; DMSO-*d6*) 9.13 (1H, s, NH), 8.47 (1H, d, *J* 5.2 Hz, H2), 8.42 (1H, d, *J* 9.0 Hz, H5), 7.90 (1H, d, *J* 2.0 Hz, H8), 7.57 (1H, dd, *J* 9.0 and 2.0 Hz, H6), 7.56 (1H, s, H12), 7.44 (1H, t, *J* 7.8 Hz, H10), 7.33 (1H, d, *J* 7.8 Hz, H9), 7.27 (1H, d, *J* 7.8 Hz, H11), 6.87 (1H, d, *J* 5.2 Hz, H3), 5.53 (1H, s, H13), 3.55 (4H, br m, 2 x H16), 2.66 (2H, t, *J* 5.6 Hz, H*15a*), 2.40 (2H, t, *J* 5.6 Hz, H*15b*), 1.69 (9H, s, 3 x H14); δ_C (101 MHz; DMSO-*d6*) 153.8, 151.7, 149.5, 147.7, 140.2, 136.6, 133.8, 129.1, 127.5, 125.1, 124.8, 124.4, 123.4, 122.0, 118.3, 101.9, 66.2 (2C), 62.9, 61.5, 50.0 (2C) and 29.5 (3C); MS (ESI) *m/z* 478.0 (M^+); (Found: C, 58.98, H, 6.60, N, 18.60 %; $C_{25}H_{28}ClN_7O.2H_2O$ Requires C, 58.42, H, 6.27, N, 19.07%), HPLC purity: 98.6%; $t_{r'}$=5.12 min.

7-*Chloro*-N-{3-[(*dimethylamino*)(1-(2-*morpholinoethyl*)-1H-*tetrazol*-5-*yl*)*methyl*]*phenyl*}*quinolin*-4-*amine*, 3.9g (TK7)

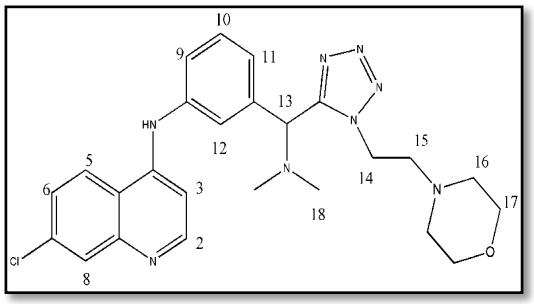

As a thick yellow oil (100 mg, 35%); R_f (DCM: MeOH, 95: 05%) 0.32, IR ν_{max} (DCM)/cm^{-1} 3413 (N-H), 1607 (Ar C=C), 1372 (N=N), 1331 (C=N), 1116 (C-O-C); δ_H (400 MHz; $CDCl_3$) 8.54 (1H, d, *J* 5.5 Hz, H2), 8.04 (1H, d, *J* 2.0 Hz, H8), 8.00 (1H, d, *J* 9.0 Hz, H5), 7.50 (1H, s, H12), 7.45 (1H, dd, *J* 9.0 and 2.0 Hz, H6), 7.43 (1H, t, *J* 7.8 Hz, H10), 7.35 (1H, d, *J* 7.8 Hz, H9), 7.24 (1H, d, *J* 7.8 Hz, H11), 6.95 (1H, d, *J* 5.5 Hz, H3), 5.03 (1H, s, H13), 4.54 (2H, m, H14), 3.60 (4H, t, *J* 4.6 Hz, 2 x H17), 2.75 (2H, m, H15), 2.45 (4H, t, *J* 4.6 Hz, 2 x H16), 2.31 (6H, s, 2 x H18); δ_C (101 MHz; $CDCl_3$) 154.3, 150.8, 150.3, 147.8, 139.9, 136.0, 135.1, 129.9, 128.1, 126.5, 125.4, 123.0, 122.4, 121.8, 118.0, 102.5, 66.7 (2C), 64.9, 57.4, 53.7 (2C), 45.2 and 42.8 (2C), MS (ESI) *m/z* 493.0 (M^+); HPLC purity: 97.5%; t_r=4.16 min.

N-{3-[(*diethylamino*)-(1-(2-*morpholinoethyl*)-1H-*tetrazol*-5-*yl*)*methyl*]*phenyl*}-7-*chloroquinolin*-4-*amine*, 3.9h (TK8)

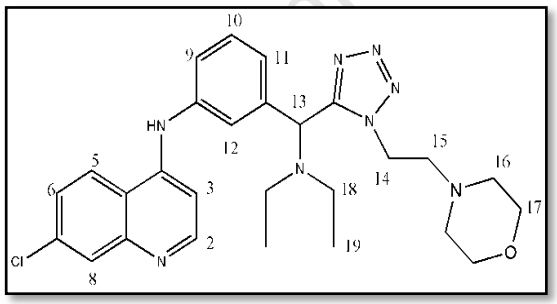

As a white paste (95 mg, 32%); R_f (DCM: MeOH, 95: 05%) 0.38, IR ν_{max} (DCM)/cm^{-1} 3422 (N-H), 1609 (Ar C=C), 1374 (N=N), 1325 (C=N), 1116 (C-O-C); δ_H (400 MHz; $CDCl_3$) 8.79 (1H, s, NH), 8.55 (1H, d, *J* 5.3 Hz, H2), 8.01 (1H, d, *J* 2.1 Hz, H8), 7.90 (1H, d, *J* 9.0 Hz, H5), 7.45 (1H, dd, *J* 9.0 and 2.1 Hz, H6), 7.38 (2H, m, H10 and H12), 7.30 (1H, d, *J* 7.9 Hz, H9), 7.18 (1H, d, *J* 7.9 Hz, H11), 6.97 (1H, d, *J* 5.3 Hz, H3), 5.41 (1H, s, H13), 4.51 (2H, m, H14), 3.69 (2H, t, *J* 4.7 Hz, H*17a*), 3.57 (2H, t, *J* 4.7 Hz, H*17b*), 2.81 (2H, m, H15), 2.63 (4H, q, *J* 7.2 Hz, 2 x H18), 2.49

(2H, m, H*16a*), 2.43 (2H, m, H*16b*), 1.04 (6H, t, *J* 7.1 Hz, 2 x H19); δ_C (101 MHz; $CDCl_3$) 154.3, 151.7, 149.7, 147.3, 140.1, 137.8, 135.5, 129.7, 128.9, 126.3, 125.2, 123.0, 122.1, 121.4, 118.5, 102.7, 66.8 (2C), 59.6, 57.3, 53.4 (2C), 45.4, 44.0 (2C) and 13.0 (2C), MS (ESI) *m/z* 521.0 (M^+); HPLC purity: 98.9%; t_r=4.29 min.

7-*Chloro*-N-{3-[1-(2-*morpholinoethyl*)-1H-*tetrazol*-5-*yl*)(*pyrrolidin*-1-*yl)methyl*]*phenyl*}*quinolin*-4-*amine*, 3.9i (TK9)

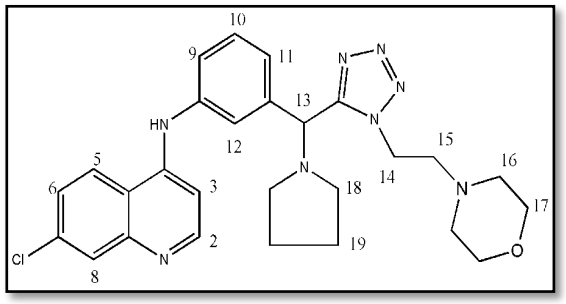

As a white paste (130 mg, 40%); R_f (DCM: MeOH, 95: 05%) 0.39, IR ν_{max} (DCM)/cm^{-1} 3422 (N-H), 1606 (Ar C=C), 1370 (N=N), 1325 (C=N), 1119 (C-O-C); δ_H (400 MHz; $CDCl_3$) 8.51 (1H, d, *J* 5.5 Hz, H2), 8.04 (1H, d, *J* 1.8 Hz, H8), 7.98 (1H, d, *J* 8.8 Hz, H5), 7.47 (1H, s, H12), 7.46 (1H, dd, *J* 8.8 and 1.8 Hz, H6), 7.40 (1H, t, *J* 7.8 Hz, H10), 7.33 (2H, m, H9 and H11), 6.94 (1H, d, *J* 5.5 Hz, H3), 5.06 (1H, s, H13), 4.53 (2H, m, H14), 3.61 (4H, t, *J* 4.6 Hz, 2 x H17), 2.81 (2H, m, H15), 2.66 (2H, m, H*18a*), 2.50 (2H, m, H*18b*), 2.44 (4H, t, *J* 4.6 Hz, 2 x H16) 1.83 (4H, m, 2 x H19); δ_C (101 MHz; $CDCl_3$) 155.1, 150.4, 150.3, 148.0, 140.1, 138.7, 136.2, 130.0, 127.8, 126.6, 124.6, 122.3, 122.1, 122.0, 118.0, 102.5, 66.7 (2C), 63.7, 57.0, 53.6 (2C), 52.4 (2C), 45.1 and 23.5 (2C), MS (ESI) *m/z* 519.0 (M^+); HPLC purity: 98.2%; t_r=4.08 min.

N-{2-[(1-tert-*butyl*-1H-*tetrazol*-5-*yl*)(*dimethylamino*)*methyl*]*phenyl*}-7-*Chloroquinolin*-4-*amine*, 3.9j (TK10)

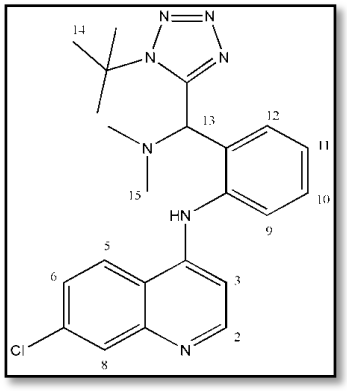

As a yellow paste (45 mg, 12%); R_f (DCM: MeOH, 95: 05%) 0.51, IR ν_{max} (DCM)/cm^{-1} 3422 (N-H), 1607 (Ar C=C), 1368 (N=N), 1325 (C=N); δ_H (400 MHz; DMSO-*d6*) 9.82 (1H, s, NH), 8.61 (1H, d, *J* 5.2 Hz, H2), 8.06 (1H, d, *J* 2.0 Hz, H8),

7.84 (1H, d, *J* 8.9 Hz, H5), 7.61 (1H, d, *J* 7.9 Hz, H12), 7.49 (1H, dd, *J* 2.1 and 8.9 Hz, H6), 7.37 (1H, t, *J* 7.8 Hz, H10), 7.13 (1H, d, *J* 5.3 Hz, H3), 6.98 (1H, t, *J* 7.8 Hz, H11), 6.60 (1H, d, *J* 7.6 Hz, H9), 5.61 (1H, s, H13), 2.55 (6H, s, 2 x H15), 1.55 (9H, s, 3 x H14); δ_C (101 MHz; DMSO-*d6*) 151.8, 149.3, 147.0, 146.8, 139.8, 129.8, 129.5, 128.9, 127.8, 126.5, 123.5, 121.4, 120.8, 120.7, 102.0, 101.9, 61.6, 59.6, 40.9 (2C) and 29.6 (3C); MS (ESI) *m/z* 436.2 (M^+); HPLC purity: 98.2%; t_r=6.87 min.

N-{2-[(1-tert-*butyl*-1H-*tetrazol*-5-*yl*)(*dimethylamino*)*methyl*]*phenyl*}-7-*Chloroquinolin*-4-*amine*, 3.9k (TK11)

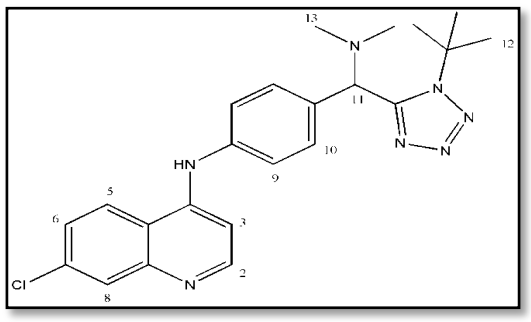

As a yellow solid (101 mg, 16%); m. p. 165-168 °C, R_f (DCM: MeOH, 90: 10%) 0.35; IR ν_{max} (KBr)/cm^{-1} 3500 (N-H), 1611 (Ar C=C), 1374 (N=N), 1323 (C=N);, δ_H (300 MHz; DMSO-*d6*) 9.53 (1H, s, NH), 8.40 (1H, d, *J* 5.4 Hz, H2), 8.20 (1H, d, *J* 9.0 Hz, H5), 7.81 (1H, d, *J* 2.2 Hz, H8), 7.67 (2H, d, *J* 7.0 Hz, 2 x H9), 7.56 (2H, d, *J* 6.9 Hz, 2 x H10), 7.53 (1H, dd, *J* 9.0 and 2.2 Hz, H6), 6.73 (1H, d, *J* 5.4 Hz, H3), 5.54 (1H, s, H11), 2.31 (6H, s, 2 x H13), 1.74 (9H, s, 3 x H12); δ_C (75 MHz; DMSO-*d6*) 153.9, 151.3, 148.9, 147.3, 141.2, 139.4, 138.3, 136.5, 133.2, 129.9, 127.3, 125.0, 124.4, 123.6, 119.8, 117.4, 100.4, 62.4, 61.3, 41.4 (2C) and 29.4 (3C); MS (ESI) *m/z* 436.4 (M^+); HPLC purity: 99.5%; t_r=7.21 min.

General procedure for the synthesis of de-*tert*-butylated deoxyamodiaquine-tetrazoles 3.10a-f.

A solution of the *tert*-butylated tetrazole **3.9a-f** (0.58 mmol) in 32% HCl acid (10 ml) was refluxed at 120 °C for 4-8 hrs. On complete consumption of the starting material, as shown by TLC, the reaction mixture was allowed to cool to room temperature, water (30 ml) added

and the pH adjusted to 12 by the addition of 5% $NaHCO_3$. The resultant mixture was washed with EtOAc (2 x 100 ml), aqueous layer neutralized to pH 7 by drop-wise addition of 32% HCl acid and allowed to stand in the fume hood overnight. The precipitate which had formed was filtered and washed with cold Et_2O to afford a crude product which was purified by preparative HPLC to give the desired de-*tert*butylated tetrazoles **3.10a-f.**

7-*Chloro*-N-{3-[(*dimethylamino*)(1H-*tetrazol*-5-*yl*)*methyl*]*phenyl*}*quinolin*-4-*amine*, 3.10a (TK1B3)

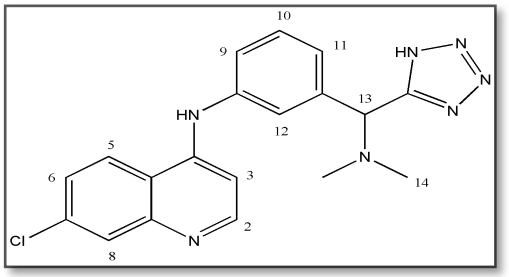

As an off-white powder (129 mg, 59%); m. p. 174- 176 °C, R_f (DCM: MeOH: NH_4OH; 90: 9.7: 0.3%) 0.17; IR ν_{max} (KBr)/cm^{-1} 3341 (N-H), 1588 (Ar C=C), 1370 (N=N), 1329 (C=N); δ_H (400 MHz; DMSO-*d6*) 9.12 (1H, br s, NH), 8.45 (1H, d, *J* 9.1 Hz, H5), 8.42 (1H, d, *J* 5.4 Hz, H2), 7.87 (1H, d, *J* 2.2 Hz, H8), 7.58 (1H, s, H12), 7.54 (1H, dd, *J* 9.1 and 2.2 Hz, H6), 7.33 (1H, t, *J* 7.6 Hz, H10), 7.26 (1H, d, *J* 7.6 Hz, H9), 7.21 (1H, d, *J* 7.6 Hz, H11), 6.89 (1H, d, *J* 5.4 Hz, H3), 4.82 (1H, s, H13), 2.14 (6H, s, 2 x H14); δ_C (101 MHz; DMSO-*d6*) 159.8, 151.7, 149.4, 148.0, 142.5, 139.5, 133.7, 128.4, 127.4, 124.6 (2C), 124.4, 123.2, 121.1, 118.2, 101.5, 66.7 and 42.8 (2C); MS (ESI) *m/z* 380.4 (M^+); (Found: C, 51.77, H, 5.83, N, 24.24%; $C_{19}H_{18}ClN_7.H_2O.NH_4HCO_2$ Requires C, 52.12, H, 5.47, N, 24.31%); HPLC purity: 98.0%; t_r,=4.23 min.

N-{3-[(*diethylamino*)(1H-*tetrazol*-5-*yl*)*methyl*]*phenyl*}-7-*Chloroquinolin*-4-*amine*, 3.10b (TK2B3)

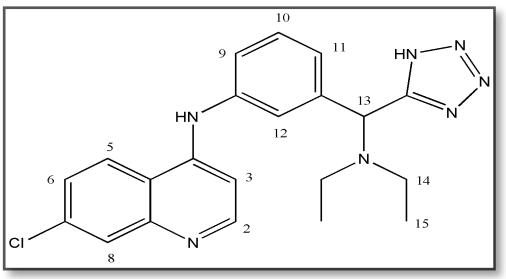

As a pale-yellow powder (99 mg, 40%), m. p. 185-187 °C, R_f (DCM: MeOH: NH_4OH; 90: 9.7: 0.3%) 0.11; IR ν_{max} (KBr)/cm^{-1} 3345 (N-H), 1593 (Ar

C=C), 1374 (N=N), 1325 (C=N); δ_H (400 MHz; DMSO-*d6*) 9.20 (1H, br s, NH), 8.47 (1H, d, *J* 5.4 Hz, H2), 8.43 (1H, d, *J* 9.0 Hz, H5), 7.91 (1H, d, *J* 2.2 Hz, H8), 7.59 (1H, s, H12), 7.58 (1H, dd, *J* 9.0 and 2.2 Hz, H6), 7.45 (1H, t, *J* 7.8 Hz, H10), 7.32 (2H, 2 x d, *J* 7.8 Hz, H9 and H11), 6.91 (1H, d, *J* 5.4 Hz, H3), 5.61 (1H, s, H13), 2.79 (2H, q, *J* 7.1 Hz, H14*a*), 2.64 (2H, q, *J* 7.1 Hz, H14*b*), 1.05 (6H, t, *J* 7.1 Hz, 2 x H15); δ_C (101 MHz; DMSO-*d6*) 157.2, 152.2, 149.8, 148.4, 140.9, 134.5, 130.0, 128.0, 125.5, 125.0, 124.9, 123.2, 122.8, 118.9, 102.6, 61.1, 55.3, 44.3 (2C) and 11.1 (2C); MS (ESI) *m/z* 408.6 (M^++H); (Found: C, 56.94, H, 6.05, N, 24.04%; $C_{21}H_{22}ClN_7.NH_4HCO_2$ Requires C, 56.11, H, 5.78, N, 23.79%); HPLC purity: 95.7%; t_r,=4.35 min.

N-{3-[(*pyrrolidin*-1-*yl*)(1H-*tetrazol*-5-*yl*)*methyl*]*phenyl*}-7-*Chloroquinolin*-4-*amine*, 3.10c (TK3B3)

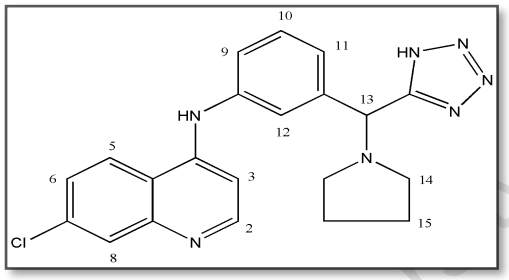

As a pale-yellow powder (134 mg, 55%), m. p. 189- 192 °C, R_f (DCM: MeOH: NH_4OH; 90: 9.7: 0.3%) 0.14; IR ν_{max} (KBr)/cm^{-1} 3360 (N-H), 1601 (Ar C=C), 1373 (N=N), 1325 (C=N); δ_H (400 MHz; DMSO-*d6*) 9.16 (1H, br s, NH), 8.48 (1H, d, *J* 5.3 Hz, H2), 8.43 (1H, d, *J* 9.1 Hz, H5), 7.91 (1H, d, *J* 2.0 Hz, H8), 7.65 (1H, s, H12), 7.58 (1H, dd, *J* 9.1 and 2.0 Hz, H6), 7.45 (1H, t, *J* 7.8 Hz, H10), 7.38 (1H, d, *J* 7.8 Hz, H9), 7.33 (1H, d, *J* 7.8 Hz, H11), 6.92 (1H, d, *J* 5.3 Hz, H3), 5.49 (1H, s, H13), 2.85 (4H, t, *J* 6.2 Hz, 2 x H14), 1.84 (4H, t, *J* 6.2 Hz, 2 x H15); δ_C (101 MHz; DMSO-*d6*) 157.8, 151.7, 149.3, 147.6, 140.4, 138.3, 133.9, 129.6, 127.4, 124.9, 124.4, 124.1, 122.4, 122.2, 118.3, 102.1, 64.2, 52.2 (2C) and 22.8 (2C); MS (ESI) *m/z* 406.3 (M^+); (Found: C, 54.05, H, 6.01, N, 22.45%; $C_{21}H_{20}ClN_7.H_2O.NH_4HCO_2$ Requires C, 54.26, H, 5.59, N, 23.01%); HPLC purity: 99.4%; t_r,=4.33 min.

N-{3-[(*piperidin*-1-*yl*)(1H-*tetrazol*-5-*yl*)*methyl*]*phenyl*}-7-*Chloroquinolin*-4-*amine*, 3.10d (TK4B3)

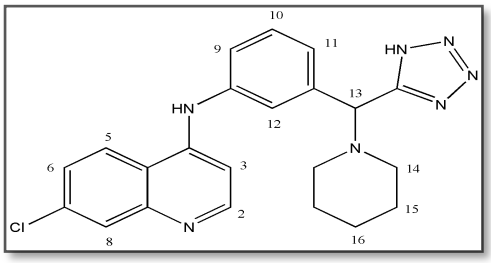

As a yellow powder (84 mg, 39%); m. p. 193- 195 °C, R_f (DCM: MeOH: NH_4OH; 90: 9.7: 0.3%) 0.16; IR ν_{max} (KBr)/cm^{-1} 3381 (N-H), 1609 (Ar C=C), 1374 (N=N), 1322 (C=N); δ_H (300 MHz; DMSO-*d6*) 9.09 (1H, br s, NH), 8.47 (1H, d, *J* 5.4 Hz, H2), 8.43 (1H, d, *J* 9.0 Hz, H5), 7.90 (1H, d, *J* 2.2 Hz, H8), 7.57 (1H, dd, *J* 9.0 and 2.2 Hz, H6),7.55 (1H, s, H12), 7.43 (1H, t, *J* 7.8 Hz, H10), 7.30 (1H, d, *J* 7.8 Hz, H9), 7.24 (1H, d, *J* 7.8 Hz, H11), 6.89 (1H, d, *J* 5.4 Hz, H3), 5.24 (1H, s, H13), 2.57 (2H, m, H*14a*), 2.45 (2H, m, H*14b*), 1.58 (4H, m, 2 x H15), 1.41 (2H, t, *J* 7.4 Hz, H16); δ_C (75 MHz; DMSO-*d6*) 156.9, 151.6, 149.3, 148.9, 147.8, 140.2, 138.4, 133.4, 129.2, 127.4, 124.8, 124.3 (2C), 122.6, 121.8, 102.0, 65.0, 51.3 (2C), 24.6 (2C) and 23.2; MS (ESI) *m/z* 420.1 (M^+); (Found: C, 56.06, H, 5.96, N, 22.45%; $C_{22}H_{22}ClN_7.0.5H_2O.NH_4HCO_2$ Requires C, 56.15, H, 5.74, N, 22.78%); HPLC purity: 96.4%; t_r=4.38 min.

N-{3-[(*morpholino*) (1H-*tetrazol*-5-*yl*)*methyl*]*phenyl*}-7-*Chloroquinolin*-4-*amine*, 3.10f (TK6B3)

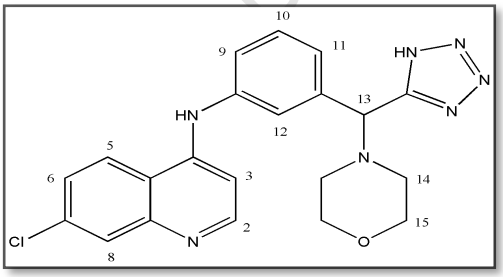

As a yellow powder (170 mg, 45%); m. p. 190-192 °C, R_f (DCM: MeOH: NH_4OH, 90: 9.7: 0.3%) 0.10; IR ν_{max} (KBr)/cm^{-1} 3340 (N-H), 1587 (Ar C=C), 1371 (N=N), 1320 (C=N); δ_H (300 MHz; DMSO-*d6*) 8.46 (1H, d, *J* 5.4 Hz, H2), 8.41 (1H, d, *J* 9.0 Hz, H5), 7.90 (1H, d, *J* 2.2 Hz, H8), 7.54 (1H, dd, *J* 9.0 and 2.2 Hz, H6), 7.51 (1H, s, H12), 7.38 (1H, t, *J* 7.8 Hz, H10), 7.28 (1H, d, *J* 7.8 Hz, H9), 7.22 (1H, d, *J* 7.8 Hz, H11), 6.88 (1H, d, *J* 5.2 Hz, H3), 5.05 (1H, s, H13), 3.60 (4H, t, *J* 4.6 Hz, 2 x H15), 2.45 (2H, m, H*14a*), 2.30 (2H, m, H*14b*); δ_C (75 MHz;

DMSO-*d6*) 156.9, 151.4, 149.1, 147.9, 140.2, 138.6, 133.9, 129.3, 127.2, 124.8, 124.4, 124.1, 122.4, 121,8, 118.2, 101.9, 65.9 (2C), 64.6 and 51.0 (2C); MS (ESI) *m/z* 422.2 (M^+); (Found: C, 54.60, H, 5.46, N, 23.53%; $C_{21}H_{20}ClN_7O.NH_4HCO_2$ Requires C, 54.49, H, 5.20, N, 23.11%); HPLC purity: 99.4%; t_r=4.47 min.

General procedure for the synthesis of 4-aminoquinoline-amines 3.13a-c.

4,7-Dichloroquinoline (1.0 eq) (**3.6**) and the respective diamine (**3.12a-c**) (5.0 eq) were heated neat at 80 °C for 1 hr without stirring and then at 135 °C for 4 hrs with stirring. The resulted mixtures were allowed to cool to room temperature, 10% NaOH (60 ml) added and a portion of products precipitated, and collected by filtration. These were then washed with distilled water and ice-cold ethanol to afford white or yellow powdery products. Excess products that remained in the aqueous solution were extracted with hot EtOAc (3 x 100 ml), washed with distilled water and dried over $MgSO_4$. Solvents were removed in *vacuo* to obtain the amines **3.13a-c** in moderate yields.

N-(7-*Chloroquinolin*-4-*yl*)*ethane*-1,2-*diamine*, 3.13a

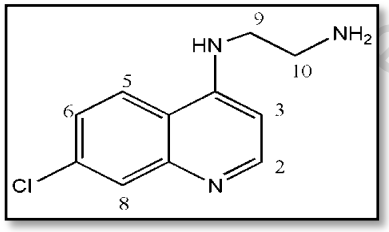

As a white powder (1.47 g, 65%); m. p. 138- 140 °C (*lit.*[2] 137- 139 °C); R_f (NH_3: MeOH, 2:98%) 0.20; δ_H (400 MHz; CD_3OD) 8.37 (1H, d, *J* 5.6 Hz, H2), 8.13 (1H, d, *J* 9.2 Hz, H5), 7.79 (1H, d, *J* 2.0 Hz, H8), 7.42 (1H, dd, *J* 9.2 and 2.0 Hz, H6), 6.69 (1H, d, *J* 6.0 Hz, H3), 3.36 (2H, t, *J* 6.4 Hz, H9), 2.98 (2H, t, *J* 6.4 Hz, H10).

N-(7-*Chloroquinolin*-4-*yl*)*propane*-1,3-*diamine*, 3.13b

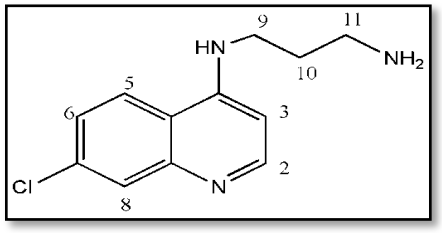

As a white-crystalline powder (1.59 g, 66%); m. p. 120-122 °C (*lit.*[2] 124- 127 °C); R_f (NH_3: MeOH,

2:98%) 0.21; δ_H (400 MHz; CD_3OD) 8.36 (1H, d, *J* 5.6 Hz, H2), 8.09 (1H, d, *J* 8.8 Hz, H5), 7.78 (1H, d, *J* 2.4 Hz, H8), 7.40 (1H, dd, *J* 8.8 and 2.4 Hz, H6), 6.54 (1H, d, *J* 5.6 Hz, H3), 3.44 (2H, t, *J* 7.2 Hz, H9), 2.84 (2H, t, *J* 7.2 Hz, H11), 1.95 (2H, m, H10).

N-(7-*Chloroquinolin*-4-*yl*)*butane*-1,4-*diamine*, 3.13c

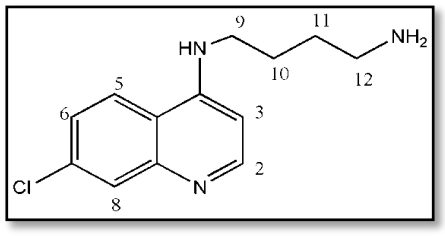

As a pale-yellow powder (1.78 g, 70%); m. p. 40-41 °C (*lit.*[2] 43- 47 °C); R_f (NH_3: MeOH, 2:98%) 0.22; δ_H (300 MHz; CD_3OD) 8.30 (1H, d, *J* 5.7, H2), 8.05 (1H, d, *J* 9.0, H5), 7.73 (1H, d, *J* 2.1, H8), 7.34 (1H, dd, *J* 9.0 and 2.1, H6), 6.44 (1H, d, *J* 5.7, H3), 3.30 (2H, t, *J* 7.2, H9), 2.76 (2H, t, *J* 7.2, H12), 1.75 (2H, m, H11), 1.62 (2H, m, H10).

General procedure[4] for the synthesis of chloroquine-like tetrazoles

Quinoline diamines **3.13a-c** (1.35 mmol) and an aromatic aldehydes (1.35 mmol) were stirred in anhydrous methanol at 26 °C for 5 minutes. Thereafter, $TMSN_3$ (1.35 mmol) was added, followed by the addition of *tert*-butyl isocyanide (1.35 mmol) and the resulting mixture was then stirred for 24 hrs. The solvent was removed in *vacuo* to afford crude tetrazole products **3.15a1-5 (**n=1**), 3.15b (**n=2**) and 3.15c (**n=3**)**.

N-{2-[(1-tert-*butyl*-1H-*tetrazol*-5-*yl*)(*phenyl*)*methylamino*]ethyl}-7-*chloroquinolin*-4-*amine*, 3.15a1 (TK900A)

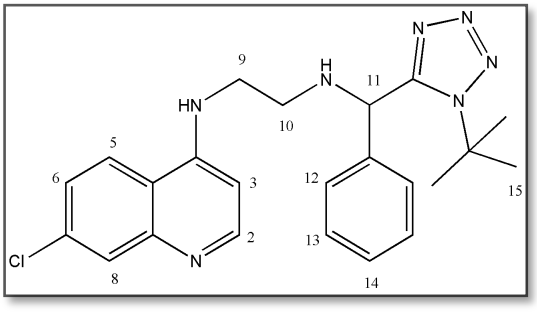

Purified by column chromatography (on silica gel; elution with DCM: MeOH; 95:05) to yield the desired product **3.15a1** (382 mg, 65%) as a pale-yellow crystalline solid; m. p. 72- 74 °C, R_f

(DCM: MeOH, 95: 05%) 0.38; IR ν_{max} (DCM)/cm^{-1} 1602 (Ar C=C), 1370 (N=N), 1330 (C=N), 1277 (C-N); δ_H (400 MHz; $CDCl_3$) 8.47 (1H, d, *J* 5.6 Hz, H2), 8.11 (1H, d, *J* 9.0 Hz, H5), 7.98 (1H, d, *J* 2.1 Hz, H8), 7.43 (1H, dd, *J* 9.0 and 2.1 Hz, H6), 7.33 (3H, m, 2 x H13 and H14), 7.23 (2H, 2 x d, *J* 7.9 Hz, 2 x H12), 6.80 (1H, br s, NH), 6.30 (1H, d, *J* 5.6 Hz, H3), 5.40 (1H, s, H11), 3.35 (2H, m, H9), 3.15 (1H, m, H*10a*), 2.99 (1H, m, H*10b*), 1.58 (9H, s, 3 x H15); δ_C (101 MHz; $CDCl_3$) 155.7, 151.0, 150.4, 147.4, 138.4, 135.7, 129.3 (2C), 128.8, 128.0 (2C), 127.1, 125.8, 122.4, 117.1, 98.6, 61.8, 59.1, 45.7, 42.7 and 29.9 (3C); MS (ESI) *m/z* 436.1 (M^+); HPLC purity: 98.5%; t_r,=6.59 min.

N-{2-[(1-tert-*butyl*-1H-*tetrazol*-5-*yl*)(4-*methoxyphenyl*)*methylamino*]ethyl}-7-*chloroquinolin*-4-*amine*, 3.15a2 (TK900B)

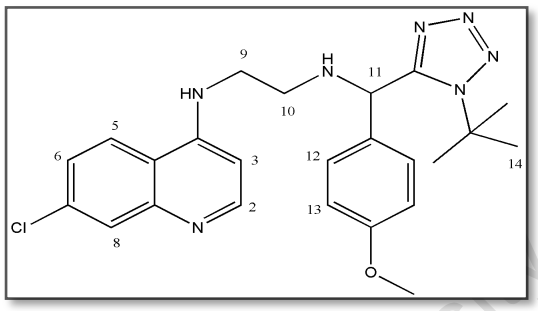

Purified by column chromatography (on silica gel; elution with DCM: MeOH; 95:05) to yield the desired product **3.15a2** (358 mg, 57%) as a pale-yellow crystalline solid; m. p. 75- 77 °C, R_f (DCM: MeOH, 95: 05%) 0.48; IR ν_{max} (DCM)/cm^{-1} 1610 (Ar C=C), 1371 (N=N), 1329 (C=N), 1241 (C-O Ester); δ_H (400 MHz; $CDCl_3$) 8.49 (1H, d, *J* 5.4 Hz, H2), 8.04 (1H, d, *J* 9.0 Hz, H5), 7.96 (1H, d, *J* 2.2 Hz, H8), 7.44 (1H, dd, *J* 9.0 and 2.2 Hz, H6), 7.13 (2H, d, *J* 8.8 Hz, 2 x H13), 6.85 (2H, d, *J* 8.8 Hz, 2 x H12), 6.40 (1H, br s, NH), 6.33 (1H, d, *J* 5.4 Hz, H3), 5.33 (1H, s, H11), 3.78 (3H, s, OCH_3), 3.36 (2H, m, H9), 3.12 (1H, m, H*10a*), 2.98 (1H, m, H*10b*), 1.59 (9H, s, 3 x H14); δ_C (101 MHz; $CDCl_3$) 159.8, 155.9, 151.7, 150.2, 147.5, 137.8, 130.5, 129.2 (2C), 128.3, 125.5, 122.0, 117.4, 114.6 (2C), 98.9, 61.7, 58.5, 55.3, 45.7, 42.5 and 29.9 (3C); MS (ESI) *m/z* 465.9 (M^+); HPLC purity: 99.0%; t_r,=6.52 min.

N-{2-[(1-tert-*butyl*-1H-*tetrazol*-5-*yl*)(p-*tolyl*)*methylamino*]ethyl}-7-*chloroquinolin*-4-*amine*, 3.15a3 (TK900C)

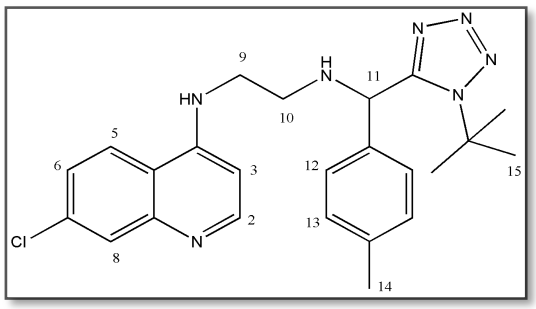

Purified by column chromatography (on silica gel; elution with DCM: MeOH; 95:05) to yield the desired product **3.15a3** (371 mg, 61%) as a pale-yellow crystalline solid; m. p. 80- 82 °C, R_f (DCM: MeOH, 95: 05%) 0.33; IR ν_{max} (DCM)/cm^{-1} 1612 (Ar C=C), 1366 (N=N), 1325 (C=N), 1265 (C-N); δ_H (400 MHz; $CDCl_3$) 8.45 (1H, d, *J* 5.5 Hz, H2), 8.09 (1H, d, *J* 9.0 Hz, H5), 7.97 (1H, d, *J* 2.1 Hz, H8), 7.44 (1H, dd, *J* 9.0 and 2.1 Hz, H6), 7.14 (2H, d, *J* 8.3 Hz, 2 x H13), 7.09 (2H, d, *J* 8.3 Hz, 2 x H12), 6.66 (1H, br s, NH), 6.31 (1H, d, *J* 5.5 Hz, H3), 5.36 (1H, s, H11), 3.36 (2H, m, H9), 3.14 (1H, m, H*10a*), 2.98 (1H, m, H*10b*), 2.32 (3H, s, H14), 1.58 (9H, s, 3 x H15); δ_C (101 MHz; $CDCl_3$) 155.7, 151.6, 150.3, 147.8, 138.9, 135.5, 135.1, 129.2 (2C), 128.3, 127.8 (2C), 125.5, 122.0, 117.4, 98.9, 61.8, 58.8, 45.7, 42.5, 29.9 (3C) and 21.1; MS (ESI) *m/z* 450.3 (M^+), HPLC purity: 99.5%; t_r=6.92 min.

N-{2-[(1-tert-*butyl*-1H-*tetrazol*-5-*yl*)(3,4-*dichlorophenyl*)*methylamino*]ethyl}-7-*chloroquinolin*-4-*amine*, 3.15a4 (TK900D)

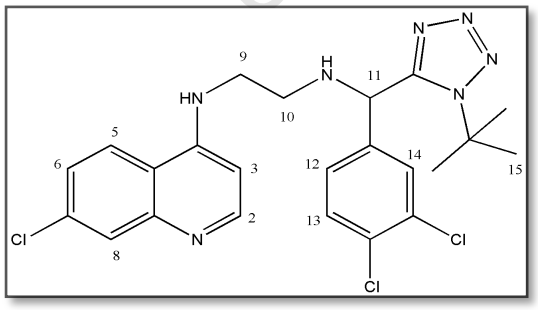

Purified by column chromatography (on silica gel; elution with DCM: MeOH; 95:05) to yield the desired product **3.15a4** (73 mg, 11%) as a pale-yellow crystalline solid; m. p. 68- 71 °C, R_f (DCM: MeOH, 95: 05%) 27; IR ν_{max} (DCM)/cm^{-1} 1583(Ar C=C), 1373 (N=N), 1333 (C=N), 1245 (C-N); δ_H (400 MHz; $CDCl_3$) 8.55 (1H, d, *J* 5.3 Hz, H2), 7.97 (1H, d, *J* 2.1 Hz, H8), 7.94 (1H, d, *J* 9.0 Hz, H5), 7.46 (1H, dd, *J* 9.0 and 2.1 Hz, H6), 7.45 (1H, d, *J* 8.2 Hz, H13), 7.42 (1H, d, *J* 2.5 Hz, H14), 7.07 (1H,

dd, *J* 8.2 and 2.5 Hz, H12), 6.35 (1H, d, *J* 5.4 Hz, H3), 6.09 (1H, br s, NH), 5.33 (1H, s, H11), 3.38 (2H, m, H9), 3.09 (1H, m, H*10a*), 2.95 (1H, m, H*10b*), 1.63 (9H, s, 3 x H15); δ_C (101 MHz; $CDCl_3$) 154.8, 151.7, 150.0, 148.9, 138.5, 135.1, 133.6, 133.3, 131.2, 130.1, 128.6, 127.1, 125.7, 121.6, 117.4, 99.0, 61.8, 58.0, 46.0, 42.4 and 29.9 (3C); MS (ESI) *m/z* 504.3 (M^+); HPLC purity: 99.2%; $t_{r'}$=7.79 min.

N-{2-[(1-tert-*butyl*-1H-*tetrazol*-5-*yl*)(4-*chlorophenyl*)*methylamino*]ethyl}-7-*chloroquinolin*-4-*amine*, 3.15a5 (TK900E)

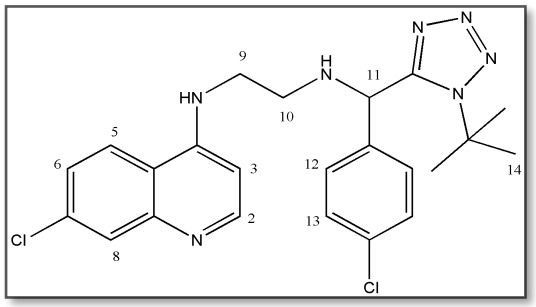

Purified by column chromatography (on silica gel; elution with DCM: MeOH; 95:05) to yield the desired product **3.15a5** (180 mg, 28%) as a pale-yellow crystalline solid; m. p. 79- 81 °C, R_f (DCM: MeOH, 95: 05%) 0.37; IR ν_{max} (DCM)/cm^{-1} 1579 (Ar C=C), 1375 (N=N), 1319 (C=N), 1269 (C-N); δ_H (400 MHz; $CDCl_3$) 8.51 (1H, d, *J* 5.3 Hz, H2), 7.98 (1H, d, *J* 9.0 Hz, H5), 7.96 (1H, d, *J* 2.1 Hz, H8), 7.44 (1H, dd, *J* 9.0 and 2.1 Hz, H6), 7.33 (2H, d, *J* 8.5 Hz, 2 x H13), 7.19 (2H, d, *J* 8.5 Hz, 2 x H12), 6.35 (1H, d, *J* 5.3 Hz, H3), 6.21 (1H, br s, NH), 5.37 (1H, s, H11), 3.39 (2H, m, H9), 3.13 (1H, m, H*10a*), 2.99 (1H, m, H*10b*), 1.62 (9H, s, 3 x H14); δ_C (101 MHz; $CDCl_3$) 155.3, 151.8, 150.0, 149.0, 136.9, 135.1, 134.9, 129.5 (2C), 129.3 (2C), 128.6, 125.6, 121.7, 117.4, 99.0, 61.8, 58.4, 45.9, 42.4 and 30.0 (3C); MS (ESI) *m/z* 470.4 (M^+), HPLC purity: 99.5%; $t_{r'}$=7.02 min.

N-{3-[(1-tert-*butyl*-1H-*tetrazol*-5-*yl*)(*phenyl*)*methylamino*]*propyl*}-7-*chloroquinolin*-4-*amine*, 3.15b (TK910)

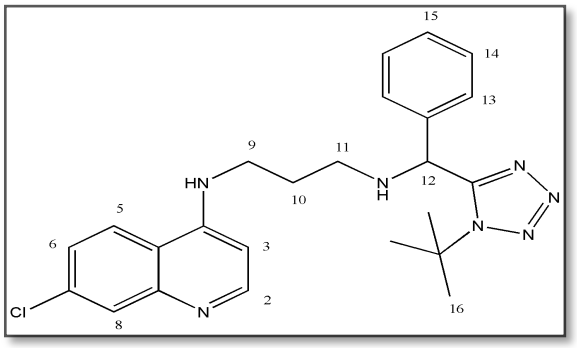

Purified by column chromatography (on silica gel; elution with DCM: MeOH; 95:05) to yield the desired product **3.15b** (291 mg, 51%) as a pale-yellow crystalline solid; m. p. 68- 70 °C, R_f (DCM: MeOH, 95: 05%) 0.38; IR ν_{max} (DCM)/cm^{-1} 1607 (Ar C=C), 1372 (N=N), 1329 (C=N), 1278 (C-N); δ_H (400 MHz; $CDCl_3$) 8.48 (1H, d, *J* 5.6 Hz, H2), 7.93 (1H, d, *J* 2.1 Hz, H8), 7.40 (3H, m, H5 and 2 x H13), 7.31 (3H, m, 2 x H14 and H15), 7.03 (1H, dd, *J* 9.0 and 2.1 Hz, H6), 6.30 (1H, d, *J* 5.6 Hz, H3), 5.31 (1H, s, H12), 3.44 (2H, t, *J* 5.9 Hz, H9), 2.95 (1H, m, H*11a*), 2.99 (1H, m, H*11b*), 1.96 (2H, m, H10), 1.59 (9H, s, 3 x H16); δ_C (101 MHz; $CDCl_3$) 155.2, 150.9, 150.7, 147.7, 138.2, 135.3, 129.4 (2C), 128.9, 128.1 (2C), 127.3, 125.9, 122.1, 117.1, 98.1, 61.6, 59.5, 47.9, 43.8, 30.0 (3C) and 27.3; MS (ESI) *m/z* 450.7 (M^++H); HPLC purity: 96.5%; $t_{r'}$=6.15 min.

N-{4-[(1-tert-*butyl*-1H-*tetrazol*-5-*yl*)(*phenyl*)*methylamino*]*butyl*}-7-*chloroquinolin*-4-*amine*, 3.15c (TK920)

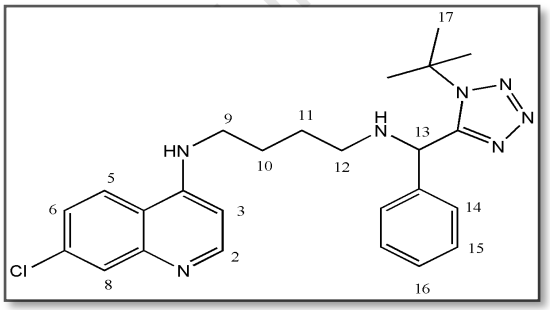

Purified by column chromatography (on silica gel; elution with DCM: MeOH; 95:05) to yield the desired product **3.15c** (282 mg, 51%) as a pale-yellow crystalline solid; m. p. 64- 66 °C, R_f (DCM: MeOH, 95: 05%) 0.39; IR ν_{max} (KBr)/cm^{-1} 1609 (Ar C=C), 1372 (N=N), 1326 (C=N), 1276 (C-N); δ_H (400 MHz; $CDCl_3$) 8.34 (1H, d, *J* 5.8 Hz, H2), 7.90 (1H, d, *J* 2.1 Hz, H8), 7.74 (1H, d, *J* 9.0 Hz, H5), 7.31 (3H, m, 2 x H15 and H6), 7.24 (3H, m, 2 x H14 and H16), 6.51 (1H, br s, NH), 6.29 (1H, d, *J* 5.8

Hz, H3), 5.26 (1H, s, H13), 3.33 (2H, t, *J* 6.8 Hz, H9), 2.62 (2H, m, H12), 1.83 (2H, m, H10), 1.68 (2H, m, H11), 1.61 (9H, s, 3 x H17); δ_C (101 MHz; $CDCl_3$) 155.6, 151.2, 149.1, 146.2, 138.6, 135.9, 129.1 (2C), 128.5, 128.0 (2C), 126.2, 125.6, 122.2, 116.7, 98.4, 61.4, 59.2, 47.3, 43.0, 30.0 (3C), 27.3 and 26.0; MS (ESI) *m/z* 464.3 (M^+); HPLC purity: 95.9%; t_r=5.84 min.

General procedure for the synthesis of de-*tert*-butylated chloroquine-like tetrazoles 3.16a1-5, 3.16b and 3.16c.

The procedure used in the synthesis of the de-*tert*-butylated deoxyamodiaquine tetrazole **3.10a-f** was followed**,** chloroquine-based tetrazoles **3.15a1-5**, **3.15b** and **3.15c** (0.46 mmol) were refluxed in 32% HCl (10 ml) for a period of 4 to 8 hours to give the desired de-*tert*-butylated products, **3.16a1-5**, **3.16b** and **3.16c**, after purification by column chromatography (on silica gel; elution with DCM: MeOH: NH_4OH; 95:0.5:01).

7-*chloro*-N-{2-[*phenyl*(1H-*tetrazol*-5-*yl*)*methylamino*]*ethyl*}*quinolin*-4-*amine,* 3.16a1 (TK900AB3)

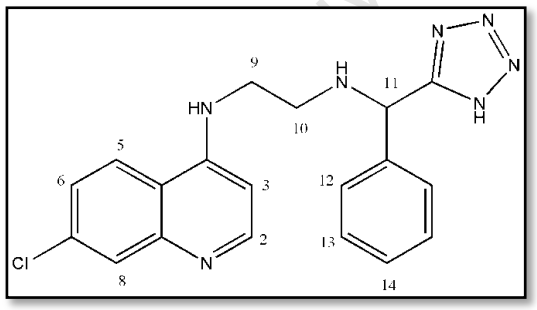

As a -yellow powder (15 mg, 8%), m. p. 144-148 °C, R_f (DCM: MeOH: NH_4OH; 95:0.9:01%) 0.12; IR ν_{max} (KBr)/cm^{-1} 1600 (Ar C=C), 1372 (N=N), 1330 (C=N); δ_H (400 MHz; $CDCl_3$) 8.49 (1H, d, *J* 9.0 Hz, H5), 8.34 (1H, d, *J* 5.4 Hz, H2), 7.76 (1H, d, *J* 2.1 Hz, H8), 7.68 (1H, br m, NH), 7.40 (3H, m, H6, 2 x H13), 7.20 (2H, 2 x d, *J* 7.2 Hz, 2 x H12), 7.14 (1H, t, *J* 7.2 Hz, H14), 6.40 (1H, d, *J* 5.4 Hz, H3), 5.09 (1H, s, H11), 3.29 (2H, m, H9), 2.79 (1H, m, H*10a*), 2.75 (1H, m, H*10b*); δ_C (101 MHz; $CDCl_3$) 151.7 (2C), 150.2, 148.9, 143.8, 133.1, 127.7 (2C), 127.5 (2C), 127.2, 126.1, 124.4,

123.8, 117.4, 98.4, 59.0, 45.7, and 42.9, MS (ESI) *m/z* 379.9 (M^+); HPLC purity: 99.0%; t_r=5.13 min.

N-{2-[(4-*methoxyphenyl*)(1H-*tetrazol*-5-*yl*)*methylamino*]ethyl}-7-*chloroquinolin*-4-*amine*, 3.16a2 (TK900BB3)

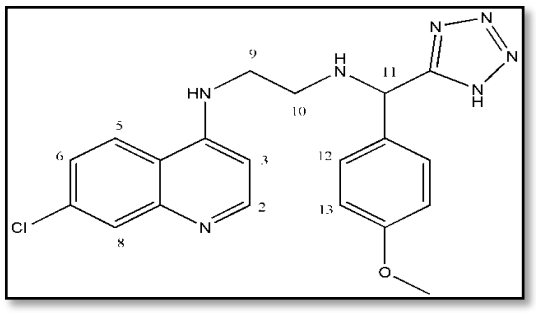

As a pale-yellow solid (68 mg, 38%), m. p. 171- 173 °C, R_f (DCM: MeOH: NH_4OH; 95:0.9:01%) 0.18; IR ν_{max} (KBr)/cm^{-1} 1615 (Ar C=C), 1370 (N=N), 1328 (C=N), 1240 (C-O Ester); δ_H (400 MHz; $CDCl_3$) 8.38 (1H, d, *J* 5.5 Hz, H2), 8.30 (1H, d, *J* 9.0 Hz, H5), 7.78 (1H, d, *J* 2.2 Hz, H8), 7.45 (1H, dd, *J* 9.0 and 2.2 Hz, H6), 7.41 (2H, d, *J* 8.7 Hz, 2 x H13), 6.87 (2H, d, *J* 8.7 Hz, 2 x H12), 6.46 (1H, d, *J* 5.5 Hz, H3), 5.40 (1H, s, H11), 3.72 (3H, s, OCH_3), 3.43 (2H, t, *J* 6.6 Hz, H9), 2.87 (2H, t, *J* 6.6 Hz, H10); δ_C (101 MHz; $CDCl_3$) 159.1, 158.7, 151.0, 150.2, 148.0, 133.7, 132.8, 129.6 (2C), 126.6, 124.3, 124.0, 117.2, 113.7 (2C), 98.6, 57.1, 55.0, 43.9 and 40.2; MS (ESI) *m/z* 410.1 (M^+); HPLC purity: 97.4%; t_r=5.70 min.

N-{2-[(1H-*tetrazol*-5-*yl*)(*p-tolyl*)*methylamino*]*ethyl*}-7-*chloroquinolin*-4-*amine*, 3.16a3 (TK900CB3)

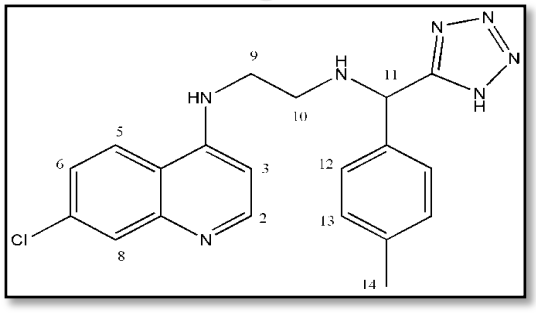

As a pale-yellow crystalline powder (54 mg, 31%), m. p. 150- 153 °C, R_f (DCM: MeOH: NH_4OH; 95:0.9:01%) 0.28; IR ν_{max} (KBr)/cm^{-1} 1610 (Ar C=C), 1376 (N=N), 1327 (C=N); δ_H (400 MHz; $CDCl_3$) 8.40 (1H, d, *J* 5.6 Hz, H2), 8.26 (1H, d, *J* 9.0 Hz, H5), 7.80 (1H, d, *J* 2.2 Hz, H8), 7.47 (1H, dd, *J* 9.0 and 2.2 Hz, H6), 7.37 (2H, d, *J* 8.3 Hz, 2 x H13), 7.14 (2H, d, *J* 8.3 Hz, 2 x H12), 6.49 (1H, d, *J* 5.6 Hz, H3), 5.46 (1H, s, H11), 3.49 (2H, t, *J* 6.4 Hz, H9), 2.90 (2H, t, *J* 6.4 Hz, H10), 2.27 (3H, s, H14);

δ_C (101 MHz; $CDCl_3$) 156.2, 155.4, 142.7, 139.1, 138.4, 137.8, 129.7, 129.4 (2C), 128.9 (2C), 126.7, 126.3, 118.8, 115.6, 98.6, 55.3, 43.5, 40.5 and 20.6; MS (ESI) *m/z* 494.4 (M^+); HPLC purity: 98.0%; t_r=6.19 min.

N-{2-[(3,4-*dichlorophenyl*)(1H-*tetrazol*-5-*yl*)*methylamino*]*ethyl*}-7-*chloroquinolin*-4-*amine*, 3.16a4 (TK900DB3)

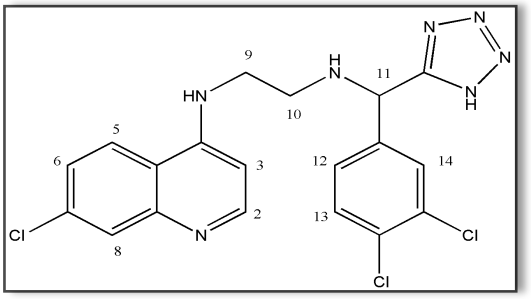

As a yellow powder (77 mg, 58%), m. p. 124-1127 °C, R_f (DCM: MeOH: NH_4OH; 95:0.9:01%) 0.21; IR ν_{max} (KBr)/cm^{-1} 1598 (Ar C=C), 1368 (N=N), 1328 (C=N); δ_H (400 MHz; $CDCl_3$) 8.49 (1H, d, *J* 9.1 Hz, H5), 8.44 (1H, d, *J* 6.4 Hz, H2), 7.90 (1H, d, *J* 1.8 Hz, H8), 7.76 (1H, d, *J* 1.9 Hz, H14), 7.61 (2H, m,H6 and H13), 7.44 (1H, dd, *J* 8.3 and 1.9 Hz, H12), 6.68 (1H, d, *J* 6.4 Hz, H3), 5.48 (1H, s, H11), 3.55 (2H, t, *J* 6.3 Hz, H9), 2.89 (2H, t, *J* 6.3 Hz, H10); δ_C (101 MHz; $CDCl_3$) 158.5, 152.8, 146.7, 143.2, 140.6, 135.6, 130.3, 130.2, 128.1, 124.9 (2C), 122.7, 122.6, 125.7, 116.3, 98.6, 56.1, 44.5 and 42.3; MS (ESI) *m/z* 449.9 (M^++H); HPLC purity: 99.0%; t_r=5.93 min.

N-{2-[(4-*chlorophenyl*)(1H-*tetrazol*-5-*yl*)*methylamino*]*ethyl*}-7-*chloroquinolin*-4-*amine*, 3.16a5 (TK900EB3)

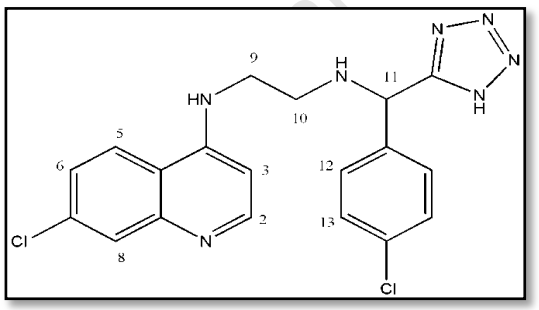

As a pale-yellow powder (47 mg, 27%), m. p. 152- 155 °C, R_f (DCM: MeOH: NH_4OH; 95:0.9:01%) 0.13; IR ν_{max} (KBr)/cm^{-1} 1620 (Ar C=C), 1378 (N=N), 1325 (C=N); δ_H (400 MHz; $CDCl_3$) 8.28 (1H, d, *J* 9.1 Hz, H5), 8.25 (1H, d, *J* 6.7 Hz, H2), 7.79 (1H, d, *J* 1.9 Hz, H8), 7.58 (1H, dd, *J* 9.1 and 1.9 Hz, H6), 7.37 (2H, d, *J* 8.4 Hz, 2 x H13), 7.19 (2H, d, *J* 8.4 Hz, 2 x H12), 6.61 (1H, d, *J* 6.7 Hz, H3), 5.23 (1H, s, H11), 3.52 (2H, t, *J* 6.1 Hz, H9), 2.80 (2H, t, *J* 6.1 Hz, H10), δ_C (101 MHz; $CDCl_3$) 159.1,

151.0, 149.9, 146.7, 138.0, 134.3, 132.5, 129.9 (2C), 128.3 (2C), 125.6, 124.6, 124.3, 117.0, 98.6, 56.9, 44.3 and 41.3; MS (ESI) *m/z* 414.1 (M^+); HPLC purity: 99.2%; $t_{r'}$=5.86 min.

7-*chloro*-N-{3-[*phenyl*(1H-*tetrazol*-5-*yl*)*methylamino*]*propyl*}*quinolin*-4-*amine*, 3.16b (TK910B3)

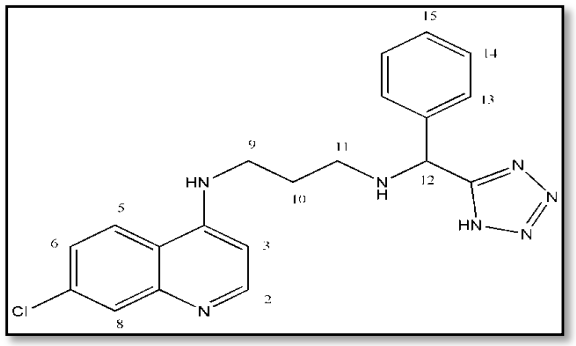

As a pale-yellow powder (91 mg, 52%), m. p. 99- 102 °C, R_f (DCM: MeOH: NH_4OH; 95:0.9:01%) 0.22; IR ν_{max} (KBr)/cm^{-1} 1608 (Ar C=C), 1374 (N=N), 1327 (C=N); δ_H (300 MHz; $CDCl_3$) 8.40 (1H, d, *J* 5.5 Hz, H2), 8.40 (1H, d, J 9.1 Hz, H5), 7.79 (1H, d, *J* 2.0 Hz, H8), 7.55 (3H, m, 2 x H13), 7.44 (1H, dd, *J* 9.1 and 2.0 Hz, H6), 7.35 (3H, m, 2 x H14 and H15), 6.49 (1H, d, *J* 5.5 Hz, H3), 5.57 (1H, s, H12), 3.33 (2H, t, *J* 6.3 Hz, H9), 2.83 (2H, t, *J* 6.2 Hz, H11), 1.96 (2H, m, H10), δ_C (75 MHz; $CDCl_3$) 158.5, 150.7, 150.2, 147.8, 137.7, 133.5, 128.1 (2C), 128.0 (2C), 127.8, 126.4, 124.0, 123.9, 117.0, 98.4, 57.9, 45.6, 44.3 and 25.6; MS (ESI) *m/z* 394.0 (M^+); HPLC purity: 98.3%; $t_{r'}$=8.63 min.

7-*chloro*-N-{4-[*phenyl*(1H-*tetrazol*-5-*yl*)*methylamino*]*butyl*}*quinolin*-4-*amine*, 3.16c (TK920B3)

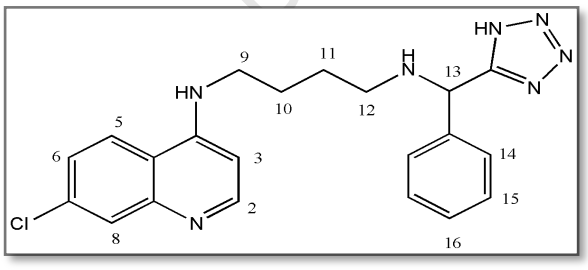

As a pale-yellow powder (98 mg, 72%), m. p. 113- 116 °C, R_f (DCM: MeOH: NH_4OH; 95:0.9:01%) 0.25; IR ν_{max} (KBr)/cm^{-1} 1605 (Ar C=C), 1370 (N=N), 1324 (C=N); δ_H (400 MHz; $CDCl_3$) 8.39 (1H, d, *J* 5.6 Hz, H2), 8.27 (1H, d, *J* 9.0 Hz, H5), 7.79 (1H, d, *J* 2.2 Hz, H8), 7.55 (2H, m, 2 x H15), 7.47 (1H, dd, *J* 9.0 and 2.2 Hz, H6), 7.35 (3H, m, 2 x H14 and H16), 6.49 (1H, d, *J* 5.6 Hz, H3), 5.60 (1H, s, H13), 3.27 (2H, t, *J* 7.0 Hz, H9), 2.76 (2H, m, H12), 1.73 (2H, m, H10), 1.65 (2H, m, H11); δ_C (101 MHz; $CDCl_3$) 158.0, 150.8, 150.3,

147.8, 136.3, 133.7, 128.6 (2C), 128.3 (2C), 126.5, 124.1, 124.0, 117.1, 98.6, 57.9, 54.7, 45.6, 41.7, 24.9 and 23.5; MS (ESI) *m/z* 408.0 (M^+); HPLC purity: 97.6%; $t_{r'}$=5.89 min.

Synthesis of Primaquine-based tetrazoles[4]

Similar to the procedure used in the synthesis of chloroquine-like compounds, primaquine-based tetrazoles were obtained from the multi-component reaction of a racemic Primaquine diphosphate (**3.17**) (1.1 mmol) in triethylamine (4.0 eq), aromatic aldehydes (1.1 mmol) $TMSN_3$ (1.1 mmol) and *tert*-butyl isocyanide (1.1 mmol) as unresolved racemic (1:1) mixture of diastereomers (**3.19a-e**) in poor to moderate yields.

N-{5-[(1-tert-*butyl*-1H-*tetrazol*-5-*yl*)(*phenyl*)*methylamino*]*pentan*-2-*yl*}-6-*methoxyquinolin-8-amine*, 3.17a (TK1000A)

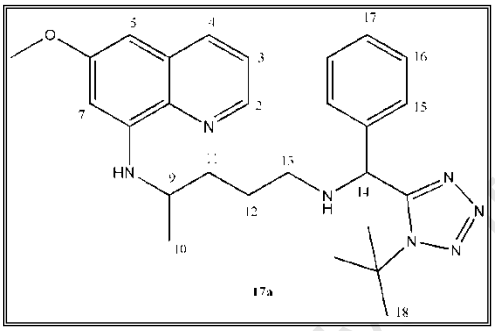

Product **3.19a** (108.4 mg, 21%) is obtained as a thick yellow oil; R_f (DCM: Acetone, 95: 05%) 0.50; IR ν_{max} (DCM)/cm^{-1} 1615 (Ar C=C), 1385 (N=N), 1315 (C=N), 1266 (C-N), 1254 (C-O Ester); δ_H (300 MHz; $CDCl_3$) 8.47 (1H, m, H2), 7.88 (1H, dd, *J* 8.3 and 1.6 Hz, H4), 7.25 (6H, m, ArH and H3), 6.29 (1H, d, *J* 2.3 Hz, H7), 6.23 (1H, d, *J* 2.5 Hz, H5), 5.99 (1H, t, *J* 8.6 Hz, NH), 5.22 (1H, d, *J* 6.7 Hz, H14), 3.85 (3H, s, OCH_3), 3.56 (1H, m, H9), 2.53 (2H, m, H13), 1.63 (4H, m, H11 and H12), 1.55 (9H, d, *J* 4.04 Hz, 3 x H18), 1.25 (3H, d, *J* 6.4 Hz, H10); δ_C (75 MHz; $CDCl_3$) 159.5, 155.7, 145.0, 144.2, 138.9, 135.4, 134.7, 129.9, 128.9 (2C), 128.2, 128.0 (2C), 121.8, 96.6, 91.6, 61.2, 59.0, 55.2, 55.1, 47.9, 34.2, 30.0 (3C), 26.5 and 20.5; MS (ESI) *m/z* 474.1 (M^+); HPLC purity: 99.3%; $t_{r'}$=16.63 min.

N-{5-[(1-tert-*butyl*-1H-*tetrazol*-5-*yl*)(*methoxyphenyl*)*methylamino*]*pentan*-2-*yl*}-6-*methoxyquinolin*-8-*amine*, 3.19b (TK1000B)

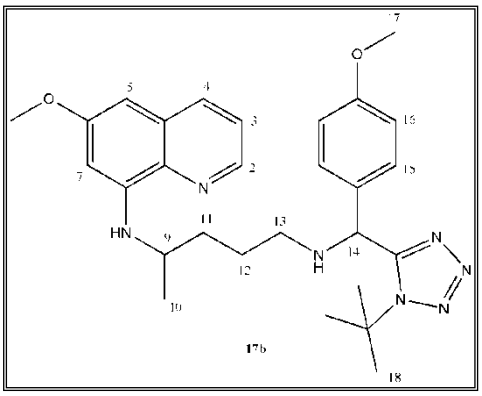

Product **3.19b** (219.6 mg, 40%) is obtained as a yellow oil; R_f (DCM: Acetone, 95: 05%) 0.54; IR ν_{max} (DCM)/cm^{-1} 1615 (Ar C=C), 1387 (N=N), 1269 (C=N), 1266 (C-N), 1217 (C-O Ester); δ_H (400 MHz; $CDCl_3$) 8.50 (1H, m, H2), 7.91 (1H, dd, *J* 8.3 and 1.8 Hz, H4), 7.29 (1H, dd, *J* 8.2 and 4.2 Hz, H3), 7.18 (2H, m, 2 x H16), 6.83 (2H, m, 2 x H15), 6.32 (1H, d, *J* 1.7 Hz, H7), 6.26 (1H, d, *J* 1.7 Hz, H5), 6.03 (1H, m, NH), 5.20 (1H, d, *J* 9.0 Hz, H14), 3.85 (3H, d, *J* 1.4 Hz, OCH_3), 3.77 (3H, d, *J* 1.0 Hz, H17), 3.61 (1H, m, H9), 2.54 (2H, m, H13), 1.67 (4H, m, H11 and H12), 1.57 (9H, d, *J* 5.3 Hz, 3 x H18), 1.28 (3H, d, *J* 6.4 Hz, H10); δ_C (101 MHz; $CDCl_3$) 159.4, 155.9, 145.1, 144.2 (2C), 135.4, 134.7 (2C), 131.0, 129.9, 129.2 (2C), 121.8, 114.3 (2C), 96.6, 91.6, 61.1, 58.3, 55.2, 47.9 (2C), 34.2, 30.0 (3C), 26.5 and 20.5; MS (ESI) *m/z* 504.6 (M^++H); HPLC purity: 99.5%; t_r,=16.62 min.

N-{5-[(1-tert-*butyl*-1H-*tetrazol*-5-*yl*)(p-*tolyl*)*methylamino*]*pentan*-2-*yl*}-6-*methoxyquinolin*-8-*amine*, 3.19c (TK1000C)

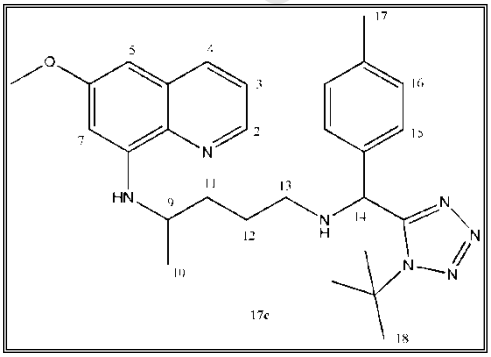

Product **3.19c** (265.9 mg, 50%) is obtained as a thick yellow oil; R_f (DCM: Acetone, 95: 05%) 0.51; IR ν_{max} (DCM)/cm^{-1} 1617 (Ar C=C), 1390 (N=N), 1325 (C=N), 1260 (C-N), 1232 (C-O Ester); δ_H (400 MHz; $CDCl_3$) 8.53 (1H, m, H2), 7.93 (1H, dd, *J* 8.3 and 1.7 Hz, H4), 7.31 (1H, dd, *J* 8.3 and 4.2 Hz, H3), 7.12-7.18 (4H, m, 2 x H16 and 2 x H15), 6.34 (1H, d, *J* 2.4 Hz, H7), 6.28 (1H, d, *J* 2.5 Hz, H5), 6.04 (1H, m, NH), 5.29 (1H, d, *J* 8.2 Hz, H14), 3.91 (3H, d, *J* 1.3 Hz, OCH_3), 3.62 (1H, m, H9), 2.57 (2H, m, H13), 2.33 (3H, s, H17),

1.69 (4H, m, H11 and H12), 1.60 (9H, d, *J* 5.4 Hz, 3 x H18), 1.25 (3H, d, *J* 6.4 Hz, H10); δ_C (101 MHz; $CDCl_3$) 159.5, 155.9, 145.1, 144.2 (2C), 138.0, 135.9, 135.2, 134.7, 129.9, 129.6 (2C), 127.9 (2C), 121.8, 96.6, 91.6, 61.2, 58.7, 55.2, 47.9, 34.2, 30.1 (3C), 26.5, 21.0 and 20.5; MS (ESI) *m/z* 488.2 (M^+); HPLC purity: 99.4%; t_r=17.14 min.

N-{5-[(1-tert-*butyl*-1H-*tetrazol*-5-*yl*)(3,4-*dichlorophenyl*)*methylamino*]*pentan*-2-*yl*}-6-*methoxyquinolin*-8-*amine*, 3.19d (TK1000D)

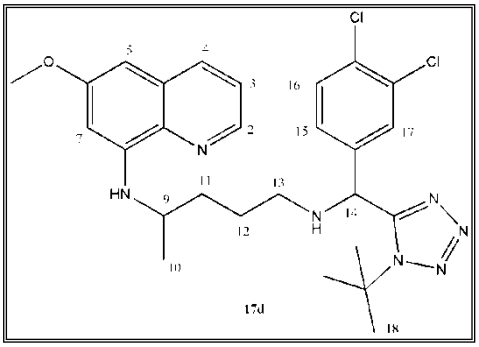

Product **3.19d** (100.5 mg, 17%) is obtained as a thick yellow oil; R_f (DCM: Acetone, 95: 0.5%) 0.29; IR ν_{max} (DCM)/cm^{-1} 1609 (Ar C=C), 1383 (N=N), 1330 (C=N), 1264 (C-N), 1245 (C-O Ester); δ_H (400 MHz; $CDCl_3$) 8.53 (1H, m, H2), 7.94 (1H, dd, *J* 8.3 and 1.6 Hz, H4), 7.42 (1H, d, *J* 2.1 Hz, H15), 7.42 (1H, d, *J* 2.1 Hz, H16), 7.38 (1H, s, H17), 7.32 (1H, dd, *J* 8.2 and 4.2 Hz, H3), 6.35 (1H, d, *J* 1.9 Hz, H7), 6.28 (1H, d, *J* 2.2 Hz, H5), 6.03 (1H, m, NH), 5.22 (1H, d, *J* 9.6 Hz, H14), 3.91 (3H, d, *J* 1.4 Hz, OCH_3), 3.62 (1H, m, H9), 2.56 (2H, m, H13), 1.69 (4H, m, H11 and H12), 1.63 (9H, d, *J* 12.1 Hz, 3 x H18), 1.25 (3H, d, *J* 6.4 Hz, H10); δ_C (101 MHz; $CDCl_3$) 159.5, 155.0, 145.0, 144.3, 139.1, 135.4, 134.7, 132.6, 130.8, 130.1, 130.0, 129.9, 127.3, 121.8, 96.6, 91.6, 61.3, 57.8, 55.2, 47.9, 34.0, 33.7, 30.0 (3C), 26.5 and 20.8; LCMS *m/z* 542.0 (M^+) and 556.3 (MH^++Na); HPLC purity: 99.5%; t_r=17.52 min.

N-{5-[(1-tert-*butyl*-1H-*tetrazol*-5-*yl*)(4-*chlorophenyl*)*methylamino*]*pentan*-2-*yl*}-6-*methoxyquinolin*-8-*amine*, 3.19e (TK1000E)

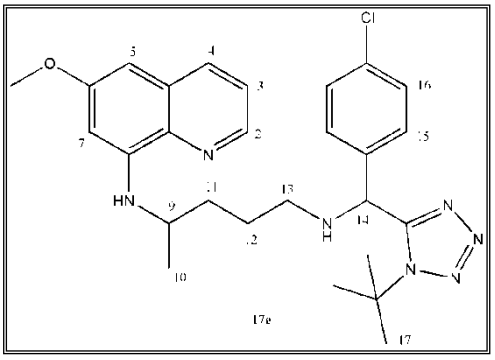

Product **3.19e** (228.5 mg, 41%) is obtained as a thick yellow oil; R_f (DCM: Acetone, 95: 0.5%) 0.52; IR ν_{max} (DCM)/cm^{-1} 1630 (Ar C=C), 1380 (N=N), 1335 (C=N), 1278 (C-N), 1246 (C-O Ester);δ_H (400 MHz; $CDCl_3$) 8.52 (1H, dd, *J* 4.2 and 1.6 Hz, H2), 7.93 (1H, dd, *J* 8.4 and 1.6 Hz, H4), 7.26- 7.42 (5H, m, ArH and H3), 7.35 (1H, d, *J* 2.4 Hz, H7), 6.28 (1H, d, *J* 2.4 Hz, H5), 6.03 (1H, m, NH), 5.24 (1H, d, *J* 12.0 Hz, H14), 3.90 (3H, d, *J* 2.2 Hz, OCH_3), 3.63 (1H, m, H9), 2.55 (2H, m, H13), 1.68 (4H, m, H11 and H12), 1.60 (9H, d, *J* 6.1 Hz, 3 x H17), 1.30 (3H, d, *J* 6.4 Hz, H10); δ_C (101 MHz; $CDCl_3$) 159.5, 155.4, 145.0, 144.2 (2C), 137.4, 135.4, 134.7, 134.2, 129.9, 129.4 (2C), 129.1 (2C), 121.8, 96.6, 91.6, 61.3, 58.2, 55.2, 47.8, 34.1, 30.0 (3C), 26.5 and 20.6; MS (ESI) *m/z* 508.3 (M^+); HPLC purity: 99.7%; t_r=17.44 min.

Synthesis of the Quinine-nucleus,[5,6] *i.e.* 6-*Methoxyquinoline*-4-*carbaldehyde*, 4.8

5-[(4-*Methoxyphenylamino*)*methylene*]-2,2-*dimethyl*-1,3-*dioxane*-4,6-*dione*, 4.5

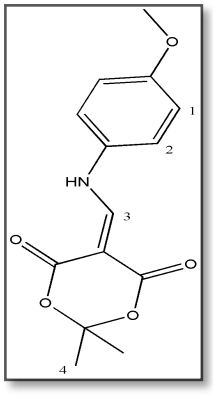

In a 25 ml ethanolic solution of *p*-anisidine (**4.3**) (2.97 g, 24.1 mmol) were added Meldrum's acid (**4.4**) (4.02 g, 27.9 mmol) followed by triethyl orthoformate (4.24 ml, 25.4 mmol) and the resultant mixture refluxed at 100 °C for 4 hrs. Theafter the mixture was cooled to room temperature and a white precipitate formed and was filtered, washed with ice cold ethanol to afford the title compound (**4.5**) (5.34 g, 80%) as a white powder and was used without further purification; δ_H (400 MHz; $CDCl_3$) 11.18 (1H, d, *J* 13.9 Hz, NH), 8.56 (1H, d *J* 13.9 Hz, H3), 7.25 (2H, m, H1), 7.01 (2H, m, H2), 3.88 (3H, s, OCH_3), 1.76 (6H, s, H4);

6-*Methoxyquinolin*-4-*ol*, 4.6

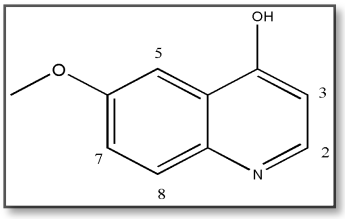

Product **4.5** (5.25 g, 18.9 mmol) was added in portions to Dowtherm A (35 ml) at 255 °C. The resultant mixture was heated for 20 minutes and allowed to cool to room temperature and diluted with diethyl ether (15 m). A precipitate which formed was filtered, washed with ice cold diethyl ether and dried in the vacuum line for 3 hrs to afford the desired product **4.6** (4.05 g, 90%) as an off-white powder which was used without further purification; δ_H (300 MHz; DMSO-*d6*) 11.62 (1H, br s, OH), 7.80 (1H, d, *J* 7.3 Hz, H2), 7.52 (1H, d, *J* 3.0 Hz, H5), 7.49 (1H, d, *J* 9.0 Hz, H8), 7.49 (1H, dd, *J* 9.0 and 3.0 Hz, H7), 5.98 (1H, d, *J* 7.3 Hz, H3), 3.83 (3H, s, OCH_3); *m*/*z* 175.01 [M^+ , 100%].

4-*Bromo*-6-*Methoxyquinoline*, 4.7

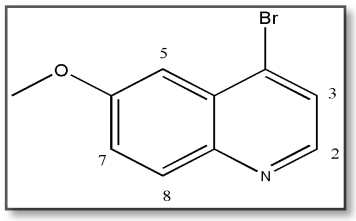

To a mixture of **4.6** (1.60 g, 9.2 mmol) in anhydrous DMF (5 ml) was added PBr_3 (1 ml, 10.6 mmol) drop-wise over a 5 minutes period. The resultant dark brown solution was stirred for a further 5 minutes under N_2 atmosphere before a brown precipitate formed. The precipitated mixture was further stirred for 2 hrs, quenched with water and pH adjusted to 10. The precipitate is then filtered, washed with ice cold water. The crude brown precipitate is purified by column chromatography (on silica gel; elution with EtOAc: Hex; 50:50) to give an off-white solid (1.65 g, 75%); δ_H (300 MHz; $CDCl_3$) 8.52 (1H, d, *J* 3.6 Hz, H2), 8.02 (1H, dd, *J* 6.6 and 0.9 Hz, H7), 7.65 (1H, d, *J* 3.6 Hz, H3), 7.39 (2H, m, H5 and H8), 3.99 (3H, s, OCH_3); *m*/*z* 238.8 [M^+ , 71%].

6-*Methoxyquinoline*-4-*carbaldehyde*, 4.8

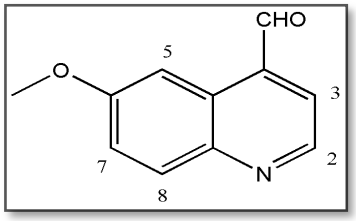

To a solution of *n*-BuLi (2.5 M, 3.5 ml, 6.3 mmol) in anhydrous diethyl ether (90 ml) at -78 °C was slowly added a

solution of **4.7** (3.00 g, 12.6 mmol) in diethyl ether (35 ml), a thick yellow suspension appeared and the mixture was stirred further for 30 minutes at -78 °C. Anhydrous DMF (10 ml) was then added, the resultant orange mixture was stirred for 3 hrs at -78 °C. The reaction was quenched with water (250 ml), diethyl ether (300 ml) was added and the organic phase separated, washed with NH_4Cl (150 ml), saturated $Na_2S_2O_3$ (150 ml) and brine (150 ml) and dried over anhydrous Na_2SO_4. The solvent was removed *in vacuo* to afford a crude product which was purified by column chromatography (on silica gel; elution with EtOAc: Hex; 50:50) to give a pale-yellow solid (**4.8**) (1.92 g, 86%); δ_H (300 MHz; $CDCl_3$) 10.41 (1H, s, CHO), 9.01 (1H, d, *J* 4.3 Hz, H2), 8.44 (1H, d, *J* 2.8 Hz, H5), 8.07 (1H, d, *J* 9.3 Hz, H8), 7.72 (1H, d, *J* 4.3 Hz, H3), 7.44 (1H, dd, *J* 9.3 and 2.8 Hz, H7), 3.99 (3H, s, OCH_3); *m*/*z* 187.01 [M^+ , 28%].

Synthesis of the Mefloquine-nucleus,[7] 2,8-bis*(trifluoromethyl)quinoline*-4-*carbaldehyde*, 4.11

4-*bromo*-2,8-bis*(trifluoromethyl)quinoline*, 4.10

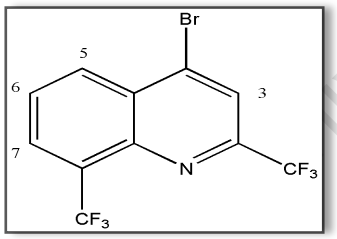

Phosphorus oxybromide (8.0 g, 28 mmol, 8.0 eq) in an oven-dried round bottom flask was heated at 75 °C until the solid melted. Thereafter, commercially available 2,8-*bis*(trifluoromethyl)quinolin-4-ol (**4.9**) (1.0 g, 3.5 mmol, 1.0 eq) was added gradually to the molten solid and the mixture was further heated at 150 °C for 2 hrs. Upon cooling to room temperature, ice-cold water was added (50 ml) to the resultant mixture resulting in the formation of a yellow precipitate which was filtered, dried on a vacuum pump for 4 hrs. The obtained pale-yellow powder (**4.10**) (0.95 g, 78%) was pure enough for use in the subsequent step without further purification; δ_H (400 MHz; $CDCl_3$) 8.55 (1H, d, *J* 7.5 Hz, H7), 8.29 (1H, d, *J* 7.5 Hz, H5), 8.05 (1H, s, H3), 7.94 (1H, t, *J* 7.6 Hz, H6);

2,8-bis*(trifluoromethyl)quinoline*-4-*carbaldehyde*, 4.11

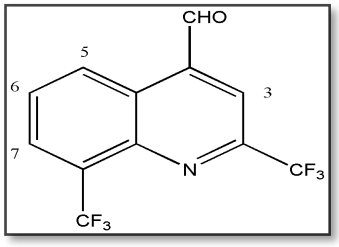

4-bromo-2,8-*bis*(trifluoromethyl)quinoline (**4.10**) (0.85 g, 2.35 mmol) was dissolved in dry THF (10 ml) and cooled to -78 °C. To the flask was added *n*-BuLi (2.5 M in hexane; 7.05 mmol, 2.9 ml, 3 eq) at once and the resultant blue solution was stirred at this temperature for 30 minutes. Thereafter, anhydrous DMF (1 ml, 11.75 mmol, 5.0 eq) was added drop-wise and the resultant solution was further stirred for 2 hrs at -78 °C. On complete consumption of the starting material the solution was poured into a separatory funnel containing 1:1 ethyl acetate:brine mixture and the aqueous layer was further extracted three times with ethyl acetate. The combined organic extract was washed with NH_4Cl (20 ml), saturated $Na_2S_2O_3$ (20 ml) and water (150 ml), and dried over anhydrous $MgSO_4$. The solvent was removed *in vacuo* to afford an oily crude product (0.35 g) which was purified by column chromatography (on silica gel; elution with EtOAc: Hex; 30:70) to give a pale-yellow paste (**4.11**) (0.20 g, 29%) which showed a presence of impurities on the ^1H NMR and was used as such in the next step; δ_H (300 MHz; $CDCl_3$) 10.47 (1H, s, C*H*O), 9.32 (1H, d, *J* 7.2 Hz, H7), 8.29 (1H, d, *J* 7.4 Hz, H5), 8.23 (1H, s, H3), 7.93 (1H, t, *J* 7.6 Hz, H6);

Synthesis of Quinine- and Mefloquine-based tetrazoles

Aldehydes **4.8** and **4.11** (1.6 mmol) with various amines (2.12 mmol) were stirred in anhydrous methanol at 26 °C for 5 minutes. Thereafter, $TMSN_3$ (2.12 mmol) was added, followed by the addition of *tert*-butyl isocyanide (2.12 mmol) and the resulting mixture was then stirred for 24 hrs. The solvent was removed in *vacuo* to afford crude tetrazole products **4.12a-f** and **4.13a-b**.

(1-tert-*butyl*-1H-*tetrazol*-5-*yl*)(6-*methoxyquinolin*-4-*yl*)-N,N-*dimethylmethanamine*, 4.12a (TK501)

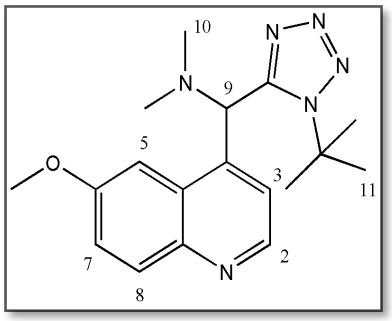

Purified by column chromatography (on silica gel; elution with EtOAc: Hex; 50:50) to yield the desired product **4.12a** (235 mg, 65%) as a white solid; m. p. 101- 103 °C, R_f (EtOAc: Hex, 50: 50%) 0.41; IR ν_{max} (DCM)/cm^{-1} 1621 (Ar C=C), 1374 (N=N), 1318 (C=N), 1278 (C-N), 1230 (C-O Ester); δ_H (400 MHz; $CDCl_3$) 8.64 (1H, d, *J* 4.5 Hz, H2), 8.07 (1H, d, *J* 9.2 Hz, H8), 7.67 (1H, d, *J* 2.7 Hz, H5), 7.43 (1H, dd, *J* 9.2 and 2.7 Hz, H7), 6.89 (1H, d, *J* 4.5 Hz, H3), 6.13 (1H, s, H9), 3.99 (3H, s, OCH_3), 2.48 (6H, s, 2 x H10), 1.56 (9H, s, 3 x H11); δ_C (101 MHz; $CDCl_3$) 158.4, 152.5, 147.2, 144.8, 140.6, 131.8, 127.9, 122.0, 121.4, 102.6, 61.3, 60.5, 55.5, 41.3 (2C) and 30.1 (3C); MS (ESI) *m/z* 341.3 (M^++H); HPLC purity: 95.2%; t_r,=6.52 min.

N-[(1-tert-*butyl*-1H-*tetrazol*-5-*yl*)(6-*methoxyquinolin*-4-*yl*)*methyl*]-N-*ethylethanamine*, 4.12b (TK502)

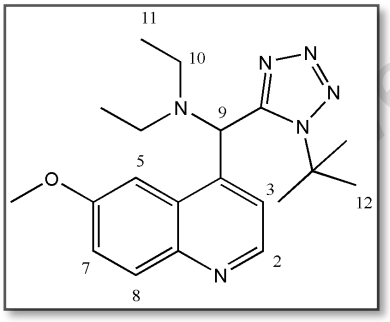

Purified by column chromatography (on silica gel; elution with DCM: MeOH; 95:05) to yield the desired product **4.12b** (312 mg, 80%) as a pale-yellow solid; m. p. 118- 121 °C, R_f (DCM: MeOH, 95: 05%) 0.59; IR ν_{max} (DCM)/cm^{-1} 1619 (Ar C=C), 1376 (N=N), 1316 (C=N), 1290 (C-N), 1236 (C-O Ester); δ_H (300 MHz; $CDCl_3$) 8.60 (1H, d, *J* 4.6 Hz, H2), 8.05 (1H, d, *J* 9.2 Hz, H8), 7.86 (1H, d, *J* 2.8 Hz, H5), 7.42 (1H, dd, *J* 9.2 and 2.8 Hz, H7), 6.60 (1H, d, *J* 4.6 Hz, H3), 6.30 (1H, s, H9), 3.98 (3H, s, OCH_3), 2.89 (4H, m, 2 x H10), 1.52 (9H, s, 3 x H12), 0.91 (6H, t, *J* 5.4 Hz, 2 x H11); δ_C (75 MHz; $CDCl_3$) 158.6, 153.1, 147.2, 145.1, 142.6, 131.7, 127.9, 122.5, 122.4, 102.6, 62.1, 58.6, 55.9, 46.3 (2C), 30.1 (3C) and 15.3 (2C); MS (ESI) *m/z* 369.3 (M^++H); HPLC purity: 99.0%; t_r,=9.46 min.

4-[(1-tert-*butyl*-1H-*tetrazol*-5-*yl*)(*pyrrolidin*-1-*yl*)*methyl*]-6-*methoxyquinoline*, 4.12c (TK503)

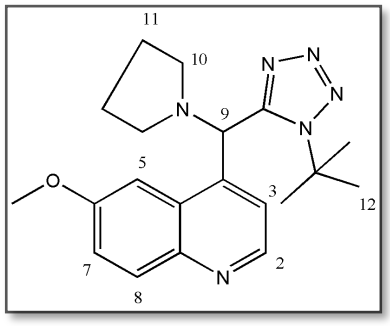

Purified by column chromatography (on silica gel; elution with DCM: MeOH; 95:05) to yield the desired product **4.12c** (179 mg, 46%) as a thick brown oil; R_f (DCM: MeOH, 95: 05%) 0.61; IR ν_{max} (DCM)/cm^{-1} 1618 (Ar C=C), 1372 (N=N), 1309 (C=N), 1279 (C-N), 1238 (C-O Ester); δ_H (400 MHz; $CDCl_3$) 8.62 (1H, d, *J* 4.5 Hz, H2), 8.05 (1H, d, *J* 9.2 Hz, H8), 7.90 (1H, d, *J* 2.4 Hz, H5), 7.43 (1H, dd, *J* 9.2 and 2.4 Hz, H7), 6.79 (1H, d, *J* 4.5 Hz, H3), 6.16 (1H, s, H9), 4.03 (3H, s, OCH_3), 3.01 (2H, m, *H10a*), 2.50 (2H, m, *H10b*), 1.59 (9H, s, 3 x H12), 1.44 (4H, m, 2 x H11); δ_C (101 MHz; $CDCl_3$) 158.2, 152.6, 147.3, 145.0, 140.3, 131.7, 128.0, 122.0, 121.7, 102.7, 62.8, 61.3, 55.5, 50.3 (2C), 30.1 (3C) and 26.8 (2C); MS (ESI) *m/z* 367.2 (M^++H); HPLC purity: 96.6%; t_r,=7.09 min.

4-[(1-tert-*butyl*-1H-*tetrazol*-5-*yl*)(*piperidin*-1-*yl*)*methyl*]-6-*methoxyquinoline*, 4.12d (TK504)

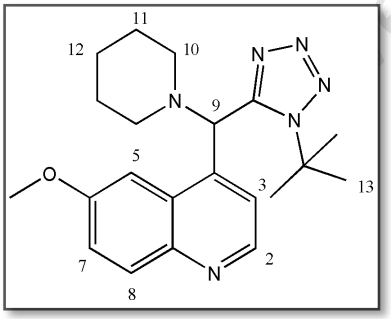

Purified by column chromatography (on silica gel; elution with DCM: MeOH; 95:05) to yield the desired product **4.12d** (179 mg, 87%) as a light brown solid; m. p. 117- 119 °C, R_f (DCM: MeOH, 95: 05%) 0.39; IR ν_{max} (DCM)/cm^{-1} 1617 (Ar C=C), 1374 (N=N), 1314 (C=N), 1260 (C-N), 1241 (C-O Ester); δ_H (400 MHz; $CDCl_3$) 8.65 (1H, d, *J* 4.5 Hz, H2), 8.06 (1H, d, *J* 9.2 Hz, H8), 7.73 (1H, d, *J* 2.2 Hz, H5), 7.42 (1H, dd, *J* 9.2 and 2.2 Hz, H7), 7.06 (1H, d, *J* 4.6 Hz, H3), 6.29 (1H, s, H9), 4.00 (3H, s, OCH_3), 3.14 (2H, m, H*10a*), 2.45 (2H, m, H*10b*), 1.80 (2H, m, H12), 1.73 (4H, m, 2 x H11), 1.60 (9H, s, 3 x H13); δ_C (101 MHz; $CDCl_3$) 158.3,

153.6, 147.5, 144.8, 140.9, 131.8, 127.7, 121.4 (2C), 102.3, 61.3, 57.2, 55.5, 49.5 (2C), 30.1 (3C), 29.9 and 24.2 (2C); MS (ESI) *m/z* 381.5 (M^++H); HPLC purity: 95.5%; t_r=9.50 min.

4-[(1-tert-*butyl*-1H-*tetrazol*-5-*yl*)(4-*methylpiperazin*-1-*yl*)*methyl*]-6-*methoxyquinolin*e, 4.12e (TK505)

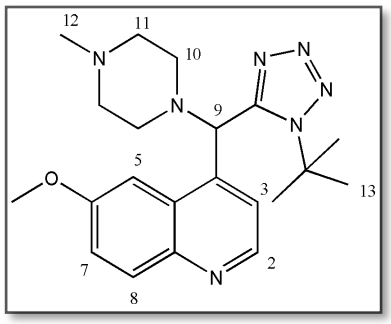

Purified by column chromatography (on silica gel; elution with DCM: MeOH; 95:05) to yield the desired product **4.12e** (117 mg, 56%) as a pale-yellow solid; m. p. 140- 144 °C, R_f (DCM: MeOH, 95: 05%) 0.32; IR ν_{max} (DCM)/cm^{-1} 1619 (Ar C=C), 1374 (N=N), 1318 (C=N), 1275 (C-N), 1223 (C-O Ester); δ_H (300 MHz; $CDCl_3$) 8.62 (1H, d, *J* 4.5 Hz, H2), 8.04 (1H, d, *J* 9.2 Hz, H8), 7.81 (1H, d, *J* 2.7 Hz, H5), 7.41 (1H, dd, *J* 9.2 and 2.7 Hz, H7), 6.93 (1H, d, *J* 4.5 Hz, H3), 6.12 (1H, s, H9), 3.99 (3H, s, OCH_3), 3.00 (2H, m, H*10a*), 2.45 (2H, m, H*10b*), 2.38 (2H, m, H*11a*), 2.31 (2H, m, H*11b*), 2.20 (3H, s, H12), 1.56 (9H, s, 3 x H13); δ_C (75 MHz; $CDCl_3$) 158.3, 152.4, 147.4, 145.0, 140.0, 131.9, 127.9, 122.3, 121.8, 102.6, 61.4, 61.0, 55.6 (3C), 49.5 (2C), 46.0 and 30.2 (3C); MS (ESI) *m/z* 396.1 (M^+); HPLC purity: 98.9%; t_r=5.38 min.

4-[(1-tert-*butyl*-1H-*tetrazol*-5-*yl*)(*morpholino*)*methyl*]-6-*methoxyquinolin*e, 4.12f (TK506)

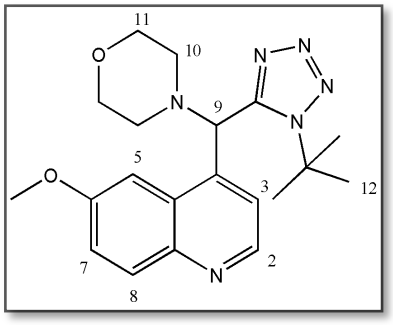

Purified by column chromatography (on silica gel; elution with DCM: MeOH; 95:05) to yield the desired product **4.12f** (302 mg, 75%) as a pale-yellow solid; m. p. 110- 112 °C, R_f (DCM: MeOH, 95: 05%) 0.45; IR ν_{max} (DCM)/cm^{-1} 1619 (Ar C=C), 1372 (N=N), 1321 (C=N), 1276 (C-N), 1239 (C-O Ester); δ_H (400 MHz; $CDCl_3$) 8.65 (1H, d, *J* 4.5 Hz, H2), 8.08 (1H, d, *J* 9.2 Hz, H8), 7.83 (1H, d, *J* 2.6 Hz, H5), 7.45 (1H, dd, *J* 9.2 and 2.6 Hz, H7), 6.90 (1H, d, *J* 4.5 Hz,

H3), 6.15 (1H, s, H9), 4.02 (3H, s, OCH_3), 3.67 (2H, m, H*11a*), 3.57 (2H, m, H*11b*), 3.06 (2H, m, H*10a*), 2.54 (2H, m, H*10b*), 1.58 (9H, s, 3 x H13); δ_C (101 MHz; $CDCl_3$) 158.4, 152.3, 147.3, 145.0, 139.1, 132.0, 127.7, 122.3, 121.6, 102.6, 67.4 (2C), 61.4, 61.2, 55.6, 49.8 (2C) and 30.2 (3C); MS (ESI) *m/z* 383.3 (M^++H); HPLC purity: 93.8%; t_r=8.35 min.

[2,8-bis*(trifluoromethyl)quinolin*-4-*yl](*tert-*butyl*-1H-*tetrazol*-5-*yl)*-N,N-*dimethylmethanamine*, 4.13a (TK710)

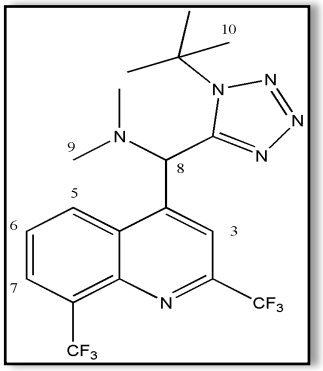

Purified by column chromatography (on silica gel; elution with EtOAc: Hex; 50:50) to yield the desired product **4.13a** as a white powder (20 mg, 22%); m. p. 171- 173 °C, R_f (EtOAc: Hex, 50: 50%) 0.35; IR ν_{max} (DCM)/cm^{-1} 1602 (Ar C=C), 1423 (N=N), 1314 (C=N), 1271 (C-N), 1090 (C-F); δ_H (400 MHz; $CDCl_3$) 8.70 (1H, d, *J* 8.5 Hz, H7), 8.23 (1H, d, *J* 7.1 Hz, H5), 7.84 (1H, t, *J* 7.9 Hz, H6), 7.40 (1H, s, H3), 6.29 (1H, s, H8), 2.46 (6H, s, 2 x H9), 1.62 (9H, s, 3 x H10); δ_C (101 MHz; $CDCl_3$) 151.4, 145.2, 144.2, 129.4, 129.3, 129.2, 128.2, 128.1, 127.8, 124.8, 122.0, 118.0, 61.6, 60.3, 41.3 (2C) and 30.2 (3C); MS (ESI) *m/z* 447.2 (M^++H); HPLC purity: 98.9%; t_r=8.60 min.

N-{[2,8-bis*(trifluoromethyl)quinolin*-4-*yl](*tert-*butyl*-1H-*tetrazol*-5-*yl)metyhyl}*-N-*ethylethanamine*, 4.13b (TK720)

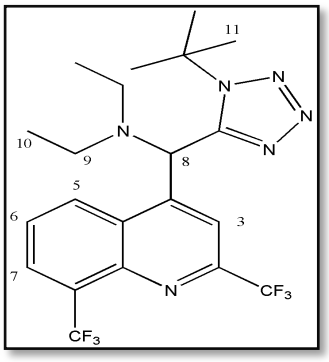

Purified by column chromatography (on silica gel; elution with EtOAc: Hex; 50:50) to yield the desired product **4.13b** as a yellow solid (13.3 mg, 22%) as a light-brown solid; m. p. 76- 78 °C, R_f (EtOAc: Hex, 50: 50%) 0.35; IR ν_{max} (DCM)/cm^{-1} 1602 (Ar C=C), 1424 (N=N), 1309 (C=N), 1279 (C-N), 1112 (C-F); δ_H (400 MHz; $CDCl_3$) 8.82 (1H, d, *J* 8.6 Hz, H7), 8.23 (1H, d, *J* 7.2 Hz, H5), 7.84 (1H, t, *J* 7.7 Hz, H6), 7.11 (1H, s, H3), 6.43 (1H, s, H8), 2.88 (4H, q, *J* 7.2 Hz, 2 x H9), 1.62 (9H, s, 3

x H11), 0.93 (6H, t, *J* 7.2 Hz, 2 x H10); δ_C (101 MHz; $CDCl_3$) 152.5, 146.6, 143.1, 129.4, 129.3, 129.2, 128.4, 128.0, 127.8, 124.8, 122.1, 118.1, 61.9, 58.4, 45.8 (2C), 30.2 (3C) and 14.7 (2C); MS (ESI) *m/z* 475.4 (M^++H); HPLC purity: 95.3%; t_r=8.93 min.

General procedure for the synthesis of de-*tert*-butylated quinine-based tetrazoles 4.14a-f

The procedure used in the synthesis of the de-*tert*-butylated deoxyamodiaquine tetrazole **3.10a-f** was followed**,** quinine-based tetrazoles **4.13a-f** (0.51 mmol) were refluxed in 32% HCl (10 ml) to give the desired products, **4.14a-f**, after purification by column chromatography (on silica gel; elution with DCM: MeOH: NH_4OH; 95:0.5:01).

(6-*methoxyquinolin*-4-*yl*)-N,N-*dimethyl(*1H-*tetrazol*-5-*yl)methanamine*, 4.14a (TK501B3)

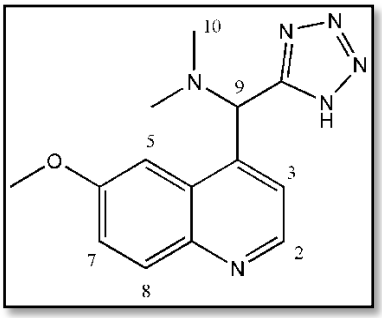

As a pale-yellow solid (55 mg, 33%); m. p. 159- 162 °C, R_f (DCM: MeOH: NH_4OH; 95:0.9:01%) 0.12; IR ν_{max} (KBr)/cm^{-1} 1588 (Ar C=C), 1369 (N=N), 1314 (C=N), 1276 (C-O Ester), 1245(C-O Ester); δ_H (400 MHz; DMSO-d*6*) 8.65 (1H, d, *J* 4.5 Hz, H2), 7.86 (1H, d, *J* 9.2 Hz, H8), 7.82 (1H, d, *J* 2.8 Hz, H5), 7.76 (1H, d, *J* 4.5 Hz, H3), 7.33 (1H, dd, *J* 9.2 and 2.8 Hz, H7), 5.37 (1H, s, H9), 3.87 (3H, s, OCH_3), 2.14 (6H, s, 2 x H10); δ_C (101 MHz; DMSO-d*6*) 159.5, 156.4, 147.3, 146.0, 143.9, 130.6, 127.7, 120.9, 120.5, 103.7, 63.3, 55.2 and 43.2 (2C); MS (ESI) *m/z* 285.1 (M^++H); HPLC purity: 95.8%; t_r=6.33 min.

N-*ethyl*-N-[(6-*methoxyquinolin*-4-*yl*)(1H-*tetrazol*-5-*yl*)*methyl*]*ethanamine*, 4.14b (TK502B3)

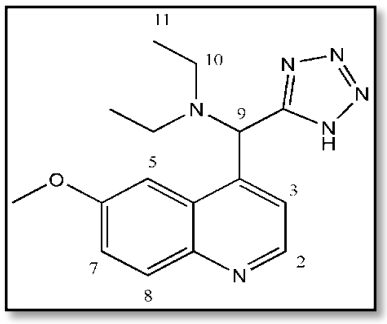

As a yellow solid (26 mg, 15%); m. p. 168- 171 °C, R_f (DCM: MeOH: NH_4OH; 95:0.9:01%) 0.11; IR ν_{max} (KBr)/cm^{-1} 1600 (Ar C=C), 1368 (N=N), 1319 (C=N), 1269 (C-N), 1225 (C-O Ester); δ_H (400 MHz; DMSO-d*6*) 8.61 (1H, d, *J* 4.5 Hz, H2), 7.91 (1H, d, *J* 2.8 Hz, H5), 7.86 (1H, d, *J* 9.2 Hz, H8), 7.52 (1H, d, *J* 4.5 Hz, H3), 7.32 (1H, dd, *J* 9.2 and 2.8 Hz, H7), 5.87 (1H, s, H9), 3.85 (3H, s, OCH_3), 2.63 (2H, q, *J* 7.1 Hz, H*10a*), 2.27 (2H, q, J 7.1 Hz, H*10b*), 0.91 (6H, t, *J* 7.1 Hz, 2 x H11); δ_C (100 MHz; DMSO-d*6*) 159.6, 156.6, 147.8, 146.1, 144.6, 131.1, 127.8, 122.1, 121.2, 104.4, 58.8, 55.8, 44.3 (2C) and 13.5 (2C); MS (ESI) *m/z* 313.2 (M^++H); HPLC purity: 96.7%; t_r,=7.38 min.

6-*methoxy*-4-*[(pyrrolidin*-1-*yl)(*1H-*tetrazol*-5-*yl)methyl]quinoline*, 4.14c (TK503B3)

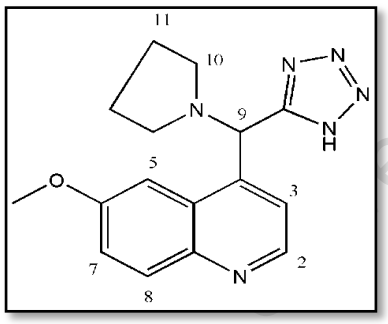

As a light-brown solid (22 mg, 13%); m. p. 211- 214 °C; R_f (DCM: MeOH: NH_4OH; 95:0.9:01%) 0.09; IR ν_{max} (KBr)/cm^{-1} 1579(Ar C=C), 1366 (N=N), 1326 (C=N), 1274 (C-N), 1215 (C-O Ester); δ_H (300 MHz; DMSO-d*6*) 8.66 (1H, d, *J* 4.4 Hz, H2), 7.96 (1H, d, *J* 2.6 Hz, H8), 7.84 (1H, d, *J* 9.2 Hz, H5), 7.79 (1H, d, *J* 4.4 Hz, H3), 7.30 (1H, dd, *J* 9.2 and 2.6 Hz, H7), 5.40 (1H, s, H9), 3.86 (3H, s, OCH_3), 2.54 (2H, m, H*10a*), 2.35 (2H, m, H*10b*), 1.65 (4H, m, 2 x H11); δ_C (75 MHz; DMSO-d*6*) 159.0, 156.2, 147.2, 146.5, 130.3, 130.1, 129.1, 127.2, 120.3, 103.7, 61.9, 58.5, 51.6 (2C) and 23.0 (2C); MS (ESI) *m/z* 311.4 (M^++H); HPLC purity: 95.1%; t_r,=7.12 min.

6-*methoxy*-4-*[(piperidin*-1-*yl)(*1H-*tetrazol*-5-*yl)methyl]quinoline*, 4.14d (TK504B3)

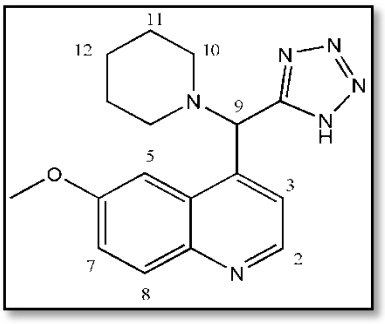

As a pale-yellow crystalline solid (49 mg, 28%); m. p. 131-134 °C, R_f (DCM: MeOH: NH_4OH; 95:0.9:01%) 0.10; IR ν_{max} (KBr)/cm^{-1} 1630 (Ar C=C), 1368 (N=N), 1309 (C=N), 1251 (C-N), 1223 (C-O Ester);δ_H (300 MHz; DMSO-d*6*) 8.62 (1H, d, *J* 4.5 Hz, H2), 7.99 (1H, d, *J* 2.8 Hz, H5), 7.85 (1H, d, *J* 9.2 Hz, H8), 7.69 (1H, d, *J* 4.5 Hz, H3), 7.31 (1H, dd, *J* 9.2 and 2.8 Hz, H7), 5.43 (1H, s, H9), 3.88 (3H, s, OCH_3), 2.45 (2H, m, H*10a*), 2.25 (2H, m, H*10b*), 1.44 (4H, m, 2 x H11), 1.35 (2H, m, H12); δ_C (101 MHz; DMSO-d*6*) 159.2, 156.1, 147.1, 145.9, 143.9, 130.3, 127.8, 120.8, 120.4, 104.0, 63.5, 55.0, 51.6 (2C), 25.8 (2C) and 24.0; MS (ESI) *m/z* 325.1 (M^++H); HPLC purity: 95.2%; t_r,=6.98 min.

6-*methoxy*-4-*[(4-methylpiperazin*-1-*yl)(*1H-*tetrazol*-5-*yl)methyl]quinoline*, 4.14e (TK505B3)

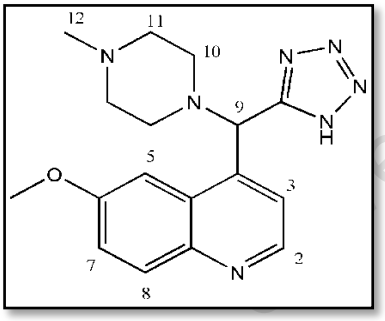

As a cream-coloured solid (58 mg, 34%); m. p. 176- 179 °C, R_f (DCM: MeOH: NH_4OH; 95:0.9:01%) 0.12; IR ν_{max} (KBr)/cm^{-1} 1590 (Ar C=C), 1368 (N=N), 1299 (C=N), 1259 (C-N), 1219 (C-O Ester);δ_H (400 MHz; DMSO-d*6*) 8.60 (1H, d, *J* 4.5 Hz, H2), 7.96 (1H, d, *J* 2.5 Hz, H5), 7.81 (1H, d, *J* 9.2 Hz, H8), 7.68 (1H, d, *J* 4.5 Hz, H3), 7.27 (1H, dd, *J* 9.2 and 2.5 Hz, H7), 5.36 (1H, s, H9), 3.84 (3H, s, OCH_3), 2.46 (2H, m, H*10a*), 2.39 (2H, m, H*10b*), 2.26 (4H, m, 2 x H11), 2.09 (3H, s, H12); δ_C (100 MHz; DMSO-d*6*) 159.5, 156.3, 147.4, 145.6, 144.0, 130.5, 127.7, 120.9, 120.8, 103.9, 63.2, 55.3, 55.0 (3C), 50.5 and 45.6; MS (ESI) *m/z* 340.4 (M^++H); HPLC purity: 95.6%; t_r,=7.22 min.

6-*methoxy*-4-*[morpholino(*1H-*tetrazol*-5-*yl)methyl]quinoline*, 4.14f (TK506B3)

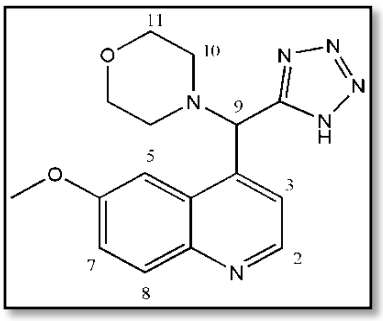

As a light-brown solid (37 mg, 21%); m. p. 137- 140 °C, R_f (DCM: MeOH: NH_4OH; 95:0.9:01%) 0.23; IR ν_{max} (KBr)/cm^{-1} 1598 (Ar C=C), 1368 (N=N), 1330 (C=N), 1273 (C-N), 1220 (C-O Ester);δ_H (300 MHz; DMSO-d*6*) 8.64 (1H, d, *J* 4.5 Hz, H2), 8.03 (1H, d, *J* 2.8 Hz, H5), 7.85 (1H, d, *J* 9.2 Hz, H8), 7.74 (1H, d, *J* 4.5 Hz, H3), 7.32 (1H, dd, *J* 9.2 and 2.8 Hz, H7), 5.44 (1H, s, H9), 3.90 (3H, s, OCH_3), 3.56 (4H, m, 2 x H11), 2.44 (2H, m, H*10a*), 2.29 (2H, m, H*10b*); δ_C (75 MHz; DMSO-d*6*) 158.9, 156.3, 147.2, 145.1, 144.0, 130.4, 127.7, 121.0, 120.6, 104.0, 66.4 (2C), 63.4, 55.2 and 51.2 (2C); MS (ESI) *m/z* 327.3 (M^++H); HPLC purity: 99.1%; t_r=6.66 min.

Synthesis of nitroimidazole-based tetrazoles and hybrids

Synthesis of *p, m* and *o*-(bromomethyl)benzaldehydes[9], 4.16a-c

Solutions of commercially available *p*-, *m*- and *o*-(bromomethly)benzonitrile (**4.15a-c**) (10.2 mmol) in dry toluene (30 ml) was cooled to 0 °C in an ice-bath under an inert N_2 atmosphere. A 1.5 M solution of DIBAL-H in toluene (15.3 mmol) was then added drop-wise over a period of 30 minutes and the resultant solution was then allowed to further stir for 1 hour at 0 °C. Thereafter, $CHCl_3$ (20 ml) and 2M HCl (25 ml) were added and mixture stirred for 12 hours at room temperature. The organic layer was separated and washed twice with water, dried over $MgSO_4$ and solvent removed *vacuo* to give the desired products (**4.16a-c**) pure enough to proceed to the next step without further purification.

2-*(bromomethyl)benzaldehyde*, 4.16a

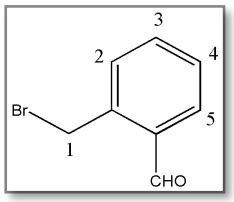

Obtained as a thick-colourless oil (1.25 g, 68%); R_f (EtOAc: Hex, 50: 50%) 0.39; δ_H (300 MHz; $CDCl_3$) 10.15 (1H, s, C*H*O), 7.91 (1H, d, *J*

5.7 Hz, H5), 7.54 (1H, m, H3), 7.41 (1H, m, H4), 7.35 (1H, d, *J* 5.4 Hz, H2), 4.91 (2H, s, H1).

3-*(bromomethyl)benzaldehyde*, 4.16b

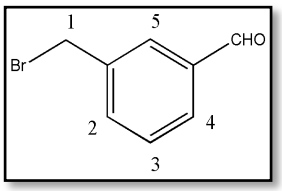

Obtained as a yellow paste (1.86 g, 85%); R_f (EtOAc: Hex, 50: 50%) 0.41; δ_H (400 MHz; $CDCl_3$) 9.96 (1H, s, C*H*O), 7.84 (1H, s, H5), 7.74 (1H, d, *J* 7.6 Hz, H4), 7.60 (1H, d, *J* 7.6 Hz, H2), 7.45 (1H, t, *J* 7.6 Hz, H3), 4.48 (2H, s, H1).

4-*(bromomethyl)benzaldehyde*, 4.16c

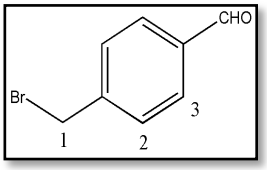

Obtained as white flakes (1.65 g, 80%); R_f (EtOAc: Hex, 50: 50%) 0.45; δ_H (300 MHz; $CDCl_3$) 10.01 (1H, s, C*H*O), 7.87 (2H, d, *J* 6.3 Hz, 2 x H3), 7.55 (2H, d, *J* 6.3 Hz, 2 x H2), 4.51 (2H, s, H1).

Synthesis of 2-nitroimidazo-oxazine aldehydes[10], 4.18a-b

At 0 °C, under N_2 atmosphere, NaH (60% mineral oil, 1.3 eq) was added to the stirred solution of *p*, *m* and *o*-(bromomethyl)benzaldehydes (1.2 eq) (**4.16a-c**) and (*S*)-2-nitro-6,7-dihydro-5H-imidazo[2,1-*b*][1,3]oxazin-6-ol (**4.17**) (1.0 eq) in anhydrous DMF (5 ml). The resultant mixture was maintained at this temperature for 30 minutes, allowed to warm to room temperature and stirred further for 12 hrs. On completion of the reaction as seen on the TLC, the solvent was removed in *vacuo* by azeotropic distillation of toluene to afford crude products **4.18a-b** (*m*- and *p*-based products). The *o*-(bromomethyl)benzaldehyde reaction did not work as evidence by the recovery of starting materials.

4-{[(*S*)-6,7-*dihydro*-2-*nitro*-5H-*imidazo*[2,1-*b*][1,3]*oxazin*-6-*yloxy*]*methyl*}*benzaldehyde*, 4.18a (PA-2A1)

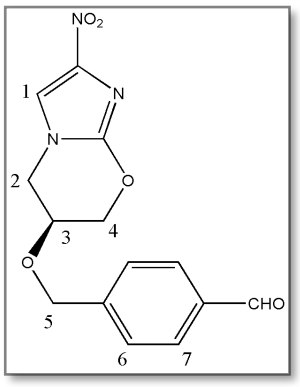

Purified by column chromatography (on silica gel; elution with DCM: MeOH; 95:05) to yield the desired product **4.18a** (91 mg, 46%) as pale-yellow flakes; m. p. 145- 148 °C, R_f (DCM: MeOH, 95: 05%) 0.27; IR ν_{max} (DCM)/cm^{-1} 1699 (C=O), 1579 (Ar C=C), 1548 (NO_2), 1266 (C-O Ether); δ_H (400 MHz; DMSO-*d6*) 9.99 (1H, s, C*H*O), 8.02 (1H, s, H1), 7.89 (2H, d, *J* 8.1 Hz, 2 x H7), 7.52 (2H, d, *J* 8.1 Hz, 2 x H6), 4.77 (2H, dd, J_{AB} 13.2 Hz, H5), 4.49 (1H, dt, *J* 2.6 and 12.1 Hz, H3), 4.48 (1H, d, *J* 11.9 Hz, H*4a*), 4.28 (3H, m, H2 and H*4b*); δ_C (101 MHz; DMSO-*d6*) 193.1, 147.6, 145.2, 136.0, 130.0 (2C), 128.2 (2C), 127.1, 118.4, 69.6, 68.4, 62.9 and 47.2; MS (ESI) *m/z* 304.1 (M^++H), HPLC purity: 98.9%; $t_{r'}$=6.98 min.

4-{[(*S*)-6,7-*dihydro*-2-*nitro*-5H-*imidazo*[2,1-*b*][1,3]*oxazin*-6-*yloxy*]*methyl*}*benzaldehyde*, 4.18b *(*PA-2A2 or PA-10A)

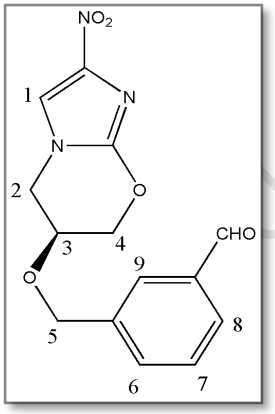

Purified by column chromatography (on silica gel; elution with DCM: MeOH; 95:05) to yield the desired product **4.18b** (131 mg, 78%) as yellow flakes; m. p. 129- 132 °C, R_f (DCM: MeOH, 95: 05%) 0.22; IR ν_{max} (DCM)/cm^{-1} 1685 (C=O), 1569 (Ar C=C), 1538 (NO_2), 1245 (C-O Ether); δ_H (400 MHz; DMSO-*d6*) 10.01 (1H, s, C*H*O), 7.99 (1H, s, H1), 7.83 (2H, m, H8 and H9), 7.65 (1H, t, *J* 7.7 Hz, H7), 7.60 (1H, d, *J* 7.7 Hz, H6), 4.76 (2H, dd, J_{AB} 12.9 Hz, H5), 4.66 (1H, dt, *J* 4.7 and 11.9 Hz, H3), 4.49 (1H, d, *J* 11.6 Hz, H*3a*), 4.28 (3H, m, H2 and H*3b*); δ_C (101 MHz; DMSO-*d6*) 192.8, 148.3, 143.2, 138.3, 135.9, 133.3, 129.0, 128.8, 127.9, 117.7, 68.9, 67.7, 66.5 and 46.5; MS (ESI) *m/z* 304.2 (M^++H), HPLC purity: 93.6%; $t_{r'}$=7.29 min.

Towards the synthesis of nitroimidazo-oxazine-tetrazole derivatives[4], 4.19a-h

The 2-nitroimidazo-oxazine aldehyde, **4.18a** (0.099 mmol) and anvarious amine (including 4-amino-7chloroquinoline diamines)[§] (0.207 mmol) were stirred in anhydrous methanol as a suspension at 26 °C for 5 minutes. Thereafter, $TMSN_3$ (0.207 mmol) was added, followed by the addition of *tert*-butyl isocyanide (0.207 mmol) and the resulting mixture was then stirred at 40 °C for 12 hrs. Thereafter, the solvent was removed in *vacuo* to afford the crude tetrazoles which were purified by column chromatography (on silica gel; elution with DCM: MeOH; 95:05) to give the desired products, **4.19a-h**, in low to excellent yields.

(4-{[(*S*)-6,7-*dihydro*-2-*nitro*-5H-*imidazo*[2,1-*b*][1,3]*oxazin*-6-*yloxy*]*methyl*}*phenyl*)(1-tert-*butyl*-1H-*tetrazol*-5-*yl*)-N,N-*dimethylmethanamine*, 4.19a (PA-3A)

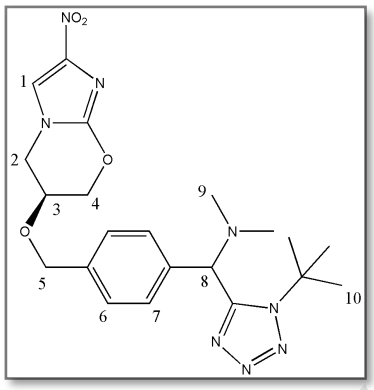

As a yellow solid (25 mg, 46%); m. p. 68- 72 °C, R_f (DCM: MeOH, 95: 05%) 0.32; IR ν_{max} (DCM)/cm^{-1} 1588 (Ar C=C), 1566 (NO_2), 1368 (N=N), 1340 (C=N), 1284 (C-O Ether); δ_H (400 MHz; $CDCl_3$) 7.42 (2H, d, *J* 8.0 Hz, 2 x H7), 7.37 (1H, d, *J* 12.9 Hz, H1), 7.27 (2H, d, *J* 8.0 Hz, 2 x H6), 5.19 (1H, s, H8), 4.72 (1H, m, H3), 4.59 (2H, m, H5), 4.35 (1H, d, *J* 12.1 Hz, H*4a*), 4.17 (3H, m, H2 and H*4b*), 2.29 (6H, s, 2 x H9), 1.69 (9H, s, 3 x H10); δ_C (101 MHz; $CDCl_3$) 154.3, 147.2, 136.9, 136.0, 130.1 (2C), 127.6 (2C), 127.0, 115.0, 70.7, 67.4, 66.7, 65.0, 63.2, 47.5; 42.4 (2C) and 30.2 (3C); MS (ESI) *m/z* 457.3 (M^+), HPLC purity: 97.5%; t_r=8.30 min.

§ HCl protected amines were neutralized by addition of the base, diisopropyl ethylamine (2 eq)

N-(4-{[((*S*)-6,7-*dihydro*-2-*nitro*-5H-*imidazo*[2,1-*b*][1,3]*oxazin*-6-*yloxy*)*methyl*]*pheny*}(1-tert-*butyl*-1H-*tetrazol*-5-*yl*)*methyl*)-N-*dimethylmethanamine*, 4.19b (PA-4A)

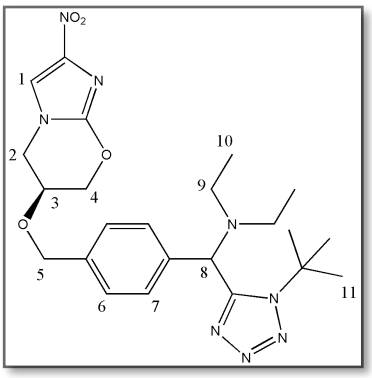

As a pale-yellow solid (30.2 mg, 63%); m. p. 48- 50 °C, R_f (DCM: MeOH, 95: 05%) 0.46; IR ν_{max} (DCM)/cm^{-1} 1601 (Ar C=C), 1536 (NO_2), 1378 (N=N), 1340 (C=N), 1260 (C-O Ether); δ_H (400 MHz; $CDCl_3$) 7.37 (1H, d, *J* 15.0 Hz, H1), 7.25 (4H,m, 2 x H6 and 2 x H7), 5.61 (1H, s, H8), 4.72 (1H, m, H3), 4.59 (2H, m, H5), 4.34 (1H, d, *J* 12.3 Hz, H*4a*), 4.16 (3H, m, H2 and H*4b*), 2.78 (2H, q, *J* 7.1 Hz, H*9a*), 2.65 (2H, q, *J* 7.1 Hz, H*9b*), 1.66 (9H, s, 3 x H11), 0.95 (6H, t, *J* 7.1 Hz, 2 x H10); δ_C (101 MHz; $CDCl_3$) 154.7, 147.1, 138.0, 136.4, 136.3, 129.7 (2C), 127.5 (2C), 127.4, 114.9, 70.8, 67.4, 67.3, 60.6, 47.5; 44.8 (2C), 30.3 (3C) and 14.1 (2C); MS (ESI) *m/z* 485.4 (M^++H), HPLC purity: 98.9%; $t_{r'}$=8.06 min.

(*S*)-6-{4-[(1-tert-*butyl*-1H-*tetrazol*-5-*yl*)(*pyrrolidin*-1-*yl*)*methyl]benzyloxy*}-*6,7-dihydro*-2-*nitro*-5H-*imidazo*[2,1-*b*][1,3]*oxazine*, 4.19c (PA-5A)

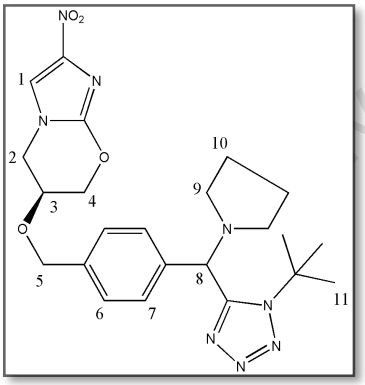

As a yellow solid (21 mg, 44%); m. p. 58- 61 °C, R_f (DCM: MeOH, 95: 05%) 0.39; IR ν_{max} (DCM)/cm^{-1} 1604 (Ar C=C), 1520 (NO_2), 1380 (N=N), 1360 (C=N), 1263 (C-O Ether); δ_H (300 MHz; $CDCl_3$) 7.50 (2H, d, *J* 8.1 Hz, 2 x H7), 7.37 (1H, d, *J* 6.7 Hz, H1), 7.26 (2H, d, *J* 8.1 Hz, 2 x H6), 5.20 (1H, s, H8), 4.72 (1H, m, H3), 4.62 (2H, m, H5), 4.34 (1H, d, *J* 12.1 Hz, H*4a*), 4.17 (3H, m, H2 and H*4b*), 2.59 (2H, m, H*9a*), 2.49 (2H, m, H*9b*), 1.79 (4H, m, 2 x H10), 1.68 (9H, s, 3 x H11); δ_C (75 MHz; $CDCl_3$) 155.5, 147.2, 136.1, 127.4, 123.1, 121.9 (2C), 119.2 (2C), 118.3, 79.9, 67.4, 63.2, 53.0, 52.2, 52.1, 41.2 (2C), 30.2 (3C) and 24.6 (2C); MS (ESI) *m/z* 483.4 (M^++H), HPLC purity: 99.6%; $t_{r'}$=7.68 min.

N-{2-[(4-{[((*S*)-6,7-*dihydro*-2-*nitro*-5H-*imidazo*[2,1-*b*][1,3]*oxazin*-6-*yloxy*)*methyl*]*pheny*}(1-tert-*butyl*-1H-*tetrazol*-5-*yl*)*methylamino*)*ethyl*]}-7-*chloroquinolin*-*4-amine*, 4.19d (PA-6A)

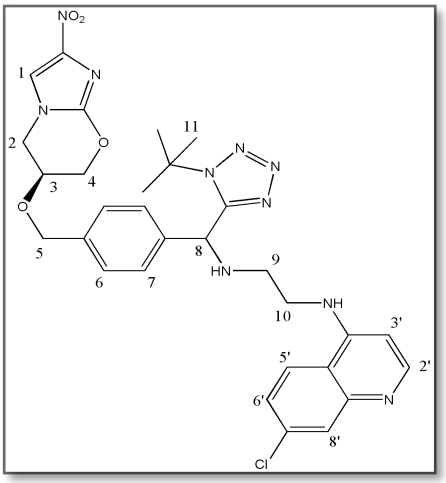

As a pale-yellow solid (27 mg, 65%); m. p. 87- 89 °C, R_f (DCM: MeOH, NH_4OH, 94: 5.5: 0.5%) 0.16; IR ν_{max} (DCM)/cm^{-1} 1610 (Ar C=C), 1550 (NO_2), 1390 (N=N), 1369 (C=N), 1250 (C-O Ether); δ_H (400 MHz; DMSO-*d6*) 8.35 (1H, d, *J* 5.4 Hz, H2'), 8.20 (1H, d, *J* 9.1 Hz, H5'), 7.99 (1H, d, *J* 4.3 Hz, H1), 7.77 (1H, d, *J* 2.2 Hz, H8'), 7.43 (3H, m, 2 x H7 and H6'), 7.26 (2H, d, *J* 8.1 Hz, 2 x H6), 7.18 (1H, t, *J* 5.3 Hz, NH), 6.43 (1H, d, *J* 5.4 Hz, H3'), 5.53 (1H, s, H8), 4.63 (3H, m, H3 and H5), 4.46 (1H, d, *J* 11.9 Hz, H*4a*), 4.23 (3H, m, H2 and H*4b*), 3.35 (2H, m, H9), 4.30 (1H, br m, NH), 2.78 (2H, m, H10), 1.62 (9H, s, 3 x H11); δ_C (101 MHz; DMSO-*d6*) 158.2, 155.8, 151.7 (2C), 149.9, 148.9, 146.5, 138.6, 137.1, 133.2, 128.1 (2C), 127.5 (2C), 127.4 (2C), 123.9, 123.8, 117.8, 98.6, 69.2, 67.7, 66.3, 55.8 46.6, 45.1; 42.5 and 29.2 (3C); MS (ESI) *m/z* 633.5 (M^+), HPLC purity: 96.2%; t_r,=8.44 min.

N-{3-[(4-{[((*S*)-6,7-*dihydro*-2-*nitro*-5H-*imidazo*[2,1-*b*][1,3]*oxazin*-6-*yloxy*)*methyl*]*pheny*}(1-tert-*butyl*-1H-*tetrazol*-5-*yl*)*methylamino*)*propyl*]}-7-*chloroquinolin*-*4-amine*, 4.19e (PA-7A)

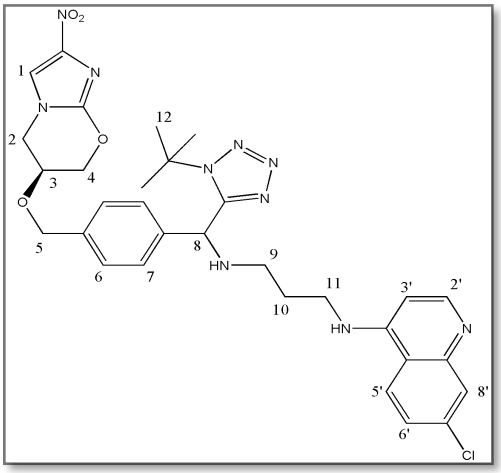

As a pale-yellow solid (20 mg, 47%); m. p. 95- 99 °C, R_f (DCM: MeOH, NH_4OH, 94: 5.5: 0.5%) 0.35; IR ν_{max} (DCM)/cm^{-1} 1613 (Ar C=C), 1576 (NO_2), 1369 (N=N), 1387 (C=N), 1265 (C-O Ether); δ_H (400 MHz; $CDCl_3$) 8.45 (1H, d, *J* 5.3 Hz, H2'), 7.86 (1H, d, *J* 2.2 Hz, H8'), 7.27 (6H, m,

2 x H7, 2 x H6, H1 and H5'), 7.15 (1H, br s, NH), 6.95 (1H, dd, *J* 9.0 and 2.2 Hz, H6'), 6.29 (1H, d, *J* 5.3 Hz, H3'), 5.30 (1H, s, H8), 4.73 (1H, m, H3), 4.63 (2H, dd, *J* 12.1 and 3.5Hz, H5), 4.36 (1H, d, *J* 12.1 Hz, H*4a*), 4.18 (3H, m, H2 and H*4b*), 3.41 (2H, m, H9), 2.88 (1H, m, H*11a*), 2.79 (1H, m, H*11b*), 1.92 (2H, m, H10), 1.53 (9H, s, 3 x H12); δ_C (101 MHz; $CDCl_3$) 156.7, 155.2, 152.0 (2C), 150.2, 149.0, 147.0, 144.1, 143.7, 138.3, 137.4, 134.4, 128.4 (2C), 128.3, 128.2, 124.8, 122.1, 117.4, 98.4, 70.5, 67.2, 67.1, 61.6, 59.0, 47.8, 47.4; 43.5 and 29.8 (3C); MS (ESI) *m/z* 647.4 (M^+), HPLC purity: 99.2%; t_r'=8.61 min.

N-{4-[(4-{[((*S*)-6,7-*dihydro*-2-*nitro*-5H-*imidazo*[2,1-*b*][1,3]*oxazin*-6-*yloxy*)*methyl*]*pheny*}(1-tert-*butyl*-1H-*tetrazol*-5-*yl*)*methylamino*)*butyl*]}-7-*chloroquinolin*-4-*amine*, 4.19f (PA-8A)

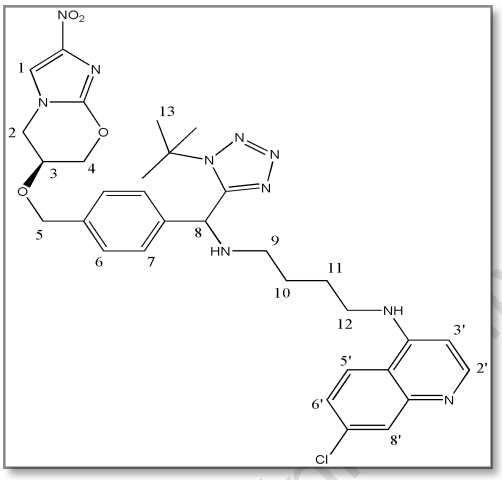

As a pale-yellow solid (37 mg, 85%); m. p. 82- 86 °C, R_f (DCM: MeOH, NH_4OH, 94: 5.5: 0.5%) 0.32; IR ν_{max} (DCM)/cm^{-1} 1619 (Ar C=C), 1555 (NO_2), 1388 (N=N), 1360 (C=N), 1248 (C-O Ether); δ_H (400 MHz; $CDCl_3$) 8.48 (1H, d, *J* 5.4 Hz, H2'), 7.92 (1H, d, *J* 2.0 Hz, H8'), 7.57 (1H, dd, *J* 9.2 and 2.0 Hz, H6'), 7.33 (1H, d, *J* 6.5 Hz, H1), 7.24 (5H, m, 2 x H7, 2 x H6 and H5'), 6.37 (1H, d, *J* 5.4 Hz, H3'), 5.48 (1H, m, NH), 5.27 (1H, s, H8), 4.67 (1H, m, H3), 4.60 (2H, m, H5), 4.32 (1H, d, *J* 11.7 Hz, H*4a*), 4.12 (3H, m, H2 and H*4b*), 3.32 (2H, m, H12), 2.62 (2H, m, H9), 1.83 (2H, m, H11), 1.69 (2H, m, H10), 1.61 (9H, s, 3 x H13); δ_C (101 MHz; $CDCl_3$) 157.4, 155.5, 151.9 (2C), 149.9, 149.8, 138.9, 137.1, 137.0, 128.6, 128.5, 128.3 (2C), 128.1, 128.0, 125.1, 121.2, 115.0, 99.0, 70.6, 67.3, 67.2, 66.9, 66.8, 58.8, 47.5, 42.9, 30.1 (3C), 27.4 and 26.3; MS (ESI) *m/z* 661.5 (M^+), HPLC purity: 96.9%; t_r'=8.66 min.

N-{5-[(4-{[((*S*)-6,7-*dihydro*-2-*nitro*-5H-*imidazo*[2,1-*b*][1,3]*oxazin*-6-*yloxy*)*methyl*]*pheny*}(1-tert-*butyl*-1H-*tetrazol*-5-*yl*)*methylamino*)*pentan*-2-*yl*]}-6-*methoxyquinolin*-*8*-*amine*, 4.19g (PA-9A)

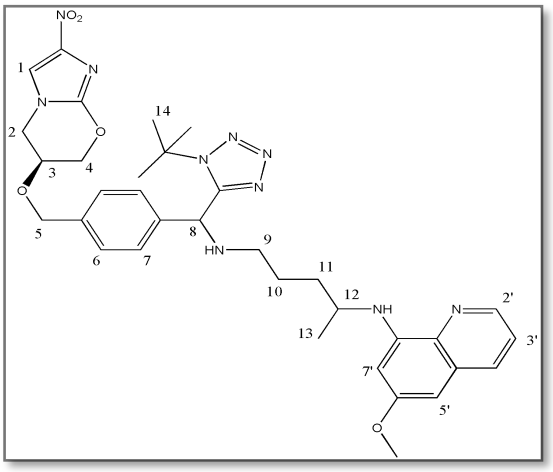

As a thick-yellow oil (55 mg, 83%; 1:1 diastereomeric mixture); R_f (DCM: MeOH, 95: 05%) 0.48; IR ν_{max} (DCM)/cm^{-1} 1601 (Ar C=C), 1539 (NO_2), 1388 (N=N), 1338 (C=N), 1238 (C-O Ester); δ_H (300 MHz; $CDCl_3$) 8.59 (1H, s, H1), 8.50 (1H, dd, *J* 4.2 and 1.6 Hz, H2'), 7.91 (1H, dd, *J* 8.3 and 1.6 Hz, H4'), 7.36 (1H, dd, *J* 8.7 and 4.4 Hz, H3'), 7.31 (2H, m, H7), 7.22 (2H, m, H6), 6.32 (1H, d, *J* 2.5 Hz, H7'), 6.24 (1H, t, *J* 2.8 Hz, H5'), 6.01 (1H, br m, NH), 5.24-5.26 (1H, 2 x s, H8), 4.68 (1H, d, *J* 12.2 Hz, H3), 4.57 (2H, m, H5), 4.31 (1H, d, *J* 12.4 Hz, H*4a*), 4.12 (3H, m, H2 and H*4b*), 3.88 (3H, s, OCH_3), 3.57 (1H, m, H12), 2.56 (2H, m, H9), 1.64 (4H, m, H10 and H11), 1.59-1.60 (9H, 2 x s, 3 x H14), 1.27 (3H, d, *J* 6.3 Hz, H13); δ_C (75 MHz; $CDCl_3$) 159.5, 155.6, 145.0, 144.3, 143.8, 139.7, 136.6, 134.8, 129.9, 128.5 (2C), 128.2, 128.1 (2C), 127.4, 121.8, 114.9, 96.6, 91.6, 70.6, 67.3, 67.2, 66.4, 58.5, 55.2, 47.9; 47.5, 47.4, 34.2, 29.8 (3C), 26.5 and 20.6; MS (ESI) *m/z* 671.6 (M^++H), HPLC purity: 98.7%; t_r=8.52 min.

N-{5-[(3-{[((*S*)-6,7-*dihydro*-2-*nitro*-5H-*imidazo*[2,1-*b*][1,3]*oxazin*-6-*yloxy*)*methyl*]*pheny*}(1-tert-*butyl*-1H-*tetrazol*-5-*yl*)*methylamino*)*pentan*-2-*yl*]}-6-*methoxyquinolin*-*8*-*amine*, 4.19h (PA-11A)

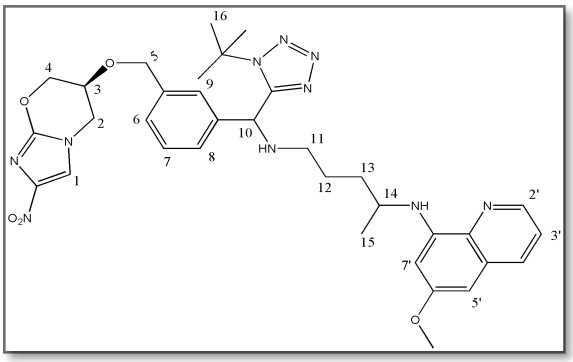

As a thick-yellow oil (140 mg, 79%; 1:1 diastereomeric mixture); R_f (DCM: MeOH, 95: 05%) 0.52; IR ν_{max} (DCM)/cm^{-1} 1610 (Ar C=C), 1545 (NO_2), 1390 (N=N), 1340

(C=N), 1228 (C-O Ester); δ_H (400 MHz; $CDCl_3$) 8.50 (1H, s, H1), 8.49 (1H, dd, *J* 4.2 and 1.7 Hz, H2'), 7.90 (1H, dd, *J* 8.3 and 1.6 Hz, H4'), 7.32 (1H, s, H9), 7.31 (2H, m, H3' and H8), 7.20 (2H, m, H6 and H7), 6.32 (1H, d, *J* 2.5 Hz, H7'), 6.24 (1H, dd, *J* 6.8 and 2.7 Hz, H5'), 5.99 (1H, br m, NH), 5.25-5.27 (1H, 2 x s, H10), 4.66 (1H, m, H3), 4.54 (2H, m, H5), 4.26 (1H, m, H*4a*), 4.09 (3H, m, H2 and H*4b*), 3.86-3.87 (3H, 2 x s, OCH_3), 3.59 (1H, m, H14), 2.55 (2H, m, H11), 1.72 (9H, s, 3 x H16), 1.66 (4H, m, H12 and H13), 1.27-1.29 (3H, 2 x d, *J* 5.9 and 6.3 Hz, H15); δ_C (101 MHz; $CDCl_3$) 159.5, 155.7, 145.0, 144.2, 139.7, 137.5, 135.3, 134.8, 129.9, 129.2, 128.1, 127.6, 127.5, 127.0, 121.9, 115.1, 96.7, 91.6, 70.9, 67.7, 66.5, 66.4, 58.6, 55.2, 47.9; 47.8, 47.4, 34.3, 29.9 (3C), 26.5 and 20.6; MS (ESI) *m/z* 671.9 (M^++H), HPLC purity: 95.6%; $t_{r'}$=8.55 min.

General procedure[1] for the synthesis of 4-aminoquinoline-imines 4.21a-g.

Quinoline diamine **3.13a-c** (1.0 mmol) and various aldehydes (1.0 mmol) were stirred in anhydrous methanol at room temperature for 24 hrs, thereafter solvent removed *in vacuo* to afford crude imines **4.21a-g** which were further dried under vacuum for 4 hrs. Imines in general are known to be unstable and they tend to break down is silica hence these were subsequently used without further purification and the reported yields are crude product yields.

N-*[(Benzylideneamino)ethyl]*-7-*Chloroquinolin*-4-*amine*, 4.21a

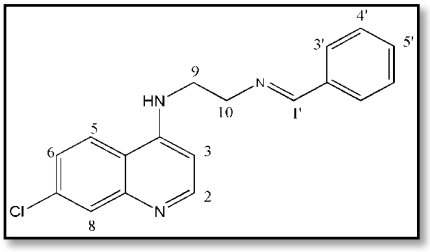

As a cream-coloured powder (0.39 g, 65%); δ_H (300 MHz; DMSO-*d6*) 8.42 (1H, d, *J* 5.4 Hz, H2), 8.36 (1H, s, H1'), 8.25 (1H, d, *J* 9.0 Hz, H5), 7.78 (1H, d, *J* 2.4 Hz, H8), 7.73 (2H, d, *J* 2.1 Hz, 2 x H3'), 7.72 (1H, dd,

J 1.5 and 3.3 Hz, H5'), 7.44 (1H, dd, *J* 9.0 and 2.3 Hz, H6), 7.43 (2H, m, 2 x H4'), 6.61 (1H, d, *J* 5.4 Hz, H3), 3.91 (2H, m, H9), 3.61 (2H, m, H10); *m*/*z* 309.85 (MH^+, 32.9%) and 133.96 (M^+-$C_9H_6N_2Cl$, 100%).

N-*[(4-Chlorobenzylideneamino)ethyl]-7-Chloroquinolin-4-amine*, 4.21b

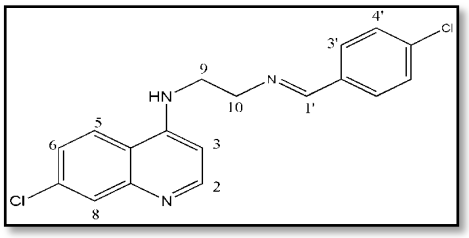

As a cream-coloured powder (0.28 g, 72.3%); δ_H (300 MHz; DMSO-*d6*) 8.42 (1H, d, *J* 5.2 Hz, H2), 8.37 (1H, s, H1'), 8.22 (1H, d, *J* 8.8 Hz, H5), 7.78 (1H, d, *J* 1.8 Hz, H8), 7.74 (2H, d, *J* 2.2 Hz, 2 x H3'), 7.48 (2H, d, *J* 2.2 Hz, 2 x H4'), 7.41 (1H, dd, *J* 8.8 and 2.0 Hz, H6), 7.17 (1H, t, *J* 0.8 Hz, NH), 6.60 (1H, d, *J* 5.2 Hz, H3), 3.91 (2H, t, *J* 5.6 Hz, H9), 3.63 (2H, m, H10); *m*/*z* 342.66 (M^+, 54.6%)

N-*[(3,4-Dichlorobenzylideneamino)ethyl]-7-Chloroquinolin-4-amine*, 4.21c

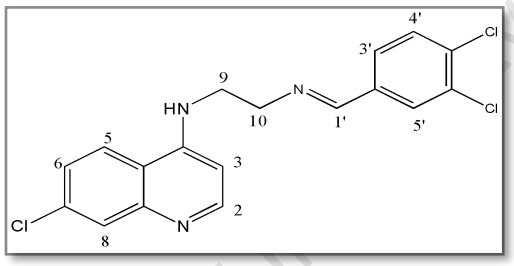

As a cream-coloured solid (0.22 g, 57.9%); δ_H (400 MHz; DMSO-*d6*) 8.42 (1H, d, *J* 5.2 Hz, H2), 8.35 (1H, s, H1'), 8.22 (1H, d, *J* 9.2 Hz, H5), 7.91 (1H, s, H5'), 7.78 (1H, d, *J* 2.4 Hz, H8), 7.67 (2H, d, *J* 2.1 Hz, H3' and H4'), 7.40 (1H, dd, *J* 9.2 and 2.4 Hz, H6), 7.19 (1H, br s, NH), 6.59 (1H, d, *J* 5.2 Hz, H3), 3.91 (2H, t, *J* 6.2 Hz, H9), 3.65 (2H, m, H10); *m*/*z* 378.73 (M^+, 6.1%) and 190.84 (M^+-$C_8H_6NCl_2$, 100%).

N-*[(4-Methoxybenzylideneamino)ethyl]-7-Chloroquinolin-4-amine*, 4.21d

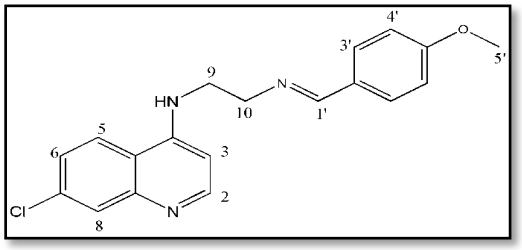

As a pale-yellow solid (0.17 g, 49%); δ_H (300 MHz; DMSO-*d6*) 8.65 (1H, d, *J* 5.0 Hz, H2), 8.55 (1H, s, H1'), 8.34 (1H, d, *J* 9.0 Hz, H5),

7.92 (1H, d, *J* 2.3 Hz, H8), 7.77 (2H, d, *J* 2.5 Hz, 2 x H3'), 7.67 (2H, d, *J* 2.5 Hz, 2 x H4'), 7.45 (1H, dd, *J* 9.0 and 2.4 Hz, H6), 7.29 (1H, s, NH), 6.65 (1H, d, *J* 5.4 Hz, H3), 3.91 (2H, t, *J* 7.2 Hz, H9), 3.65 (2H, t, *J* 7.4 Hz, H10).

N-*[(4-Methylbenzylideneamino)ethyl]*-7-*Chloroquinolin*-4-*amine*, 4.21e

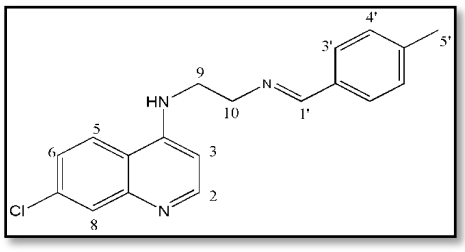

As a pale-yellow solid (0.21 g, 59%); δ_H (400 MHz; DMSO-*d6*) 8.41 (1H, d, *J* 5.4 Hz, H2), 8.39 (1H, d, *J* 9.2 Hz, H5), 8.29 (1H, s, H1'), 8.24 (1H, d, *J* 1.5 Hz, H8), 7.83 (2H, d, *J* 7.3 Hz, 2 x H3'), 7.78 (1H, dd, *J* 9.o and 1.6 Hz, H6), 7.33 (1H, br m, NH), 7.21 (2H, d, *J* 7.3 Hz, 2 x H4'), 6.59 (1H, d, *J* 5.4 Hz, H3), 3.86 (2H, m, H9), 3.59 (2H, m, H10).

N-*[3-(Benzylideneamino)propyl]*-7-*Chloroquinolin*-4-*amine*, 4.21f

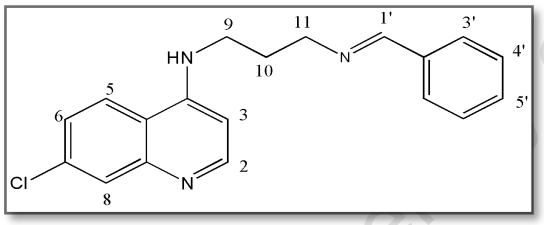

As a pale-yellow paste (0.11 g, 39%); δ_H (400 MHz; DMSO-*d6*) 8.39 (2H, d, *J* 5.6 Hz, H2 and H1'), 8.28 (1H, d, *J* 9.0 Hz, H5), 7.96 (1H, d, *J* 2.0 Hz, H8), 7.75 (1H, dd, *J* 9.0 and 2.0 Hz, H6), 7.45 (5H, m, ArH), 7.37 (1H, br m, NH), 6.49 (1H, d, *J* 5.6 Hz, H3), 3.71 (2H, t, *J* 6.8 Hz, H9), 3.40 (2H, m, H11), 2.40 (2H, m, H10).

N-*[4-(Benzylideneamino)butyl]*-7-*Chloroquinolin*-4-*amine*, 4.21g

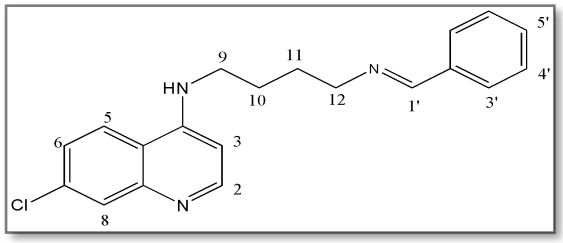

As a yellow paste (0.25 g, 79%); δ_H (400 MHz; DMSO-*d6*) 8.37 (1H, d, *J* 5.1 Hz, H2), 8.34 (1H, s, H1'), 8.27 (1H, d, *J* 9.1 Hz, H5), 7.01 (1H, d, *J* 9.0 Hz, H6), 7.75 (1H, s, H8),

7.44 (5H, m, ArH), 7.32 (1H, br m, NH), 6.47 (1H, d, *J* 5.1 Hz, H3), 3.61 (2H, t, *J* 5.7 Hz, H9), 3.31 (2H, m, H12), 1.74 (4H, m, H10 and H11);

General procedure[1] for the synthesis of 4-aminoquinoline- β-lactams 4.22a-g

Imines **4.21a-g** (1.0 eq) and Et_3N (3.0 eq) were stirred in dry DCM (5 ml) at -78 °C under inert N_2 atmosphere, followed by drop-wise addition of the methoxy acetyl chloride (1.5 eq) in dry DCM (2 ml). The resulting mixtures were allowed to warm to room temperature and further stirred overnight. Thereafter, saturated $NaHCO_3$ was added to the mixture and the organic layer extracted with DCM, washed with brine and water, dried over $MgSO_4$ and solvent removed *in vacuo* to yield crude products, which were purified by column chromatography to obtain the desired β-lactams **4.22a-g**. The synthesized β-lactams were obtained as the *cis* (coupling constant 4.5 ppm) configuration. This is so because the coupling constants between ^1H and ^2H are usually between 4-6 ppm for *cis* configuration.[8]

1-[2-(7-*Chloroquinolin*-4-yl*amino*)*ethyl*]-3-*methoxy*-4-*phenylazetidin*-2-*one*, 4.22a (BL1)

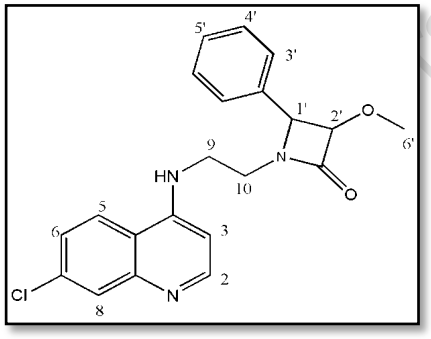

As a white solid (55 mg, 30%); m. p. 142- 146 °C, R_f (DCM: MeOH, 95: 0.5%) 0.21; IR ν_{max} (DCM)/cm^{-1} 1744 (C=O), 1620 (Ar C=C), 1264 (C-O Ester); δ_H (400 MHz; $CDCl_3$) 8.49 (1H, d, *J* 5.4 Hz, H2), 8.00 (1H, d, *J* 2.1 Hz, H8), 7.84 (1H, d, *J* 9.0 Hz, H5), 7.42 (1H, dd, *J* 9.0 and 2.1 Hz, H6), 7.35 (5H, m, ArH), 6.26 (1H, d, *J* 5.4 Hz, H3), 4.97 (1H, d, *J* 4.4 Hz, H1'), 4.74 (1H, d, *J* 4.4 Hz, H2'), 3.54 (2H, m, H9), 3.46 (2H, m, H10), 3.12 (3H, s, H6'); δ_C (101 MHz; $CDCl_3$) 168.9, 151.5, 149.8, 148.8, 135.3, 133.2, 129.1, 128.7 (2C), 128.4, 128.3 (2C), 125.8, 121.9, 117.3, 98.5, 85.4, 63.3, 58.2, 42.4 and 41.1; MS (ESI) *m/z* 382.1 (M^+), HPLC purity: 95.6%; t_r'=8.37 min.

1-[2-(7-*Chloroquinolin*-4-yl*amino*)*ethyl*]-4-*(*4-*chlorophenyl*)-3-*methoxyazetidin*-2-*one*, 4.22b (Bl2)

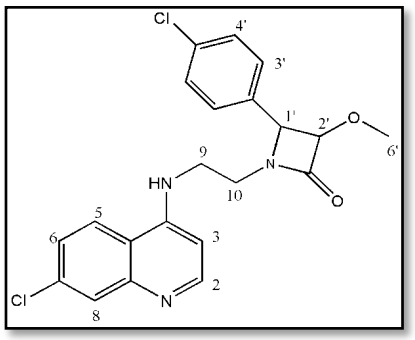

As a pale-yellow solid (20.3 mg, 14%); m. p. 135- 138 °C, R_f (DCM: MeOH, 95: 0.5%) 0.14; IR ν_{max} (DCM)/cm^{-1} 1740 (C=O), 1598 (Ar C=C), 1265 (C-O Ester); δ_H (400 MHz; $CDCl_3$) 8.46 (1H, d, *J* 5.3 Hz, H2), 7.95 (1H, d, *J* 1.9 Hz, H8), 7.85 (1H, d, *J* 9.0 Hz, H5), 7.39 (1H, dd, *J* 9.0 and 1.9 Hz, H6), 7.31 (2H, d, *J* 8.5 Hz, 2 x H4'), 7.24 (2H, d, *J* 8.5 Hz, 2 x H3'), 6.47 (1H, br s, NH), 6.24 (1H, d, *J* 5.3 Hz, H3), 4.77 (1H, d, *J* 4.3 Hz, H1'), 4.72 (1H, d, *J* 4.3 Hz, H2'), 3.54 (1H, m, H*10a*), 3.47 (3H, m, H9 and H*10b*), 3.13 (3H, s, H6'); δ_C (101 MHz; $CDCl_3$) 168.7, 151.2, 150.0, 148.4, 135.4, 135.1, 131.2, 129.7 (2C), 128.9 (2C), 128.0, 125.9, 122.0, 117.2, 98.5, 85.4, 62.6, 58.3, 42.3 and 41.0; MS (ESI) *m/z* 416.1 (M^+), HPLC purity: 99.2%; t_r'=8.63 min.

1-[2-(7-*Chloroquinolin*-4-yl*amino*)*ethyl*]-4-*(*3,4-*dichlorophenyl*)-3-*methoxyazetidin*-2-*one*, 4.22c (BL3)

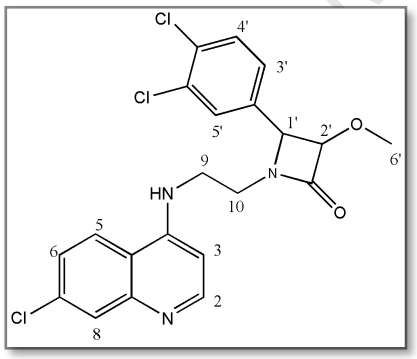

As a pale-yellow solid (17.3 g, 4%); m. p. 152- 156 °C, R_f (DCM: MeOH, 95: 0.5%) 0.16; IR ν_{max} (DCM)/cm^{-1} 1739 (C=O), 1601 (Ar C=C), 1277 (C-O Ester); δ_H (400 MHz; $CDCl_3$) 8.45 (1H, d, *J* 5.6 Hz, H2), 7.96 (1H, d, *J* 2.1 Hz, H8), 7.89 (1H, d, *J* 9.0 Hz, H5), 7.39 (3H, m, ArH), 7.16 (1H, dd, *J* 9.0 and 2.1 Hz, H6), 6.74 (1H, br s, NH), 6.25 (1H, d, *J* 5.6 Hz, H3), 4.78 (1H, d, *J* 4.4 Hz, H1'), 4.74 (1H, d, *J* 4.4 Hz, H2'), 3.49 (2H, m, H9), 3.43 (2H, m, H10), 3.18 (3H, s, H6'); δ_C (101 MHz; $CDCl_3$) 168.6, 150.5, 150.1, 147.2, 136.0, 133.7, 133.2, 130.6, 130.4, 127.6, 127.0, 126.2, 126.1, 122.2, 117.0, 98.3, 85.5, 62.1, 58.6, 42.2 and 41.0; MS (ESI) *m/z* 450.3 (M^+), HPLC purity: 99.5%; t_r'=8.81 min.

1-[2-(7-*Chloroquinolin*-4-yl*amino*)*ethyl*]-3-*methoxy*-4-(4-*methoxyphenyl*)*azetidin*-2-*one*, 4.22d (BL4)

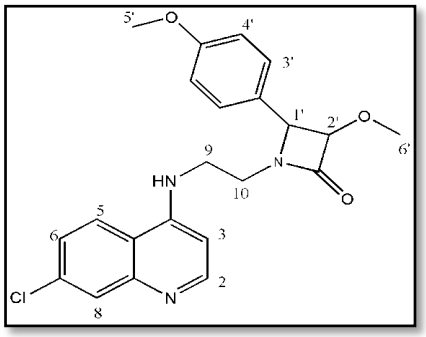

As a yellow solid (44.6 mg, 9%); m. p. 144- 147 °C, R_f (DCM: MeOH, 95: 0.5%) 0.21; IR ν_{max} (DCM)/cm^{-1} 1746 (C=O), 1610 (Ar C=C), 1267 (C-O Ester);δ_H (400 MHz; $CDCl_3$) 8.48 (1H, d, *J* 5.5 Hz, H2), 7.98 (1H, s, H8), 7.84 (1H, d, *J* 8.9 Hz, H5), 7.41 (1H, d, *J* 9.0, H6), 7.24 (2H, d, *J* 8.6 Hz, 2 x H4'), 6.86 (2H, d, *J* 8.6 Hz, 2 x H3'), 6.45 (1H, br s, NH), 6.25 (1H, d, *J* 5.5 Hz, H3), 4.74 (1H, d, *J* 4.4 Hz, H1'), 4.71 (1H, d, *J* 4.4 Hz, H2'), 3.79 (3H, s, H5'), 3.52 (2H, t, *J* 4.6 Hz, H9), 3.47 (1H, m, H*10a*), 3.41 (1H, m, H*10b*), 2.92 (3H, s, H6'); δ_C (101 MHz; $CDCl_3$) 169.0, 160.3, 151.1, 150.1, 148.3, 135.5, 129.7 (2C), 127.9, 125.9, 124.8, 122.0, 117.2, 114.1 (2C), 98.4, 85.3, 62.9, 58.2, 55.3, 42.5 and 40.9; MS (ESI) *m/z* 412.1 (M^+), HPLC purity: 95.6%; t_r'=8.43 min.

1-[2-(7-*Chloroquinolin*-4-yl*amino*)*ethyl*]-3-*methoxy*-4-p-*tolylazetidin*-2-*one*, 4.22e (BL5)

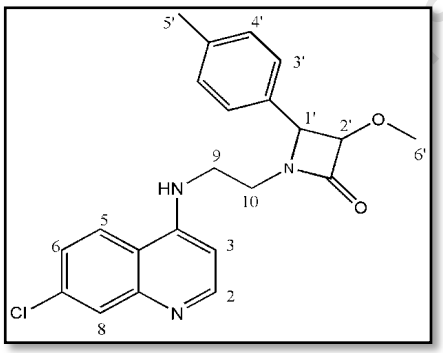

As a yellow solid (21 mg, 6%); m. p. 78- 82 °C, R_f (DCM: MeOH, 95: 0.5%) 0.31; IR ν_{max} (DCM)/cm^{-1} 1744 (C=O), 1604 (Ar C=C), 12652 (C-O Ester); δ_H (400 MHz; $CDCl_3$) 8.49 (1H, d, *J* 1.3 Hz, H8), 8.04 (1H, d, *J* 5.7 Hz, H2), 7.88 (1H, d, *J* 9.0 Hz, H5), 7.41 (1H, dd, *J* 9.0 and 1.3 Hz Hz, H6), 7.20 (2H, d, *J* 8.0 Hz, 2 x H4'), 7.14 (2H, d, *J* 8.0 Hz, 2 x H3'), 6.78 (1H, br s, NH), 6.24 (1H, d, *J* 5.7 Hz, H3), 4.77 (1H, d, *J* 4.3 Hz, H1'), 4.73 (1H, d, *J* 4.3 Hz, H2'), 3.52 (2H, m, H9), 3.47 (2H, m, H10), 3.13 (3H, s, H6'), 2.35 (3H, s, H5'); δ_C (101 MHz; $CDCl_3$) 169.0, 150.7, 150.1, 147.1, 139.1, 136.0, 129.4 (2C), 128.9, 128.4 (2C), 126.8, 126.1, 122.3, 117.0, 98.2, 85.3, 63.1, 58.2, 42.5, 40.9 and 21.6; MS (ESI) *m/z* 396.2 (M^+), HPLC purity: 94.6%; t_r'=8.29 min.

1-[3-(7-*Chloroquinolin*-4-yl*amino*)*propyl*]-3-*methoxy*-4-*phenylazetidin*-2-*one*, 4.22f (BL6)

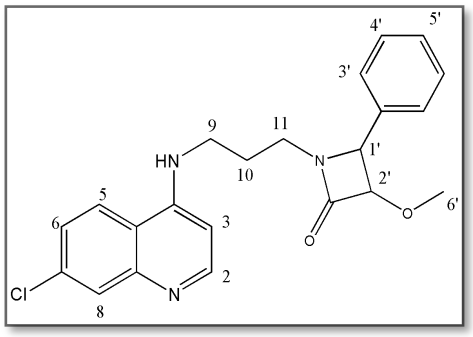

As a yellow paste (19.6 mg, 5%); R_f (DCM: MeOH, 95: 0.5%) 0.41; IR ν_{max} (DCM)/cm^{-1} 1745 (C=O), 1609 (Ar C=C), 1269 (C-O Ester); δ_H (300 MHz; $CDCl_3$) 8.50 (1H, d, *J* 5.4 Hz, H2), 7.95 (1H, d, *J* 2.0 Hz, H8), 7.84 (1H, d, *J* 9.0 Hz, H5), 7.40 (1H, m, H6), 7.36 (5H, m, ArH), 6.36 (1H, d, *J* 5.4 Hz, H3), 6.08 (1H, br s, NH), 4.73 (1H, d, *J* 4.4 Hz, H1'), 4.70 (1H, d, *J* 4.4 Hz, H2'), 3.49 (3H, s, H6'), 3.43 (2H, m, H11), 3.18 (2H, m, H9), 1.80 (1H, m, H*10a*), 1.64 (1H, m, H*10b*); δ_C (75 MHz; $CDCl_3$) 169.2, 155.2, 147.5, 140.1, 136.8, 136.2, 129.0, 128.7, 128.5, 128.1, 126.6, 125.9, 124.3, 122.1, 117.5, 98.5, 85.1, 61.9, 57.8, 42.1, 40.5 and 26.7; MS (ESI) *m/z* 396.7 (M^++H), HPLC purity: 97.2%; t_r'=9.06 min.

1-[4-(7-*Chloroquinolin*-4-yl*amino*)*butyl*]-3-*methoxy*-4-*phenylazetidin*-2-*one*, 4.22g (BL7)

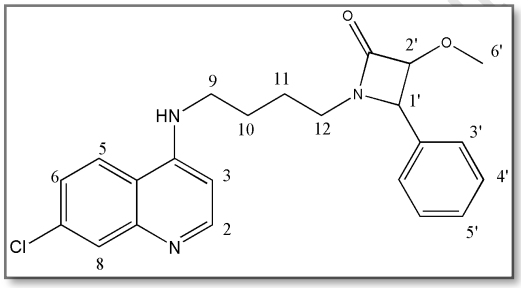

As a yellow solid (28 mg, 9%); m. p. 86- 89 °C, R_f (DCM: MeOH, 95: 0.5%) 0.31; IR ν_{max} (DCM)/cm^{-1} 1739 (C=O), 1599 (Ar C=C), 1258 (C-O Ester); δ_H (400 MHz; $CDCl_3$) 8.39 (1H, d, *J* 9.0 Hz, H5), 8.28 (1H, d, *J* 5.6 Hz, H2), 8.05 (1H, s, H8), 7.92 (1H, br s, NH), 7.36 (6H, m, H6 and ArH), 6.39 (1H, d, *J* 5.6 Hz, H3), 4.76 (1H, d, *J* 4.3 Hz, H1'), 4.73 (1H, d, *J* 4.3 Hz, H2'), 3.44 (4H, m, H9 and H12), 3.09 (3H, s, H6'), 1.92 (2H, m, H10), 1.72 (2H, m, H11); δ_C (101 MHz; $CDCl_3$) 167.7, 153.5, 145.6, 142.7, 137.7, 133.5, 128.8, 128.5 (2C), 128.4, 126.7, 126.2, 124.1, 123.1, 116.3, 98.1, 85.4, 62.4, 58.1, 43.2, 40.9, 25.6 and 25.1; MS (ESI) *m/z* 410.5 (M^+), HPLC purity: 98.0%; t_r'=9.12 min.

6.5 Procedures for biological evaluation

6.5.1 *In vitro* Antiplasmodial assays:[11] 3D7 and K1 strains (London School of Hygiene and Tropical Medicine, UK)

Two clones of *P. falciparum* were used: (a) the 3D7 clone of NF54 which is known to be sensitive to all anti-malarials, (b) the K1 strain originating from Thailand that is resistant to chloroquine and pyrimethamine, but sensitive to mefloquine. The cultures are naturally, asynchronous (65-75% ring stage) and were maintained in continuous log phase growth in RPMI 1640 supplemented with 5% washed human A+ erythrocytes , 25mM HEPES, 32nM $NaHCO_3$ and AlbuMAXII (lipid rich bovine serum albumin) (GIBCO, Grand Island, NY) (CM). All cultures and assays were conducted at 37°C under an atmosphere of 5% CO_2 and 5% O_2, with a balance N_2. These assays were performed in various stages i.e. the primary and secondary screens.

Drug sensitivity assays

Stock drug solutions were prepared in 100% DMSO (dimethylsulfoxide) at 20 mg/ml unless otherwise suggested by the supplier. The compound is further diluted to the appropriate concentration using complete medium RPMI1640 supplemented with 15nM cold hypoxanthine and AlbuMAXII.

Assays were performed in sterile 96-well microtitre plates, each plate containing 100 µl of parasite culture (0.5% parasitemia, 2.5% hematocrit). The test compounds were tested in triplicate and parasite growth compared to the control and blank (uninfected erythtocytes) wells. After 24h of incubation at 37°C, 3.7Bq of [^{3}H]hypoxanthine was added to each well [1]. Cultures were incubated for a further 24 h before they were harvested onto glass-fiber filter mats. The radioactivity was counted using a Wallac Microbeta 1450 scintillation

counter. The results were recorded as counts per minute (CPM) per well at each compound concentration, control and blank wells. Percentage inhibition was calculated from comparison to blank and control wells, and IC_{50} values calculated using GraphPad Prism 4.0.

Primary Screen

The primary screen used the 3D7 strain. The test compounds were tested at 6 concentrations (30, 10, 3, 1, 0.3, and 0.1µg/mL). Compounds that did not affect parasite growth at 10µg/mL are considered inactive, between 10 and 11µg/mL are designated as partially active and if <1µg/mL the compound was classified as active and was further evaluated by three-fold serial dilutions in a repeat test.

Secondary Screen

In this screen both 3D7 and K1 were used. The test drug was diluted 3-fold over at 12 different concentrations with an appropriate starting concentrations based on the primary screen. The IC_{50} values were determined by sigmoidal dose response analysis using Microsoft XLFit (IDBS, UK). For each assay, the IC_{50} values for each parasite line were determined against CQ and other standard compounds appropriate for the assay.

6.5.2 *In vitro* Antiprotozoan and cytotoxicity assays: *T.b. brucei rhodesiense* STIB900, K1 and L6 mammalian cell-line (Swiss Tropical and Public Health Institute, Switzerland)

Activity against *Trypanosoma brucei rhodesiense* STIB900[12,13,14]

This stock was isolated in 1982 from a human patient in Tanzania and after several mouse passages was cloned and adapted to axenic culture conditions (Baltz et al 1985) Minimum Essential Medium (50 µl) supplemented with 25 mM HEPES, 1g/l additional glucose, 1% MEM non-essential amino acids (100x), 0.2 mM 2-mercaptoethanol, 1mM Na-pyruvate and

15% heat inactivated horse serum were added to each well of a 96-well microtiter plate. Serial drug dilutions of eleven three-fold dilution steps covering a range from 100 to 0.002 µg/ml were prepared. Then, $4x10^3$ bloodstream forms of *T. b. rhodesiense* STIB 900 in 50 µl was added to each well and the plate incubated at 37 °C under a 5 % CO_2 atmosphere for 70 h. 10 µl Alamar Blue (resazurin, 12.5 mg in 100 ml double-distilled water) was then added to each well and incubation continued for a further 2–4 h (Raz et al 1997). Then the plates were read with a Spectramax Gemini XS microplate fluorometer (Molecular Devices Cooperation, Sunnyvale, CA, USA) using an excitation wave length of 536 nm and an emission wave length of 588 nm. The IC50 values were calculated by linear regression (Huber 1993) from the sigmoidal dose inhibition curves using SoftmaxPro software (Molecular Devices Cooperation, Sunnyvale, CA, USA).

Activity against K1 strain of *P. falciparum*,[11,15]

In vitro activity against erythrocytic stages of *P. falciparum* was determined using a ^{3}H-hypoxanthine incorporation assay, using the chloroquine and pyrimethamine resistant K1 strain that originate from Thailand and the standard drug chloroquine (Sigma C6628). Compounds were dissolved in DMSO at 10 mg/mL and added to parasite cultures incubated in RPMI 1640 medium without hypoxanthine, supplemented with HEPES (5.94 g/l), $NaHCO_3$ (2.1 g/l), neomycin (100 U/mL), Albumax^R (5 g/l) and washed human red cells A^+ at 2.5% haematocrit (0.3% parasitaemia). Serial drug dilutions of eleven three-fold dilution steps covering a range from 100 to 0.002 µg/ml were prepared. The 96-well plates were incubated in a humidified atmosphere at 37 °C; 4% CO_2, 3% O_2, 93% N_2. After 48 h 50 µl of ^{3}H-hypoxanthine (=0.5 µCi) was added to each well of the plate. The plates were incubated for a further 24 h under the same conditions. The plates were then harvested with a Betaplate™ cell harvester (Wallac, Zurich, Switzerland), and the red blood cells transferred onto a glass fibre filter then washed with distilled water. The dried filters were inserted into a

plastic foil with 10 mL of scintillation fluid, and counted in a Betaplate™ liquid scintillation counter (Wallac, Zurich, Switzerland). IC_{50} values were calculated from sigmoidal inhibition curves by linear regression using Microsoft Excel.

***In vitro* cytotoxicity with L-6 cells**[16,17]

Assays were performed in 96-well microtiter plates, each well containing 100 µl of RPMI 1640 medium supplemented with 1% L-glutamine (200mM) and 10% fetal bovine serum, and 4000 L-6 cells (a primary cell line derived from rat skeletal myoblasts). Serial drug dilutions of eleven three-fold dilution steps covering a range from 100 to 0.002 µg/mL were prepared. After 70hours of incubation the plates were inspected under an inverted microscope to assure growth of the controls and sterile conditions. 10µl of Alamar Blue was then added to each well and the plates incubated for another 2 hours. Then the plates were read with a Spectramax Gemini XS microplate fluorometer (Molecular Devices Cooperation, Sunnyvale, CA, USA) using an excitation wave length of 536 nm and an emission wave length of 588 nm. The IC50 values were calculated by linear regression (Huber 1993) from the sigmoidal dose inhibition curves using SoftmaxPro software (Molecular Devices Cooperation, Sunnyvale, CA, USA).

6.5.3 *In vitro* Antiplasmodial assays:[18,19] W2 strain (Department of Medicine, San Francisco General Hospital, University of San Francisco)

The protocol to this assay is as described by Rosenthal, *et al*,[18] 1996. The W2 (CQ resistant) strain of *P. falciparum* (1% parasitemia, 2% hematocrit), were cultured in 0.5ml of medium in 48-well culture dishes. Stock solutions of inhibitors (10mM) in DMSO were added to cultured parasites to a final concentration of 20µM. From the 48-well plates, 125µM of culture was transferred to two 96-well plates (duplicates). Serial dilutions (1%) of inhibitors were made to final concentrations of 10µ*M*, 2µ*M*, 0.4µ*M*, 80n*M*, 16n*M*, and 3.2nM. Cultures

were maintained at 37^{o}C for 2 days after which the parasites were washed and fixed with 1% formaldehyde in PBS. After 2 days parasitemia was measured by flow cytometry using the DNA stain YOYO-1 as a marker of cell survival.

6.5.4 *In vitro* Antimycobacterial evaluation:[20,21,22] MABA and LORA Assays

(Institute of Tuberculosis Research, College of Pharmacy, Univirsity of Chicago)

MIC vs. replicating *M. tuberculosis* H_{37}Rv.

All compounds were evaluated for MIC vs. *M. tuberculosis* H_{37}Rv (ATCC 27294) using the microplate Alamar Blue assay (MABA) as previously described[20] except that we now use 7H12 media (3) (instead of 7H9 + glycerol + casitone + OADC). In the case of compounds exhibiting significant background fluorescence, luciferase reporter strains of *M. tuberculosis* H_{37}Rv were utilized as well as measurement of intracellular adenosine triphosphate. Cultures were incubated in 200 ul medium in 96-well plates for 7 days at 37C. Alamar Blue and Tween 80 are added and incubation continued for 24 hours at 37C. Fluorescence is determined at excitation/emission wavelengths of 530/590 nm, respectively. The MIC is defined as the lowest concentration effecting a reduction in fluorescence (or luminescence) of 90% relative to controls. Six control compounds are run in each experiment including isoniazid, rifampin, moxifloxacin, streptomycin, PA-824 and metronidazole.

Activity against non-replicating persistant (NRP) *M. tuberculosis*

This Low Oxygen Recovery Assay (LORA)[21] was designed to detect compounds which may have the potential for shortening the duration of therapy through (more) efficient killing of the non-replicating persistor (NRP) population. The assay involves 1) adaptation of M. tuberculosis to low oxygen through gradual, monitored, self-depletion of oxygen during culture in a sealed flask with slow stirring, 2) exposure for 10 days of the low-oxygen adapted culture to test compounds in microplates that are maintained under an anaerobic

environment using an Anoxomat system, thus precluding growth and 3) subsequent evaluation of M. tuberculosis viability as determined by the ability to recover. Recovery/viability is determined by the extent to which a luciferase-expressing strain can recover the ability to produce luminescence. This assay is HTS-compatible. Compounds such as isoniazid and ethambutol which are considered to be devoid of "sterilizing activity", are inactive in this assay Confirmation of new classes with activity was made by immediate subculture (without recovery phase) onto solid, drug-free media and determination of colony forming units. While the rifamycins and the more potent fluoroquinolones, which do appear to eliminate some proportion of the persistor population and thus can affect treatment duration, are active, albeit at concentrations higher than the MICs for replicating cultures. Correlation between the cfu and luminescence readout has been good with the exception of the fluoroquinolone class for which luminescence underestimates absolute activity but not relative activity.

Cytotoxicity Assay

Compounds are routinely tested for cytotoxicity using VERO cells[22]. After 72 hours exposure, viability is assessed on the basis of cellular conversion of MTS into a soluble formazan product using the Promega CellTiter 96 Aqueous Non-Radioactive Cell Proliferation Assay. Rifampin is included as a control. For compounds with IC_{50}:MIC >10, cytotoxicity will be repeated, this time using the J774.1 macrophage cell line since these are used in the macrophage assay and are usually somewhat more sensitive than VERO cells. This is important for interpreting data from the macrophage assay. Since much more comparative data is available for VERO cells, the use these for primary cytotoxicity testing is preferred. Additional cell lines include HepG2 and the new metabolically active HepaRG.

6.5.5 *In vitro* Antimycobacterial evaluation:[23] 7 and 14 day assays

Culture preparation of the mycobacterium

Mycobacterial tuberculosis $H_{37}Rv$ drug-sensitive strain was grown on Middlebrook 7H10 (Merck) supplemented with 0.5% glycerol and 10% Middlebrook Oleic acid Dextros catalase (OADC) enrichment (Merck) for five days at 37 °C, without shaking. To prepare the suspension for inoculation, the cultures were vortexed, left for 45 seconds to allow heavy particles to settle, followed by dilution.

Broth microdilution method assay

The broth microdilution method allows a range of antibiotic concentrations to be tested, on a single 96-well (8 by 12) microtitre plate, to determine the minimum inhibitory concentration (MIC). Briefly, a 10 mL culture of *M. tuberculosis* is grown to an OD600 of 0.7. The culture is then diluted 1:500 in 7H9 media. In a 96- well microtitre plate, 50 µl of 7H9 media was added to all wells starting from Rows 2-12. In the first and last wells of Row 1, 100 µl of 7H9 media was added as a control. The test compounds were added to Row 1 at a final concentration of 640 µM (stock concentration of 12.8 mM in DMSO, diluted to final concentration in 7H9 media). A serial dilution was prepared using a multichannel pipette by transferring 50 µl of the liquid in Row 1 to Row 2, followed by aspirating to mix. A 50 µl of the liquid in Row 2 was transferred to Row 3 and aspirated. The procedure was repeated until Row 12 was reached, where 50 µl of the liquid in Row 12 was discarded to bring the final volume in each well to 50 µl.

Finally, the 50 µl of the diluted *M. tuberculosis* culture was added to all the wells starting from Row 2 to 12. The microtitre plate was stored in a ziplock bag and incubated at 37°C.

6.6 References

1. Feng, T-S, PhD Thesis, University of Cape Town, **2009**.

2. Peck, R. M.; Preston, R. K.; Creech, H. J., *J. Am. Chem. Soc*., **1959**, *81*, 3984.

3. Mobilio, D.; Musser, J. H., US Patent Ser number 592411, **1993**.

4. Mayer, J.; Umkemhrer, M.; Kalinski, C.; Ross, G.; Kolb, J.; Burdack, C.; Hiller, W., *Tetrahedron Lett.* **2009**, *46*, 7393.

5. Damiers, R.; Price, A. T., PCT/WO**2007**/016610/A2.

6. Davidson, D.; Bernhald, S. A., *J. Am. Chem. Soc*., **1948**, *70*, 3426.

7. Milner, E.; McCalmont, W.; Bhonsle, J.; Caridha, D.; Carroll, D.; Gardner, S.; Gerena, L.; Gettayacamin, M.; Lanteri, C.; Luong, T.; Melendez, V.; Moon, J.; Roncal, N.; Sousa, J.; Tungtaeng, A.; Wipf, P.; Dow, G., *Bioorg. Med. Chem. Lett.*, **2010**, *20*, 1347.

8. Jiao, L.; Liang, Y.; Xu, J., *J. Am. Chem. Soc*., **2006**, *128*, 6060.

9. Illiashevsky, O.; Amir, L.; Glaser, R.; Marks, R. S.; Lemcoff, N. G., *J. Mater. Chem*., **2009**, *16*, 6616.

10. Jiricek, J.; Patel, S.; Keller, T. H.; Barry, C. E.; Dowd, C. S., US **2008**/0275035 A1.

11. Desjardins, R. E., C. J. Canfield, J. D. Haynes, and J. D. Chulay., *Antimicrob. Agents Chemother*., **1979**, *16*, 710.

12. Baltz, T. D.; Giroud, C.; Crockett, J., *EMBO J*., **1985**, *4*, 1273.

13. Rätz, B.; Iten, M.; Grether-Buhler, Y.; Kaminsky, R., *Acta. Trop*., **1997**, *68*, 139.

14. Huber, W.; Koella, J. C., *Acta. Trop*., **1993**, *55*, 232.

15. Thaithong, S.; Beale, G. H.; Chutmongkonkul, M., *Trans. Royal Soc. Trop. Med. Hygiene,1993*, *77*, 228.

16. Page, C. M.; Noel, C., *J. Oncology*, **1993**, *3*, 473

17. Ahmed, S. A.; Gogal, R. M.; Walsh, J. E., *J. Immunol. Methods*, **1994**, *170*, 211.

18. Rosenthal, P. J.; Olson, J. E.; lee, G. K.; Palmer, J. T.; Klaus, J. L.; Rasnick, D.; *Antimicrob. Agents Chemother*., **1996**, *40*, 1600.

19. Greenbaum, D. C.; Mackey, Z.; Hansell, E.; Doyle, P.; Gut, J.; Caffrey, C. R.; Lehrman, J.; Rosenthal, P. J.; McKerrow, J. H.; Chibale, K., *J. Med. Chem*., **2004**, *47*, 3212.

20. Collins, L.; Franzblau, S. G.; *Antimicrob. Agents Chemother*., **1997**, *41*, 1004.

21. Cho, S. H.; Warit, S.; Wan, B.; Hwang, C. H.; Pauli, G. F.; Franzblau, S. G., *Antimicrob. Agents Chemother.*, **2007**, *51*, 1380.

22. Falzari, K.; Zhu, Z.; Pan, D.; Liu, H.; Hongmanee, P.; Franzblau, S. G., *Antimicrob. Agents Chemother.*, **2005**, *49*, 1447.

23. Leite, C. Q.; Beretta, L. A.; Anno, I. S.; Telles, M. A., *Mem Inst Oswaldo Cruz*, **2000**, *95*, 127.